

AD-A233 959

ONR-URI Composites Program
Technical Report No. 90-05

UIUC-NCCMR-90-05

**NOVEL INTERPHASES: SYNTHESIS, MOLECULAR
ORIENTATION AND GRAFTING OF LIQUID CRYSTAL
POLYMERS ON CARBON FIBERS**

Satya Bhamu Sastri* and Samuel I. Stupp**

January, 1990

National Center for Composite Materials Research
at University of Illinois, Urbana - Champaign
A DoD University Research Initiatives Center funded by the
Office of Naval Research, Arlington, VA

* Graduate Research Assistant

** Professor of Material Science and Engineering

91 3 27 092

NOVEL INTERPHASES: SYNTHESIS, MOLECULAR ORIENTATION AND
GRAFTING OF LIQUID CRYSTAL POLYMERS ON CARBON FIBERS

Satya Bhama Sastri, Ph.D.

Department of Materials Science and Engineering

University of Illinois at Urbana-Champaign, 1990

Samuel Stupp, Advisor

The objective of this research has been to study composite material systems containing liquid crystal polymers either as matrices or in interfacial boundary zones. The fundamental point of interest here is the interfacial response that fiber surfaces can potentially induce in self ordering polymers. This investigation includes studies in three broad categories: molecular orientation of nematic melts containing dispersed carbon fibers, the chemical grafting of a liquid crystal polymer to these fibers by in-situ polymerization of monomeric melts, and the synthesis and anchoring on fibers of specially designed liquid crystal monomers and polymers containing pendant chemical functions on their mesogenic groups.

The matrix polymer used in orientation studies is a thermotropic liquid crystal polyester synthesized from the monomers p-acetoxybenzoic acid, diacetoxyhydroquinone and pimelic acid. This aliphatic-aromatic polymer was characterized by ^{13}C -NMR as a chemically disordered copolymer of the three structural units which exhibits a nematic phase above 150°C . Broadline proton NMR above the solid to liquid crystal transition was used to measure the rate of magnetic alignment of molecules in the matrix. Enhanced rates of magnetic orientation in the polymer melt were observed when carbon fibers are dispersed in the medium. Polarized optical microscopy studies of these composite samples revealed that fiber surfaces influence the orientation of liquid crystal polymer matrix in their immediate surroundings. In spite of this orienting influence of

DIST A PER TELECON MR. Y BARSOUM
ONR/CODE 1132 SM
4/1/91 CG

A-1

fibers on the matrix molecules, fracture surface analysis of composite specimens by SEM revealed poor wetting of the fibers by the matrix polymer. It was possible to induce excellent wetting of this polymer on carbon fibers by in-situ polymerization of the monomers in the presence of functionalized fibers. This in-situ growth of liquid crystal polymer chains results in covalent grafting of mesogenic chains on fiber surfaces. New hydroxy-functionalized side chain liquid crystal polymers were synthesized which could be useful in the molecular design of interfacial boundary layers in polymer-based composites. A protection-polymerization-deprotection scheme was developed for the synthesis of these functionalized polymers. Optical observations reveal that the phenolic monomer has an exceptionally strong tendency for orthogonal anchoring on glass surfaces. However, this anchoring by glass is disturbed around carbon fibers dispersed in the monomeric melt. From studies with a compensator, it is inferred that these "boundary zones" around fibers contain arrays of molecules oriented in two different directions. Comparative studies with similar compounds which contain different terminal substituents reveal that the presence of phenolic functional groups facilitates perpendicular alignment of molecules on glass substrates. In contrast to the monomer, the orienting behavior of the polymer on either glass or carbon surfaces is less defined. This property of the polymer could be improved significantly by replacing some phenolic groups by bulky, nonpolar silyl ether groups presumably due to the "plasticizing" effect of these substituents bound to polymer backbones. This observation suggests that the mobility of mesogenic side chains is an important factor for substrate-induced alignment of comb polymers.

ACKNOWLEDGEMENTS

The author wishes to express her sincere gratitude to her advisor, Professor Samuel Stupp, for his unflagging enthusiasm for research. By creating a working environment which has encouraged her to pursue a relatively independent research program, and providing constructive suggestions and criticism, Professor Stupp has contributed significantly to her development as a research scientist.

Members of the committee, Professor Philip H. Geil, Professor Steve Granick, and Professor Su Su Wang are gratefully acknowledged for their counsel and helpful discussions.

Support from the National Center for Composite Materials Research funded by the Office of Naval Research, University of Illinois, is appreciated.

Much gratitude is extended to all fellow graduate students and friends for their helpful discussions, comments and enjoyable company.

The author is sincerely thankful to her parents, brother and sisters for their contribution to the pursuit and attainment of goals which at one time were only dreams.

Above all, the author would like to express her thanks and appreciation to her husband, Bhima Sankar Sastri, for his patience, encouragement, moral support, but mostly for being the nice person that he is.

TABLE OF CONTENTS

	<u>Page</u>
INTRODUCTION	1
CHAPTER 1	
Molecular Orientation and Grafting of a Liquid Crystal Polymer on Carbon Fibers	
1.1 Introduction	4
1.1.1 Orientation Studies by NMR	7
1.1.2 Interphases in Carbon Fiber-Containing Composites	9
1.2 Results and Discussion	11
1.2.1 Synthesis and Characterization of a Liquid Crystal Polymer Matrix Material	11
1.2.2 Magnetic Alignment Studies	16
1.2.3 Optical Microscopy Studies	21
1.2.4 Grafting and Interfacial Adhesion	26
1.2.4.1 Grafting <i>via</i> Melt-phase Transesterification	26
1.2.4.2 Grafting <i>via</i> Esterification in Solution	41
1.3 Summary	43
1.4 Experimental	45
1.4.1 Polymer Synthesis and Characterization	45
1.4.2 Grafting by In-Situ Polymerization	48
1.4.3 Grafting <i>via</i> Carbodiimide-based Esterification	49
References	50
CHAPTER 2	
Synthesis of Functionalized Side Chain Liquid Crystal Polymers	
2.1 General Introduction	55
2.1.1 Structural Principles	56
2.1.2 General Synthetic Routes	64
2.1.3 Functionalized Side Chain Liquid Crystal Polymers	68
2.1.4 Target Polymers	72

2.2	Results and Discussion	75
2.2.1	Overview of the Synthetic Plan	75
2.2.2	Stepwise Construction of Functionalized Monomers	76
2.2.3	Polymerization Strategy	80
2.2.3.1	Initial Attempts	80
2.2.3.2	Synthesis of Target Polymers	91
2.3	Summary	99
2.4	Experimental	101
2.4.1	General Information	101
2.4.1.1	Reagents, Supplies, and Purification	102
2.4.2	Experimental Procedures	104
2.4.2.1	Hydroxy-Functionalized Monomer Synthesis	104
2.4.2.2	Protected Monomer Synthesis	117
2.4.2.3	Protected Polymer Synthesis	124
2.4.2.4	Deprotection of Polymers	130
References		133

CHAPTER 3

Properties of Hydroxy-Functionalized Monomers, Polymers and Derivatives

3.1	Structure-Property Correlations in Liquid Crystalline Compounds	143
3.1.1	Structural Criteria	143
3.1.1.1	Hydrogen Bonding and Mesomorphism	146
3.1.2	Molecular Structure and Mesomorphism	152
3.1.3	Influence of Substituents on Transition Temperatures	153
3.1.4	Surface Phenomena	155
3.2	Results and Discussion	160
3.2.1	Properties of Hydroxy-Functionalized Monomers and Polymers	160
3.2.2	Properties of O-Derivatized Monomers and Polymers	173

3.2.3	Influence of Fibers on Molecular Alignment . . .	187
3.2.4	Partially Protected Hydroxy-Functionalized Polymers	202
3.3	Summary	214
3.4	Experimental	215
3.4.1	Synthesis of O-Derivatized Monomers and Polymers	215
References	223
FINAL CONCLUSIONS	227
VITA	230

INTRODUCTION

One common feature of all liquid crystal phases is their ability to acquire spontaneously molecular order without significantly freezing out molecular mobility. The various classes of liquid crystal phases differ in degree of molecular mobility. Constituents of the nematic phase, for example, display orientational correlation only among their long axes, while the ends of the molecules in smectic phases exhibit positional correlation (the molecules are arranged in layers). The unusual combination of order and mobility brought together by the liquid crystal phase creates a physical environment capable of exhibiting cooperative reorientation upon application of weak external fields. Solidification of oriented arrays is of interest to study properties of highly ordered or anisotropic materials. In small molecule liquid crystals, this opportunity is not readily apparent since the formation of an unoriented polycrystalline microstructure is very probable when the oriented fluid solidifies. With macromolecular liquid crystals there exist more possibilities to form oriented materials based on the fact that they have slower crystallization and /or longer relaxation times.

The orienting effect of surfaces on liquid crystals is a well known phenomenon. Surface-related forces at liquid crystal-solid interfaces may be considered as local-external fields exerting their aligning influence on self-ordering molecules similar to electric, magnetic or flow fields. However, many aspects of these surface-guided orientations in macromolecular liquid crystals remain unknown at this stage.

The purpose of the present investigation is to contribute to the understanding of how surface forces influence the alignment of self-ordering polymer molecules. In particular, this study focuses on carbon fibers and

thermotropic liquid crystal polymers. Guiding forces originating from fiber surfaces may have a significant influence on the alignment of molecules in the interphase regions. Studies on these systems are relevant for the modification of properties of composites containing liquid crystalline polymers as matrices or interfacial zones. For instance, orientational organization of mesomorphic molecules in interphase regions may result in highly ordered boundary zones around fibers. Such an interphase might manifest itself in superior mechanical properties of the composite specimen. In addition, with liquid crystal polymers, it may be possible to dictate the molecular orientation within these zones with respect to the fiber axis. From a properties standpoint, the occurrence of high density surface layer with significant orientation of molecular backbone normal to the fibers could offer advantages in environmental stability and isotropic strength in processed composites.

The first part of this study involved synthesis of a main chain liquid crystal polyester for studies on magnetic field orientation of liquid crystal polymer-carbon fiber composites. In principle, these polymeric chains can also be grafted onto fiber surfaces with suitable functional groups. Chapter 1 presents results of the molecular orientation studies and also the implications of grafting mesogenic chains to fiber surfaces on interfacial bonding. The chapter concludes with detailed experimental procedures employed in the synthesis of matrix polymer and characterization of composite specimens.

The next phase of research involved design of a new class of functionalized polymers that could have potential to control interphases in a number of composite systems. The target polymers designed for this purpose were hydroxy-functionalized side chain liquid crystal polymers. It was desirable to place the hydroxyl groups on the mesogenic units so as to lock these groups in the ordered mesophases. The concerted behavior of functional groups in the

interphase regions may very well influence the reactivity of these interphases towards organic matrices. Synthesis of the target polymers involved identifying suitable protecting groups for preparation of phenolic polymers by addition polymerization mechanism. The synthetic strategy employed for their synthesis and the experimental procedures are discussed in chapter 2. Properties of the phenolic monomer, the corresponding polymer and the influence of fibers on their properties are addressed in chapter 3. The Final Conclusions section briefly outlines the salient findings of the entire study.

CHAPTER 1

Molecular Orientation and Grafting of a Liquid Crystal Polymer on Carbon Fibers

1.1: Introduction

The observation by Reinitzer in 1888 (1) of what appeared to be two melting transitions in cholesteryl benzoate is usually cited as the event that initiated the study of mesomorphism or liquid crystalline behavior. This phenomenon continues to draw a great deal of attention from the scientific community. The subject of small molecule liquid crystals (LCs) (2-7) and liquid crystalline polymers (LCPs) (8-11) have been extensively reviewed in the literature. While the science of LCs is well developed and these systems are technologically exploited, LCPs have gained popularity only over the last two decades and still remain an open subject for materials scientists to explore. This study is aimed at addressing the properties of these polymeric materials in contact with surfaces for their potential application in composite systems. The present chapter focuses on thermotropic LCPs, i. e. LCPs which show mesomorphic behavior upon heating, and in particular, on main chain LCPs which have mesogens as a part of the polymer backbone. The following chapters elaborate on LCPs of a side chain variety which have pendant mesogenic moieties linked to the polymeric backbone *via* flexible spacers.

A theoretical understanding of liquid crystallinity in polymers was first offered by the work of Flory in 1956 (12). His calculations on thermodynamic properties of polymer solutions (12) predicted that polymers containing rigid segments of appropriate dimensions would exhibit an anisotropic phase above some minimum concentration as a consequence of repulsive forces. Over

the past few decades, a number of other theoretical attempts to describe the spontaneous ordering of rigid molecules into an anisotropic phase have been reported. Lars Onsager (13) showed that steric interactions between rigid rods can lead to anisotropic phases as a consequence of the balance between orientational and rotational entropy. Maier and Saupe (14-16) developed a theory of liquid crystallinity utilizing the assumption that anisotropic dispersion forces were alone responsible for the generation of the mesomorphic state. Flory and Ronca (17), utilizing a lattice model, showed that a critical molecular axial ratio of 6.4 in rod-like molecules would lead to an anisotropic phase as a result of repulsive forces only. More contemporary theoretical attempts provide more realistic models of the polymeric systems by incorporating flexibility terms. Ronca and Yoon (18) incorporated semiflexibility into the theory of nematic systems utilizing a worm-like chain model. ten Bosch, Maissa and Sixou (19) incorporated semiflexibility into a Landau de Gennes free energy expression and presented the nematic to isotropic transition as a function of chain length and chain flexibility. Khokhlov and Semenov (20) examined several different models of partial flexibility and employed both attractive and repulsive forces in the theory. This theory balances the orientational and translational entropy with the repulsive and attractive forces of chain segments. In general, the results indicate that steric forces play the dominant role in self ordering of molecules while the attractive forces are secondary.

Interest in thermotropic LCPs stems from the possibility of combining the unique properties of small molecule LCs with those of high molecular weight compounds to generate new materials with extraordinary properties. Due to their properties, small molecule LCs have been utilized in a variety of electro-optical applications (21-23). However, small molecule LCs fail to form useful

solids due to their low melting points close to ambient temperatures. On the other hand, macromolecular liquid crystals are useful due to their significantly higher melting temperatures and excellent physical properties. In addition, it is known that these materials respond to external fields (electric, magnetic, flow) and surfaces which offers a unique method of directing the molecular orientation of polymeric melts. A rich body of knowledge is available regarding the orienting effects of surfaces (22, 24-37), electric fields (30, 38-49) and magnetic fields (48-51) on small molecule liquid crystals. At this time thermotropic polymers do not harbor this abundance of information. Due to the long chain nature of these molecules, there is a potential to lock in the oriented microstructure by vitrifying the melt to create solids with controlled levels of orientation.

One attractive application for thermotropic LCPs based on this potential to form oriented microstructures could be in composite systems. The driving force for formation of such oriented microstructures may be the orienting effect that fiber surfaces can have on self ordering molecules. In small molecule LCs, this orienting effect of surfaces has been theoretically explained on the basis that orientation avoids high energy elastic distortions in mesophases that are in contact with specific types of surfaces (24, 52). The types of surfaces that are known to have this "guiding effect" on liquid crystal's orientation include chemically modified surfaces and also those containing topological features such as uniaxial grooves or cavities. Should it be possible to extend these effects of fiber surfaces to macromolecular liquid crystals incorporated in composite systems, many possibilities would exist for the control of properties through highly ordered films formed at interfaces. It is our objective to understand the principles and limitations of fiber surface forces affecting molecular organization of self ordering matrices.

Composites containing liquid crystalline polymers are relatively new systems. To our knowledge, only Stamatoff et al. (54) have addressed the issue regarding orienting effects of fibers on LCP chains. In their composite specimens, a preferential alignment of LCP chains in the solid state was observed along the axis of the carbon fibers. However, little is known about the organization of molecules around fibers in a fluid matrix and even less is known about the orientation dynamics of molecules in the presence of fibers. Therefore, an attempt is made here to study the molecular orientation in LCP-carbon fiber composite systems by nuclear magnetic resonance (NMR) spectroscopy and optical microscopy. The magnetic field in NMR measurements which serves as the external orienting force can be considered analogous to a flow field. Polymeric mesophases are oriented readily by flow fields at quite low shear rates (54). It is anticipated that these experiments which couple magnetic and surface forces would shed some light on the combined influence of flow field and surface forces which the polymeric chains experience under processing conditions of composite specimens.

1.1.1: Orientation Studies by NMR

Information regarding the degree of order in a liquid crystal is given by macroscopic order parameter ($S_{z'z'}$) defined as,

$$S_{z'z'} = \frac{3}{2} \cos^2 \theta_0 - \frac{1}{2} \quad \text{..... (1.1)}$$

where θ_0 is the angle which the macroscopic director makes with the external field. Measurement of macroscopic order parameter as a function of time was first conducted independently by Blumstein and coworkers (55) and Samulski

(56) using NMR studies. Recent work by Moore and Stupp (57) has shown that the kinetics of molecular orientation could be derived from these experiments.

From the proton spectra collected as a function of time at temperatures above the solid to liquid crystal transition, it is possible to obtain values of second moment, $\langle \Delta v^2 \rangle$, defined as,

$$\langle \Delta v^2 \rangle = \frac{\int_{-\infty}^{\infty} [v - \langle v \rangle]^2 g(v) dv}{\int_{-\infty}^{\infty} g(v) dv} \quad \text{..... (1.2)}$$

where $g(v)$ represents the functional form of the NMR line shape, v is the frequency at which resonance occurs and $\langle v \rangle$ is the average frequency of the resonance band. The relationship between $\langle S_{zz}^2 \rangle$ and second moment can be written as,

$$\langle S_{zz}^2 \rangle = \frac{\langle \Delta v^2 \rangle - f_I \langle \Delta v^2 \rangle_I}{\langle \Delta v^2 \rangle^0 - f_I \langle \Delta v^2 \rangle_I} \quad \text{..... (1.3)}$$

where $\langle \Delta v^2 \rangle_I$ is the second moment associated with the isotropic component of the signal, and $\langle \Delta v^2 \rangle^0$ is the experimentally measured second moment of a perfectly aligned specimen. Moore and Stupp have shown that the values of $\langle \Delta v^2 \rangle^0$, $\langle \Delta v^2 \rangle_I$ and f_I can be determined from low molecular weight samples that completely align in the field (57). This value of $\langle S_{zz}^2 \rangle$ as measured by NMR should be equal to 0.2 for a randomly oriented sample and should increase to 1.0

for a fully aligned system. The fitting of the $\langle S_{zz}^2 \rangle$ vs. time data to a theoretical model described at length in (57) enables one to obtain a characteristic orientation time, τ , for the macroscopic reorientation process. This τ is defined as the time it takes the macroscopic order parameter to reach a value $1/e$ and can serve as a measure of how fast the LCP chains reorient parallel to the external field.

1.1.2: Interphases in Carbon Fiber-Containing Composites

The success of composites as engineering materials depends critically on the ability of the matrix material to transfer stresses to the reinforcing phase. This stress transfer in interphase regions requires ideally the formation of interfacial chemical bonds. While the importance of a strong interfacial bond is widely recognized, a global understanding of all properties as affected by chemistry and morphology of interphases is still lacking.

In recent years, several research groups have investigated fiber-matrix chemical interactions mostly in connection with glass fibers (58-61). In many of these investigations, the formation of durable bonds at the interface has been claimed. Even though much less is known about interfacial chemistry when carbon fibers are involved, it is clear that their surfaces are less reactive than those of glass fibers. Nonetheless, a range of active functional groups such as those shown in figure 1.1 can be introduced on carbon surfaces by oxidative treatments such as heating in oxygen or treatment with nitric acid (62, 63). These active groups exist preferentially at the edges and defect sites of the basal planes (62) and therefore covalent bonds can form between the fibers and chemical functions in matrix molecules.

In-situ polymerization of monomers which can react with surface functionalities offers a unique route to modify the interphase chemistry and morphology in composite systems. Kochinski and Reighert (64) used this

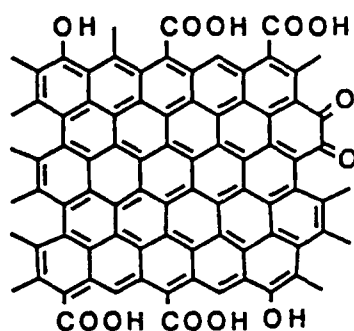


Figure 1.1 : Chemical structure of the carboxy-functionalized carbon fiber (81)

approach in an attempt to modify poly(phenylene sulphide)-carbon fiber composite systems. They observed improved fiber/matrix adhesion, an increased resistance to corrosive media and only a marginal improvement in strength relative to composites prepared by physical blending. In another investigation by Zeng and Bailing (65), in-situ polymerization of nylon 10,10 in the presence of carbon fibers was attempted but resulted in poor properties of the composite specimens as compared to the control samples. This was attributed by the authors to the low molecular weight of the matrix material.

In the present context of self ordering matrices, it is important to have good adhesion between the fiber and the matrix in order to fully exploit the guiding influence of fiber surface forces that could create highly ordered interphases. One possible way to accomplish a good interfacial adhesion would be by covalent grafting of mesogenic chains on functionalized carbon fiber surfaces. Grafting in these systems may be viewed as not only a mechanism to achieve interfacial binding but also an approach to modify the interphase physical structure.

In the following section, results of the magnetic alignment studies of a number of composite systems studied are presented. Results of the optical

microscopy studies that assist in the interpretation of alignment kinetics of these composite specimens are also presented. In addition, grafting of nematogenic chains on carbon fibers and its impact on adhesion of a liquid crystal polymer matrix are discussed. Specific details regarding the preparation of monomers and matrix polymer are offered in the experimental section. This section also presents details concerning characterization of the pure matrix polymer and the composite specimens. Finally, grafting procedures by in-situ polymerization of monomers in the presence of functionalized fibers and by solution-based carbodiimide chemistry are presented.

1.2: Results and Discussion

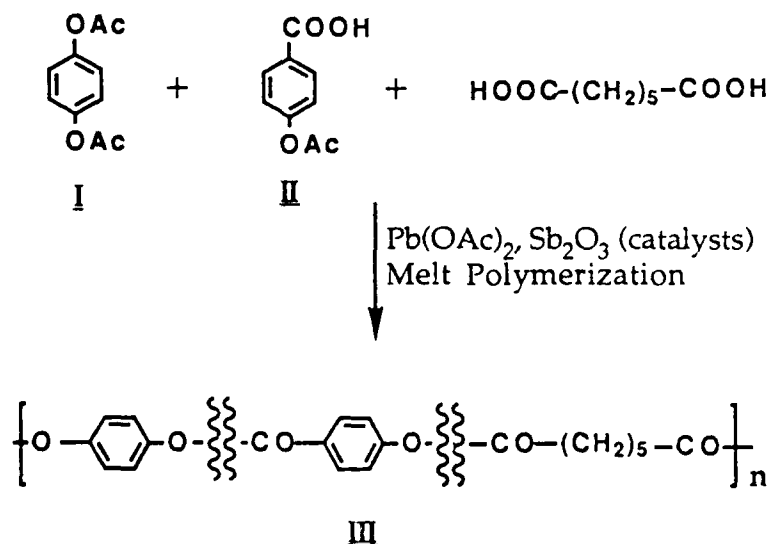
1.2.1: Synthesis and Characterization of a Liquid Crystal Polymer Matrix Material

Synthesis of monomers diacetoxyhydroquinone (**I**) and p-acetoxybenzoic acid (**II**) were easily accomplished by acylation reaction (66) in 76% and 82% yields, respectively. Polycondensation of these monomers in the presence of pimelic acid was designed to synthesize aliphatic-aromatic polyesters with melting transitions below 200°C for orientation studies. Synthesis of high molecular weight polyesters by transesterification often employ conditions of stoichiometric imbalance at the start of the reaction. These conditions are necessary when one monomer is volatile under high-vacuum and high-temperature conditions, in order to drive the system to stoichiometric balance. In our early attempts at synthesizing this polyester by the melt polymerization procedure, a white crystalline solid (3-4% by weight of the reaction mixture) was always found to sublime from the reaction flask. Even when the contents were heated very slowly from 180°C and the pressure was reduced over an extended period of time, sublimation was still observed. Using NMR the predominant

component of the sublimate was identified to be unreacted diacetoxyhydroquinone contaminated with a small quantity of unreacted pimelic acid. On the basis of the integral heights of the aliphatic and aromatic regions, it was determined that the polymerization of high molecular weights by virtue of stoichiometric balance might be carried out successfully with an initial 10% molar excess of diacetoxyhydroquinone.

The synthesis of the liquid crystal polyester was accomplished by melt polymerization of monomers in two stages as shown in scheme 1.1. The first step yielded an oligomeric product, the molecular weight of which increased under high-vacuum and high-temperature conditions employed in the second stage. This liquid crystal polyester **III** can be alternatively synthesized by the condensation of the asymmetric diester of p-hydroxybenzoic acid and hydroquinone with pimelic acid (67). The $^1\text{H-NMR}$ spectrum of the polyester obtained from the synthetic procedures employed is shown in figure 1.2.

SCHEME 1.1



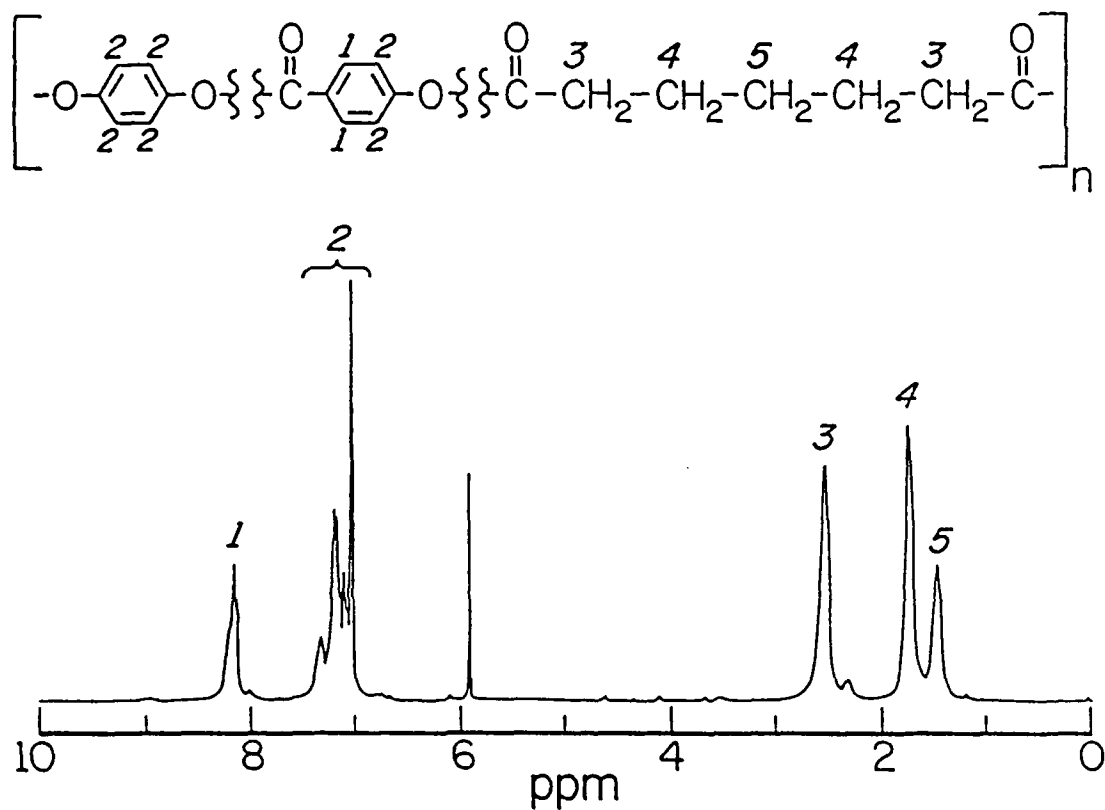
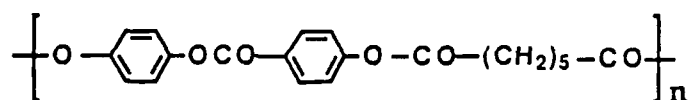


Figure 1.2 : ^1H -NMR spectrum of the liquid crystalline polyester used as the matrix polymer in magnetic alignment studies

Peak assignments can be made easily by comparison with spectra corresponding to the three monomers. A small multiplet seen in the range 2.20-2.40 δ corresponds to the polymer end groups. Since the acetoxy and the methylene α to the carboxylic acid groups appear in the same region, it is not possible to know which end groups dominate. This multiplet also indicates that the molecular weight of the synthesized polymer is not high. Based on the intrinsic viscosity obtained for polymer solutions (0.41dL/g) and Mark-Houwink constants calculated in previous work from this laboratory (67), the molecular weight of the polymer is estimated to be approximately 5500. No further attempts to increase the molecular weight of the polymer were made as this range of molecular weight was ideally suited for magnetic alignment studies.

The ^{13}C -NMR spectrum of the polymer is shown in figure 1.3. For a chain with a periodic sequence as shown in IV, one would expect three different carbonyl peaks with equal intensities. However, careful inspection of the ^{13}C



IV

spectrum reveals four different carbonyl peaks with unequal intensities, indicating the polymer has an aperiodic sequence of the three structural units. The appearance of the small peak at δ 164.2 is indicative of the presence of oxybenzoate diads in the polymer backbone.

Optical microscopic analysis of the molten samples between cross polars revealed as expected for a liquid crystalline polymer, a highly birefringent fluid. Flow was detected near 145 $^{\circ}\text{C}$ and similarly to the polymer synthesized by the alternative method (67), the polymer showed a broad biphasic texture between

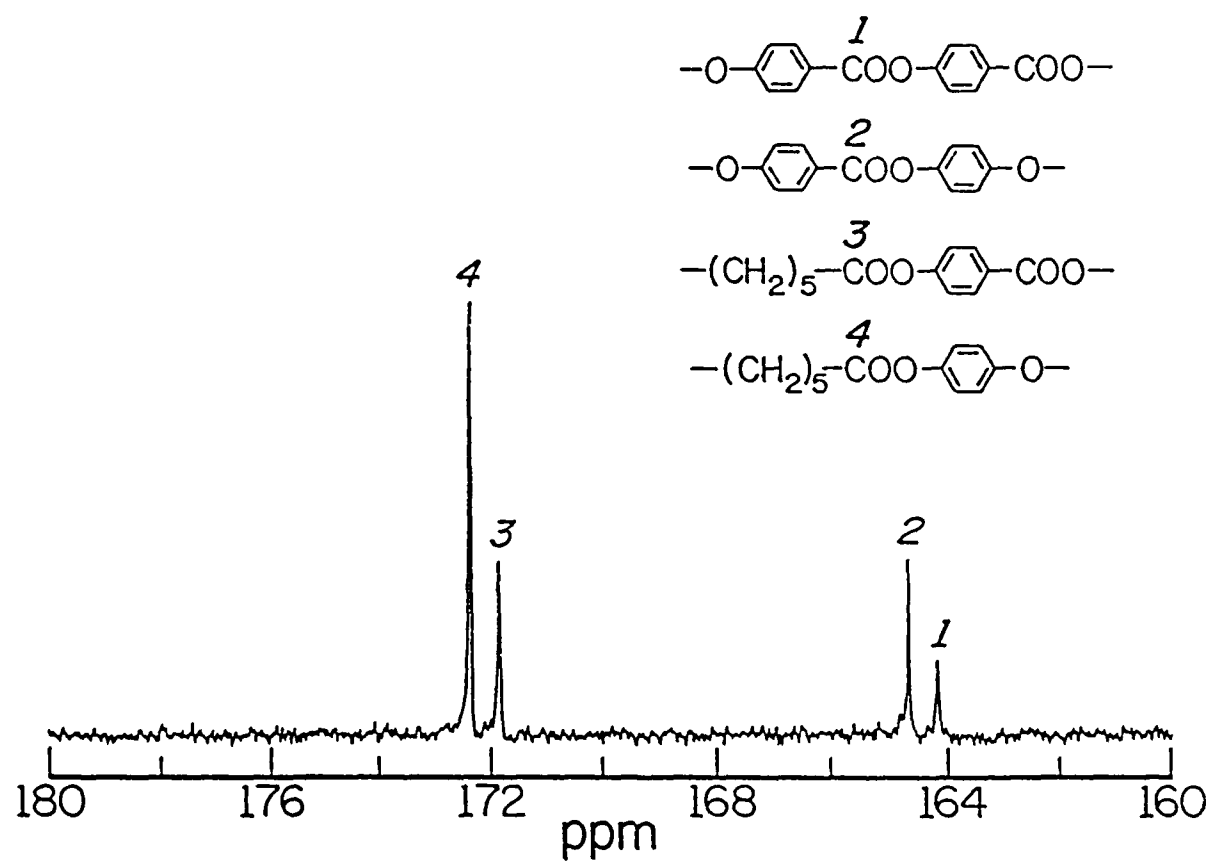


Figure 1.3 : ^{13}C -NMR spectrum of the matrix polymer synthesized by melt phase transesterification

220°C and 350°C. In this temperature range, a nematic phase and an isotropic phase coexist and the entire sample becomes isotropic above 350°C. A DSC scan of the polyester obtained during the second heating cycle is shown in figure 1.4. A well defined endotherm at 133°C corresponds to the solid to liquid crystal transition. A second endotherm corresponding to the liquid crystal to the isotropic transition is not clearly defined in the DSC scan presumably because of the gradual transition to isotropic phase as observed by the optical microscopy.

1.2.2: Magnetic Alignment Studies

Liquid crystalline polymers can acquire macroscopic orientation in a magnetic field (68-75). The goal in our experiments has been to establish if carbon fibers in a composite system can affect in any way the course of magnetic orientation of the LCP matrix. The question has been addressed by ¹H-NMR experiments in LCP-carbon fiber composites. Figure 1.5 shows the gradual change observed in broadline NMR spectrum of the LCP sample with time under the influence of a magnetic field. The gradual appearance of two well defined bands symmetric in frequency above and below the central resonance peak is an indication of macroscopic orientation in the liquid sample. This effect is caused by dipolar interactions between protons in the orientationally ordered fluid (76).

Second moment values as a function of time were calculated from the proton spectra for a number of composite specimens from which the time dependence of the macroscopic order parameter $\langle S_{zz}^2 \rangle$ could be assessed. Plots of $\langle S_{zz}^2 \rangle$ vs. time for two such composite specimens are shown in figure 1.6. By fitting these curves to a theoretical model (57), characteristic orientation times were calculated for LCP matrices in contact with varying fractions of carbon fibers. Results of orientation times for various composite specimens are

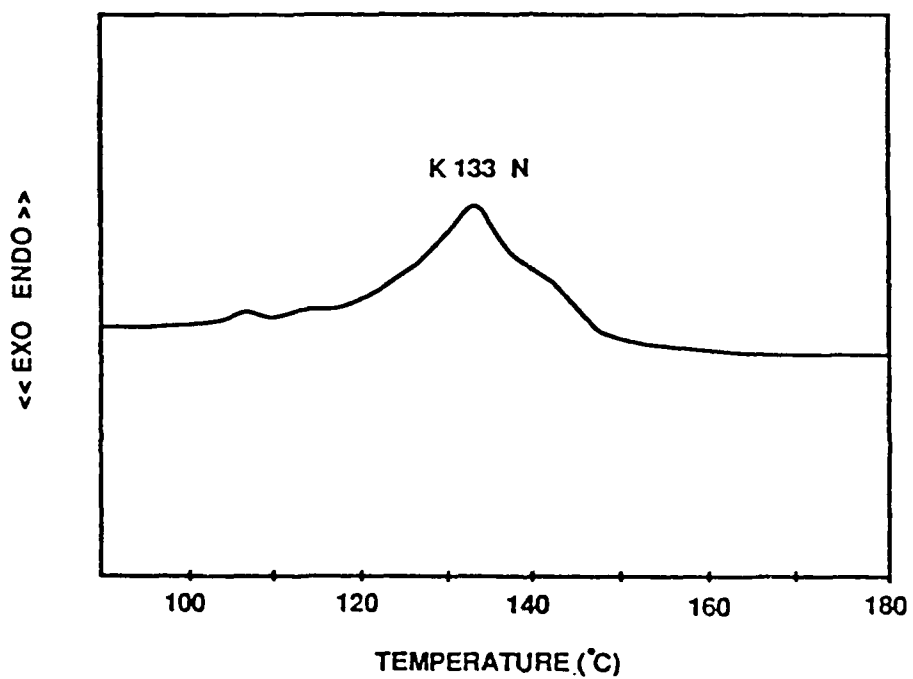


Figure 1.4 : DSC scan of the liquid crystalline polyester obtained during the second heating cycle, at a heating rate of 10°C/min

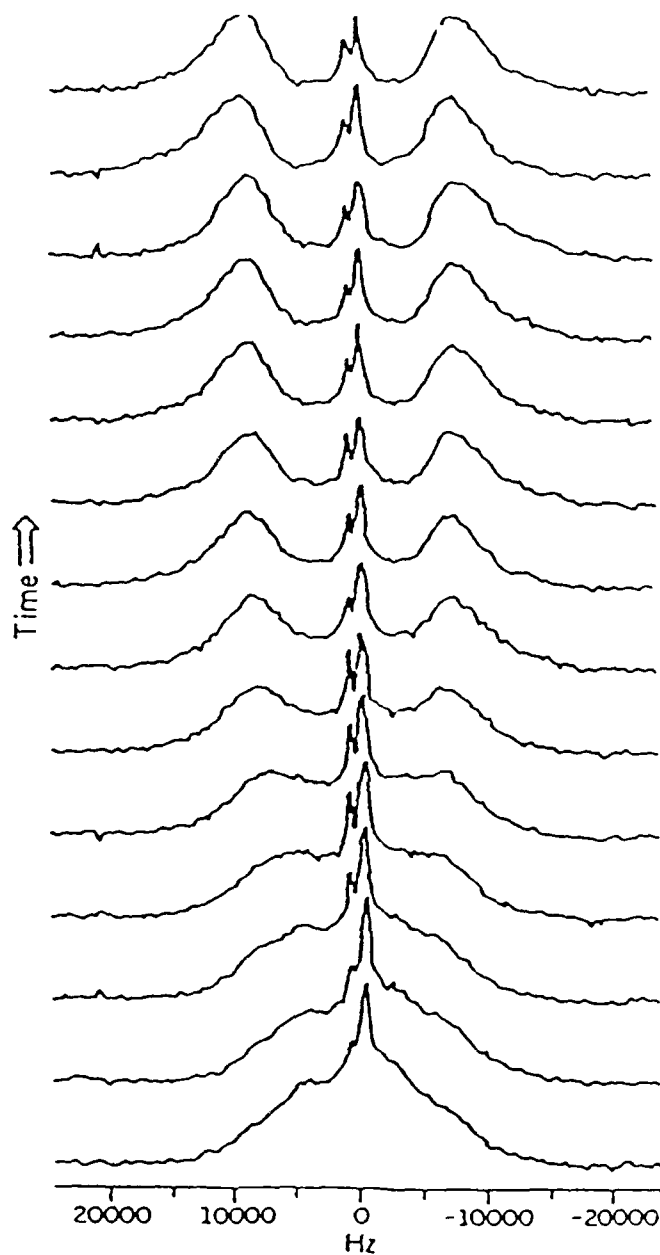


Figure 1.5: Broadline ^1H -NMR spectra of the matrix polyester in the fluid state with increasing time in the magnetic field ($T=170^\circ\text{C}$)

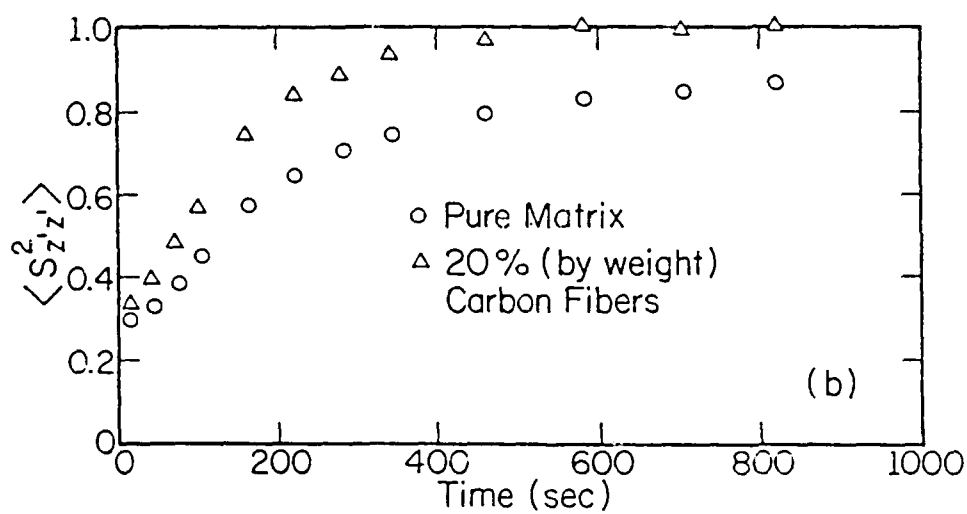
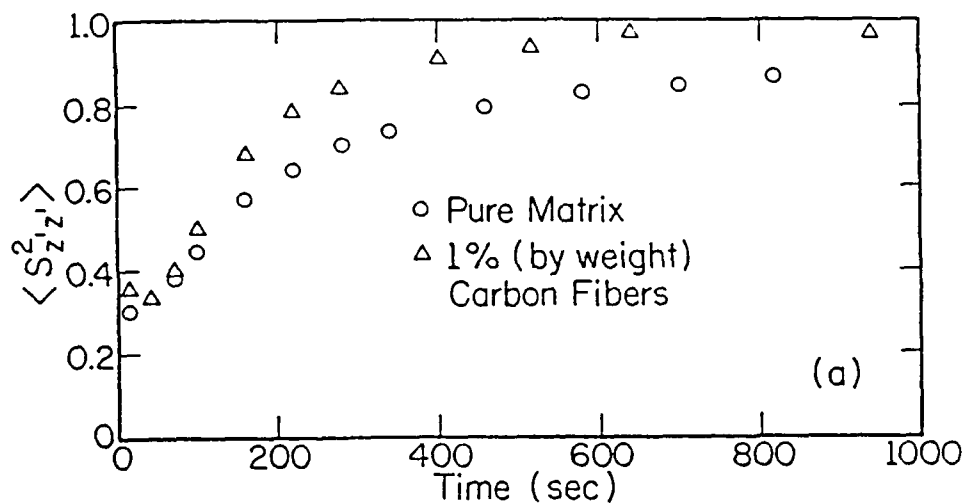


Figure 1.6: Plot of macroscopic order parameter $\langle S_{zz}^2 \rangle$ as a function of time for the pure matrix and matrix containing 1% by weight (a) and 20% by weight (b) dispersed carbon fibers

summarized in table 1.1. Interestingly, these results suggest that the LCP matrix orients at a significantly faster rate when in contact with dispersed carbon fibers. This reduction in orientation time is observed with a small fraction (1% by weight) of fibers with no further significant decrease with higher fiber contents.

Wt.% of carbon fibers	τ (sec)
0	239
1	137
5	134
20	138
40	152

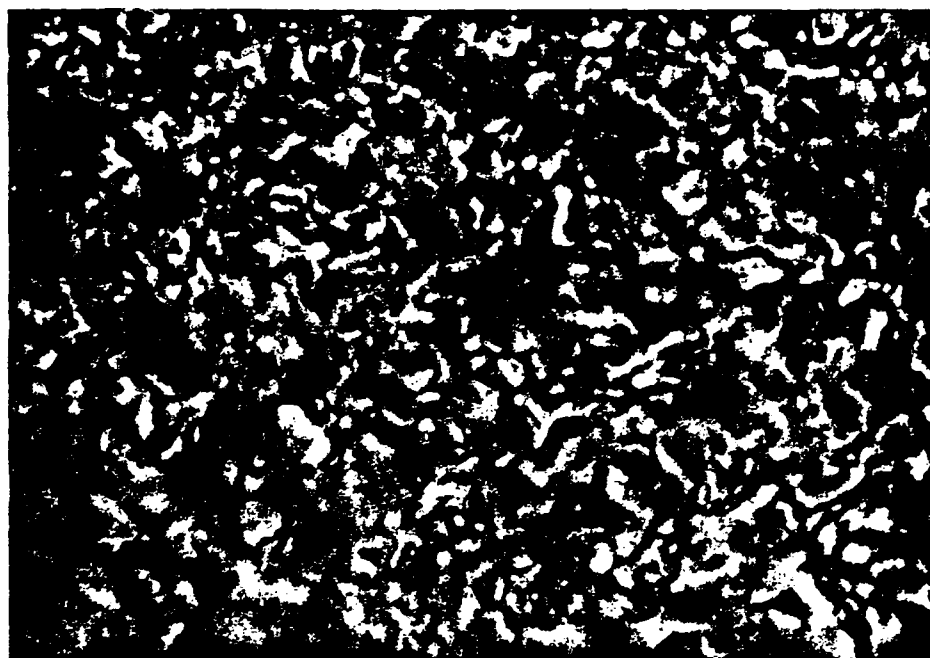
Table 1.1: Orientation times of LCP-carbon fiber composites obtained from ^1H -NMR studies

The enhanced orientation rates of matrix molecules in composite systems clearly indicate that the presence of fibers facilitates macroscopic orientation of polymer chains. As mentioned previously, surfaces may guide the orientation of liquid crystals. Uniaxial orientation of fibers could therefore facilitate matrix orientation if the surface anchoring direction were to coincide with that of the external field. However, in the present case, fibers were randomly oriented before exposure to magnetic field and their random orientation after the magnetic alignment experiment was confirmed by scanning electron microscopy (SEM) studies. Furthermore, SEM studies on the fibers alone revealed that the

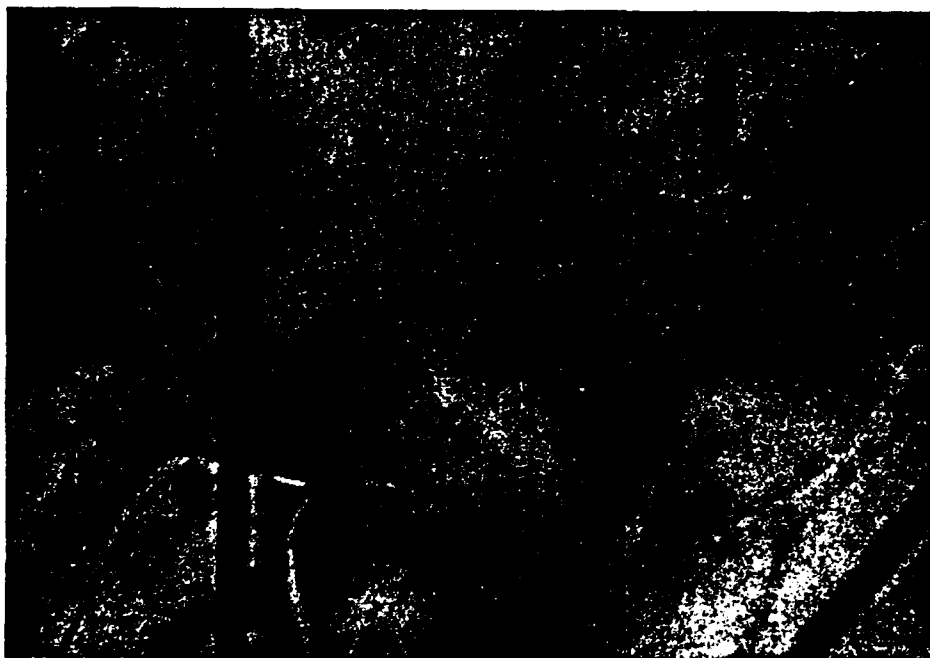
surfaces were devoid of any topological features such as grooves or cavities that could be responsible for their guiding effect on liquid crystals. Therefore, it is not clear what might be the mechanism of their "catalytic effect" on molecular orientation in the matrix. It is possible that the fiber surfaces organize molecules in their immediate surroundings along a common direction. When the spatial range of common orientation increases, in this case as a result of the organizing effect of fibers, macroscopic realignment into the external field may occur more readily. Thus, these alignment experiments suggest that surface forces can very effectively couple with external fields to enhance the alignment of polymeric liquid crystals. This synergistic effect of surface and field on macroscopic alignment of molecules in the composite specimen is in accordance with an earlier finding by Martin, Moore and Stupp (77) in which a grooved-surface tube was found to facilitate orientation in a magnetic field.

1.2.3: Optical Microscopy Studies

Optical microscopy of the composite specimens revealed a number of interesting phenomena in the LCP matrix relative to the polymer melt. For example, the molten birefringent matrix acquires readily a more uniform color over considerable distances when in contact with fibers. The presence of carbon fibers also seems to facilitate the elimination of defects in the liquid crystalline medium. Both observations are illustrated by optical micrographs shown in figure 1.7. Examination of the micrographs reveals that disclination lines and a polychromatic field of view is more prevalent in the pure LCP fluid. These experiments also reveal that the course of phase separation into liquid crystalline and isotropic zones is affected by the presence of carbon fibers. Upon heating, it is observed that the matrix zones in contact with carbon fibers are the last to undergo the nematic to isotropic transition. That is, contact with the carbon



(a)

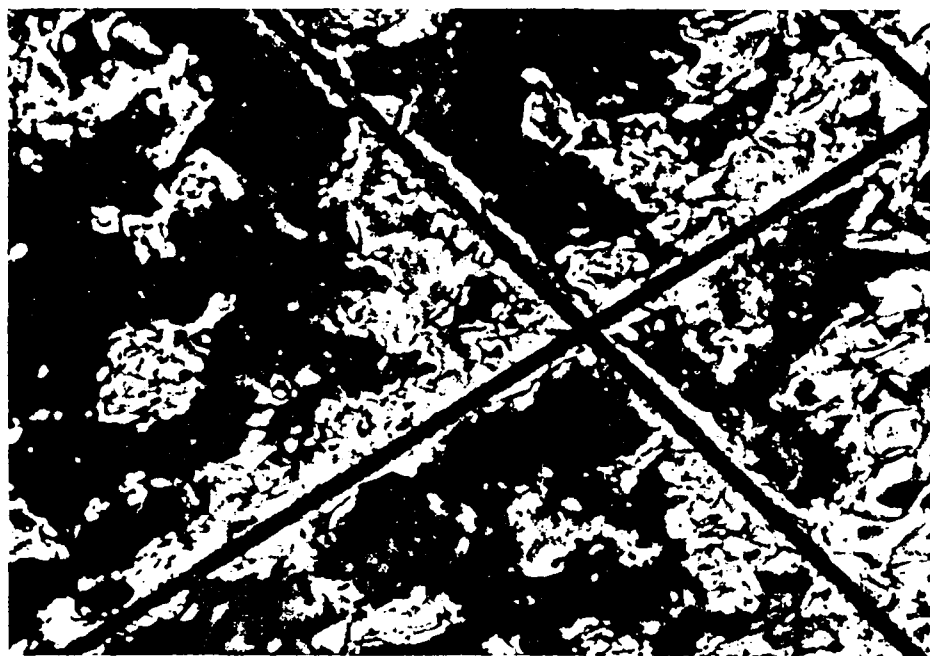


(b)

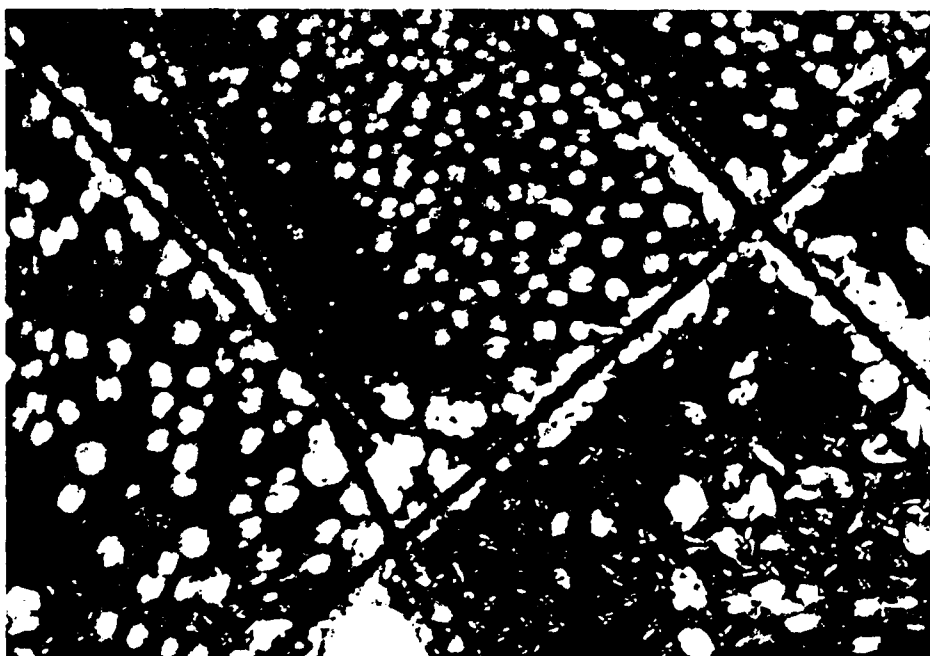
Figure 1.7 : Optical micrographs between cross polars of the liquid crystalline polymer melt (a) and matrix polymer in contact with carbon fibers (b) at 170°C (415x)

surfaces appears to stabilize orientational ordering of polymer molecules in the fluid matrix. This observation is illustrated by the micrograph in figure 1.8(a), showing birefringent zones surrounding carbon fibers and isotropization of the melt in more remote regions. Upon cooling, as revealed by micrograph in figure 1.8(b), nucleation of liquid crystallinity appears to occur preferentially at fiber-matrix interfaces. Even though this phenomenon may be related to surface nucleation of liquid crystallinity upon cooling, it is also possible that it is caused by lower temperature on carbon fiber surfaces relative to the bulk matrix. If the latter case were true based on the fact that carbon fibers have higher thermal conductivity than the polymeric melt, then the heating cycle should reveal an early isotropization of the polymeric melt in contact with fibers, contrary to that seen in figure 1.8(a).

These microscopic observations support the idea that fibers organize the orientation of molecules in the LCP melt. For example, the homogeneous color and the defect-free texture of the matrix material suggest the formation of large orientational domains near fibers. The uniform color of the molten matrix over large distances also suggests that the fibers exert their aligning influence over considerable distances. However, it is unclear why the orienting influence of fibers spans over such macroscopic distances from the fiber surface. While this may be related to the synergistic influence of several fibers dispersed in the medium, it is also important to consider the thermal effects of the fibers in the LCP fluid. The long range nature of this effect may in fact be limited to the early saturation of enhanced alignment rate at low fiber content. The slight increase in orientation time observed with composite containing 40% by weight carbon fibers could be related to increased viscosity in the medium as a result of a multiplicity of anchoring orientations induced by the zone of influence of many fibers. Finally, shown in figure 1.9 is a micrograph of the solidified composite



(a)



(b)

Figure 1.8 : Optical micrographs between cross polars of the LCP-carbon fiber composite obtained during heating at 265°C (a) and cooling at 290°C (b) (415x)

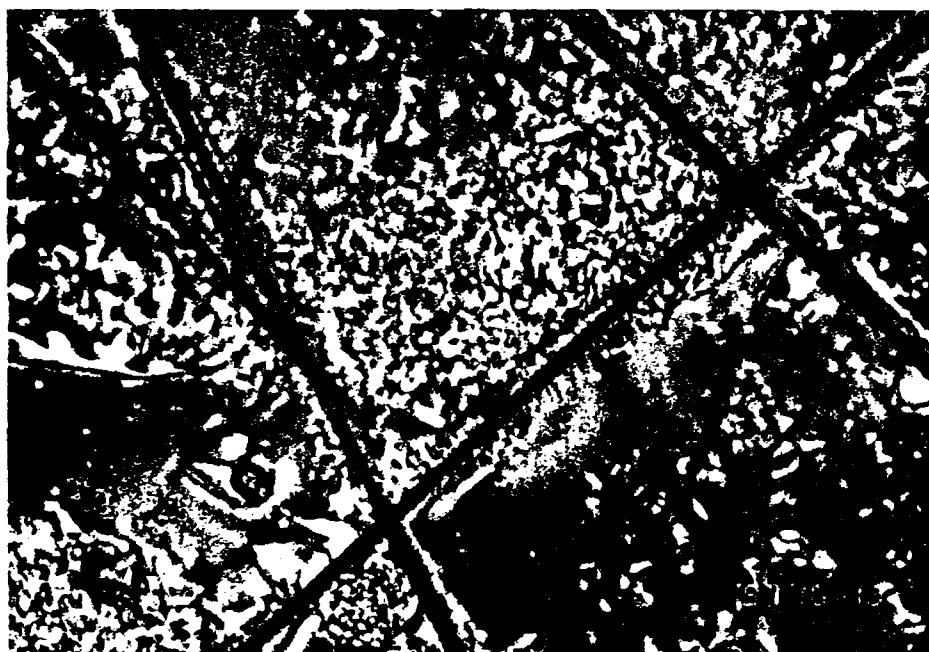


Figure 1.9 : Optical micrograph between cross polars of the solidified composite specimen showing trans-crystalline zones around fibers

which clearly reveals the influence of the fiber on the matrix structure. A well defined zone analogous to the so called trans-crystalline layer in other thermoplastic/carbon fiber composites (78-80) is observed in the composite microstructure.

When these composite specimens are examined under a scanning electron microscope, in spite of the strong orientational guiding influence that fiber surfaces have on polymeric melt, it is surprising to see that this melt does not wet the fibers. De-wetting of these fiber surfaces from the polymer occurs easily upon solidification as seen in the scanning electron micrograph in figure 1.10. So, the very concept of liquid crystallinity and ordered interphases cannot be fully exploited in these systems with poor interfacial adhesion. The next phase of this study was therefore the grafting of matrix chains onto fiber surfaces as a means to improve adhesion.

1.2.4: Grafting and Interfacial Adhesion

1.2.4.1: Grafting via Melt-phase Transesterification

Grafting of polymeric chains onto fiber surfaces was attempted by in-situ polymerization of monomers in the presence of carboxy-functionalized carbon fibers. This grafting of nematogenic chains by in-situ polymerization was designed to utilize the functional groups on the fiber surface. Therefore, in order to insure good exposure of fiber surfaces to the monomeric melt the grafting preparation used only a small fraction of fibers, 2% by weight of the total reaction mixture. As far as the chemical mechanism is concerned, the acetylation of the phenolic groups in the monomers should activate multiple transesterification events involving the polyfunctional fibers and monomers. This is inferred on the basis of other work in our laboratory (67, 81) in which it was established that carboxyl groups are the most active functions in the transesterification reactions



Figure 1.10 : Scanning electron micrograph of the fracture surface of a composite specimen revealing the poor wetting of the fiber by the matrix polymer (scale bar 10 μ)

involved in this grafting preparation. In principle, the polycondensation reactions should append chains to the surface in a variety of conformations and topologies and some of these have been illustrated in figure 1.11.

Analysis of the fibers by the XPS technique provides quantitative data on the elements present on the surface and to a limited extent on the nature of functional groups (82, 83). Typical XPS spectra of the fibers before and after the grafting reaction are shown in figure 1.12. The areas under peaks indicate the relative abundance of the elements on the fiber surface. Relative concentrations of carbon and oxygen as derived by XPS analysis are summarized in table 1.2.

Fiber Type	O/C Ratio (± 0.01)
Untreated fibers	0.27
Untreated fibers blended with LCP	0.27
Untreated fibers grafted with LCP	0.34
Functionalized fibers	0.25
Functionalized fibers blended with LCP	0.42
Functionalized fibers grafted with LCP	0.61

Table 1.2: X-ray photoelectron spectroscopy data (after Soxhlet extraction)

It is observed that following the grafting preparation the oxygen to carbon ratio (O/C ratio) on functionalized fibers increases from 0.25 to 0.61. A smaller increase, from 0.25 to 0.42 is observed when functionalized fibers were simply blended with the same liquid crystalline polymer which forms during grafting

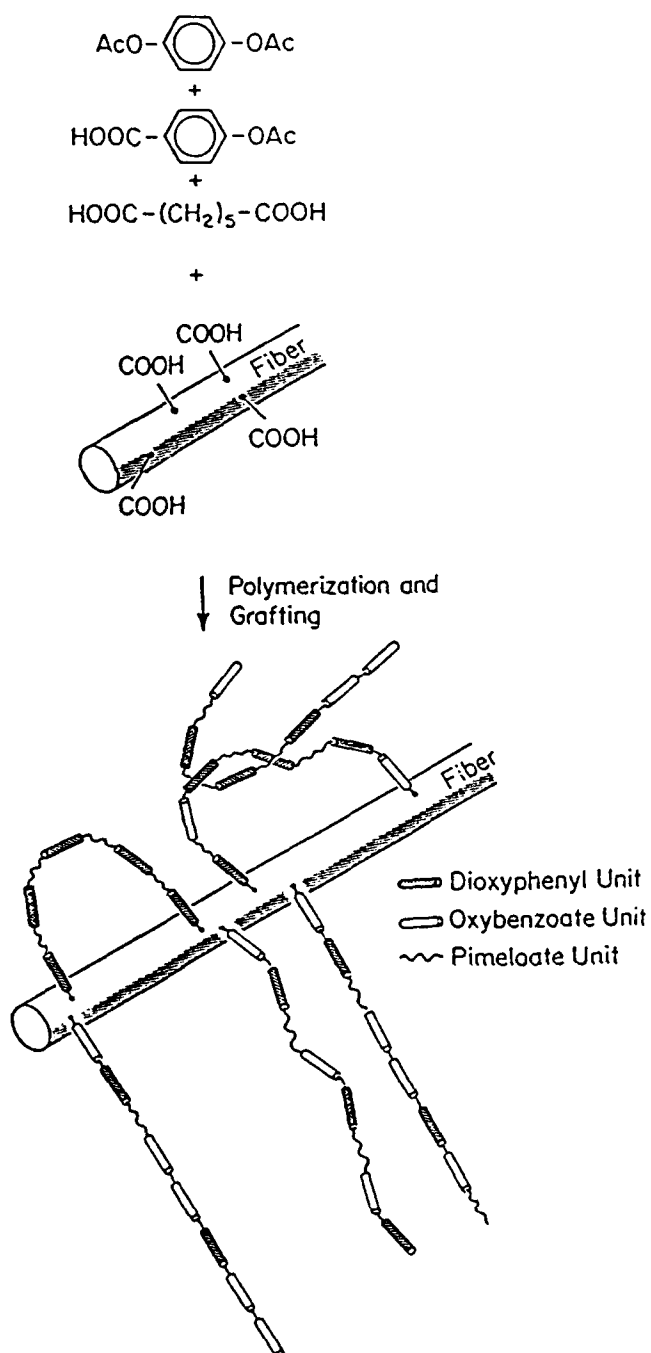


Figure 1.11 : Schematic diagram for the grafting of nematogens and molecular loops on functionalized carbon fibers

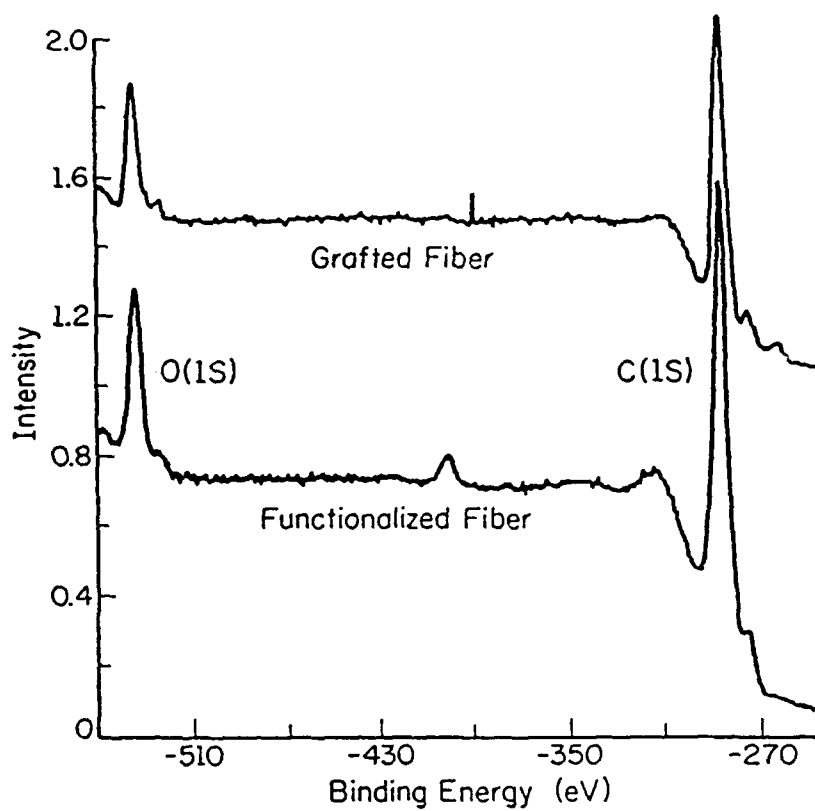


Figure 1.12 : Typical X-ray photoelectron spectroscopy (XPS) scans of the functionalized and polymer-grafted carbon fibers

but prepared in the absence of fibers. When untreated fibers are used, the O/C ratio is not even altered after blending and following the grafting procedure, it increases only by a small amount, from 0.27 to 0.34. The implication of XPS data is that a significant amount of polyester remains on polymer-grafted functionalized fibers even after the rigorous Soxhlet extraction with polymer solvent.

Figures 1.13 and 1.14 show scanning electron micrographs of the functionalized and untreated fibers exposed to Soxhlet extraction after in-situ polymerization. The micrographs in figure 1.15 and 1.16 correspond to functionalized and untreated fibers subjected to Soxhlet extraction after they were physically blended with molten liquid crystal polymer. Surfaces of grafted functionalized fibers reveal a rougher texture relative to all other fibers and thus seem to be covered with organic material. Figure 1.17 shows a close up view on a single functionalized fiber exposed to extraction after the grafting reaction.

It is interesting to consider what might be the molecular nature of the material detected by SEM on grafted functionalized fibers. If polymer chains are indeed transesterified to the fiber surface at one or both termini, the subsequent process of Soxhlet extraction to which fibers were exposed after the reaction would only dissolve weakly physisorbed polymer. The material left on fiber surfaces after rigorous extraction would include not only covalently grafted chains but also polymer which is strongly associated with the grafted molecules. An example would be chains physically "entangled" with grafted loops (as shown in figure 1.11). Another important consideration in the system is that end grafted nematogens on surfaces could produce interfacial zones of high density. For the general case of polymers at an interface, Alexander considered theoretically the problem of adsorption of chains with a polar head (84), predicting under certain conditions a transition from a low to a high density

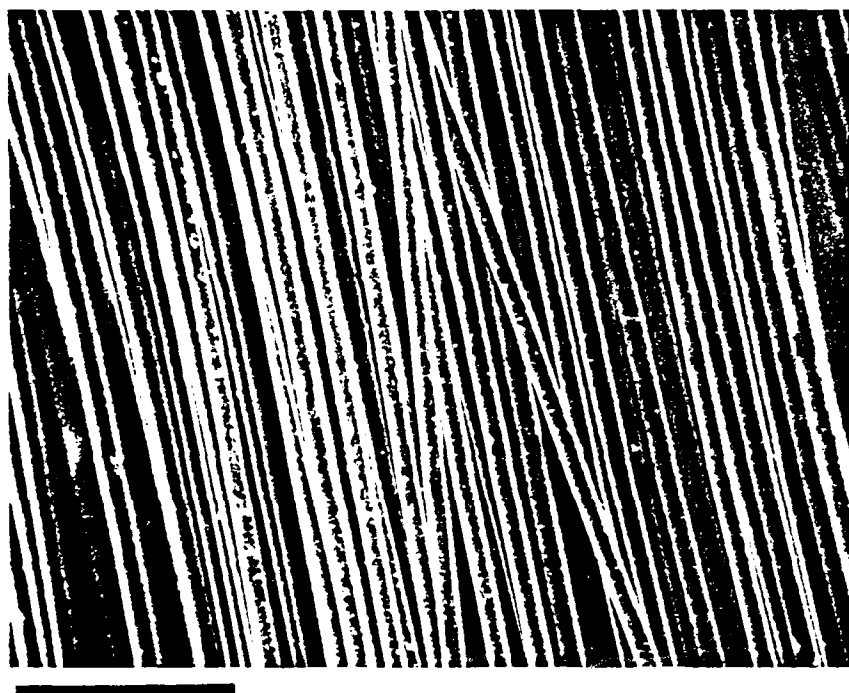


Figure 1.13 : Scanning electron micrograph of functionalized carbon fibers subjected to in-situ polymerization followed by Soxhlet extraction with polymer solvent (scale bar 100 μ)



Figure 1.14 : Scanning electron micrograph of untreated carbon fibers after in-situ polymerization and Soxhlet extraction with polymer solvent (scale bar 100 μ)



Figure 1.15 : Scanning electron micrograph of untreated carbon fibers exposed to polymer solvent after being physically blended with liquid crystal polymer (scale bar 100 μ)



Figure 1.16 : Scanning electron micrograph of functionalized carbon fibers subjected to Soxhlet extraction with polymer solvent after being physically blended with liquid crystal polymer (scale bar 100 μ)



Figure 1.17 : Scanning electron micrograph of a polymer-grafted functionalized fiber after rigorous extraction with polymer solvent (scale bar 10 μ)

adsorbed layer. In our present problem, the grafted ends can be considered physically analogous to the strong specific interaction between a polar head and a surface site. This is in contrast to the more uniform adsorption of chains where a weak to moderate attractive force prevails between structural units and the surface. In this case, equilibrium surface states have a relatively low density (84). When a specific and strong interaction is involved the surface density can become quite large and the chain dimensions are smaller than the adsorbed layer thickness. Interestingly in his paper Alexander found that when the chain interaction dominates but a significant uniform attraction still exists one may observe changes in adsorbed layer structure by a first order transition. For example, as the parameters of the system are changed one may observe a transition from a high density adsorbed-layer where chain ends interact with the surface to a dilute adsorbed layer characteristic of uniform attraction. In the high density regime,

$$\gamma \sim N^{-1/5} C^{6/5} \quad \text{..... (1. 4)}$$

where γ is the surface density of monomers, N is the chain length and C is the surface interaction of the chain end. In the low density regime,

$$\gamma \sim \delta^{1/2} \quad \text{..... (1. 5)}$$

$$D \sim \delta^{-3/2} \quad \text{..... (1. 6)}$$

where δ is the uniform surface interaction of chain structural units and D is the adsorbed layer thickness. It is very interesting to consider in our system the probability of high density surface states not only because of grafting but also since the surface concentration of chains increases continuously as the reaction

proceeds. This is because the solvents of adsorbing chains are the monomers and oligomers participating in condensation reactions. Furthermore, in this specific system the growing chains become nematogens and with rising concentration will eventually undergo an Onsager orientational transition. From a properties point of view the occurrence of a high density surface layer with significant orientation of the molecular backbone normal to the fibers could offer advantages in thermal expansion, interfacial hydrolytic stability and isotropic strength in processed composites.

Preliminary investigations of the fractured surfaces of composites prepared during grafting of functionalized fibers or prepared using untreated fibers blended with liquid crystalline polymers were conducted by scanning electron microscopy. The objective was to explore the impact of grafting on adhesion of fibers to the matrix polymer. Micrographs shown in figures 1.18 and 1.19 correspond to the fracture surface of composite specimens prepared during grafting and after blending, respectively. Fracture surface analysis by SEM definitely reveals better adhesion between grafted fibers and the matrix. But it remains to be seen at this stage if the improved adhesion between the fiber and the matrix translates to improved mechanical properties of the composite specimen.

Elemental analyses results of the functionalized fibers exposed to extraction after the grafting reaction are presented in table 1.3. The oxygen content derived by this method should correspond to the concentration of oxygen which is present only on the fiber surface. It is interesting to see that the fibers exposed to the same grafting reaction conditions show very different surface oxygen content, clearly suggesting a nonuniform distribution of surface functionalities. XPS data presented earlier in table 1.2 correspond to the average O/C ratio obtained by analyzing three different regions of the same specimen.



Figure 1.18 : Scanning electron micrograph of the fracture surface of a composite specimen prepared by in-situ polymerization in the presence of functionalized fibers (scale bar 10 μ)



Figure 1.19 : Scanning electron micrograph of the fracture surface of a composite specimen prepared by blending of the matrix polymer with functionalized carbon fibers (scale bar 100 μ)

Trial	% Carbon	%Oxygen
I	88.85	6.22
II	86.72	8.28
III	84.66	10.42
IV	83.59	11.31

Table 1.3: Elemental analysis data of the polymer-grafted functionalized fibers

The large scatter in the elemental analysis results also suggests that in general, the surface composition data needs to be handled cautiously.

1.2.4.2: Grafting *via* Esterification in Solution

Given the promising SEM results involving polymer-grafted fibers, alternative efforts to graft suitable functionalized-polymer chains onto fiber surfaces were initiated using solution-based carbodiimide chemistry. A model esterification reaction employing a fluorinated alcohol (2,2,2, trifluoroethanol) and carboxy-functionalized fibers was attempted in methylene chloride solvent at room temperature. The choice of the alcohol was based on the fact that fluorine atoms can be easily detected by XPS technique. XPS scan of these grafted fibers after Soxhlet extraction is shown in figure 1.20. The small peak seen around 688.2 eV is a clear indication of grafted molecules on the fiber surface. Thus, it seems possible to employ carbodiimide chemistry to graft functionalized polymeric chains onto fiber surfaces. Preliminary XPS results of carbon fibers that are subjected to an esterification reaction with a phenolic monomer and its corresponding polymer are presented in table 1.4. The synthesis of these

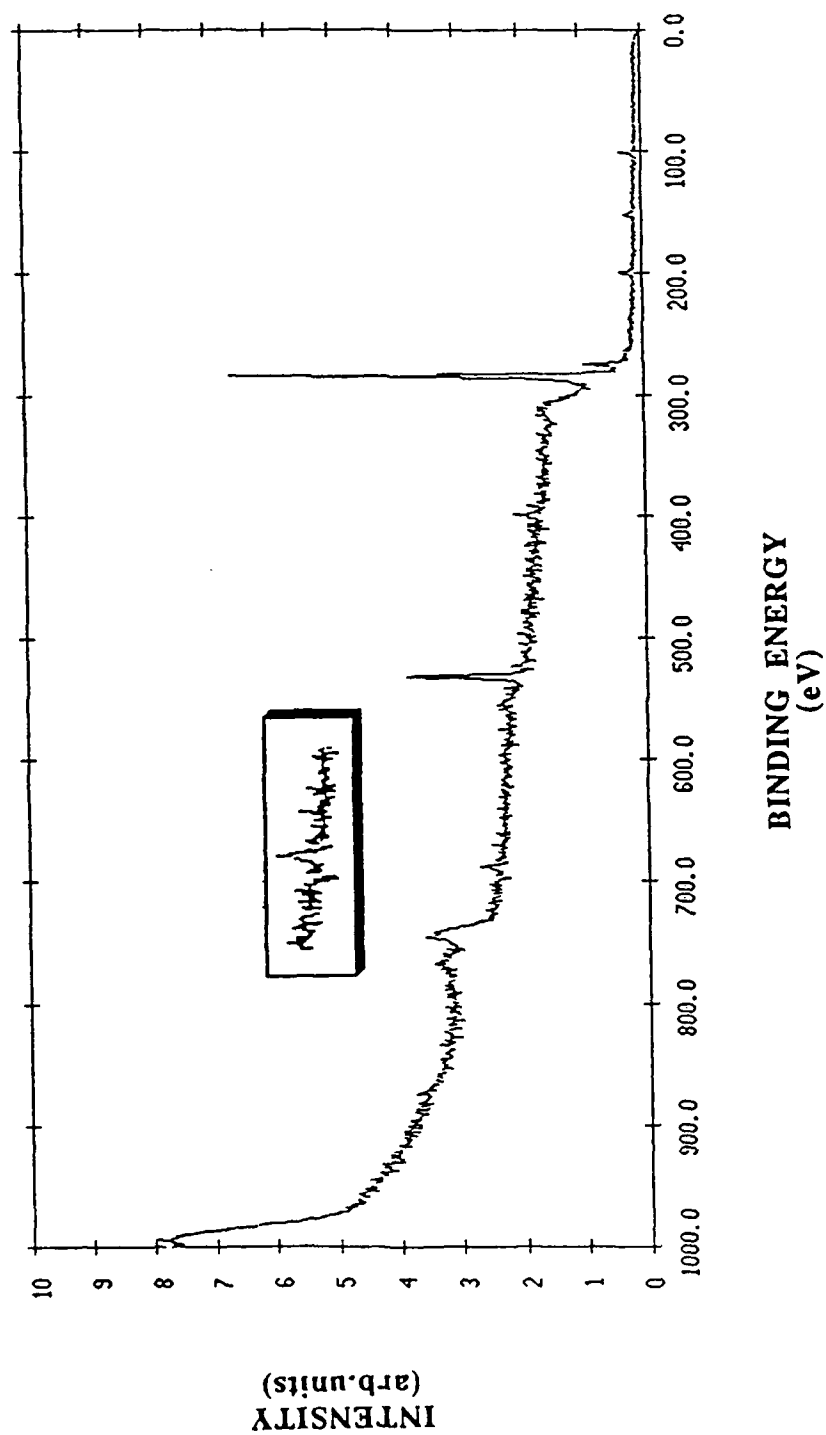


Figure 1.20 : XPS scan of functionalized fibers showing the presence of fluorine on the fiber surface after a grafting reaction

Fiber Type	O/C Ratio (± 0.01)
Functionalized fibers grafted with monomer <u>8a</u>	0.49 (0.27)
Control experiment with monomer <u>8a</u>	0.26
Functionalized fibers grafted with polymer <u>1a</u>	0.46 (0.27)
Control experiment with polymer <u>1a</u>	0.29

Table 1.4: XPS data of the functionalized fibers grafted with a phenolic monomer and a phenolic polymer *via* carbodiimide esterification. Figures in the parenthesis correspond to O/C ratio of the pure monomer and polymer as obtained from elemental analysis

phenolic compounds is discussed in the following chapter. These XPS results suggest the presence of grafted monomeric and polymeric compounds on the fiber surfaces. However, SEM analysis of these fibers do not reveal the presence of such grafted-molecules on fiber surfaces as seen earlier on fibers subjected to the in-situ polymerization procedure.

1.3: Summary

A liquid crystal polymer matrix material has been successfully synthesized from the monomers, p-acetoxybenzoic acid, diacetoxyhydroquinone and pimelic acid. The polymer was characterized by ^{13}C NMR studies to be a random copolyester of the three structural units. The polymer melts into a nematic phase at temperatures above 145°C , as inferred from optical observations. Fiber surfaces of a composite specimen were found to influence the orientation and

orientational dynamics of the liquid crystal polymer matrix. This was revealed by enhanced rates of magnetic orientation in the polymer melt when carbon fibers are dispersed in the medium. Optical microscopy studies with these composite systems revealed that fibers have a tendency to organize molecules in their immediate surroundings. This orienting effect of fibers is presumably the reason why fibers have a "catalyzing effect" on macroscopic orientation. These studies also reveal that fiber surfaces stabilize nematic ordering of the melt when heated towards or cooled from the isotropic phase.

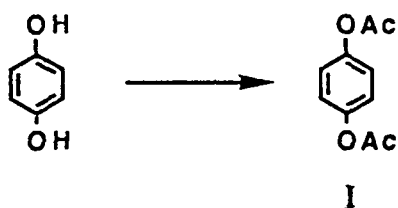
In-situ polymerization of monomers in the presence of functionalized carbon fibers leads to strong attachment of liquid crystal polymer chains on the fiber surface. This strong attachment most likely involves covalent grafting of chain ends on the surface. Evidence for the presence of grafted chains was obtained from XPS and SEM analyses. Fracture surface analysis by SEM reveals an improved adhesion between grafted fibers and the matrix polymer and a rather poor wetting of the same matrix on untreated fiber surfaces. The phenomena discovered here, orientational guiding influence of fibers on self ordering molecules and the possibility of grafting such molecules to surfaces can be of great importance to the control of mechanical properties and environmental stability of composite materials.

1.4: Experimental

1.4.1: Polymer Synthesis and Characterization

Synthesis of Monomers

Diacetoxyhydroquinone (I)



In a reaction blender was placed 55.0 g (0.50 mol) of hydroquinone and 200 ml of 5 N NaOH and 375 g crushed ice. After vigorous stirring for 5 min, 170 ml of acetic anhydride was added and stirred for an additional 10 min. The product was filtered, washed, air dried and recrystallized twice from water and benzene.

I

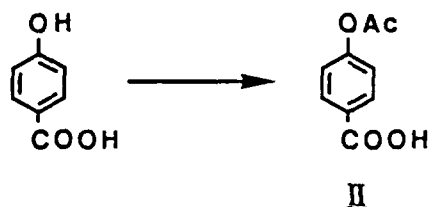
MW: 194

yield: 76% after recrystallizations

$^1\text{H-NMR}$ (300 MHz, CDCl_3): δ 2.15(s, 6H), 7.05 (s, 4H).

$\text{C}_{10}\text{H}_{10}\text{O}_4$	calcd	C 61.85	H 5.19
	found	C 61.86	H 5.18

p-Acetoxybenzoic acid (II)



Interfacial synthesis of p-acetoxybenzoic acid was carried out combining

69.10 g (0.50 mol) p-acetoxybenzoic acid with 200 ml of 6.25 N NaOH and 375 g of crushed ice in a reaction blender. 85 ml (0.90 mol) of acetic anhydride was added in one portion to the rapidly stirred mixture. After 10 min of stirring, 200 ml of 6.25 N HCl was added and the solid product was collected by suction filtration. The precipitate was washed thoroughly with water and dried in *vacuo* at 60°C. The crude product was purified by two successive recrystallizations from benzene.

II

MW: 180.15

yield: 82% after recrystallizations

¹H-NMR (300 MHz, d₆-DMSO): δ 2.31 (s, 3H); 7.26(d, J=8.86 Hz, 2H); 8.03(d, J=8.79 Hz, 2H)

C ₉ H ₈ O ₄	calcd	C 60.00	H 4.47
	found	C 59.96	H 4.47

Polymerization

As received pimelic acid was recrystallized three times, first from benzene, then from water and finally from benzene. All the monomers were dried in *vacuo* at 60°C for 12h before use.

A typical polycondensation reaction employed 3.000g (18.750 mmol) of pimelic acid, 4.001 g (20.600 mmol) of diacetoxyhydroquinone (**I**) and 3.375 g (18.750 mmol) of p-acetoxybenzoic acid (**II**) in the presence of 4.0 mg of antimony oxide and 4.5 mg of lead acetate as catalysts (10% molar excess of diacetoxyhydroquinone was used to compensate for loss by sublimation). Polymerization was carried out in two stages. In the first stage, the contents were placed in a 25 ml pear-shaped flask equipped with a nitrogen bubbler, a condenser and a receiver. The system was then heated in a sand bath from 180°C

to 220°C over a period of 1h. Nitrogen gas was bubbled after 1h to remove acetic acid and the temperature was raised to 260°C over a span of 2h. The second stage involved heating the contents in a sublimation apparatus under vacuum at 270°C for 2h to increase the molecular weight of the product. The product was dissolved in hot tetrachloroethane and precipitated into ether. The precipitate was dried in *vacuo* for 18h at 100°C yielding 4.500 g (64%) of polymer.

Characterization

¹H and ¹³C NMR spectra of the polymer were recorded on a GE-300 NMR spectrometer in deuterated tetrachloroethane. Viscosity of a 1% solution of polymer in tetrachloroethane was measured using a Ubbelohde type viscometer at 30°C. Differential scanning calorimetry was carried out in a Perkin Elmer DSC-4, using 5-10 mg samples at heating or cooling rates of 10°C/min. A constant flow of helium was maintained during DSC experiments.

NMR experiments utilized a Varian XL-200 instrument and the samples were placed in standard 5mm diameter tubes. Each tube contained 0.400 g of polymer, blended with varying fractions of carbon fiber (AS4, Hercules Inc.). The polymer was first melted on a hot plate at 180°C in a small vial and mixed with the fibers using a thin glass rod (fibers ranged from 1-2mm in length). The composite sample was divided into 4 portions and packed into the NMR tube, each portion was heated to 180°C for 1/2 a min and compacted lightly with a glass rod after addition of each portion. Once in place within the NMR instrument, all samples were first heated to 140°C to melt the polymer and maintained for 5 min before starting to collect data at 170°C. A spectral width of 80 KHz, a pulse width of 1.0 μs (90° pulse width = 13 μs) and an acquisition time of 100 ms were used for data collection. The Fourier transformation utilized 256 data points and the magnetic field and radiation frequency were 4.7 T and 200 MHz respectively.

Optical analysis was carried out in a Leitz Laborlux 12 pol polarizing microscope equipped with a Leitz hot stage and a micristar thermocontroller. The glass slides utilized to prepare samples for optical microscopy were carefully cleaned, exposed sequentially for 30 min to reagent grade 2-propanol, acetone and methyl ethyl ketone. The slides were then immersed in concentrated chromic acid solution for 24h, and finally fire polished at 600°C for 1h. The composite samples analyzed by optical microscopy were approximately 10 μ thick and were placed between two cleaned glass slides.

1.4.2: Grafting by In-situ Polymerization

Procedure for In-situ Polymerization

The in-situ synthesis of chain-grafted fibers involved polycondensation of p-acetoxybenzoic acid, diacetoxyhydroquinone and pimelic acid in the presence of carboxy-functionalized carbon fibers. A typical polymerization employed 2.700 g (16.850 mmol) of pimelic acid, 3.600 g (18.500 mmol) of diacetoxyhydroquinone, 3.039 g (16.850 mmol) of p-acetoxybenzoic acid, 4.0 mg of lead acetate and 3.6 mg of antimony oxide as catalysts and 0.186 g of carbon fibers. The reaction was performed in a 25 ml pear-shaped flask fitted with a nitrogen inlet, a condenser and a receiver. The experimental protocol involved carrying out simultaneously three polymerization reactions in an oil bath, two of which had either functionalized or untreated fibers (AS4 and AU4 from Hercules Inc.) and the third contained no fibers at all. The reaction mixtures were placed in an oil bath maintained at 180°C and the temperature was slowly increased to 240°C over a period of 1h. After 1h, nitrogen was bubbled through the mixture and the temperature raised to 265°C for an additional 1h in order to increase the molecular weight of the product.

Analysis of Fibers and Composite Samples

The pure polymer was divided into two portions, one half mixed with 0.093 g of functionalized fiber and the other half with the same amount of untreated fibers. Both mixtures were heated to 200°C and homogeneously blended with a glass rod for 5 min. These samples are referred to as the blended samples. Approximately 2 g of each of the composite samples were stirred for 1h in 50 ml of boiling tetrachloroethane to dissolve the polymer matrix. Subsequently, the fibers were subjected to Soxhlet extraction for 24h using tetrachloroethane as the solvent. The fibers were then dried in vacuo at 100°C for 24h before analysis by x-ray photoelectron spectroscopy (XPS) and scanning electron microscopy (SEM). XPS spectra were recorded on a PHI 5400 photoelectron spectrometer with a magnesium K- α x-ray source operated at 400 Watts. The base pressure in the sample chamber was in the range 10^{-9} - 10^{-10} torr and the data were analyzed using ESCA 5000 series system software in an Apollo host computer. SEM micrographs were obtained using a JSM-25 S JEOL scanning electron microscope. Composite samples for fracture surface analysis were notched with a blade and fractured after exposure to liquid nitrogen. The fracture surfaces were sputtered with gold prior to microscopic analysis.

1.4.3: Grafting *via* Carbodiimide-based Esterification

A 50 ml round bottom flask equipped with a Claisen adapter and a nitrogen inlet was charged with phenolic monomer, **8a** (0.250 g, 0.520 mmol). The same quantity of phenolic polymer **1a** was placed in a similar reaction assembly. Into each of these flasks were added, 0.200 g of carboxy-functionalized fibers (AS4, Hercules Inc.), DPTS (0.030 g), DIPC (0.12 ml) and dry DMF (20 ml). The reaction flasks were purged thoroughly with nitrogen and the contents were stirred under nitrogen atmosphere overnight at room temperature. The next

morning, fibers were transferred to a Soxhlet extractor and subjected to extraction by DMF for 24h. Following the extraction, the fibers were dried in *vacuo* at 100°C for 24h and their surface analyzed as described before by electron microscopy. Control experiments were carried out under similar conditions in the absence of the esterification agent, 1,3-diisopropylcarbodiimide (DIPC).

References

- (1) Reinitzer, F., *Monatsch. Chem.*, **1888**, *9*, 421.
- (2) Chandrasekar, S., "*Liquid Crystals*", (Cambridge University Press, Cambridge), **1977**.
- (3) Gray, G. W. and Goodby, J. W. G., "*Smectic Liquid Crystals*", (Leonard Hill, Philadelphia), **1984**.
- (4) Priestly, E. B., Wojtowicz, P. J. and Sheng, P., (eds) "*Introduction to Liquid Crystals*", (Plenum, NY), **1974**.
- (5) Vertogen, G. and de Jeu, W. H., "*Thermotropic Liquid Crystals, Fundamentals*", (Springer-Verlag), **1987**, 45.
- (6) Gray, G. W. and Winsor, P. A., "*Liquid Crystals and Plastic Crystals*", (Halstead Press), **1974**, 1.
- (7) Gray, G. W., "*Molecular Structure and the Properties of Liquid Crystals*", (Academic Press, London), **1962**.
- (8) Ciferri, A., Krigbaum, W.R and Meyer, R. B., (eds), "*Polymer Liquid Crystals*", (Academic Press, NY), **1982**.
- (9) Blumstein, A., (ed), "*Liquid Crystalline Order in Polymers*", (Academic Press), **1978**.
- (10) Finkleman, H. and Rehage, G., *Adv. in Polym. Sci.*, **1984**, *60/61*, 99.

- (11) Shibaev, V. P. and Plate', N. A., *Adv. in Polym. Sci.*, 1984, 173.
- (12) Flory, P. J., *Proc. Royal Soc. London*, 1956, A234, 73.
- (13) Onsager, L., *Ann. N. Y. Acad. Sci.*, 1949, 51, 627.
- (14) Maier, W. and Saupe, A., *Z. Naturforsch*, 1958, 13A, 564.
- (15) *ibid*, 1959, 14A, 882.
- (16) *ibid*, 1960, 15A, 287.
- (17) Flory, P. J. and Ronca, G., *Mol. Cryst. Liq. Cryst.*, 1979, 54, 289.
- (18) Ronca, G. and Yoon, D. Y., *J. Chem. Phys.*, 1982, 76, 3295.
- (19) ten Bosch, A., Maissa, P. and Sixou, P., *J. Physique Lettres*, 1983, 44, 1-105.
- (20) Khokhlov, A. R. and Semenov, A. N., *Macromol.*, 1986, 19, 373.
- (21) Castellano, J. A., *Optics and Laser Technology*, 1975, 7, 259.
- (22) Creagh, L. T., *IEEE*, 1973, 61, 814.
- (23) Castellano, J. A. and Brown, G. H., *Chemtech*, 1973, April, 229.
- (24) Wolff, V., Greubel, W. and Kruger, H., *Mol. Cryst, Liq. Cryst.*, 1973, 23, 187.
- (25) Creagh, L. T. and Kmetz, A. R., *Mol. Cryst. Liq. Cryst.*, 1973, 23, 187.
- (26) Kahn, F. J., Taylor, G. N. and Schonhorn, H., *Proc. IEEE*, 1973, 61, 823.
- (27) Kutty, T. R. N. and Fisher, A. G., *Mol. Cryst. Liq. Cryst.*, 1983, 89, 301.
- (28) Goodman, L. A., McGinn, J. T., Anderson, C. H. and Digeronimo, F., *IEEE Trans. on Electron Devices*, 1977, 24, 795.
- (29) Kahn, F. J., *Appl. Phys. Lett.*, 1973, 22, 386.
- (30) Chabicosky, R. and Kocmann, G., *IEEE Trans. on Electron Devices*, 1977, 24, 807.
- (31) Van Sprang, H. A., *Mol. Cryst. Liq. Cryst.*, 1983, 97, 255.
- (32) Uchida, T., Oghawara, M. and Shibata, Y., *Mol. Cryst. Liq. Cryst.*, 1983, 98, 149.

- (33) Oghawara, M., Uchida, T. and Wada, M., *Mol. Cryst. Liq. Cryst.*, 1981, 74, 227.
- (34) Castellano, J. A., *Liq. Cryst. Ordered Fluids*, 1984, 4, 763.
- (35) Urbach, W., Boix, M. and Guyon, E., *Appl. phys. Lett.*, 1974, 25, 479.
- (36) Cognard, J., *Mol. Cryst. Liq. Cryst. Supp. Ser.*, 1982, 1.
- (37) Janning, J. L., *Appl. Phys. Lett.*, 1972, 21, 173.
- (38) Schadt, M. and Helfrich, W., *Appl. Phys. Lett.*, 1971, 18.
- (39) Carr, E. F., *Mol. Cryst. Liq. Cryst.*, 1969, 7, 253.
- (40) Carrol, T. O., *J. Appl. Phys.*, 1972, 43, 1342.
- (41) Penz, P. A. and Ford, G. W., *Phys. Rev. A*, 1972, 6, 414.
- (42) Penz, P. A., *Phys. Rev. Lett.*, 1970, 24, 1405.
- (43) Williams, R. J., *Chem. Phys.*, 1963, 39, 384.
- (44) Greubel, W. and Wolff, U., *Appl. Phys. Lett.*, 1971, 19, 213.
- (45) Helfrich, W., *J. Chem. Phys.*, 1970, 52, 4318.
- (46) Nehring, J. and Petty, M. S., *Phys. Lett.*, 1972, 40A, 307.
- (47) Mclemore, D. P. and Carr, E. F., *Mol. Cryst. Liq. Cryst.*, 1972, 57, 3245.
- (48) Flink, W. F. and Carr, E. F., *Mol. Cryst. Liq. Cryst.*, 1973, 22, 1.
- (49) Helfrich, W., *Mol. Cryst. Liq. Cryst.*, 1973, 21, 187.
- (50) Gerritsma, C. J., de Jeu, W. H. and Van Zanten, P., *Phys. Lett.*, 1971, 36a, 389.
- (51) Fujiwara, F. Y., Reeves, L. W., Vist, M. R., Rodger, C. and Marcondes Helene, M. E., *J Amer. Chem. Soc.*, 1981, 103, 690.
- (52) Berreman, D. W., *Mol. Cryst. Liq. Cryst.*, 1973, 23, 215.
- (53) Stamatoff, J. B., Chung, T. S. and Gurion, Z. I., *Polym. Compos.*, 1986, 6, 181.
- (54) Krigbaum, W. R. in "Polymer Liquid Crystals", eds: Ciferri, A., Krigbaum, W. R. and Meyer, R. B., 1982, 297.

- (55) Volino, F., Alloneau, J. M., Giroud-Grodguin, A. M., Blumstein, R. B., Stickles, E. M. and Blumstein, A., *Mol. Cryst. Liq. Cryst. Lett.*, 1984, 21, 102.
- (56) Samulski, E. J., *Polymer*, 1985, 26, 177.
- (57) Moore, J. S. and Stupp, S. I., *Macromol.*, 1987, 20, 282.
- (58) Ishida, H., *Polym. Compos.*, 1984, 5, 101.
- (59) Ericson, P. W. and Plueddemann, E. P., in "*Composite Materials, 6: Interfaces in Polymer Matrix Composites*", ed: Plueddemann, E. P., (Academic Press, NY), 1974, 1.
- (60) Hoh, K., Ishida, H. and Koenig, J. L., in "*Composite Interphases*", eds: Ishida, H. and Koenig, J. L., (Elsevier Sci. Publishing Co.), 1986, 251.
- (61) Chiang, H. H. and Koenig, J. L., *J. Coll. Interface Sci.*, 1981, 361, 83.
- (62) Mckee, D. W. and Memeault, V. J., *Chem. Phys. Carbon*, 1973, 9, 151.
- (63) Dauksys, R. J., *J. Adhesion*, 1973, 5, 211.
- (64) Kochinski, I. and Reichert, K. H., *Makroinol. Chem. Rapid Commun.*, 1988, 9, 291.
- (65) Zeng, H. and Bailing, K., in "*Composite Interfaces*", eds: Ishida, H. and Koenig, J. L., (Elsevier Sci. Publishing Co.), 1986, 55.
- (66) Horton, D., *Org. Synth. Collec.*, 1973, 5, 1.
- (67) Moore, J. S. and Stupp, S. I., *Macromol.*, 1987, 20, 273.
- (68) Martins, A. F., Ferreira, J. B., Volino, F., Blumstein, A. and Blumstein, R. B., *Macromol.*, 1983, 16, 279.
- (69) Hardouin, F., Achard, M. F., Gasparoux, H., Liebert, L. and Strzelecki, L., *J. Polym. Sci., Polym. Phys. Ed.*, 1982, 20, 975.
- (70) Maret, G. and Blumstein, A., *Mol. Cryst. Liq. Cryst.*, 1982, 88, 296.
- (71) Noel, C., Monnerie, L., Achard, M. F., Hardouin, F., Sigaud, G. and Gasparoux, H., *Polymer*, 1981, 22, 578.

- (72) Sigaud, G., Yoon, D. Y. and Griffin, A. C., *Macromol.*, **1983**, 16, 875.
- (73) Platanov, V. A., Litichenko, G. D., Belousova, T. A., Milkova, L. P., Shablygin, M. V., Kuhlichikhin, V. G. and Papkov, S. P., *Polym. Sci. USSR, (Engl. Trans.)*, **1976**, 18, 256.
- (74) Panar, M. and Beste, L. F., *Macromol.*, **1977**, 10, 1401.
- (75) Sridhar, C. G., Hines, W. A. and Samulski, E. T., *J. Chem. Phys.*, **1974**, 61, 947.
- (76) Doane, J. W., in "*Magnetic Resonance of Phase Transitions*", eds: Owens, F. J., Poole, C. P. and Farach, H. A. Jr., (Academic Press, NY), **1971**, 171.
- (77) Martin, P. G., Moore, J. S. and Stupp, S. I., *Macromol.*, **1986**, 19, 2459.
- (78) Porter, R. S. and Lee, Y., *Polym. Engg. Sci.*, **1986**, 26, 673.
- (79) Kardos, J. L., *J. Adhesion*, **1973**, 5, 119.
- (80) Kardos, J. L., Cheng, F. S. and Tolbert, T. L., *Polym. Engg. Sci.*, **1973**, 13, 455.
- (81) Wu, J. and Stupp, S. I., Unpublished Results.
- (82) Kozlowski, C. and Sherwood, M. A., *J. Chem. Soc., Faraday Trans.*, **1985**, 1, 2745.
- (83) Hammer, G. E. and Drzal, L. T., *Appl. Surf. Sci.*, **1980**, 4, 340.
- (84) Alexander, S., *Le Journal de Physique*, **1977**, 38, 983.

CHAPTER 2

Synthesis of Functionalized Side Chain Liquid Crystal Polymers

2.1: General Introduction

Side chain liquid crystalline polymers constitute an important class of liquid crystalline polymers (LCPs) in which mesogenic side groups are appended to flexible polymer chains. Although research in this area began in the early 1970's, it gained phenomenal momentum only in the last decade. Prior to this, the conventional synthetic strategy to obtain these side chain LCPs was predominantly to link low molecular weight liquid crystalline compounds directly to polymeric backbones (1-4). Such an approach, however, did not lead to a synthetic method which could systematically produce side chain LCPs (*vide infra*).

Systematic investigations of the synthesis, characterization and applications of side chain LCPs began after 1978 when Ringsdorf and coworkers proposed a new structural criterion to observe liquid crystallinity in these polymers. They introduced a spacer model in which the motions and ordering tendencies of the mesogenic group are decoupled from that of the backbone (5-7). Based on this model, a large number of side chain liquid crystalline polymers and copolymers have been synthesized and details are currently available in the literature (8-14). Different smectic, nematic and cholesteric mesophases may be exhibited by these polymers depending upon the nature of the mesogenic groups and the polymer backbones.

Although side chain LCPs form a relatively new class of polymeric materials, they already command great theoretical and experimental interest, not only because of the deeper insight that their study can lend to understanding of

ordering processes in both polymers and liquid crystals, but also because of their potential applications. A variety of potential applications for side chain LCPs has been considered to date. Broadly speaking, these applications fall into two categories: electro-thermo-optical effects and separation and complexation effects.

The former class of applications are based on, optical data storage capabilities of cholesteric and smectic side chain LCPs (15-18), optically nonlinear effects of side chain LCPs containing appropriate dyes (19-21), photo effects from thermotropic and lyotropic side chain LCPs bearing photoconductive groups (23-26), conductivity of some side chain LCP systems (27, 28), and ferroelectric properties associated with chiral side chain LCPs (29-32). Examples from ongoing research in the latter class of applications include side chain LCPs as stationary phase in gas chromatography systems (33, 34), control of permeation of gases and simple drugs using side chain LCP membranes (35) and use of side chain LCPs with oxyethylene spacers as pseudo-crown ethers (36) and as 'solid' polymer electrolytes (37, 38).

The various synthetic and structural principles which are now accepted by investigators active in this field are discussed briefly in the following sections.

2.1.1: Structural Principles

Mesogenic Groups

The basic structural principles currently used to synthesize side chain LCPs are outlined in figure 2.1. Numerous other variations of these pathways have also been explored and are detailed in the above cited general references. Most of these polymers have rigid mesogenic units which could be *rod-like* or *semiflexible* moieties appended to the polymer backbones. *Rod-like mesogens* are usually selected from the literature on low molecular weight liquid crystals

(39-45). Traditional synthetic pathway to such mesogenic units involves the interconnection of two or more rigid cyclic units, which may be similar or dissimilar. Therefore, aromatic, trans-cyclohexane, bicyclooctane, 1,3-dithiane and 1,3-dioxathiane groups are preferred. Linking units containing multiple bonds such as $-(C\equiv C)_n-$, $-CH=N-$, $-N=N-$, $-(CH=CH)_n$ and $-CH=N-N=CH-$ are

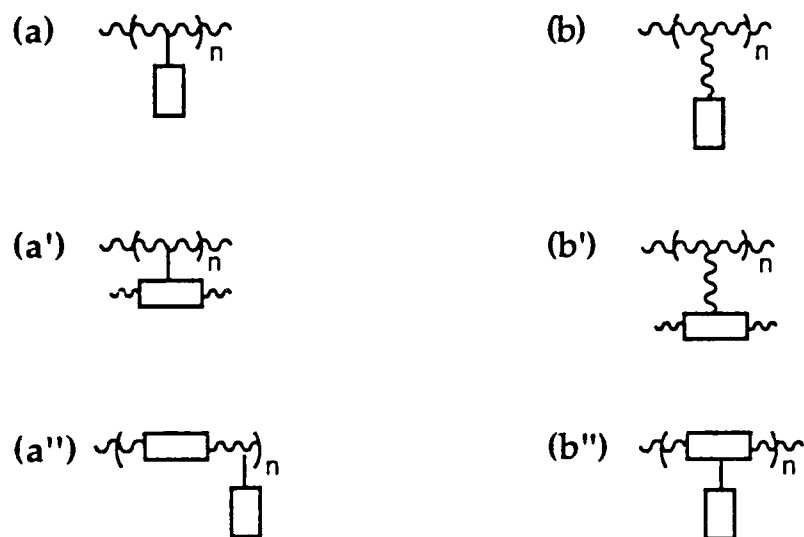


Figure 2.1 : Schematic of side chain LCPs in which mesogens are attached (1) longitudinally to the backbone without a spacer (a) and with a spacer (b); (2) parallel to the backbone without a spacer (a') and via spacer (b'); and (3) to the flexible part (a'') and rigid part (b'') of a main chain polymer (combined LCPs)

frequently employed since they restrict the freedom of rotation. Such groups can conjugate with the aromatic rings, thus enhancing the anisotropic polarizability. This increases the mesogenic length and also maintain the rigidity in these units. The ester group is also effective since resonance interactions confer double bond character to the $-C(O)-O-$ link, thereby restricting the rotation from the trans to cis

conformer. Therefore, the extended conformation of the mesogen is accomplished and maintained through the rigidity of its constituents.

Semiflexible mesogens are obtained when the rigid link is replaced with flexible ethane or methylenoxy units. Although ethane and methylenoxy units can adopt an extended chain conformation which is similar to the trans conformation provided by an ester unit, they are flexible and undergo free rotation, leading to a number of different conformational isomers which are in dynamic equilibrium. In general, an increase in length of either of these types of mesogenic units leads to an enhancement of the thermal stability and a more ordered mesophase as well (46).

Concept of Partial Decoupling by the Spacer

The formation of a thermotropic mesophase from a flexible backbone containing mesogenic side groups requires reconciliation of the main chain's tendency to form a statistical random coil conformation and the side group's tendency to arrange anisotropically. The principle that the motions of both the main chain and the side groups are coupled when the mesogenic groups are directly attached to the flexible backbone is well accepted. In such cases, the conformation of the main chain is disturbed when side groups adopt an anisotropic arrangement. As a consequence, most polymers with the mesogenic groups directly attached to the backbone are amorphous (2, 10). Nonetheless, when side chain ordering is sufficiently strong to overcome the normal barrier associated with the random-coil conformation of the backbone, the polymer does exhibit liquid crystalline behaviour (47-53).

In order to balance the competition between the backbone's random coil conformation and the side group's alignment, Ringsdorf and coworkers predicted that the motion of the polymer main chain must be decoupled from that of the anisotropic side groups in the fluid state (5, 7, 54). The structure of a

side chain LCP with this feature is schematically illustrated in figure 2.2. The spacer concept, therefore, assumes that the main chain should do little to hinder the orientation of the side groups, i. e. for a given mesogen and a spacer, the nature of the polymer backbone should in principle not affect the type of mesophase formed or its thermal stability. However, the polymer backbone does in fact affect both these aspects of mesomorphic behaviour and this has been clearly illustrated in the later work of Ringsdorf (55, 56) and Spiess (57). Their conclusion was that the spacer helps to decouple the mesogenic groups from the main chain and that the decoupling becomes more effective with increasing spacer length, but decoupling is nevertheless, incomplete. Consequently, a more accurate visualization of a side chain LCP is the interaction of two semi-independent subsystems through a flexible spacer, i. e. a section of the spacer plasticizes the main chain while another section of the spacer stabilizes the mesogenic units (57-59).

Additional support for such a partial decoupling by the spacer unit was obtained from neutron scattering experiments performed on deuterated side chain LCP backbones. These experiments demonstrated that the radius of gyration in the nematic phase has an anisotropy of approximately 25% (60). In a similar investigation by Keller et al. (61), the backbone was found to be highly anisotropic in the aligned smectic phase and was confined to a few smectic layers. Further evidence for incomplete decoupling by the spacer is also derived from the investigations of Geib and coworkers (55). In order to relate the properties of these materials to the mobility of different building blocks, they carried out ^2H -NMR studies of partially labelled molecules. Interestingly, they observed that the motions of the mesogen were completely frozen at temperatures below the glass transition temperature, with the exception of 180° rotational jumps of the phenyl ring about the mesogen's molecular axis.

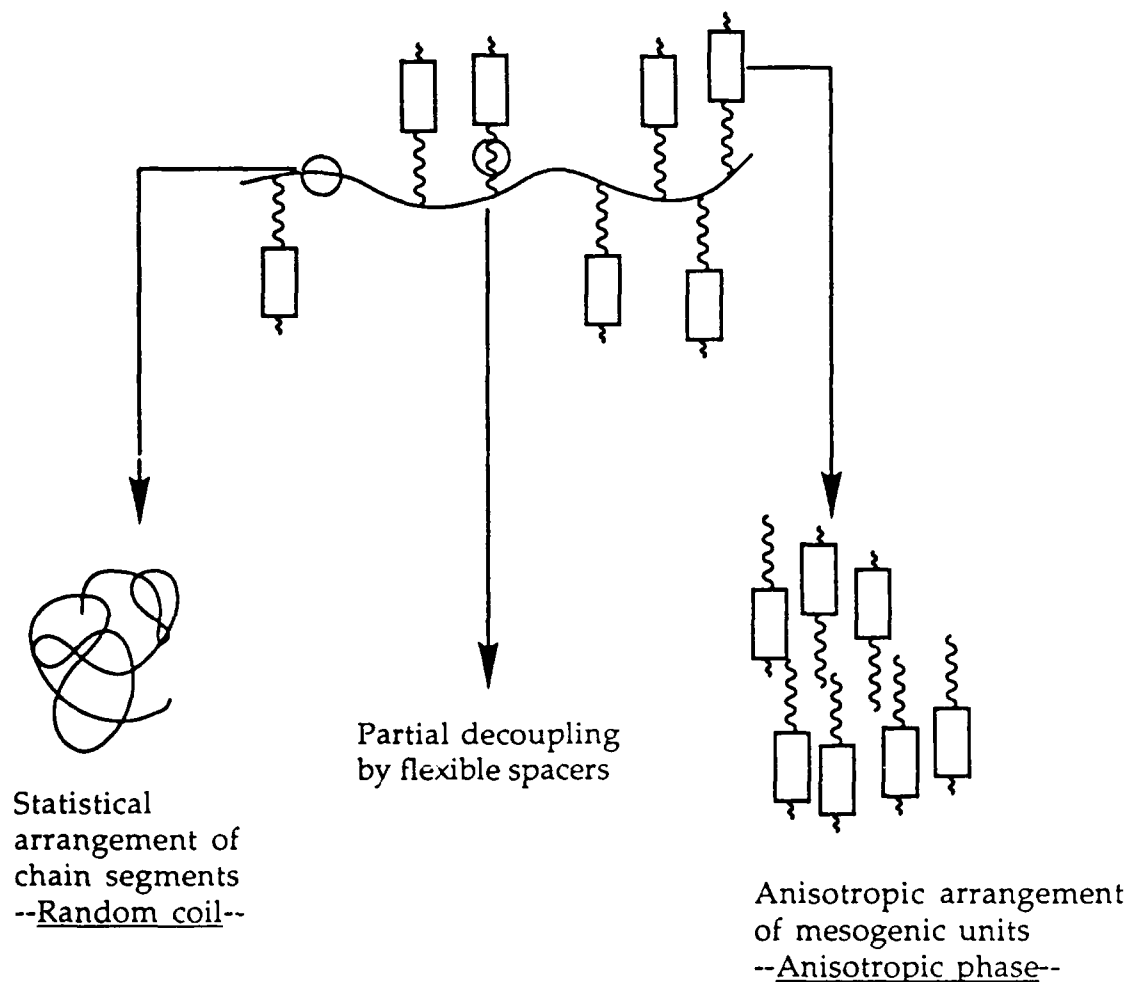


Figure 2.2 : Schematic of a side chain liquid crystalline polymer based on the spacer concept (57)

The spacer concept has also been successfully extended to the preparation of synthetic lipids by some investigators (14, 62, 63). In this context, an interesting series of polymeric lipids synthesized by Laschewsky and coworkers (64) is shown in figure 2.3. The three polymers (A), (B) and (C) shown here may be easily visualized as being very similar to the three corresponding thermotropic analogs, i. e. (A') a thermotropic homopolymer containing flexible spacer; (B') a copolymer of nonmesogenic monomers and monomers containing

mesogens directly attached to the polymerizable group and (C') a copolymer containing nonmesogenic monomers and monomers containing mesogens attached to the polymerizable group through a flexible spacer. However, the mechanistic details of the decoupling process itself in these polymeric lipids await further investigation. Intuitively, at least highly decoupled side chain liquid crystalline polymers if not fully decoupled systems might result by the combination of main chain and side chain spacers as shown in figure 2.3 C and C'.

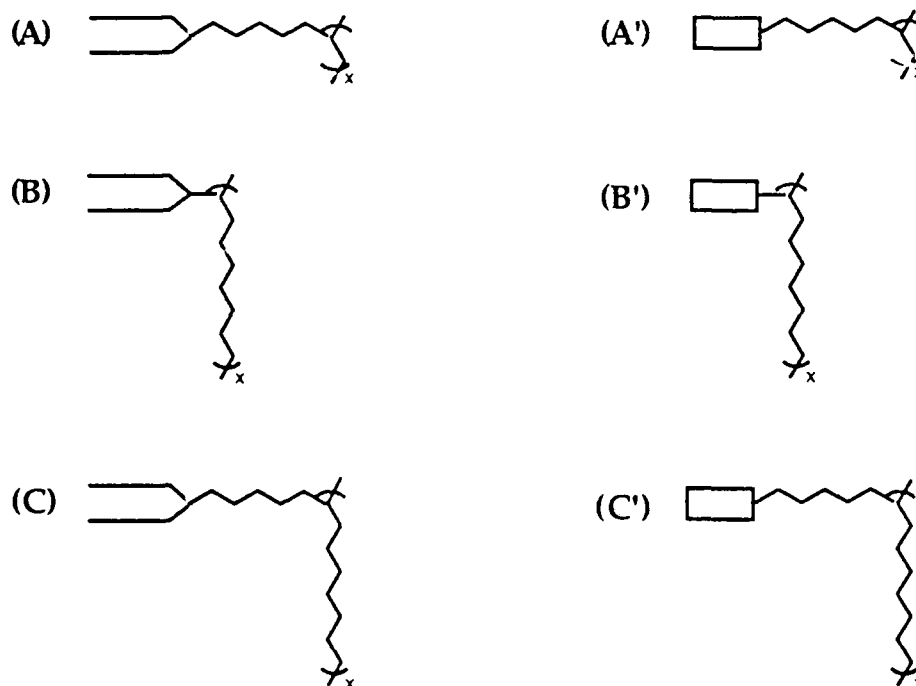
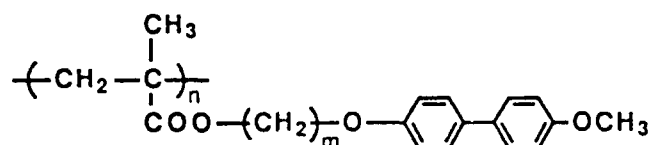


Figure 3 : Schematic representation of polymeric lipids containing hydrophilic spacers and their corresponding thermotropic side chain LCPs: (A, A') side group spacer; (B, B') main chain spacer and (C, C') main chain and side chain spacers (64)

For a given mesogenic unit and a polymer backbone, the length of the flexible spacer has also been shown to influence the extent of decoupling. In

most cases, the nature of the least ordered mesophase exhibited by a polymer with a given mesogen is dictated primarily by the spacer length. For instance, the polymer shown in table 2.1 displays a nematic mesophase with a short spacer ($n=2$) and smectic mesophases with longer spacers, presumably due to more effective decoupling (65, 66).



Spacer Length, m	Phase Transitions, °C
2	g 120 N 152 I
6	K 119 S 136 I
11	g 54 S _c 87 S _A 142 I

Table 2.1 : Influence of spacer length on the phase transition of a side chain LCP (65, 66)

Alternatively, the chemical nature of the spacer group may be altered to enhance the degree of decoupling. In this regard, several research groups have synthesized side chain LCPs containing oligooxyethylene, $-(\text{O}-\text{CH}_2-\text{CH}_2-\text{O})_m-$, and oligosiloxane, $-(\text{O}-\text{Si}(\text{CH}_3)_2)_m-$, spacers (67-73). With the former class of spacers, the mesophase formation strictly depended upon the nature of the substituents on the mesogen. For instance, with nitrile groups as substituents, no mesomorphic behaviour was observed (67, 72). In these systems, presumably, the electron donating character of the spacer enables it to interact with the

electron deficient nitrile substituent. Therefore, lack of mesomorphic ordering may be related to the lack of effective decoupling provided by the spacer unit. Whereas, with an electron donating moiety such as a p-methoxy group on the mesogen, the mesophase formation was not disturbed by the oligoethylenic spacer. However, in these cases, the thermal stability of the mesophase was found to be strongly depressed in comparison to that of a homologous polymer containing a paraffinic spacer (67-71). On the other hand, oligosiloxane spacers required longer mesogenic units in comparison to paraffinic spacers to induce liquid crystallinity, presumably due to the built-in flexibility of the siloxane linkages. Based on this observation, Engel et al. (67) concluded that such a flexible spacer should be divided into at least two units, one which stabilizes the mesophase and the other which provides the real decoupling as outlined in figure 2.4. Lastly, the nature of the group connecting the mesogen to the spacer and the spacer to the backbone has also been found to have subtle implications on the type of the mesophase formed as well as the transition temperatures. Although data available in this regard is scanty, there is some insight derived from Shibaev's work (74).

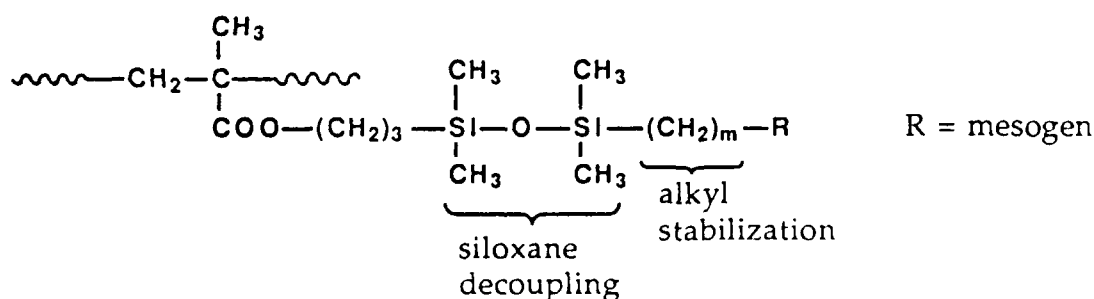


Figure 2.4: Side chain LCP with flexible siloxane unit in the spacer (67)

2.1.2: General Synthetic Routes

The synthetic issue addressed in this work concerns design of a new class of functionalized side chain liquid crystalline polymers, in which hydroxyl groups are present on the mesogenic units. Such a task first involved exploring the various possible polymerization techniques available in the literature. A brief overview of this search is presented in the following section.

Addition Polymerization Reactions

Monomers containing mesogenic groups are frequently synthesized as methacrylates, acrylates, acrylamides, itaconates and styrene derivatives (75, 76). To date, the most convenient method to polymerize such mesogenic monomers is by free radical initiation. However, in order to obtain different tacticities, molecular weights and narrow molecular weight distributions, methacrylates, acrylates and styrene derivatives could be polymerized anionically while methacrylates, acrylates and acrylamides could be polymerized by group transfer polymerization. Although both anionic (77, 78) and group transfer polymerization (79, 80) have already been used to prepare side chain LCPs, living polymers were not obtained experimentally. This was attributed to the *side reactions due to the presence of ester linkages in the mesogen*. Cationic polymerization of nucleophilic olefins and heterocyclic monomers offers additional synthetic avenues to vary the nature of the polymer backbone. Several side chain liquid crystalline polymers have been prepared by cationic polymerization of monomers containing vinyl and propenyl ethers (81, 82), cyclic imino ethers (83) and oxiranes (84) as polymerizable groups.

Step Polymerization Reactions

Step polymerization reactions have been successfully employed to synthesize a large variety of side chain LCPs. However, this method has so far been restricted to synthesis of side chain polyesters (85, 86). The common

synthetic strategy involves appending the mesogen to a monomer such as substituted malonate derivative and then polyesterifying it with a simple diol or with a diol containing a mesogenic unit. Alternatively, the mesogenic side groups can be attached to hydroquinone, and then condensed with either a flexible or a rigid dicarboxylic acid. These two routes allow insertion of the pendant mesogenic groups into either a flexible (a) or a rigid (b) structural unit of the polymer backbone as shown in figure 2.5 (85, 87, 88).

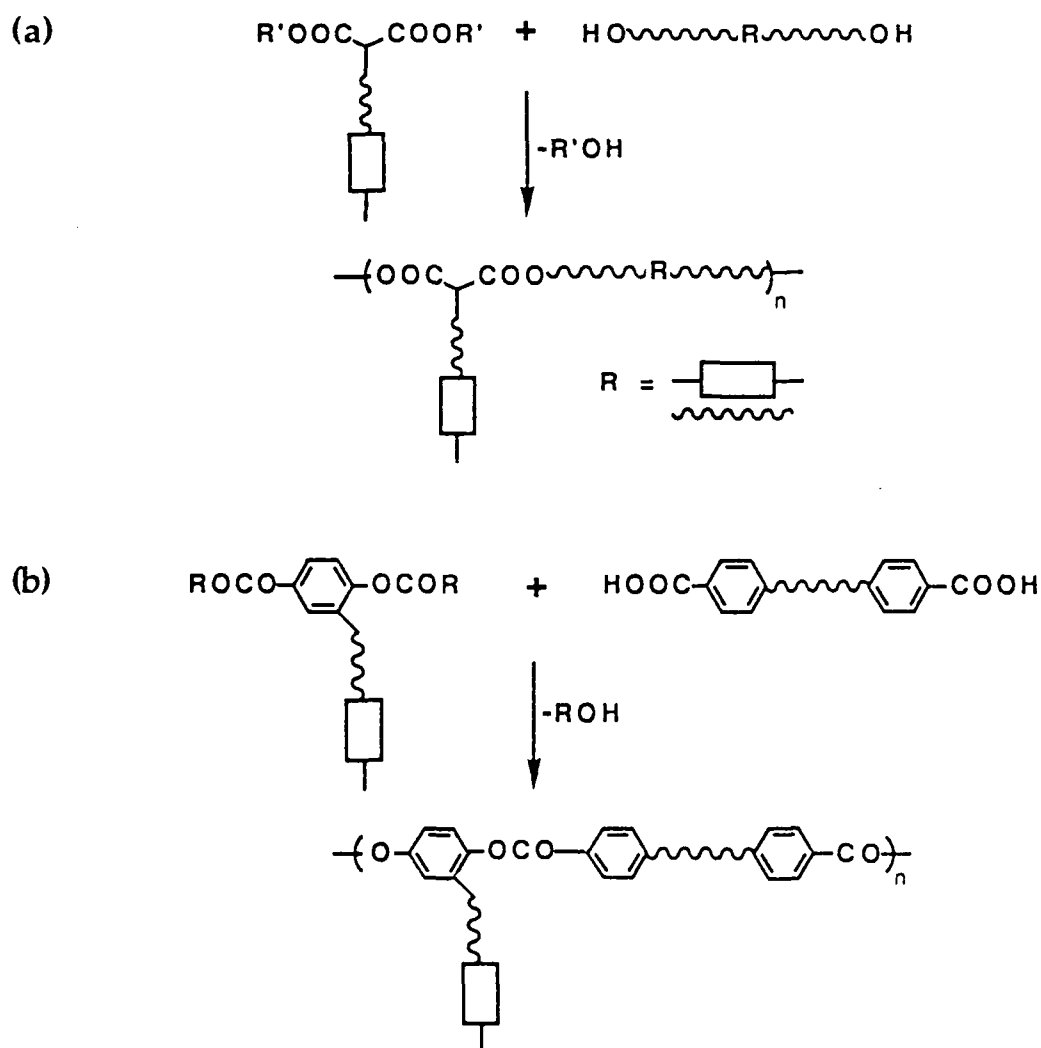


Figure 2.5 : Synthesis of combined side chain LCPs by polycondensation reactions (85, 87, 88)

Polymer Homologous Reactions

Two other reactions that are frequently employed to synthesize side chain LCPs are nucleophilic displacement and hydrosilation. In principle, the reactivity of a functional group should not be altered by attachment to a polymer (15). However, in practice, it has been observed that factors such as the neighboring group effect, or stereoisomerism can either activate or inhibit the reactivity of functional groups in polymeric systems (90). Since such effects often limit the conversion of polymer homologous reactions, they should be considered in attempts to prepare side chain LCPs.

Nucleophilic displacement reactions can be further divided into two categories. The first of these consists of reactions performed on a polymer backbone containing side groups which are displaced by mesogenic units containing a nucleophile at the opposite end of the flexible spacer. This includes displacement of halides from polyacryloyl or methacryloyl chloride (91, 92), poly(epichlorohydrin) (93, 94) and poly(dichlorophosphazene) (95, 96). Alternatively, the reactive species in the polymer and the mesogen can be interchanged to bring about a similar reaction. Keller has prepared several polyacrylates (97), polymethacrylates (98), polyitaconates (99) and poly(methyl vinyl ether-co maleate) (100) by displacing bromine from bromoalkyl containing mesogens with polymeric nucleophiles. An example of these two categories of nucleophilic displacement reactions is shown schematically in figure 2.6.

As suggested by Keller, these nucleophilic reactions can be performed by either liquid-liquid (97-100) or solid-liquid (101) phase transfer catalyzed reactions. Under these conditions, the reaction medium is fairly basic due to the presence of sodium salts of weak acids and therefore, can bring about side reactions such as aromatic ester hydrolysis in the mesogenic units. Therefore, even though easy to perform, synthesis of side chain LCPs by displacement

reactions is often limited to *mesogens that are devoid of ester linkages* (93-102).

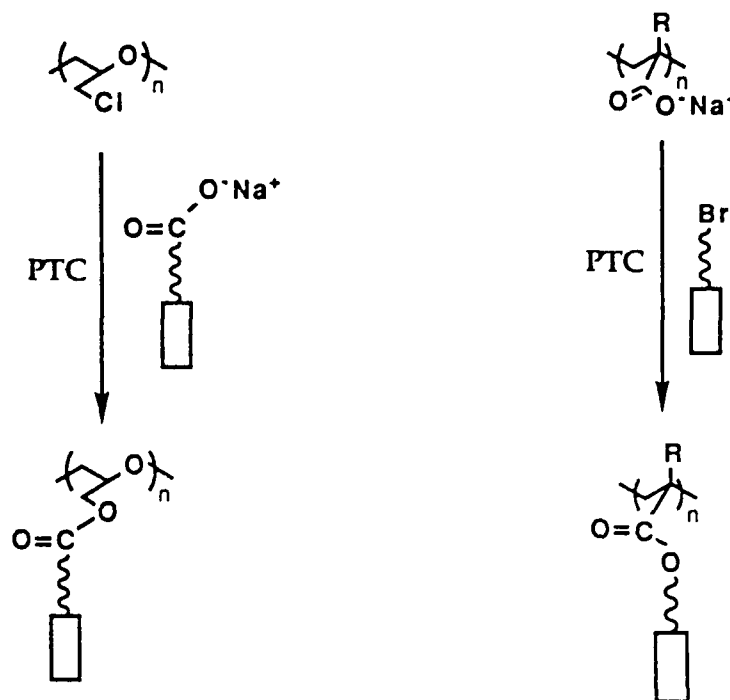


Figure 2.6 : Synthesis of side chain LCPs by polymer homologous reactions

Lastly, one of the most frequently used polymer homologous reaction is hydrosilation. Hydrosilations are difficult to perform to completion, and are accompanied by a number of side reactions (103-107). Nonetheless, they offer a convenient synthetic route to prepare elastomeric side chain liquid crystalline polysiloxanes, copolysiloxanes and crosslinked polysiloxanes, as shown schematically in figure 2.7.

In summary, addition polymerizations involving anionic and group transfer initiators are not suitable for mesogens which have ester linkages. In order to use cationic polymerization initiators, very specific monomers containing electron donor groups to stabilize the propagating species are

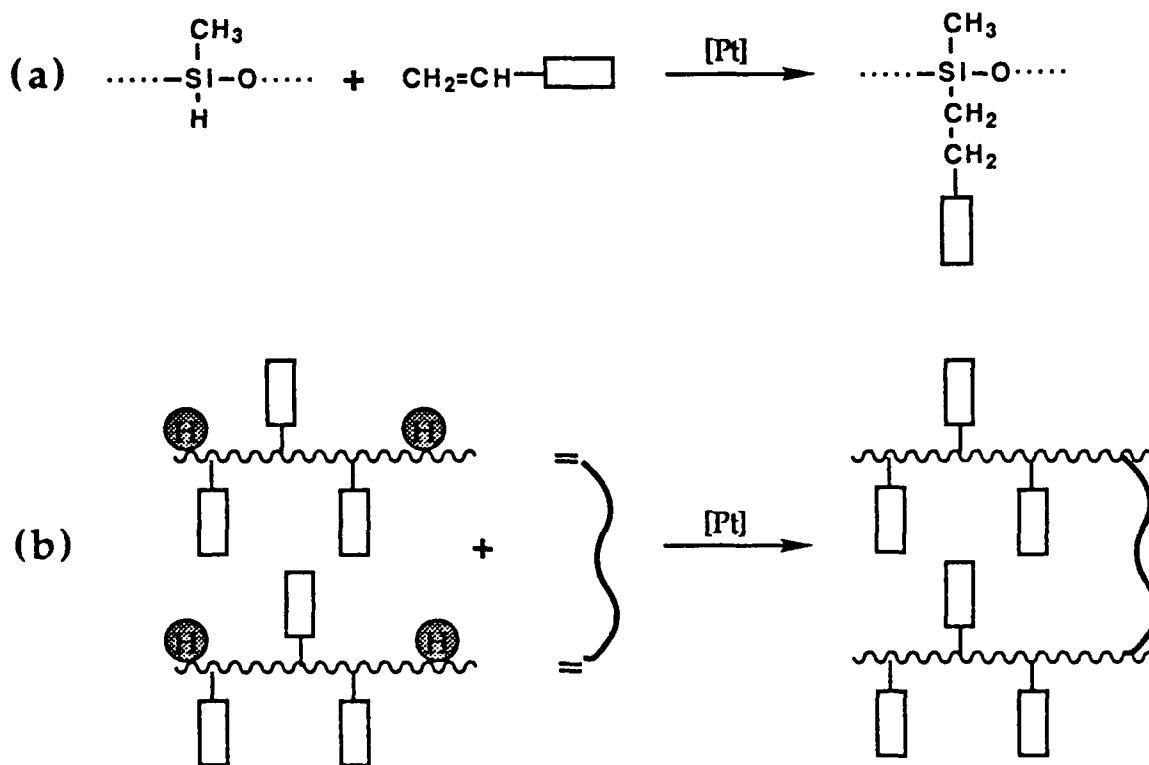


Figure 2.7 : Synthesis of (a) linear and (b) crosslinked side chain LCP by hydrosilation reaction

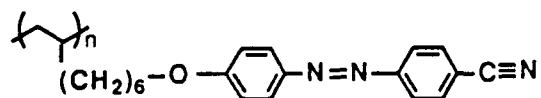
required. Step polymerization reactions are limited to polyester backbones and as such, are not suitable for synthesis of hydroxy-functionalized polymers. And finally, homologous reactions involve strongly basic conditions and hence have not been very successful for mesogens with ester linkages. Hence, the best suited mechanism to synthesize the hydroxy-functionalized side chain LCPs was identified as addition polymerization involving free radical initiators.

2.1.3: Functionalized Side Chain Liquid Crystal Polymers

Functionalization of liquid crystalline polymers is a relatively new concept and hence little information is available in the literature on the subject. It is

somewhat more extensively studied with main chain thermotropic polymers, in which it is desirable to lower the melting and clearing temperatures of the rigid rod-like polymers for ease during processing. In this context, alkoxides, nitriles and nitro groups were found to be effective in depressing the melting and clearing temperatures for some polymers (108), this depression itself being a subtle balance between the steric effects which limit molecular packing and the polar effects which facilitate the ordering. On the contrary, with side chain liquid crystalline polymers, such alterations in transition temperatures can be very finely tuned by modifying either the flexible spacer or the flexibility of the backbone itself. Typical functional groups on the mesogens of side chain liquid crystalline polymers reported in the literature are the carboxylic acids (109, 110), nitriles (111, 112) and alkoxides (111). Functionalization in side chain polymeric systems has been aimed at accomplishing very specific properties, two of which are elaborated below.

Organic compounds with extended π -electron systems and forming non-centrosymmetric crystals have nonlinear optical properties. Several possibilities exist in using polymers as matrix materials for such optically non-linear systems (113). One way to fulfill this requirement may be by use of a side chain liquid crystal polymer such as polymer 19 which contains functional groups with strong dipole moments in the mesogenic units. Poling this polymer as it cools from the



19

isotropic state or possibly advantageously in a mesophase and then quenching into a glassy state would preserve the order (114). In this context, another

interesting system studied by Meredith et al. (20) involves solid solutions of optically non-linear molecules in a liquid crystalline host. Specifically, they have focussed on solid solutions of the optically non-linear molecule DANS (4-dimethylamino-4'-nitrostilbene) in copolyacrylates containing functionalized mesogenic side groups as shown in Figure 2.7.

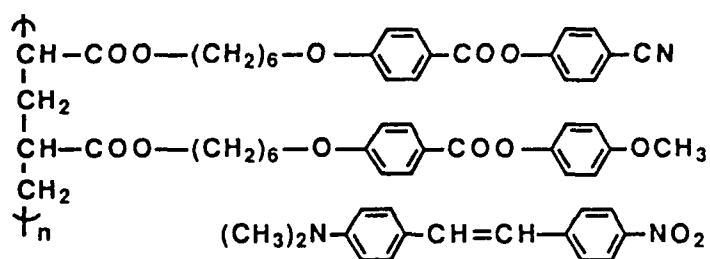


Figure 2.7 : Solid solution of DANS in a side chain liquid crystalline copolymer host for improved polar ordering (20)

Yet another approach in this regard which eliminates the problems associated with solubility of the non-linear molecules in polymer matrices is addressed by Le Barny et al. (21). In order to increase the concentration of optically non-linear molecules in polymer matrices and simultaneously make use of liquid crystal assisted induced polar ordering, copolymers of mesogenic side chain moieties and of optically non-linear side groups (stilbene derivatives) were synthesized. The structure of such a polymer is shown below in Figure 2.8.

A second specific application of functionalized side chain LCPs takes advantage of the functionality as well as the highly ordered structures that such functional group bearing polymers exhibit. For example, the possibility of converting preformed polymers into Langmuir-Blodgett films to tailor-make polymer monolayers and multilayers is being actively investigated by several

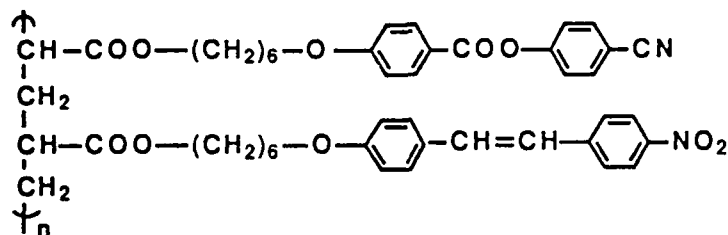


Figure 2.8: Copolymer containing mesogenic and optically non-linear side groups for improved polar ordering (21)

research groups (115-118). Such monolayers and multilayers of side chain LCPs are of great interest in the general area of optical devices and in particular, in waveguides that take advantage of the films' non-linear optical properties.

Preformed amphiphilic polymers containing hydrophilic functional groups either in the backbone or in the side chains are suitable to prepare such monolayers and multilayers. One family of polymers as an example of the former case that has been successfully used to prepare multilayers by Vickers et al. (116) is shown in Table 2.2. An interesting synthetic approach involving

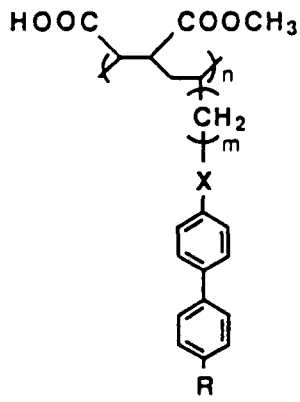
	-R	- x -	m
	-H	-COO-	9
	-H	-CO-	8
	-C ₅ H ₁₁	-CO-	2
	-C ₅ H ₁₁	-CH ₂ -	2

Table 2.2: Functionalized side chain LCPs used in the preparation of Langmuir-Blodgett films (13)

radical copolymerization of maleic anhydride with olefins containing mesogenic groups followed by monoesterification of the anhydride units with methanol was employed to prepare this class of functionalized side chain LCPs (116, 119).

Preformed side chain LCPs containing hydrophilic functional groups attached at the end of the mesogenic group have also been successfully used in the preparation of Langmuir-Blodgett monolayers which exhibit non-linear optical properties (117). One such series is illustrated in figure 2.9 (117).

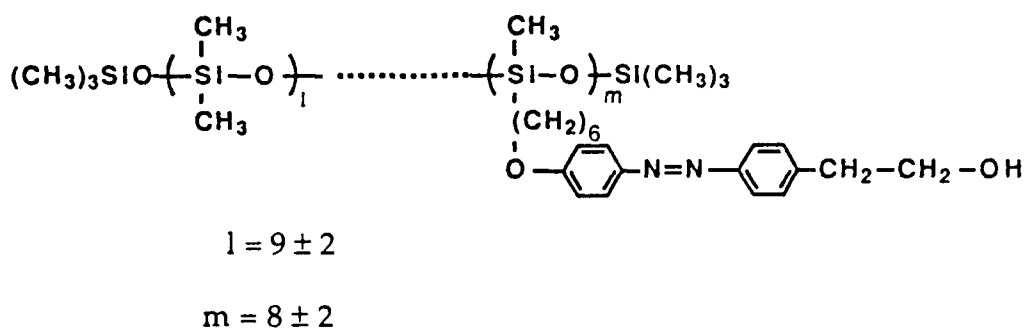
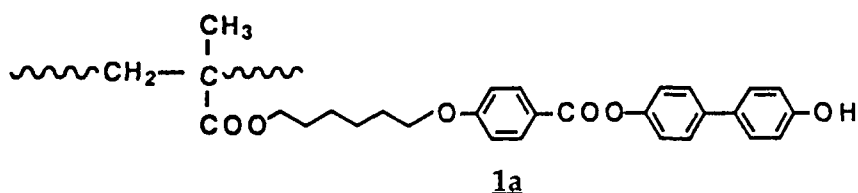


Figure 2.9 : An example of a preformed side chain liquid crystalline polysiloxane used in the preparation of Langmuir-Blodgett films (117)

Langmuir-Blodgett multilayers were also obtained from thermotropic side chain liquid crystalline polymalonates of oligooxyethylene glycols (120). These polyesters contain mesogenic azobenzene units in the side chains, and highly flexible and hydrophilic oligooxyethylene segments in the main chain.

2.1.4: Target Polymers

The structure of the target polymer chosen as a part of our study on liquid crystalline polymer-carbon fiber composite systems is shown as **1a**. A hydroxy-functionalized comb-shaped polymer such as **1a** constitutes a new member of the



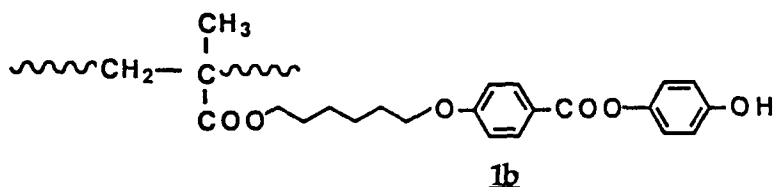
family of functionalized side chain LCPs. Of the numerous small molecule liquid crystals that have been synthesized to date, few have phenolic functionality of the type shown above (121, 122). The following chapter discusses these few examples at length. To our knowledge, polymeric liquid crystals either of the main chain or of the side chain variety containing *phenolic* functional groups have not been reported in the literature.

The choice of the functional group itself was primarily based on the potential ability of these hydroxyl groups to interact with a variety of substrates with polar or nonpolar groups on the surface. In particular, since the present work has been focussed on carbon fiber based composites, fibers with active carboxyl groups may be amenable to reaction with such polymers. Studies with these two components, i. e. the functionalized polymer and the functionalized fibers may be useful in studies of self-ordering molecules at an interphase. From an application point of view, one common feature with many organic matrices is their reactivity towards phenolic groups. For instance, matrices such as liquid crystalline copolyesters, epoxies and unsaturated polyesters are capable of reacting with hydroxyl groups under processing conditions (123). Thus, we envisage this polymer **1a** as a potential coupling agent in the context of composite materials. Viewing it differently, the functionality of this coupling agent molecule is similar to that of the commercially employed silane coupling agents for glass fibers or poly(vinyl alcohol) sizing agent used with carbon fibers (123-125).

The choice of the biphenylic mesogen, the hexamethylenic spacer and the

methacrylic backbone are all based on numerous similar structures of side chain LCPs cited in the literature (5, 126). The preference for placing the hydroxyl groups on the mesogen was predominantly to lock these groups in the ordered mesophases. The ordering of functional groups in the interphase region may very well influence the reactivity of the interphase and hence the mechanical properties of the composite specimen significantly.

One another representative member of this class of functionalized polymer is **1b**, differing from **1a** only in the rigidity of the mesogen. Many



polymers with similar structure have been reported to show mesomorphic behavior (126-128). Therefore, synthesis of **1b** was also pursued along with that of **1a**. The synthetic strategy adopted to prepare the vinylic monomers **8a** and **8b** and their corresponding polymers **1a** and **1b** and the experimental details are discussed in the remainder of this chapter. The following chapter focusses on the systematic investigation of the properties of these monomers as well as their polymers, the influence of fibers on their properties and the modification of their properties by altering the chemical nature of the functionality. The target polymers designed for this study may behave quite differently from hydroxylated-polymers such as that shown in figure 1.19. For instance, the ordering of the phenolic functional groups may be better coupled with the ordering of the mesogenic units due to their direct linkage to the aromatic rings. The fundamental information gained from investigation of the effect of

phenolic groups on the properties will presumably contribute to the discovery of a new class of functionalized liquid crystalline polymers that allow anchoring of ordered phases to a variety of substrates. While this was the motivating factor underlying this research work, we speculate that the molecular architecture of these target polymers may also permit other applications such as formation of Langmuir-Blodgett films elaborated in the earlier part of this section.

2.2: Results and Discussion

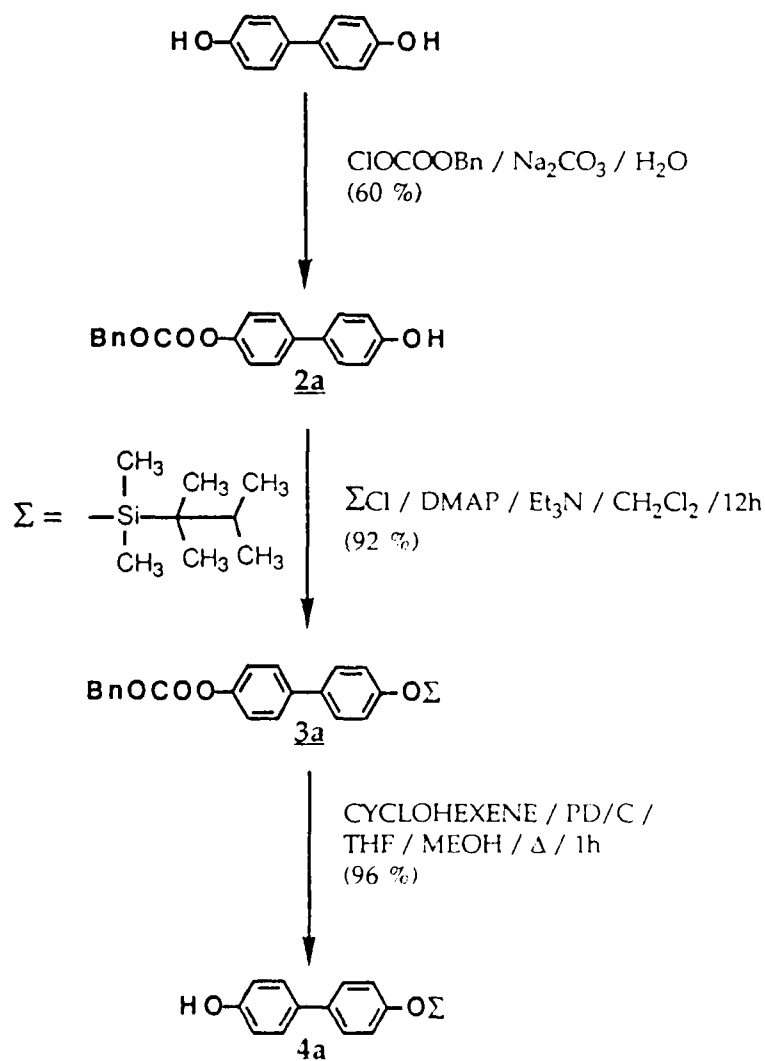
2.2.1: Overview of the Synthetic Plan

Polymers **1a** and **1b** shown in the preceeding section can be easily visualized as being derived by addition polymerization of the corresponding methacrylic monomers. At the start of this work, only a few methods were known to *prepare functionalized polymers with free phenolic groups*, the most common one being free radical polymerization of the acetylated monomers followed by removal of the protecting groups by alkaline hydrolysis (129). Such an approach, however, is restricted to simple monomers and polymers that are stable to strong alkaline media and therefore is not applicable in the present context. Direct free radical initiated polymerization of the phenolic monomers was a possibility but some uncertainty was associated with this route based on the contradictory findings reported in the literature (130-132). Alternatively, a protection-polymerization-deprotection method could be employed to prepare these polymers. Unfortunately, a precedent for such a scheme was unavailable and therefore, a search was initiated to identify a convenient synthetic route for this purpose. These results are described in the following section.

2.2.2: Stepwise Construction of Functionalized Monomers

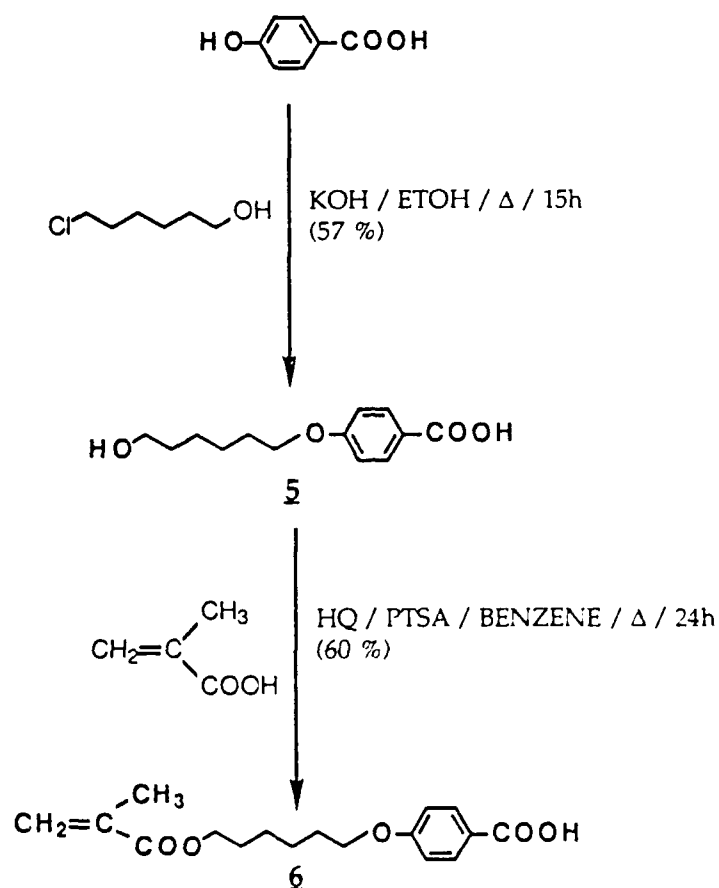
The first step towards the monomer synthesis involved synthesis of the functionalized mesogen. This was accomplished as shown in scheme 2.1. Synthesis of **2a** was a simple extension of the well known hydroquinone chemistry to selectively protect one of the phenolic groups (133). Thus, the monocarbonylbenzyloxy derivatives, **2a** and **2b**, were prepared by overnight reaction of the corresponding diols with benzylchloroformate in the presence of

SCHEME 2.1



sodium carbonate in water. 60-65% of analytically pure compound was recovered after 2 or 3 recrystallizations from toluene and ethanol-water mixtures, the major impurity being the diprotected compound. Alternatively, purification of this crude product could also be achieved by flash chromatography in 65-70% yields. Next, a silyl ether group was selected for protection of the other phenolic group, primarily because of its ease of removal with fluoride ions under mild conditions. The dimethylthexylsilyl ether was chosen over other silyl ethers (134) because of its availability (135) and its stability to survive the conditions of decarbonylbenzyloxy reaction. Thus, **3** was prepared in 89-92% yield by the reaction of **2** with 1.1 equiv. of dimethylthexylsilylchloride, 1.1 equiv. of triethylamine and catalytic quantities of DMAP (136). Analytically pure **3a** was recovered as a slow crystallizing solid and **3b** as a colorless oil after purification by silica gel chromatography. Finally, selective deprotection of the carbonylbenzyloxy group was achieved by catalytic transfer hydrogenation mechanism (137, 138). This method employs refluxing a solution of **3** in THF with a hydrogen donor (cyclohexene, 20 equiv.) in the presence of Pd/C (200% by weight of **3**) as a catalyst. Reaction yields were significantly improved from 60% to 90% when a protic solvent such as methanol was added to the reaction mixture (139). However, the course of the reaction had to be carefully monitored by TLC analysis and the crude product immediately purified because the dimethylthexylsilyl ether group was also prone to deprotection at longer time scales. This method afforded pure **4a** and **4b** in 96% and 90% yields respectively after chromatographic purification.

Synthesis of the second fraction of the monomer molecule with a methacrylic fragment attached to a flexible spacer is outlined in scheme 2.2. First, the flexible spacer was introduced by an etherification reaction of p-hydroxybenzoic acid with 6-chlorohexanol to obtain **5** (126). Analytically pure **5**

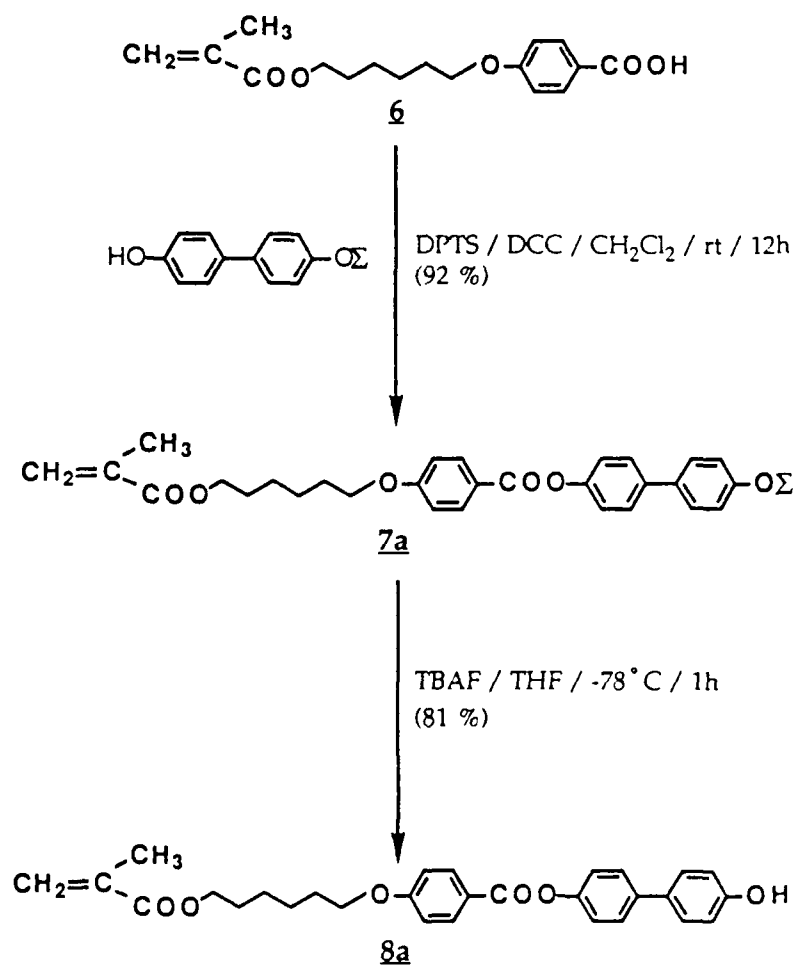
SCHEME 2.2

was obtained by recrystallization from ethanol in 57% yield. Next, the polymerizable double bond was incorporated by azeotropic esterification of **5** with a four-fold excess of methacrylic acid in benzene with PTSA as a catalyst and hydroquinone as the polymerization inhibitor (29). Purification of the product **6** could be achieved in 60% yield by recrystallization either with isopropanol or with ethanol-hexane mixture. In both these cases, recrystallization was very slow and required about 3-4 days standing in the refrigerator for the crystals to appear.

Synthesis of the functionalized monomer was achieved as shown in

scheme 2.3. Esterification of compound **6** with the biphenylic fragment was attempted by the carbodiimide chemistry (140, 141). Initial conditions involving the acid, 1.1 equiv. of 1,3-dicyclohexylcarbodiimide (DCC) and 0.2 equiv. of DMAP as catalyst afforded a product yield of only 50% after chromatographic

SCHEME 2.3



purification, the major impurity being N-acyl urea. Based on a recent discovery in our laboratory of 4-dimethylaminopyridinium p-toluenesulphonate (DPTS) as being a more effective esterification catalyst, the isolated yield of the pure ester

could be improved to 90% (142). Thus, DPTS was first synthesized by mixing a benzene solution of anhydrous p-toluenesulphonic acid (PTSA) with a solution containing an equivalent of DMAP and recrystallizing the resulting crude product from dry dichloroethane. The protected monomer 7 was then desilylated with n-tetrabutylammonium fluoride (TBAF) at -78°C in THF. Complete deprotection required only 45 min even at this temperature. Analytically pure functionalized monomers, 8a and 8b, were isolated by chromatographic purification with silica gel followed by recrystallization from heptane in 81% and 84% yields respectively. $^1\text{H-NMR}$ spectra of monomers 8a and 8b are shown in figures 2.10 and 2.11 respectively. Of particular note is the vinylic proton region (δ 5.50-6.00 ppm) and phenolic proton region (δ 9.70-9.80 ppm). The extent of polymerization could be monitored by the disappearance of the vinylic protons while the integral height of the phenolic peak could be a measure of extent of the deprotection.

2.2.3: Polymerization Strategy

2.2.3.1: Initial Attempts

Our initial efforts to polymerize the monomer 8a (as shown in scheme 2.4) by free radical initiation mechanism afforded only partial success. The polymerization reaction itself failed when 1-2 mole% AIBN initiator was employed and the starting material was recovered back in quantitative yields. 3 mole% initiator concentration afforded a polymeric residue that was insoluble in most organic solvents and was only sparingly soluble in DMF, which was later on identified to be the best solvent for the target polymer. Furthermore, $^1\text{H-NMR}$ analysis in deuterated DMF and elemental analysis identified this polymer to be the corresponding polymer of 8a. However, attempts to characterize this material by microscopic and thermal analysis revealed the infusible nature of

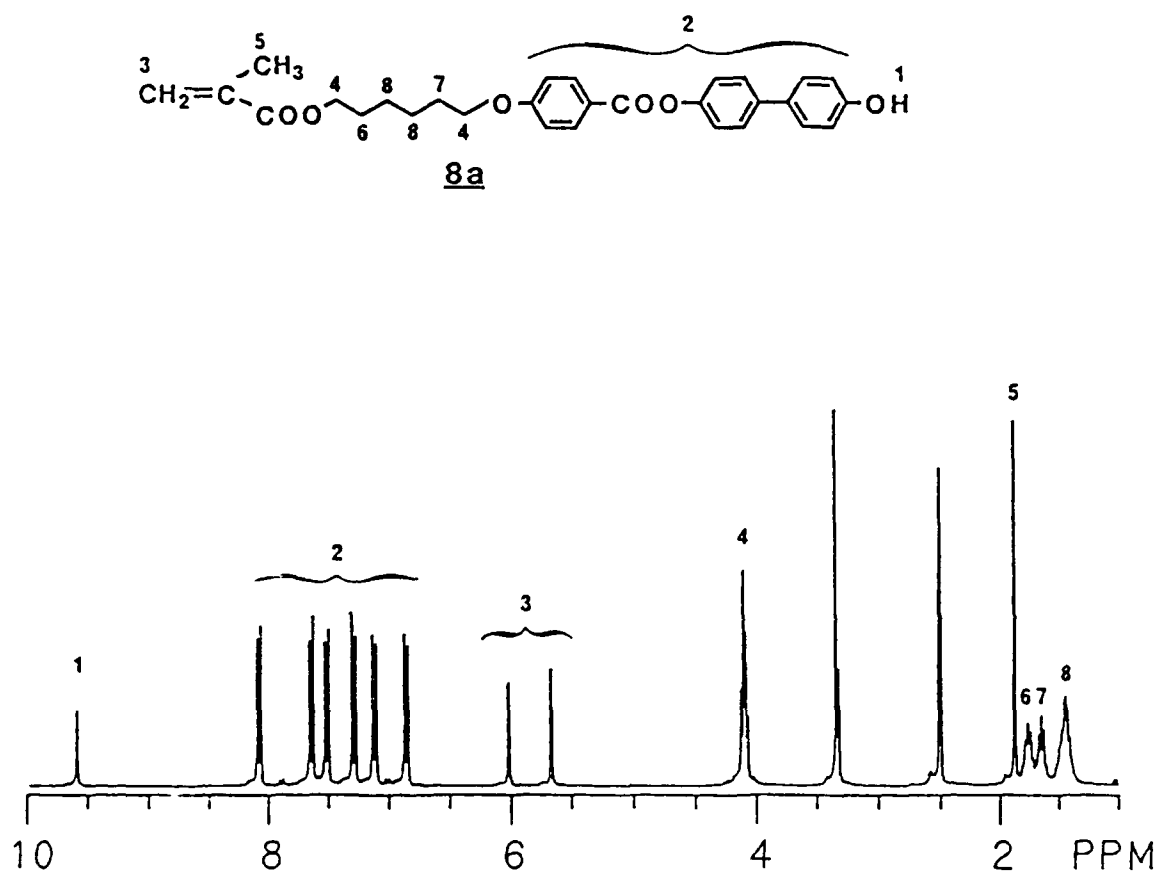


Figure 2.10 : ^1H -NMR spectrum of the hydroxy-functionalized monomer 8a

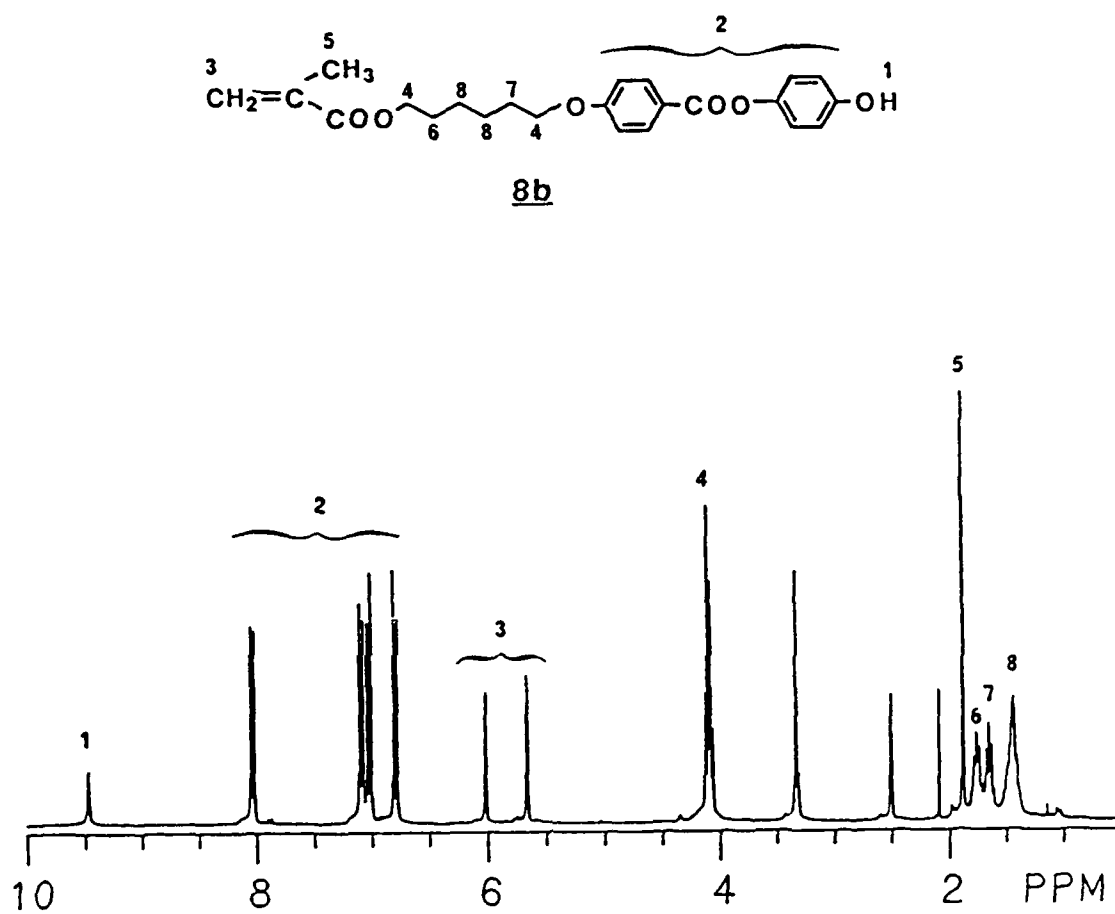
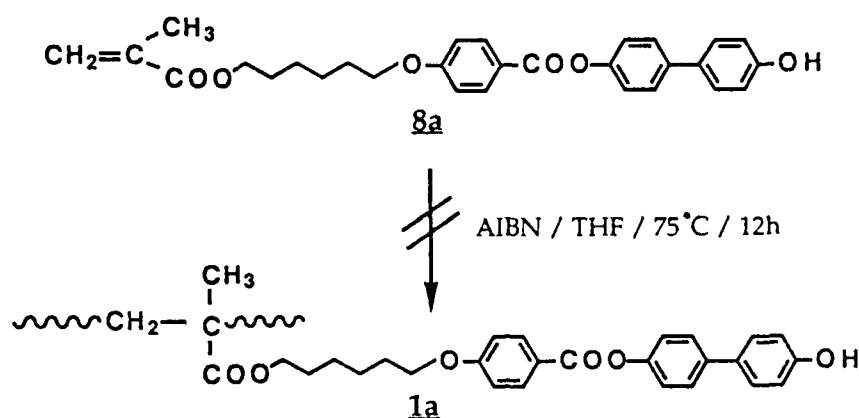


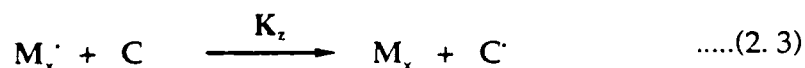
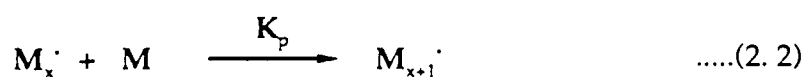
Figure 2.11 : ¹H-NMR spectrum of the hydroxy-functionalized monomer **8b**

SCHEME 2.4



this polymer.

Results of earlier investigations of polymerization of phenolic monomers by free radical initiation that are reported in the literature are of a somewhat contradictory nature. While some investigators observed no influence of the phenolic group on the polymerization mechanism (130), some others have reported a total inhibition due to the presence of these groups (131, 132). In general, initiation, propagation and inhibition for a radical initiated polymerization mechanism may be written as,



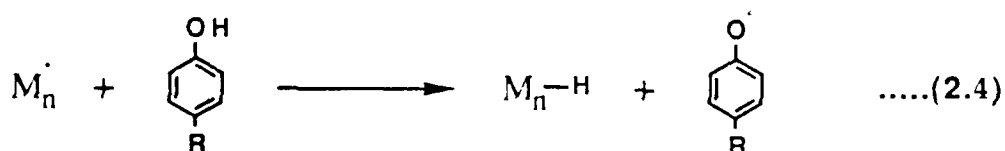
where, K_i , K_p and K_z are the respective rate constants and R^\cdot , M and C are the initiator, monomer and inhibitor respectively. The ratio of the rate constants for

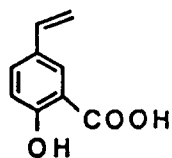
inhibition and propagation is referred to, as the inhibitor constant, Z . The inhibitor constant for any particular compound has been observed to vary considerably depending upon the reactivity and the polarity of the propagating radical. In particular, with methyl methacrylate as the monomer, the inhibitor constant of some compounds are listed in table 2.3 (143).

Inhibitor	$Z = K_z / K_p$
<i>p</i> -benzoquinone	5.7
oxygen	33,000
phenol	0.0002

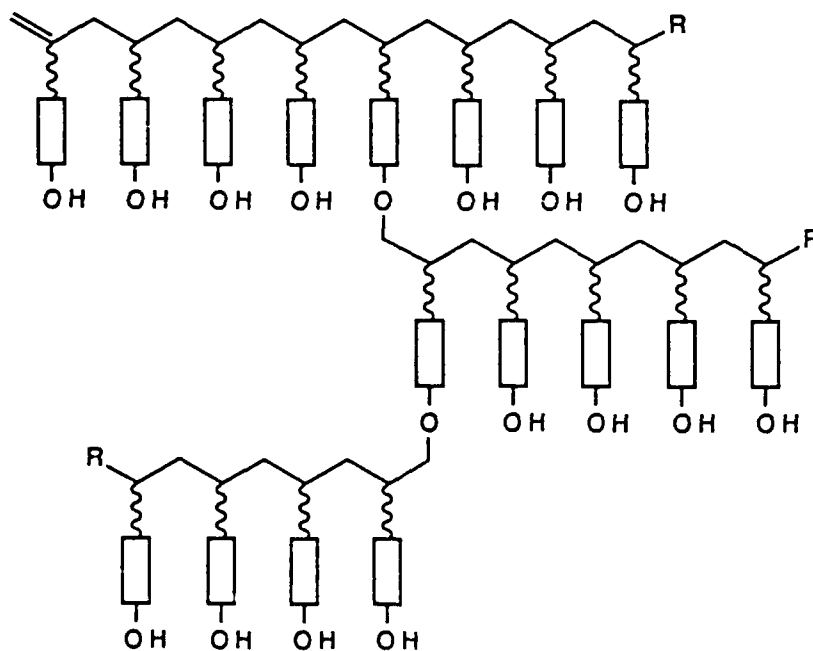
Table 2.3: Inhibitor constants for methyl methacrylate polymerization (143)

Thus, contrary to the general impression, phenol is only a poor inhibitor. However, alkyl and alkoxy substitutions on the ring make them more powerful inhibitors (131). In general, it has been observed that the presence of sufficient electron donating groups facilitate the inhibition, presumably involving hydrogen abstraction to generate the stable phenoxy radicals as shown in equation 2.4. On the other hand, the presence of electron withdrawing groups on the ring has the completely opposite effect, since monomers such as 5-vinylsalicylic acid, 20, undergo polymerization without difficulty (130).



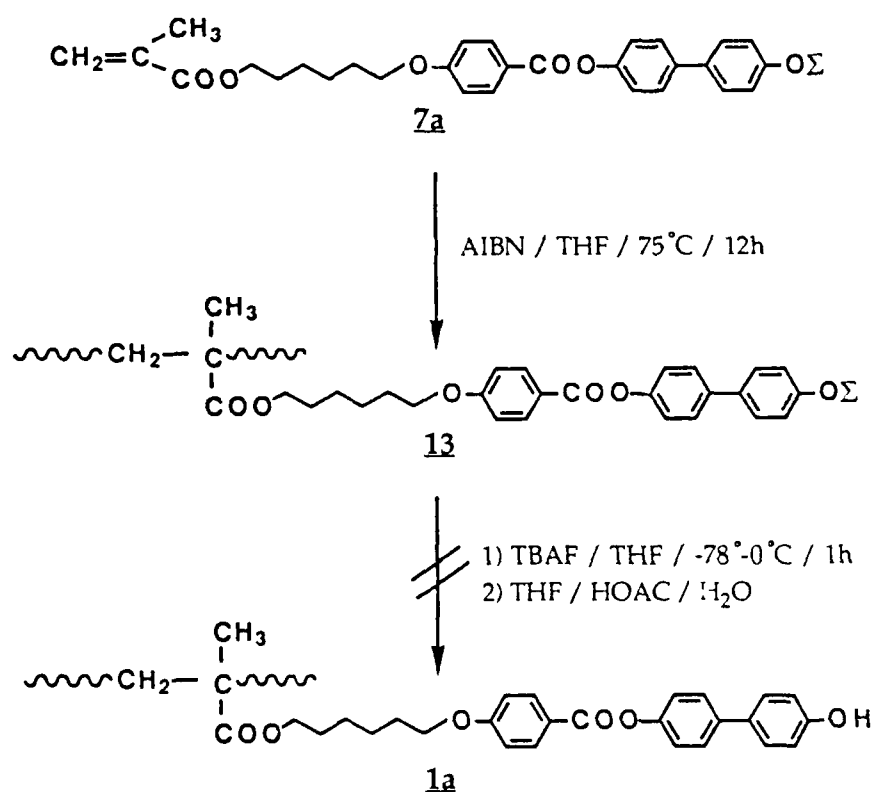
20

In the present investigation, firstly, extreme care was taken to eliminate oxygen by repeated vacuum freeze-thaw method. Secondly, other polymerizations under similar conditions but involving monomers without the phenolic group were successful. Therefore, the need for higher initiator concentration to polymerize this phenolic monomer is unclear at this stage. Furthermore, formation of the phenoxy radicals of the type shown above in equation 2.4 might bring about light crosslinking in the system as shown in 1c. Such a lightly crosslinked product can account for the poor solubility in DMF as

1c

well as the infusibility associated with it. Therefore, other less direct approaches to **1a** and **1b** involving protecting groups were initiated at this stage. The possibility of polymerizing dimethylhexylsilyl ether protected monomer that could be deprotected following the polymerization was pursued next (as shown in scheme 2.5).

SCHEME 2.5



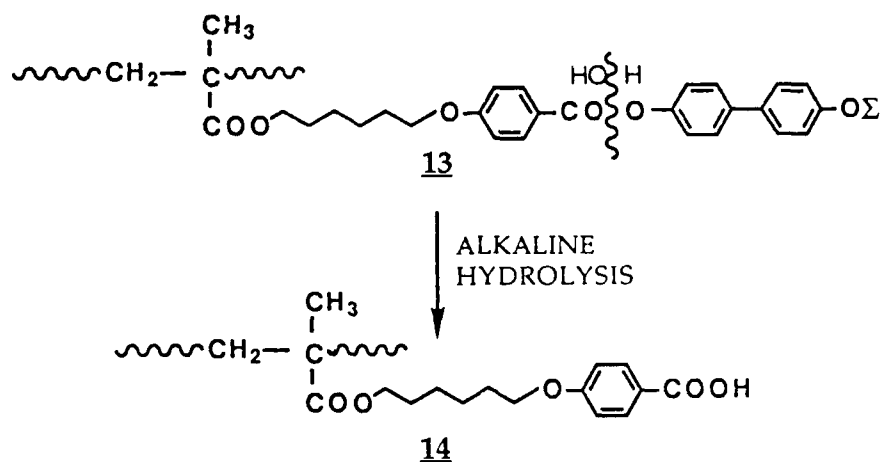
Polymerization of the silyl ether protected monomer using the general polymerization conditions of 2 mole% initiator concentration and THF as solvent afforded polymer **13**. This could be further purified by dissolving in chloroform and precipitating into methanol to obtain 88% yield of the polymer. This material was identified to be very pure by elemental analysis. ¹H-NMR

analysis showed no detectable end groups in the vinylic region and based on the nitrogen content from elemental analysis, the dp of this polymer is ca 200 (assuming termination by combination and disproportionation to be equally likely).

Deprotection of the silyl ether groups by the commonly employed fluoride reagent (TBAF) proved to be a surprisingly difficult reaction to accomplish. This reaction involved dropwise addition of a 1M solution of TBAF to a solution of 13 in THF maintained at -78°C . However, during this addition process, it was extremely difficult to keep the polymer in solution and as little as 1 drop of this reagent caused the polymer to precipitate out of solution. This was presumably due to the addition of a very polar reagent to a very nonpolar polymer solution. Additional solvent at this stage could not provide a homogeneous solution once initial precipitation had occurred. Adding a very dilute solution of TBAF did not help prevent this situation either. However, addition of 0.25M TBAF solution at 0°C instead of -78°C as used earlier did result in a clear solution. After stirring the contents for 45 min at this temperature, the reaction was quenched with acetic acid and a white solid product was isolated after precipitation with ether. Unfortunately, ^1H -NMR analysis identified this polymer to be 14, presumably due to the alkaline nature of the TBAF solution bringing about a base-catalyzed ester hydrolysis of the more susceptible biphenyl benzoate linkage as shown in scheme 2.6.

Quantitative yields of the hydrolysed products under similar reaction conditons as those employed here with TBAF reagent have also been observed by another investigator (144). Repeated attempts to use mixed solvents, keeping in mind the opposing polarity of the two components all failed. Problems encountered with other deprotection conditions employing either THF/ acetic acid/ H_2O mixtures or aqueous methanolic solution were of a different nature

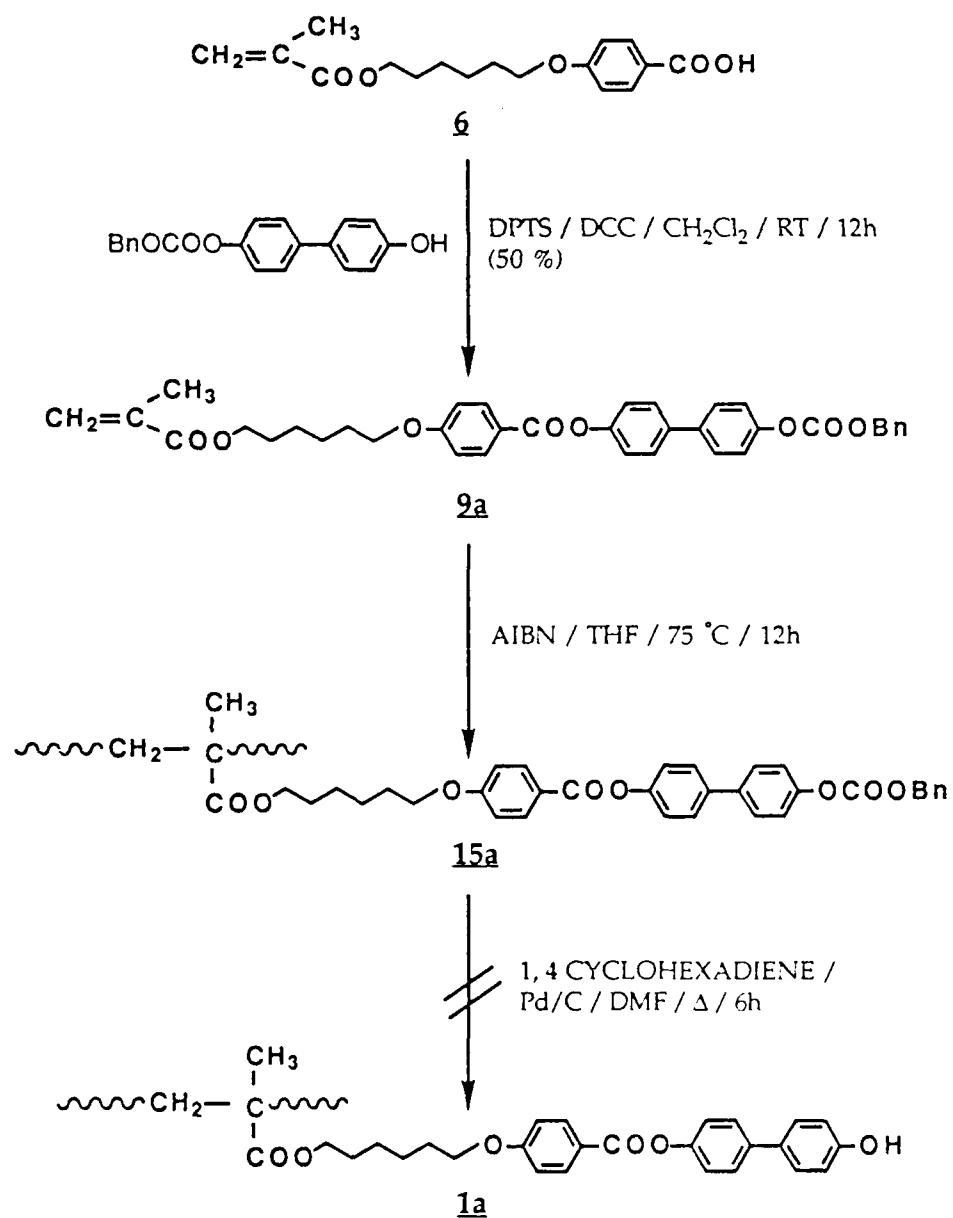
SCHEME 2.6



altogether. In both these cases, partially deprotected polymers were isolated. We return to a discussion on some of the interesting properties associated with such polymers in the next chapter.

The ease of the deprotection chemistry associated with the carbonylbenzyloxy group paved the way for many a useful reaction related to peptide synthesis (145). This was the basis of our next approach to synthesize functionalized polymers, involving carbonylbenzyloxy intermediates as shown in scheme 2.7. The fragments needed to synthesize monomers **9a** and **9b** happened to be intermediates used in the earlier part of the hydroxy-functionalized monomer synthesis. Thus, **6** and **2** were esterified using the carbodiimide chemistry and analytically pure monomers were obtained in 50-60% yields by successive recrystallization from ethanol and isopropanol-heptane mixture. Furthermore, polymerization of these monomers was also straightforward and afforded pure polymers **15a** and **15b** of dp ca 150 in both cases. Deprotection of these polymers by catalytic hydrogen transfer mechanism first required optimizing the conditions for decarbonylbenzyloxy reaction. For this purpose, compound **2a** was chosen as the model compound and the reaction

SCHEME 2.7



medium was restricted to DMF based on the excellent solubility of the target polymer in this solvent. Having established the conditions, the reaction was attempted with polymers **15a** and **15b** employing 20 equiv. of 1,4-cyclohexadiene as hydrogen donor and 5% Pd/C as catalyst. Unfortunately, attempts to isolate

the deprotected polymers from the reaction mixture proved to be a difficult task. Repeated filtrations through the celite beds to eliminate Pd/C yielded a clear solution but with a grey tinge due to very finely suspended carbon particles. Ultracentrifugation of the resultant solution at $17\text{--}20 \times 10^3$ rpm for 2h improved the clarity further, but did not provide a colorless solution. It was suspected that the high viscosity of the DMF solvent was hindering the clean filtration and therefore, other solvents were explored at this stage. Similar difficulty was encountered with 1,4-dioxane which was the only other suitable solvent for this polymer. However, concentration of this light grey solution and precipitation with ether yielded a solid product, the ^1H -NMR of which corresponded to that of a fully deprotected polymer **1a** (and **1b**). Elemental analysis results did not agree very well with the theoretically predicted values. Furthermore, attempts to melt the polymer on a microscopic slide for optical observations was very difficult below 300°C and microscopic analysis revealed only a slow degradation of the polymer upon heating to temperatures above 350°C . Alternative debenzylation routes involved catalysts such as palladium chloride or palladium acetate with triethylsilylhydride (146). However, these methods required very specific solvents such as pyridine and methanol, neither of which were suitable for the present investigation.

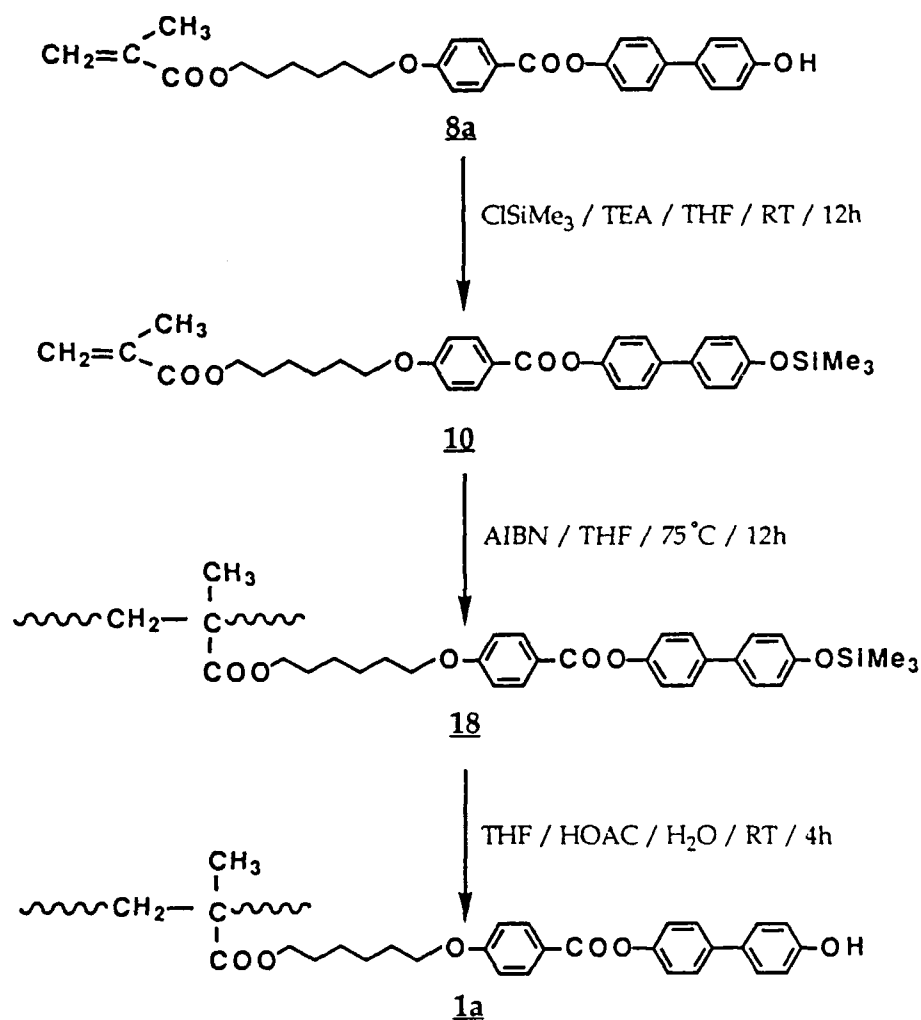
Based on the optical observations, we suspect that the infusibility of this material may be due to the strong adsorption of the polymer on carbon black surfaces. An alternative explanation may be based on the fact that the carbon dioxide gas evolved as a byproduct in this reaction acts as a transesterifying agent. This has been proved to be an excellent transesterification catalyst even at room temperature (147, 148). Even though such an ester-exchange reaction could not be inferred from the ^1H -NMR spectrum which showed a strong peak around δ 9.80 ppm corresponding to the phenolic group, a small extent of this reaction can

account for a lightly crosslinked material. This in turn can explain the observed infusibility of the material. This route was therefore abandoned and the search went back to exploring a suitable protecting group from a wide spectrum of silyl ether protecting groups that are cited in the literature (134).

2.2.3.2: Synthesis of Target Polymers

Of the numerous silyl ether protecting groups that could be employed in principle, one particularly attractive group is the trimethylsilyl ether group because of the ease of its removal under mild conditions (134). However, an obvious disadvantage associated with this group is its instability to purification by silica gel chromatography, this instability itself being a consequence of the acidic nature of the silica gel. An attempt at this route (as shown in scheme 2.8) involved synthesis of the trimethylsilyl ether protected monomer **10** using 1.1 equiv. of chlorotrimethylsilane and 1.1 equiv. of triethylamine. Efforts to purify this monomer by preparative TLC technique using neutral silica gel plates were all unsuccessful and gave back the starting material in quantitative yields. Replacing the trimethylsilyl ether group by a bulkier triethylsilyl ether group also posed a similar difficulty at the purification stage. Therefore, byproduct trimethylamine hydrochloride was filtered off from the reaction mixture and without further purification of this monomer, polymerization was attempted with 2 mole% AIBN concentration. The resultant polymer was purified by precipitating into cold methanol (0-5°C), redissolving in chloroform and reprecipitating into the same solvent. However, the solubility of this product decreased dramatically after drying and a more polar solvent (DMF) had to be employed for NMR studies. Interestingly, ¹H-NMR spectrum of this polymer (shown in figure 2.12) revealed a sharp peak around δ 9.70 ppm and only a small peak around δ 0.20 ppm corresponding to the phenolic and the trimethylsilyl

SCHEME 2.8



ether protons respectively. Based on the integral heights of the two peaks, we infer that on an average, ca one out of every twenty teeth has a protecting group appended to it. Therefore, we reassign the structure of this intermediate polymer **18** as **1d**.

The observed deprotection in **1d** is presumably due to the hydrolysis brought about by the precipitant, methanol, that was not dried before use. Complete deprotection of this partially protected polymer was easily

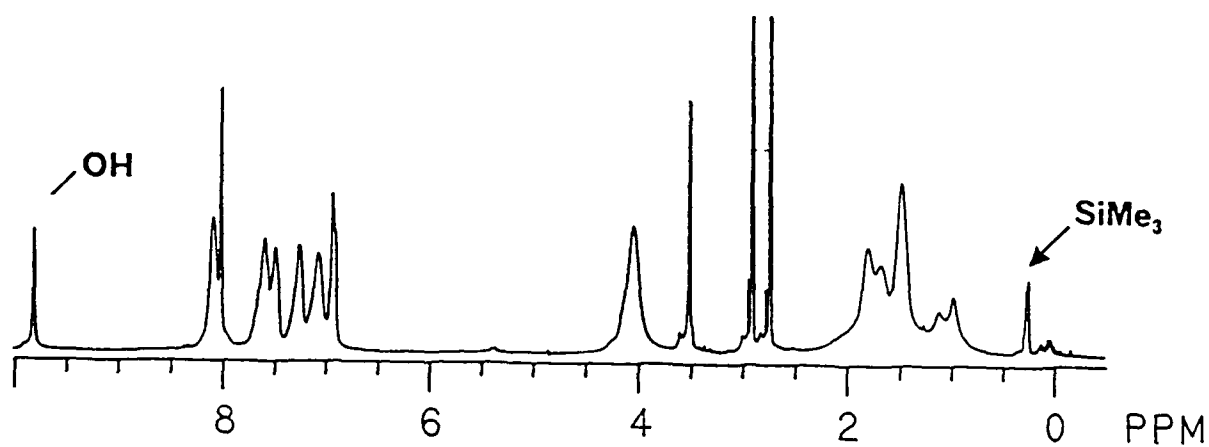
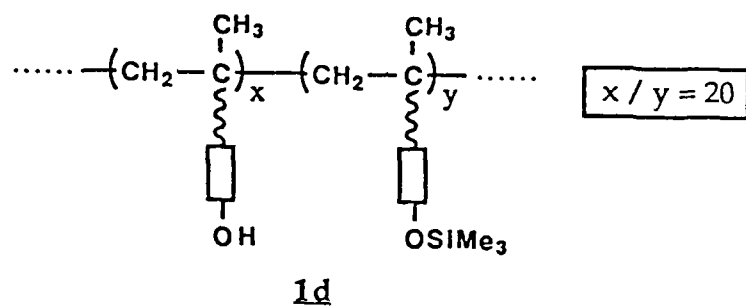
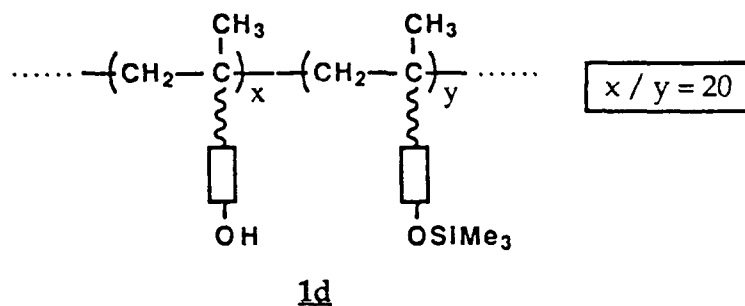


Figure 2.12 : ^1H -NMR spectrum of the trimethylsilyl ether protected polymer in d_7 -DMF after attempted purification

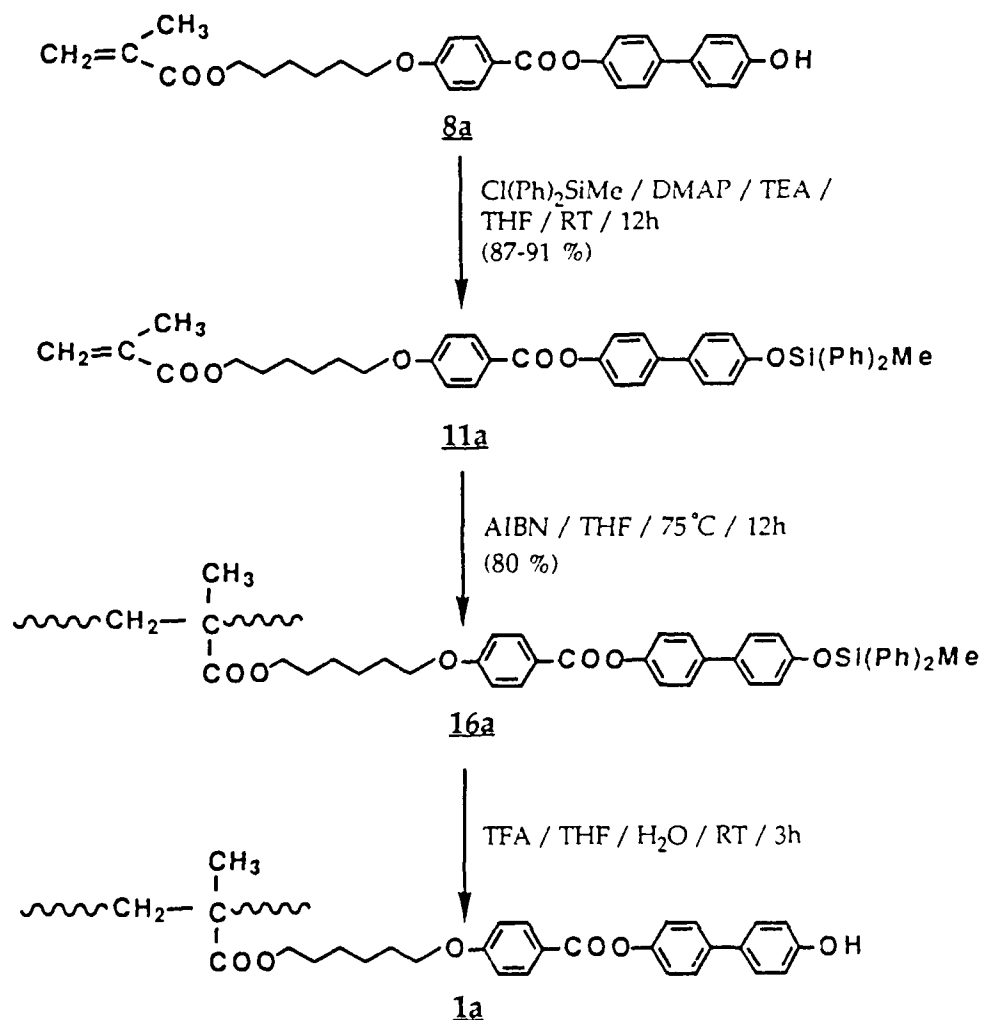


accomplished by stirring a solution of the polymer in THF with acetic acid/ H₂O mixture for 4h at room temperature. ¹H-NMR and elemental analysis identified this polymer to be 1a. Furthermore, based on the nitrogen content of this polymer, we infer that the dp of this polymer is ca 50. The somewhat lower value of dp of this polymer in comparison to other polymers prepared by an identical procedure is presumably due to the use of the unpurified monomer.

At the same time as this investigation, the possibility of using two other protecting groups were also pursued actively. One of these was the diphenylmethylsilyl ether group (DPMS) and it was hoped that this protecting group would satisfy the intermediate requirements of stability to acidic silica gel chromatography and be removable under mild conditions. The selection of this protecting group was aided by Sommer's classic work on the rates of acidic and basic hydrolysis of silyl ethers as a function of the ligands on silicon (149). Sommer found that under basic hydrolysis conditions, steric and electronic effects oppose one another. The net result is that larger alkyl groups strongly decelerate hydrolysis (Me₃Si >> Et₃Si) while phenyl groups have little effect (Me₃Si ≈ Ph₃Si). On the other hand, under acidic conditions, steric and electronic effects both decelerate hydrolysis but the rate is more strongly influenced by electronic effects (Me₃Si = 400 × Ph₃Si) than the steric effects (Me₃Si = 60 × Et₃Si). In accordance with these findings, Denmark et al. (150) observed that the DPMS groups had the same base lability as Me₃Si but a much greater acid stability

thereby enabling purification with silica gel. Thus, the protected monomer **11** was conveniently prepared with 1.1 equiv. of chlorodiphenylmethylsilane in the presence of 1.1 equiv. of base as shown in scheme 2.9. Purification was achieved by flash chromatography, yielding 84% of a white crystalline product. Polymers **16a** and **16b** of dp ca 100 and 80 respectively were prepared using general polymerization conditions in 75-80% yields.

SCHEME 2.9



Even though the deprotection of DPMS ether groups on many small organic molecules could be accomplished in 1 min or less with TBAF reagent, considerable difficulty was encountered with the protected polymer, **16**. The nature of this problem was similar to the solubility problems encountered with the deprotection of polymer, **13**. Other deprotection conditions involving THF/acetic acid/water mixtures or aqueous methanolic solutions also posed a similar problem. However, initial attempts with THF/ TFA/ H₂O mixtures were surprisingly promising. By using low concentrations of water (10:7.5:1), a homogeneous reaction mixture was attainable which was later on identified to be the key factor to accomplish complete deprotection. Thus, pure polymers **1a** and **1b**, were successfully synthesized in 82-90% yields. Furthermore, polymer **1a** obtained by this method was identical to that obtained *via* trimethylsilyl ether protection chemistry. ¹H-NMR spectra of the polymers **1a** and **1b** in d₇-DMF are shown in figures 2.13 and 2.14 respectively.

The other protecting group that was under simultaneous investigation was the tetrahydropyranylether (THP) group (scheme 2.10). It was anticipated that the intermediate polymer with these protecting groups would show better solubility than that observed with the silylether groups in polar solvents. Therefore, the protected monomer **12** was prepared by using 1.5 equiv. of 3,4-dihydropyran and PTSA as the catalyst in methylene chloride. Purification by flash chromatography followed by recrystallization from heptane afforded 60% of pure monomer **12**. Standard polymerization conditions were employed to obtain polymer **17** of dp ca 200 in 84% yield. Deprotection of **17** could be accomplished under same conditions as that employed for diphenylmethylsilyl ether protected polymer, i. e. by using THF/ TFA/ H₂O except that longer reaction times were needed to observe 100% deprotection. However, as expected, it was easy to maintain a homogeneous solution throughout the course of

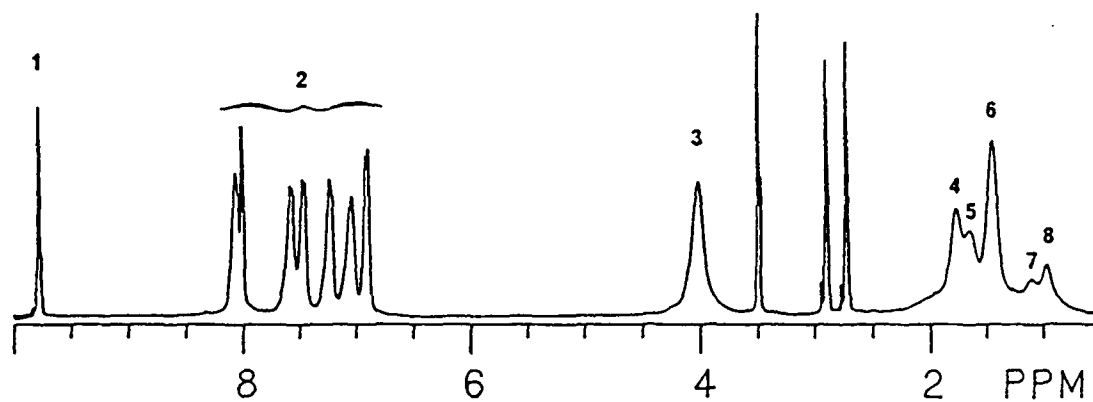
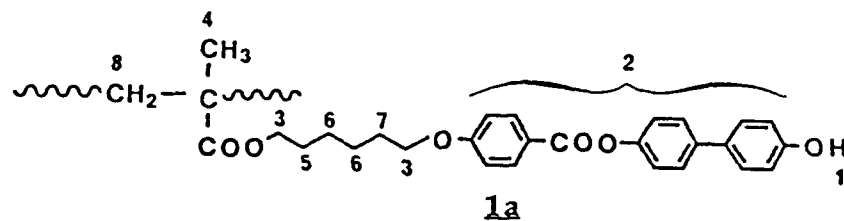


Figure 2.13 : ^1H -NMR spectrum of the hydroxy-functionalized polymer **1a** in $\text{d}_7\text{-DMF}$

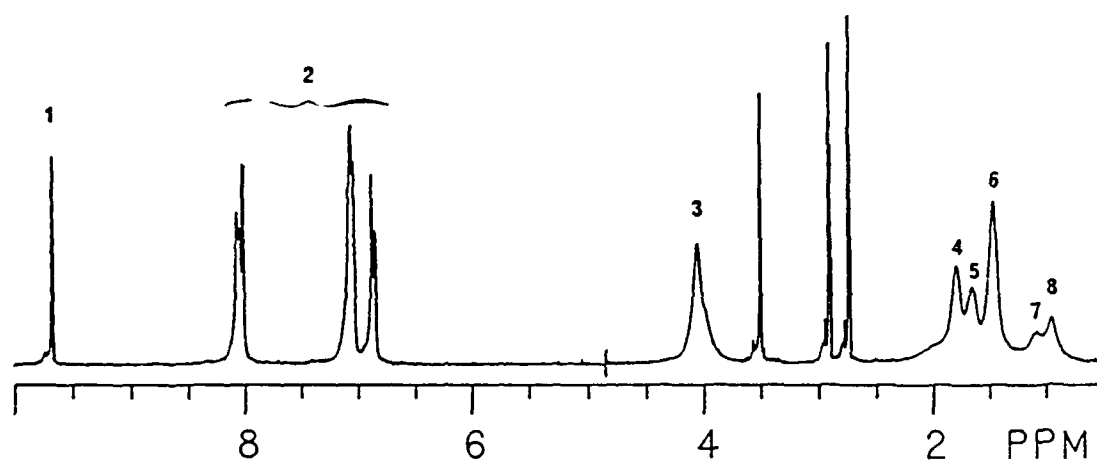
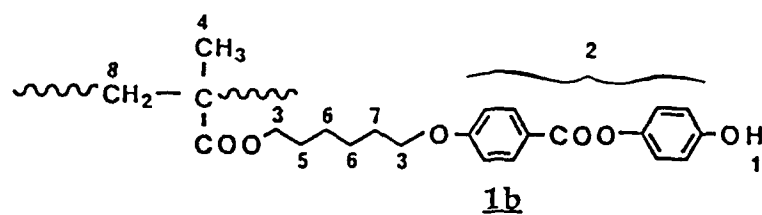
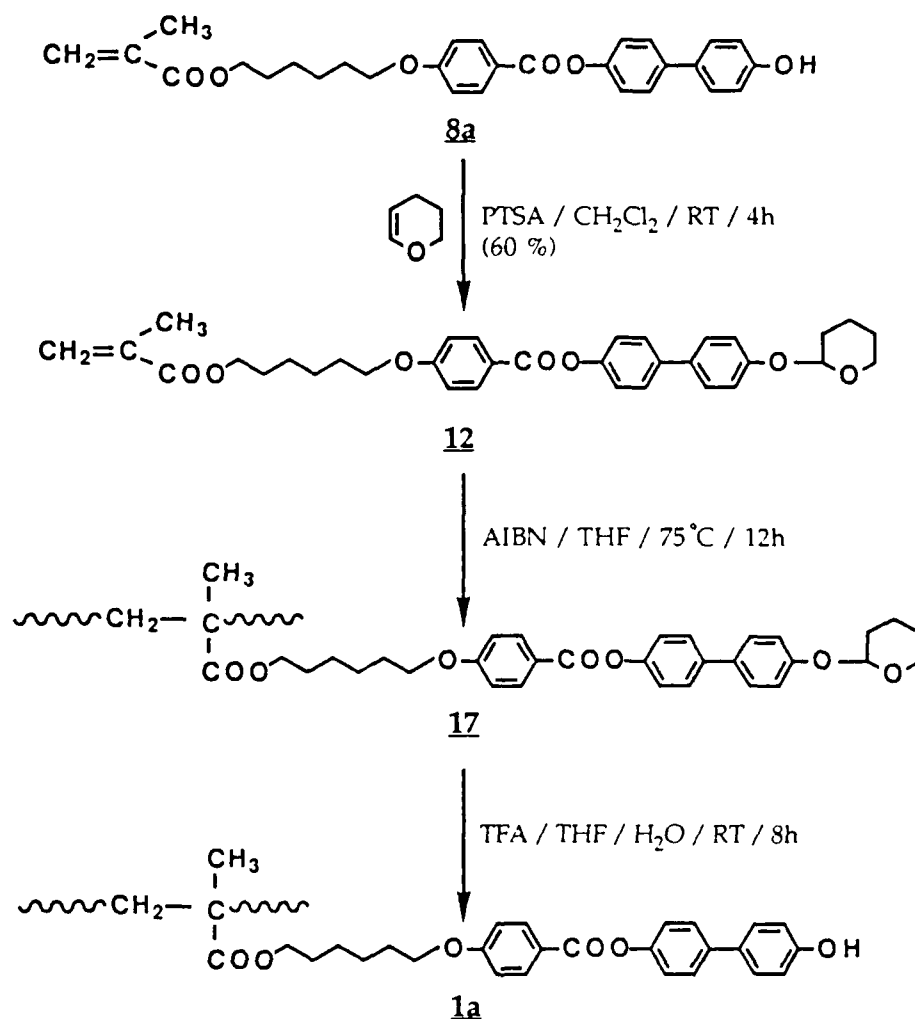


Figure 2.14 : ^1H -NMR spectrum of the hydroxy-functionalized polymer 1b in $\text{d}_7\text{-DMF}$

SCHEME 2.10



deprotection. The polymer isolated by this route in 86% yield was identical to that obtained by scheme 2.8 and scheme 2.9.

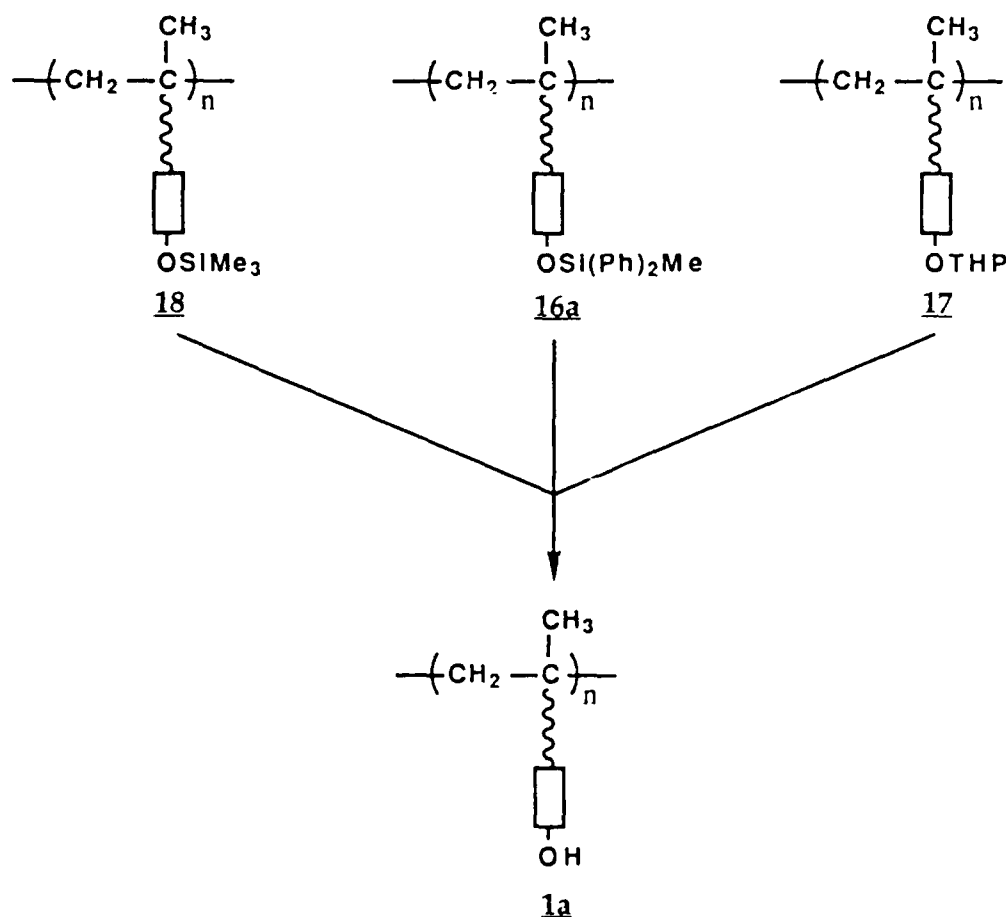
2.3: Summary

The synthesis of hydroxy-functionalized comb polymers **1a** and **1b** was accomplished. Most notably, this involved establishing suitable conditions for

general synthesis of phenolic polymers *via* free radical addition polymerization mechanism. The first task towards this goal was to synthesize the functionalized monomers 8a and 8b. These were prepared by a 7-step synthetic route in overall yields of 39% and 36% respectively.

The second task was to polymerize these phenolic monomers using AIBN as the free radical initiator. Polymerization of the phenolic monomer in the unprotected form resulted in a crosslinked polymer. This invoked the need to polymerize monomers in the protected form which could be subsequently

SCHEME 2.11



deprotected under mild conditions. Of the several protection-polymerization-deprotection routes explored, three were successful and are summarized in scheme 2.11. The use of the labile trimethylsilyl ether protecting group was a limiting factor in purifying this monomer and is presumably responsible for the lower dp (ca 50) obtained by this route. Chemistry with diphenylmethysilyl (DPMS) ether and tetrahydropyranyl (THP) ether as protecting groups on the other hand, was readily reproducible and a higher dp of ca 100-200 was attainable by these methods. The various protected and deprotected monomers as well as their corresponding polymers all showed interesting properties which are discussed in the following chapter.

2.4: Experimental

2.4.1: General Information

Proton NMR spectra were recorded on either a Varian XL-200 at 200 MHz or a General Electric QE-300 at 300 MHz. Solvents used included d_1 -chloroform ($CDCl_3$), d_6 -acetone, d_6 -dimethylsulfoxide (d_6 - Me_2SO), and d_7 -N, N dimethylformamide (d_7 -DMF). Me_2SO was usually employed for small molecule phenolic compounds and DMF for phenolic polymers to facilitate observation of the hydroxyl proton. Spectra were referenced to an internal standard of either tetramethylsilane (TMS) or corresponding solvents [Me_2SO at 2.49 (s); $CDCl_3$ at 7.26 (s) and DMF at 8.01 (b) ppm] as indicated. 1H -NMR data are presented in a condensed format as follows: chemical shift (ppm), multiplicity, scalar coupling constant (Hz), integrated intensity. Multiplicities are abbreviated by s (singlet), d (doublet), t (triplet), q (quartet), or m (multiplet) and broad signals are indicated by b. Carbon NMR shifts are given in ppm with solvents as the internal reference [Me_2SO at 39.50 (m), $CDCl_3$ at 77.00 (t), and DMF at 30.10 (m) ppm].

Carbon-hydrogen substitution patterns were determined either by attached proton test (APT) or the distortionless enhancement by polarization transfer (DEPT) pulse sequences. Substitution patterns are represented by CH₃ (methyl), CH₂ (methylene), CH (methine) and C (quarternary). Electron ionization (EI) mass spectra were recorded on a Varian MAT CH-5 spectrometer with ionization voltages of 10 and 70 eV. EI data are presented in the form m/z (intensity relative to the base peak of 100 units). Elemental analyses were performed by the University of Illinois Microanalytical Service Laboratory. Melting points (mp) were determined on a Perkin-Elmer DSC-4 at a heating rate of 40°C min⁻¹. Infrared spectra were recorded on a Beckman 4240 spectrometer. Analytical and preparative TLC utilized Merck silica gel plates with QF-254 indicator. Silica gel chromatography was performed by the method of Still (151) using Woelm, 32-63 μ m silica gel.

Reactions were carried out in oven-dried glassware (12h @ 150°C). Nitrogen gas was purified by passing through a column of CaCl₂ (1"x 1') and column of granular P₂O₅ (1"x 1'). Argon gas employed for some polymerizations was purified by passing through a column (1"x 5') of CaCl₂, a deoxygenation column (1"x 5') containing activated BTS catalyst (BASF Chemical), and finally a column (1"x 5') of granular P₂O₅.

2.4.1.1: Reagents, Supplies, and Purification

acetone	Fisher
acetic acid	Mallinckrodt
azoisobutyronitrile	Aldrich
barium oxide	Aldrich
benzene, distilled (CaH ₂)	Fisher
benzophenone	Aldrich

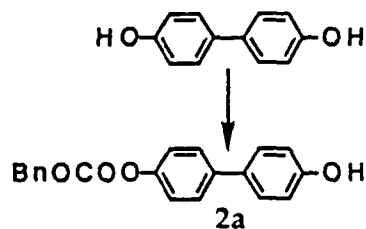
benzyl chloroformate	Aldrich
4,4'-biphenol	Aldrich
calcium chloride	Fisher
chloroform, washed, dried and distilled	Fisher
d ₁ -chloroform	Aldrich
6-chlorohexanol	Aldrich
chlorodiphenylmethysilylchloride	Aldrich
chlorotrimethylsilane	Aldrich
chlorotriethylsilane	Aldrich
1,4-cyclohexadiene	Aldrich
cyclohexene	Aldrich
1,2-dichloroethane	Aldrich
1,3-dicyclohexylcarbodiimide	Aldrich
diethyl ether, distilled (sodium/benzophenone)	Fisher
3,4-dihydro 2H-pyran	Aldrich
4-dimethylaminopyridine	Aldrich
d ₇ -N,N-dimethylformamide	Fisher
N,N-dimethylformamide, distilled (CaH ₂)	Fisher
d ₆ -dimethylsulfoxide, stored over 4A*mol sieves	Aldrich
dimethylthexylsilylchloride	Aldrich
1,4-dioxane	Mallinckrodt
ethanol	Midwest Products
ethyl acetate	Fisher
heptane	b & j
hexane	b & j
hydrochloric acid	Mallinckrodt
hydroquinone	Aldrich
p-hydroxybenzoic acid	Aldrich
isopropanol	Aldrich
methacrylic acid	Eastman
methanol	Fisher
methylene chloride, distilled (P ₂ O ₅)	Fisher
4A* molecular sieves, dried @ 150°C	Union Carbide
palladium/carbon (5%)	Aldrich
pentane	b & j

petroleum ether	Fisher
phosphorus pentoxide (granulated/powder)	Mallinckrodt
potassium hydroxide	Fisher
sodium bicarbonate	Fisher
sodium carbonate	Fisher
sodium chloride	Mallinckrodt
sodium hydroxide	Fisher
tetrabutylammonium fluoride (1.0 M in THF)	Aldrich
tetrahydrofuran, distilled (sodium/benzophenone)	Fisher
p-toluenesulfonic acid monohydrate	Aldrich
triethylamine, distilled (CaH ₂)	Mallinckrodt
trifluoroacetic acid	Aldrich

2.4.2: Experimental Procedures

2.4.2.1: Hydroxy-Functionalized Monomer Synthesis

Benzyl[4-(4'-hydroxyphenyl)phenyl]carbonate (2a)



A three-necked, 3 liter round bottomed flask equipped with mechanical stirrer, nitrogen bubbler and pressure equalized addition funnel was charged with sodium carbonate (13.600 g, 0.128 mole), acetone (1.5 liters) and distilled water (1 liter). The solution was purged with a stream of nitrogen for 15 min followed by addition of 4,4'-biphenol (48.000 g, 0.258 mole). With constant stirring, benzyl chloroformate (49.230 g, 0.288 mole) was added dropwise and within 10 min of stirring, a white solid precipitated out. The suspension was stirred for an additional 12h, the solid product was collected by suction filtration

and washed thoroughly with water. Analytically pure material was obtained by recrystallization from toluene followed by recrystallization from an ethanol-water mixture. An identical procedure was used with equal success to prepare 2b from hydroquinone.

2a

MW: 320.31

yield: 49.500 g (60%) after recrystallizations

mp: 125-126°C

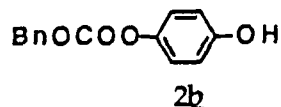
MS (70 eV): 320(24, M⁺), 276(85), 185(100), 157(43), 92(64), 91(99).

¹H-NMR (300 MHz, d₆-DMSO): δ 5.27(s, 2H); 6.82(d, J=8.6 Hz, 2H); 7.24(d, J=8.6 Hz, 2H); 7.42(d, J=8.1 Hz, 2H); 7.46(m, 5H); 7.59(d, J=8.7 Hz, 2H); 9.59(s, 1H).

¹³C-NMR (75 MHz, d₆-DMSO): δ 69.82(CH₂); 115.78(CH); 121.41(CH); 126.97(CH); 127.71(CH); 128.22(CH); 128.27(CH); 128.49(CH); 129.98(CH); 134.99(C); 138.26(C); 149.49(C); 153.02(C); 157.26(C).

C ₂₀ H ₁₆ O ₄	calcd	C 74.96	H 5.04
	found	C 75.14	H 5.06

Benzyl(4-hydroxyphenyl)carbonate (2b)



2b

MW: 244.26

yield: 74% after purification

mp: 73-74°C

MS (70 eV): 244(10, M⁺), 201(10), 200(70), 92(100), 89(21).

$^1\text{H-NMR}$ (300 MHz, CDCl_3): δ 5.22(s, 2H); 6.74(d, $J=8.86$ Hz, 2H); 6.99(d, $J=8.83$ Hz, 2H); 7.42(m, 5H); 9.53(s, 1H).

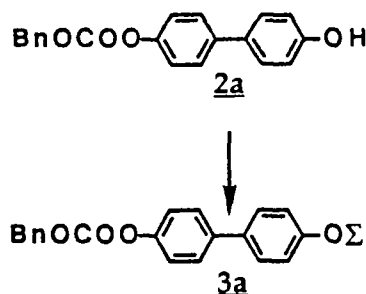
$^{13}\text{C-NMR}$ (75 MHz, CDCl_3): δ 69.79(CH_2); 115.83(CH); 122.17(CH); 128.45(CH); 128.68(CH); 135.28(C); 143.33(C); 153.76(C); 155.54(C).

$\text{C}_{14}\text{H}_{12}\text{O}_4$

calcd C 68.84 H 4.75

found C 68.85 H 4.78

Benzyl[4-(4'-dimethylthexylsiloxyphenyl)phenyl]carbonate (3a)



To a 250 ml single-necked round bottomed flask equipped with a stir bar was added 2a (15.000 g, 0.047 mole) and 4-dimethylaminopyridine (1.144 g, 0.009 mole). A Claisen adapter attached to a nitrogen inlet and a septum was connected to the reaction flask and the system carefully evacuated and purged with nitrogen. The reaction flask was charged with dry dichloromethane (70 ml) and after stirring for 15 min, dry triethylamine (5.214 g, 0.052 mole) and dimethylthexylsilylchloride (9.200 g, 0.052 mole) were added dropwise *via* a syringe. Triethylamine hydrochloride precipitated out instantly. The reaction mixture was stirred at room temperature for 10h under a nitrogen atmosphere. The mixture was transferred to a separatory funnel containing 250 ml ether. The organic phase was washed with 1N HCl (2x250), water (2x250), brine (1x250) and

dried (Na_2SO_4). The solvent was evaporated in *vacuo* and the residue purified by flash chromatography (silica, 15% acetone in petroleum ether). The same procedure was used with equal success to prepare **3b**.

3a

MW: 462.03

yield: 20.000 g (92%) after purification

mp: 44-45°C

MS (70 eV): 462(21, M^+), 418(15), 327(62), 243(15), 91(100), 73(45).

^1H -NMR (300 MHz, CDCl_3): δ 0.27(s, 6H); 0.96(d, $J=8.93$ Hz, 6H); 0.98(s, 6H); 1.78(m, 1H); 5.30(s, 2H); 6.88(d, $J=8.56$ Hz, 2H); 7.21(d, $J=8.59$ Hz, 2H); 7.41(d, $J=8.68$ Hz, 2H); 7.52(d, $J=8.72$ Hz, 2H).

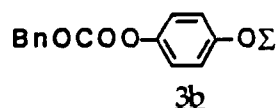
^{13}C -NMR (75 MHz, CDCl_3): δ -2.56(CH_3); 18.46(CH_3); 20.03(CH_3); 24.88(C); 33.40(CH); 70.08(CH_2); 120.27(CH); 121.02(CH); 127.51(CH); 127.90(CH); 128.35(CH); 128.48(CH); 128.53(CH); 133.06(CH); 136.66(CH); 138.67(C); 149.92(C); 153.50(C); 155.05(C).

$\text{C}_{28}\text{H}_{34}\text{O}_4\text{Si}$

calcd C 72.60 H 7.40

found C 72.79 H 7.45

Benzyl[(4-dimethylhexylsiloxy)phenyl]carbonate (**3b**)



3b

MW: 386.54

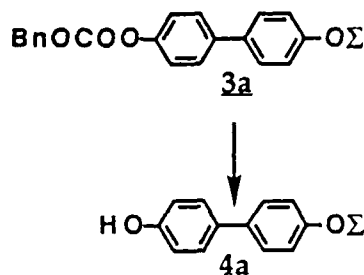
yield: 89% after purification

^1H -NMR (300 MHz, CDCl_3): δ 0.22(s, 6H); 0.94(d, $J=6.87$ Hz, 6H); 0.95(s, 6H); 1.74(m, 1H); 5.26(s, 2H); 6.79(d, $J=9.01$ Hz, 2H); 7.01(d, $J=8.94$ Hz, 2H); 7.40(m, 5H).

C₂₂H₃₀O₄Si

calcd C 68.36 H 7.82

found C 68.99 H 7.77

4-(4'-Dimethylhexylsiloxyphenyl)phenol (4a)

A three-necked 1 liter flask equipped with a condenser connected to a drying tube, a stir bar, an addition funnel and a nitrogen inlet was charged with 5% Pd/C (40.000 g, 200% by weight of 3) and thoroughly flushed with nitrogen. 3a (20.000 g, 0.043 mole) was taken up in THF (200 ml) and the solution was added to the catalyst by momentarily removing the addition funnel. After stirring the contents for 5 min, a mixture of cyclohexene (90 ml, 0.866 mole) and methanol (100 ml) was added dropwise through the addition funnel. Following the addition, the contents were heated in a water bath to the reflux temperature and maintained at that temperature for 1h. TLC analysis (developed with 15% acetone in petroleum ether) showed that no starting material remained. The reaction mixture was cooled to room temperature and filtered twice through a celite bed. The solvent was evaporated and the crude oil was purified by flash chromatography in two batches (silica, 15% acetone in petroleum ether) to obtain a white crystalline solid. A similar procedure was used to synthesize 4b.

4a

MW: 328.5

yield: 13.500 g (96%) after purification

mp: 40-41 °C

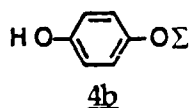
MS (70 eV): 328(43, M⁺), 245(12), 244(51), 243(100), 75(31), 73(12), 43(12).

¹H-NMR (300 MHz, CDCl₃): δ 0.27(s, 6H); 0.97(d, J=6.8 Hz, 6H); 0.98(s, 6H); 1.76(m, 1H); 6.87(d, J=8.5 Hz, 2H); 6.88(d, J=8.65 Hz, 2H); 7.39(d, J=8.6 Hz, 2H); 7.41(d, J=8.58 Hz, 2H).

¹³C-NMR (75 MHz, CDCl₃): δ -2.44(CH₃); 18.55(CH₃); 20.12(CH₃); 25.00(C); 34.07(CH); 115.62(CH); 120.34(CH); 127.57(CH); 127.90(CH); 133.67(C); 133.80(C); 154.37(C); 154.51(C).

C ₂₀ H ₂₈ O ₂ Si	calcd	C 73.12	H 8.59
	found	C 73.20	H 8.50

4-(Dimethylhexylsiloxyl)phenol (4b)



4b

MW: 252.41

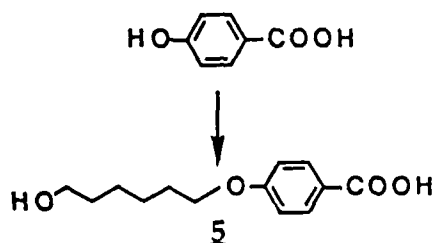
yield: 90% after purification

MS (70 eV): 252(8, M⁺), 205(12), 168(20), 167(50), 84.2(26), 75(100), 69(12).

¹H-NMR (300 MHz, CDCl₃): δ 0.10(s, 6H); 0.93(d, J=6.82 Hz, 6H); 0.94(s, 6H); 1.78(m, 1H); 6.69(s, 4H).

¹³C-NMR (75 MHz, CDCl₃): δ -2.88(CH₃); 18.28(CH₃); 19.86(CH₃); 24.61(C); 33.86(CH); 115.82(CH); 120.46(CH); 148.52(C); 153.82(C).

C ₁₄ H ₂₄ O ₂ Si	calcd	C 67.11	H 9.51
	found	C 66.97	H 9.50

4-(6'-Hydroxyhexyloxy)benzoic acid (5)

A three-necked 300 ml flask equipped with a stir bar, an addition funnel and a condenser was charged with 4-hydroxybenzoic acid (46.000 g, 0.333 mole), KI (20.0 mg), ethanol (120 ml) and KOH solution (50.000 g in 50 ml water). To the resulting light yellow solution was added 6-chlorohexanol (50.090 g, 0.068 mole) dropwise through the addition funnel. The mixture was heated to reflux for 15h using an oil bath maintained at 110°C. Subsequently, the reaction mixture was cooled to room temperature, stirred with water (100 ml) and acidified with aqueous conc. HCl. The solid product was collected by suction filtration, washed thoroughly with water and purified by recrystallization from ethanol.

5

MW: 238.27

yield: 45.000 g (57%) after recrystallization

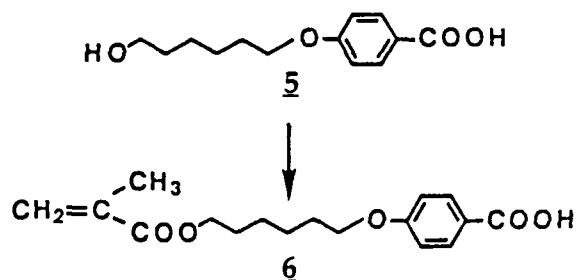
mp: 87-88°C

MS (70 eV): 238(14, M⁺), 138(100), 121(52), 82(50), 65(22), 55(99), 41(51).
¹H-NMR (300 MHz, d₆-acetone): δ 1.41(m, 4H); 1.76(m, 2H); 2.01(m, 2H); 3.50(t, J=6.36 Hz, 2H); 4.05(t, J=6.47 Hz, 2H); 6.98(d, J=8.92 Hz, 2H); 7.94(d, J=8.88 Hz, 2H).

¹³C-NMR (75 MHz, d₇-DMF): δ 25.92(CH₂); 26.00(CH₂); 29.32(CH₂); 33.05(CH₂); 61.67(CH₂); 68.27(CH₂); 114.38(CH); 123.39(C); 131.81(CH); 163.03(C); 167.53(C).
C₁₃H₁₈O₄

calcd C 65.53 H 7.61

found C 65.50 H 7.70

4-(6'-Isopropenylcarbonyloxyhexyloxy)benzoic acid (6)

A 1 liter single-necked flask was charged with 5 (23.300 g, 0.097 mole), 4-toluenesulphonic acid monohydrate (11.680 g, 0.061 mole), hydroquinone (3.886 g, 0.035 mole), methacrylic acid (33.500 g, 0.389 mole) and benzene (600 ml). A Dean Stark apparatus fitted with a condenser and drying tube was connected to the reaction flask and the whole assembly was immersed in an oil bath. The temperature of the bath was slowly raised to 120°C and maintained at that temperature for 24h. The contents were cooled to room temperature and taken up in 2l of ether. The ether extract was washed twice with water, then with brine, dried over Na₂SO₄ and concentrated in *vacuo*. Recrystallization from isopropanol yielded analytically pure sample.

6

MW: 306.27

yield: 17.800 g (60%) after recrystallization

mp: 56-57°C

MS (70 eV): 306(8, M⁺), 138(42), 87(55), 83(70), 41(100).

¹H-NMR (300 MHz, CDCl₃): δ 1.46(m, 4H); 1.70(m, J=6.63 Hz, 2H); 1.81(m, J=6.58 Hz, 2H); 1.87(s, 3H); 4.01(t, J=6.26 Hz, 2H); 4.14(t, J=6.54 Hz, 2H); 5.50(s, 1H); 6.10(s, 1H); 6.91(d, J=8.53 Hz, 2H); 8.04(d, J=8.46 Hz, 2H).

¹³C-NMR (75 MHz, d₆-DMSO): δ 18.11(CH₃); 25.41(CH₂); 25.49(CH₂); 28.28(CH₂);

28.73(CH₂); 64.38(CH₂); 67.80(CH₂); 114.16(CH); 123.13(CH₂); 125.40(C); 131.54(CH); 136.21(C); 162.49(C); 166.73(C); 167.31(C).

$C_{17}H_{22}O_5$	calcd	C 66.65	H 7.24
	found	C 66.33	H 7.19

Preparation of 4-dimethylaminopyridinium 4'-toluenesulphonate (DPTS)

Hydrated 4-toluenesulphonic acid (PTSA) was dried by azeotropic distillation of a benzene solution using a Dean Stark trap. An equimolar solution of 4-dimethylaminopyridine (DMAP) in warm benzene was then added to the anhydrous solution of PTSA. After thorough mixing, the resulting suspension was cooled to room temperature, and the solid product was collected by suction filtration. The crude product was purified by recrystallization from dry dichloroethane yielding white needles.

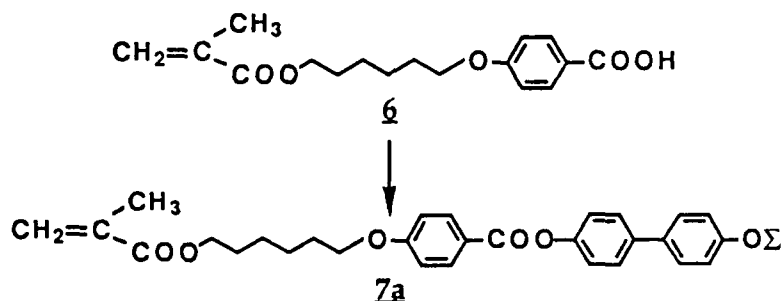
MW: 294.36

yield: 75% after purification

mp: 165°C

¹H-NMR (300 MHz, CDCl₃): δ 2.27(s, 3H); 3.16(s, 6H); 6.95(d, J=7.71 Hz, 2H); 7.09(d, J=8.15 Hz, 2H); 7.46(d, J=8.03 Hz, 2H); 8.19(d, J=7.69 Hz, 2H).

$C_{14}H_{18}N_2SO_3$	calcd	C 57.12	H 6.16	N 9.52
	found	C 57.08	H 6.26	N 9.69

Esterification ProcedureHexyl-6-oxy-{4'-[4''-(4'''-dimethylhexylsiloxyphenyl)phenyl]benzoyloxy}-methacrylate (7a)

A single-necked 250 ml round bottomed flask containing a stir bar and fitted with a Claisen adapter connected to a septum and a nitrogen inlet was assembled hot and flushed thoroughly with nitrogen. The Claisen adapter was briefly removed and replaced with a powder funnel through which was added **6** (12.290 g, 0.040 mole), **4** (14.500 g, 0.044mole), DPTS (2.300 g, 0.008 mole) and 1,3-dicyclohexylcarbodiimide (12.380 g, 0.060 mole). The Claisen adapter was returned and the system was again flushed with nitrogen. Dry dichloromethane (200 ml) was added *via* syringe and the contents were stirred at room temperature. Within 15 min, urea precipitated out of solution. Stirring continued under nitrogen atmosphere for additional 12h at room temperature following which urea was filtered off and the solution was concentrated to obtain a viscous oil. A slow crystallizing product was obtained after purification by column chromatography in 3 batches of 8.000 g each (silica, 15% acetone in petroleum ether). An identical procedure was employed to synthesize **7b**.

7a

MW: 616.79

yield: 92% after purification

mp: 61-62°C

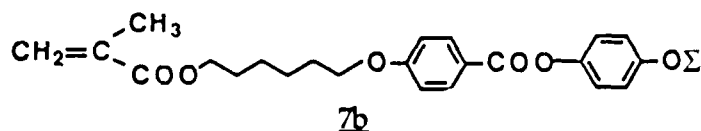
MS (70 eV): 616(10, M⁺); 288(100); 121(67); 69(18); 73(11).

¹H-NMR (300 MHz, CDCl₃): δ 0.22 (s, 6H); 0.92(d, J=6.84 Hz, 6H); 0.94(s, 6H); 1.46(m, 4H); 1.70(m, J=6.63 Hz, 2H); 1.76(m, 1H); 1.81(m, J=6.58 Hz, 2H); 1.87(s, 3H); 3.93(t, J=6.56 Hz, 2H); 4.09(m, J=6.56 Hz, 2H); 5.48(s, 1H); 6.06(s, 1H); 6.83(d, J=8.55 Hz, 2H); 6.88(d, J=8.90 Hz, 2H); 7.17(d, J=8.59 Hz, 2H); 7.38(d, J=8.56 Hz, 2H); 7.49(d, J=8.58 Hz, 2H); 8.08(d, J=8.80 Hz, 2H).

¹³C-NMR (75 MHz, CDCl₃): δ -22.79(CH₃); 17.94(CH₃); 18.23(CH₃); 19.81(CH₃); 24.68(C); 25.33(CH₂); 25.43(CH₂); 28.19(CH₂); 28.64(CH₂); 33.83(CH); 64.13(CH₂); 67.65(CH₂); 113.88(CH); 120.03(CH); 121.25(C); 121.60(CH); 124.76(C); 127.17(CH); 127.62(CH); 131.85(CH); 133.06(CH); 136.08(C); 138.01(C); 149.70(C); 154.75(C); 163.05(C); 164.35(C).

C ₃₇ H ₄₈ O ₆ Si	calcd	C 72.05	H 7.84
	found	C 72.16	H 7.91

Hexyl-6-oxy-[4'-(4''-dimethylhexylsiloxyphenyl)benzoyloxy]methacrylate (7b)



7b

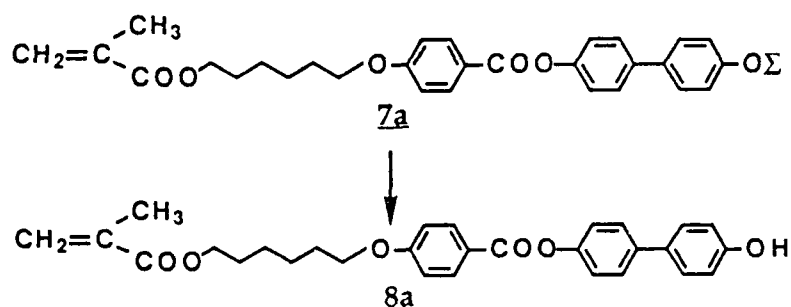
MW: 536.16

yield: 83%

¹H-NMR (300 MHz, CDCl₃): δ 0.23(s, 6H); 0.93(d, J=6.86 Hz, 6H); 0.94(s, 6H); 1.41(m, 4H); 1.62(m, 2H); 1.73(m, 2H); 1.74(m, 1H); 1.87(s, 3H); 4.04(t, J=6.97 Hz, 2H); 4.14(t, J=7.01 Hz, 2H); 5.55(s, 1H); 6.10(s, 1H); 6.83(d, J=7.01 Hz, 2H); 6.94(d, J=8.9 Hz, 2H); 7.31(d, J=8.95 Hz, 2H); 8.10(d, J=8.84 Hz, 2H).

C ₃₁ H ₄₄ O ₆ Si	calcd	C 69.96	H 8.29
	found	C 69.29	H 8.37

Hexyl-6-oxy-[4'-[4''-(4'''-hydroxyphenyl)]phenyl]benzoyloxy]methacrylate (8a)



A dry, 250 ml single-necked flask fitted with a Claisen adapter connected to a nitrogen inlet and a septum was charged with 7a (11.000 g, 0.018 mole) and dry THF (100 ml). The solution was cooled to -78°C and n-tetrabutylammonium fluoride (26.7 ml of a 1N solution in THF, 0.027 mole) was added dropwise through a syringe. After stirring the resulting pale yellow solution at -78°C for 1h, a small quantity of the reaction mixture was removed and extracted with ether and washed with 1N HCl. TLC analysis (developed with 35% acetone in petroleum ether) of the ether layer showed that no starting material remained. At this point, a solution of acetic acid (5 ml) in ether (50 ml) was added in one portion to the flask at -78°C and the mixture was transferred to a separatory funnel containing ether (200 ml) and saturated sodium bicarbonate (300 ml). The layers were separated, the organic phase washed with water (3x200), dried (Na_2SO_4), and concentrated. Purification was achieved by flash chromatography (silica, 35% acetone in petroleum ether) followed by recrystallization from a mixture of heptane and isopropanol (2:1). A similar procedure was employed to convert 6b to 8b.

8a

MW: 474.53

yield: 81% after purification

mp: 127-130°C

MS (70 eV): 474(7, M⁺), 290(34), 289(100), 185(11), 121(79).

IR (KBr disc, ν_{\max} , cm⁻¹): 3309, 2443, 2858, 1886, 1731, 1682, 1604, 1562, 1506, 1435, 1302, 1252, 1196, 1154, 1055, 985, 942, 872, 844, 794, 752.

¹H-NMR (300 MHz, d₆-DMSO): δ 1.43(m, 4H); 1.62(m, J=6.72 Hz, 2H); 1.75(m, J=6.57 Hz, 2H); 1.87(s, 3H); 4.06(2t, J=6.67 Hz, 4H); 5.65(s, 1H); 6.01(s, 1H); 6.83(d, J=8.62 Hz, 2H); 7.09(d, J=8.98 Hz, 2H); 7.26(d, J=8.68 Hz, 2H); 7.48(d, J=8.67 Hz, 2H); 7.61(d, J=8.72 Hz, 2H); 7.64(d, J=8.91 Hz, 2H); 9.58(s, 1H).

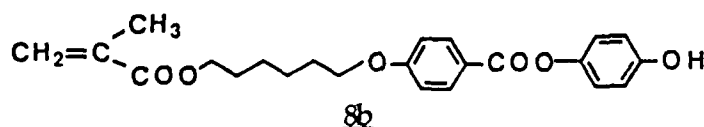
¹³C-NMR (75 MHz, d₆-DMSO): δ 17.69(CH₃); 24.91(CH₃); 25.02(CH₂); 27.87(CH₂); 28.24(CH₂); 64.00(CH₂); 67.76(CH₂); 114.41(CH); 115.63(CH); 120.84(CH₂); 121.87(CH); 124.98(C); 126.66(CH); 127.48(CH); 130.04(C); 131.74(C); 135.91(C); 137.74(C); 149.33(C); 157.07(C); 163.02(C); 164.02(C); 166.35(C).

C₂₉H₃₀O₆

calcd C 73.46 H 6.36

found C 73.52 H 6.41

Hexyl-6-oxy-[4'-(4''-hydroxyphenyl)benzoyloxy]methacrylate (8b)



8b

MW: 398.53

yield: 84% after purification

mp: 96-97°C

MS (70 eV): 398(14, M⁺), 290(100), 289(100), 219(12), 203(32), 133(21), 122(59), 120(57).

IR (KBr disc, ν_{\max} , cm⁻¹): 3380, 2929, 2858, 1724, 1682, 1590, 1506, 1464, 1433, 1309, 1252, 1182, 1161, 1062, 992, 928, 837.

¹H-NMR (300 MHz, d₆-DMSO): δ 1.41(m, 4H); 1.61(m, J=6.77 Hz, 2H); 1.72(m, J=6.63

Hz, 2H); 1.86(s, 3H); 4.05(2t, J=7.07 Hz, 4H); 5.65(s, 1H); 6.01(s, 1H); 6.77(d, J=8.87 Hz, 2H); 7.00(d, J=8.86 Hz, 2H); 7.06(d, J=8.91 Hz, 2H); 8.01(d, J=8.9 Hz, 2H); 9.46(s, 1H).

^{13}C -NMR (75 MHz, d_6 -DMSO): δ 18.02(CH_3); 25.21(CH_2); 25.31(CH_2); 28.11(CH_2); 28.51(CH_2); 64.26(CH_2); 67.86(CH_2); 114.46(CH); 115.63(CH); 121.17(CH_2); 122.56(CH); 125.40(C); 131.86(CH); 136.05(C); 142.89(C); 155.18(C); 163.06(C); 164.60(C); 166.53(C).

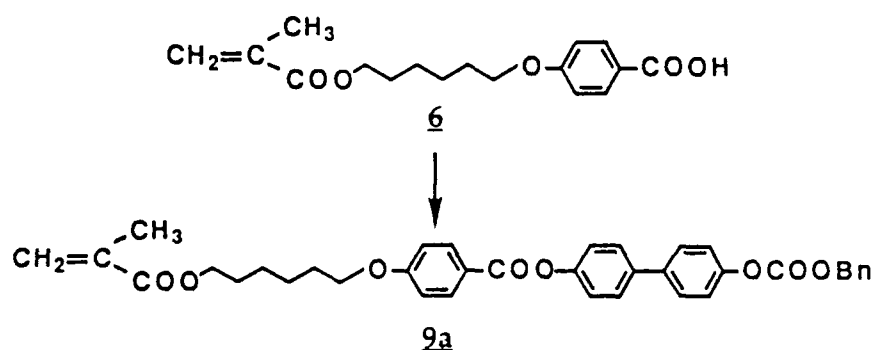
$\text{C}_{23}\text{H}_{26}\text{O}_6$

calcd C 69.33 H 6.58

found C 69.13 H 6.62

2.4.2.2: Protected Monomer Synthesis

Hexyl-6-oxy-[4'-[4''-(4'''-benzyloxycarbonyloxyphenyl)phenyl]benzoyloxy]-methacrylate (9a)



A 100 ml single-necked flask equipped with a stir bar and a Claisen adapter with a nitrogen inlet and a septum was charged with **6** (1.500 g, 4.987 mmol), **2a** (1.721 g, 5.373 mmol), DPTS (0.288 g, 0.978 mmol) and 1,3-dicyclohexylcarbodiimide (1.513 g, 7.334 mmol). The reaction flask was flushed with nitrogen and dry dichloromethane (50 ml) was added *via* syringe. Instantly, urea precipitated out of solution. Stirring continued overnight following which urea was filtered off and the solution concentrated. Analytically

pure monomer was obtained by two recrystallizations from ethanol followed by isopropanol-heptane mixture. An identical procedure was used with equal success to synthesize **9b**.

9a

MW: 608.66

yield: 50% after recrystallizations

mp: 70-71 °C

MS (70 eV): 608(14, M⁺), 291(41), 290(100), 219(15), 204(33)

IR (KBr disc, ν_{max} , cm⁻¹): 2929, 2844, 1772, 1590, 1492, 1449, 1379, 1252, 1196, 1154, 1062, 992.

¹H-NMR (300 MHz, CDCl₃): δ 1.40(m, J=6.18 Hz, 4H); 1.62(m, J=6.72 Hz, 2H); 1.73(m, J=6.94 Hz, 2H); 1.87(s, 3H); 4.06(m, J=6.41 Hz, 4H); 5.29(s, 2H); 5.65(s, 1H); 6.01(s, 1H); 7.09(d, J=8.9 Hz, 2H); 7.33(2d, J=8.62 Hz, 4H); 7.40(m, 5H); 7.72(2d, J=8.64 Hz, 4H); 8.06(d, J=8.83 Hz, 2H).

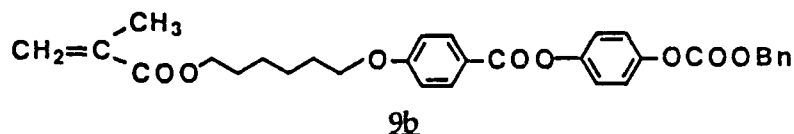
¹³C-NMR (75 MHz, d₆-DMSO): δ 17.97(CH₃); 25.72(CH₂); 25.38(CH₂); 28.12(CH₂); 28.57(CH₂); 64.15(CH₂); 67.63(CH₂); 69.90(CH₂); 113.90(CH); 120.97(CH); 121.05(CH₂); 121.81(CH); 124.88(C); 127.59(CH); 127.63(CH); 128.08(CH); 128.27(CH); 128.32(CH); 131.88(CH); 134.40(C); 136.03(C); 137.13(C); 150.17(C); 150.24(C); 153.14(C); 163.05(C); 164.30(C); 166.89(C).

C₃₇H₃₆O₈

calcd C 73.01 H 5.96

found C 72.98 H 6.08

Hexyl-6-oxy-[4'-(4''-benzyloxycarbonyloxyphenyl)benzoyloxy]methacrylate (9b)



9b

MW: 532.57

yield: 60% after recrystallizations

mp: 85-86°C

MS (70 eV): 533(30, M⁺), 425(40), 323(40), 289(100), 221(68), 155(40), 121(100)

IR (KBr disc, ν_{\max} , cm⁻¹): 2929, 2858, 1752, 1724, 1604, 1506, 1379, 1316, 1259, 1189, 1154, 1062, 1006, 935, 837.

¹H-NMR (300 MHz, d₆-DMSO): δ 1.35(m, 4H); 1.55(m, J=6.64 Hz, 2H); 1.66(m, J=6.54 Hz, 2H); 1.80(s, 3H); 4.01(m, J=6.43 Hz, 4H); 5.21(s, 2H); 5.58(s, 1H); 5.94(s, 1H); 7.02(d, J=8.62 Hz, 2H); 7.26(m, 5H); 7.32(2d, J=8.62 Hz, 4H); 7.98(d, J=8.81 Hz, 2H).

¹³C-NMR (75 MHz, CDCl₃): δ 18.16(CH₃); 25.48(CH₂); 25.57(CH₂); 28.33(CH₂); 28.76(CH₂); 64.37(CH₂); 67.76(CH₂); 70.19(CH₂); 114.09(CH); 121.08(CH₂); 121.71(CH); 122.52(CH); 125.09(C); 128.34(CH); 128.49(CH); 128.58(CH); 132.09(CH); 134.50(C); 136.24(C); 148.20(C); 148.38(C); 152.28(C); 163.30(C); 164.44(C); 167.22(C).

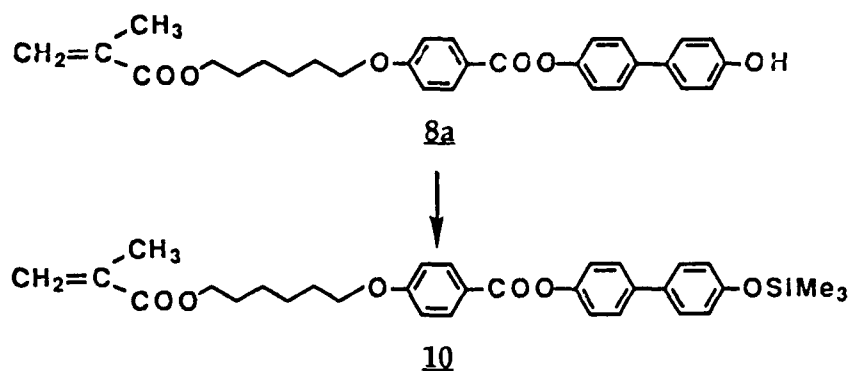
C₃₁H₃₂O₈

calcd C 69.91 H 6.06

found C 69.78 H 6.11

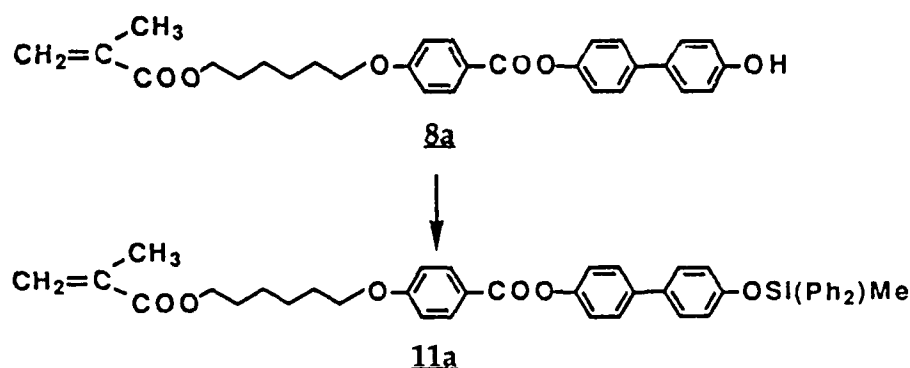
Hexyl-6-oxy-[4'-[4''-(4'''-trimethylsiloxyphenyl)phenyl]benzoyloxy]methacrylate

(10)



A 10 ml single-necked flask equipped with a Claisen adapter connected to a nitrogen inlet and a septum was charged with 8a (200 mg, 0.421 mmole). The reaction flask was thoroughly purged with argon and the solid was dissolved in freshly dried THF (2 ml). Triethylamine (0.064 ml, 0.463 mmole) and chlorotrimethylsilane (0.059 ml, 0.463 mmole) were added dropwise *via* syringe. Within 10 min of stirring, triethylamine hydrochloride precipitated out of solution. Stirring continued for additional 8h at ambient temperature under argon atmosphere. TLC analysis at this point (developed with 18% acetone in petroleum ether) showed no trace of starting material in the reaction mixture. Attempts to purify the protected monomer by preparative TLC (neutral silica) offered little success. Triethylamine hydrochloride was carefully filtered off under nitrogen atmosphere and the resultant clear solution was immediately transferred *via* a syringe to the flame dried polymerization flask.

Hexyl-6-oxy-[4'-[4''-(4'''-diphenylmethylsiloxyphenyl)phenyl]benzoyloxy]-methacrylate (11a)



A 250 ml single-necked flask equipped with a stir bar and a Claisen adapter connected to a nitrogen inlet and a septum was charged with **8a** (7.700 g, 0.013 mole) and 4-DMAP (0.339 g, 0.003 mole). The reaction flask was thoroughly flushed with nitrogen and the contents were then dissolved in dry THF (100 ml). To the resultant clear solution, dry triethylamine (1.938 ml, 0.014 mole) followed by chlorodiphenylmethylsilane (2.30 ml, 0.014 mole) were added dropwise *via* syringe with continuous stirring. Within 10 min, triethylaminehydrochloride precipitated out of solution. Stirring continued overnight at room temperature under nitrogen atmosphere. The next morning, the reaction mixture was transferred to a separatory funnel containing 100 ml ether and washed with water (2x100) and brine (1x200). The organic phase was dried over Na₂SO₄ and concentrated to obtain a viscous oil. Purification by flash chromatography (silica, 12% acetone in petroleum ether) yielded analytically pure crystalline solid. The same procedure was employed to synthesize **11b** from **8b**.

11a

MW: 670.84

yield: 87-91% after purification

mp: 56-57°C

MS (70 eV): 670(12, M⁺), 290(18), 289(100), 197(14), 121(68), 69(16)

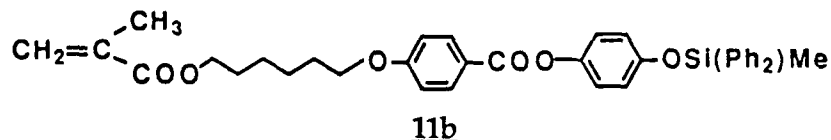
¹H-NMR (300 MHz, CDCl₃): δ 0.75(s, 3H); 1.46(m, 4H); 1.69(m, J=7.03 Hz, 2H); 1.78(m, J=7.08 Hz, 2H); 1.9(s, 3H); 4.03(t, J=6.4 Hz, 2H); 4.10(t, J=6.59 Hz, 2H); 5.51(s, 1H); 6.06(s, 1H); 6.85(d, J=8.64 Hz, 2H); 6.91(d, J=8.92 Hz, 2H); 7.16(d, J=8.64 Hz, 2H); 7.37(m, 10H); 7.48(d, J=8.63 Hz, 2H); 7.62(d, J=9.01 Hz, 2H); 8.09(d, J=8.92 Hz, 2H).
¹³C-NMR (75 MHz, CDCl₃): δ -2.64(CH₃); 18.12(CH₃); 25.57(CH₂); 25.65(CH₂); 28.43(CH₂); 28.87(CH₂); 64.67(CH₂); 67.97(CH₂); 114.21(CH); 120.16(CH); 121.57(CH₂); 121.83(CH); 125.10(C); 127.54(CH); 127.72(CH); 127.90(CH); 130.07(CH); 132.16(CH); 133.72(C); 134.26(CH); 135.25(C); 136.28(C); 138.24(C); 150.00(C); 154.61(C); 163.34(C); 164.79(C); 167.34(C).

C₄₂H₄₂O₆Si

calcd C 75.19 H 6.31

found C 74.99 H 6.23

Hexyl-6-oxy-[4'-(4''-diphenylmethoxysiloxymethyl)benzoyloxy]methacrylate (11b)



11b

MW: 594.74

yield: 84% after purification

MS (70 eV): 594(32, M⁺), 374(11), 290(100), 214(14), 203(30), 199(45).

¹H-NMR (300 MHz, CDCl₃): δ 0.77(s, 3H); 1.49(m, 4H); 1.71(m, J=6.99 Hz, 2H); 1.81(m, J=7.16 Hz, 2H); 1.94(s, 3H); 4.02(t, J=6.39 Hz, 2H); 4.15(t, J=6.58 Hz, 2H); 5.50(s, 1H); 6.10(s, 1H); 6.84(d, J=8.75 Hz, 2H); 6.98(d, J=8.97 Hz, 2H); 7.40(m, 10H); 7.65(d, J=9.06 Hz, 2H); 8.09(d, J=8.86 Hz, 2H).

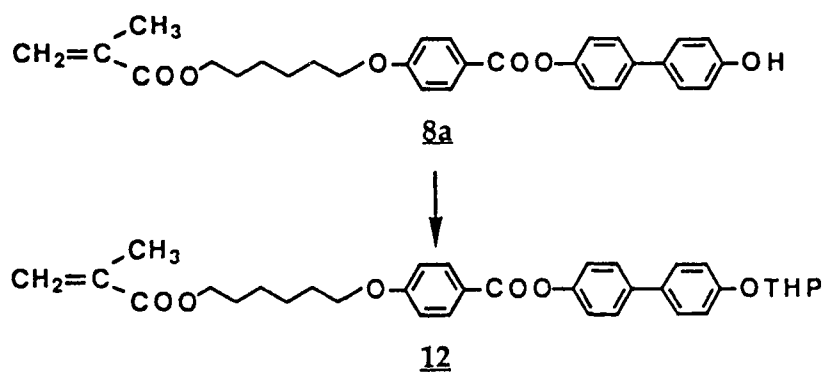
^{13}C -NMR (75 MHz, CDCl_3): δ -3.02(CH_3); 18.01(CH_3); 25.31(CH_2); 25.4(CH_2); 28.17(CH_2); 28.6(CH_2); 64.25(CH_2); 67.64(CH_2); 113.90(CH); 120.13(CH); 125.25(CH_2); 122.19(CH); 125.03(C); 127.72(CH); 129.90(CH); 131.84(CH); 134.00(CH); 134.82(C); 136.04(C); 144.89(C); 152.21(C); 163.02(C); 164.67(C); 167.05(C).

$\text{C}_{36}\text{H}_{38}\text{O}_6\text{Si}$

calcd C 72.70 H 6.44

found C 72.79 H 6.35

Hexyl-6-oxy-[4'-(4''-(4'''-tetrahydropyranyloxyphenyl)phenyl]benzoyloxy]-methacrylate (12)



A 100 ml, single-necked flask equipped with a stir bar and a Claisen adapter connected to a nitrogen inlet and a septum was charged with **8a** (1.000 g, 2.107 mmole) and PTSA (50 mg, 0.263 mmole). The flask was thoroughly flushed with nitrogen and the contents were dissolved in dry dichloromethane (25 ml). 3,4-dihydropyran (0.288 ml, 3.157 mmoles) was added *via* syringe and the contents were stirred at ambient temperature for 4h. After ensuring by TLC that no starting material remained unreacted (developed with 15% acetone in petroleum ether), the solution was transferred to a separatory funnel containing 100 ml ether. The ether layer was washed with water (3x100), brine (1x100) and

dried over Na_2SO_4 . Concentration yielded a light yellow solid which was first purified by flash chromatography (silica, 30% acetone in petroleum ether) and then followed by recrystallization from heptane.

12

MW: 558.65

yield: 60% after recrystallization

mp: 96-97°C

MS (70 eV): 558(12, M^+), 474(57), 290(100), 289(100), 203(15), 186(32), 185(25).

^1H -NMR (300 MHz, CDCl_3): δ 1.49(m, 4H); 1.61(m, 4H); 1.72(m, 8H); 1.92(s, 3H); 3.58(m, 1H); 3.91(m, 1H); 4.05(t, $J=7.07$ Hz, 2H); 4.19(t, $J=6.98$ Hz, 2H); 5.48(t, 1H); 5.65(s, 1H); 6.01(s, 1H); 6.98(d, $J=8.87$ Hz, 2H); 7.19(d, $J=8.89$ Hz, 2H); 7.24(d, $J=8.86$ Hz, 2H); 7.51(d, $J=8.91$ Hz, 2H); 7.60(d, $J=8.93$ Hz, 2H); 8.21(d, $J=8.93$ Hz, 2H).

$\text{C}_{34}\text{H}_{38}\text{O}_4$	calcd	C 73.09	H 6.86
	found	C 73.02	H 6.98

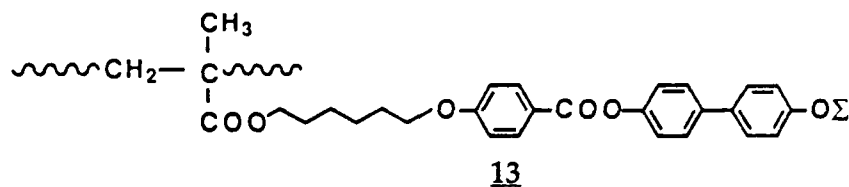
2.4.2.3: Protected Polymer Synthesis

General Polymerization Procedure

A single-necked flask containing a stir bar was fitted with a Claisen adapter. One end of the adapter was connected to a septum and the other end was attached to a reflux condenser with an argon inlet. The whole set up was assembled hot, flame dried and flushed thoroughly with argon. The assembly was evacuated for ca 15 min and flushed again with argon. Two pear shaped flasks were connected to septa while hot and allowed to cool under inert atmosphere of argon. Into one of the flasks the preweighed monomer was transferred by momentarily removing the septum. Similarly, into the other flask was transferred the initiator, AIBN, (1-2 mole%). The monomer was

dissolved in freshly dried THF (0.8-1 ml per 100 mg monomer) and was transferred to the polymerization flask *via* syringe. The initiator was dissolved in THF (0.003 g in 0.2-0.3 ml) and added to the monomer solution. In some cases it was more convenient to weigh accurately larger quantities of the initiator and use appropriate amounts of the solution. Polymerization was most successful when performed with minimum quantity of solvent (0.200 mmol in ca 1 ml THF). The polymerization flask was placed in an oil bath and the temperature was gradually increased to 75°C and maintained at that temperature for 12h. The solution was then cooled to room temperature, concentrated and redissolved in chloroform. The resultant solution was filtered under gravity, concentrated to near dryness and precipitated with a large excess of methanol. This procedure yielded analytically pure polymer in most cases. For some polymers, further purification was achieved by redissolution in CHCl₃ followed by precipitation with ether or pentane or a mixture of both the solvents. The resultant precipitate was refrigerated for 4h, collected by suction filtration and dried at 60°C for 18h in *vacuo*.

Poly(hexyl-6-oxy-{4'-[4''-(4'''-dimethylhexylsiloxyl)phenyl]phenyl}benzoyloxy)-methacrylate) (13)



13

FW: 616.79

dp: ca 200

yield: 88%

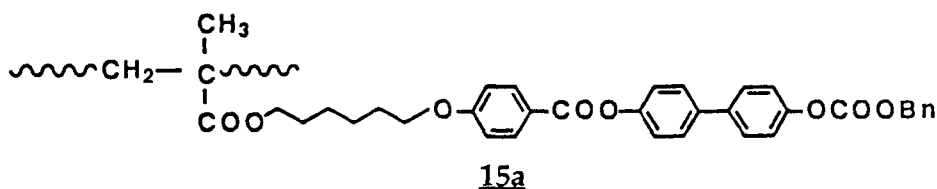
$^1\text{H-NMR}$ (300 MHz, CDCl_3): δ 0.22(b, 6H); 0.91(b, 2H); 1.08(b, 2H); 1.44(b, 4H); 1.66(b, 2H); 1.80(s, 3H); 4.01(b, 4H); 6.86(d, $J=8.54$ Hz, 2H); 6.92(d, $J=8.50$ Hz, 2H); 7.20(d, $J=8.70$ Hz, 2H); 7.38(b, 2H); 7.50(b, 2H); 8.10(d, $J=8.80$ Hz, 2H).

$(\text{C}_{37}\text{H}_{48}\text{O}_6\text{Si})_n$

calcd C 69.96 H 8.29

found C 69.20 H 8.06 N < 0.03

Poly(hexyl-6-oxy-{4'-[4''-(4'''-benzyloxycarbonyloxyphenyl)phenyl]benzoyloxy}-methacrylate) (15a)



15a

FW: 608.66

dp: ca 150

yield: 88%

mp: 134-142° C

IR (KBr disc, ν_{max} , cm^{-1}): 2929, 1717, 1591, 1485, 1379, 1252, 1189, 1154, 1062, 999, 837.

$^1\text{H-NMR}$ (300 MHz, CDCl_3): δ 0.89(b, 2H); 1.08(b, 2H); 1.45(b, 4H); 1.60(b, 2H); 1.77(b, 3H); 3.92(b, 4H); 5.28(b, 2H); 6.81(d, $J=8.79$ Hz, 2H); 7.21(2d, $J=8.81$ Hz, 4H); 7.29(b, 14H); 8.03(b, 2H).

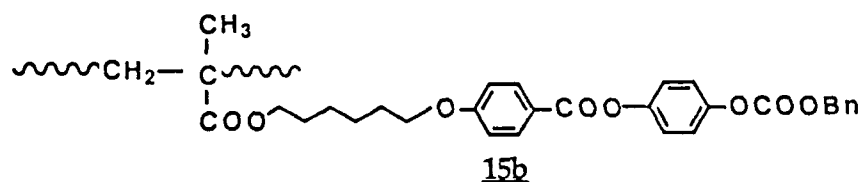
$(\text{C}_{37}\text{H}_{36}\text{O}_8)_n$

calcd C 73.01 H 5.96

found C 72.96 H 5.94 N 0.04

Poly(hexyl-6-oxy-[4'-(4''-benzyloxycarbonyloxyphenyl)benzoyloxy]methacrylate)

(15b)



15b

FW: 532.5

dp: ca 150

yield: 75%

mp: 82-87°C

IR (KBr disc, ν_{\max} , cm^{-1}): 2929, 1724, 1597, 1499, 1372, 1252, 1154, 1048, 999, 837, 759.

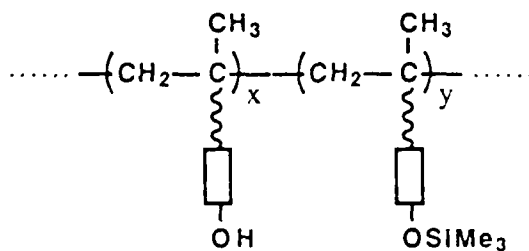
$^1\text{H-NMR}$ (300 MHz, CDCl_3): δ 0.91(b, 2H); 1.18(b, 2H); 1.46(b, 4H); 1.68(b, 2H); 1.81(b, 3H); 3.84(b, 4H); 5.25(b, 2H); 6.89(d, $J=8.80$ Hz, 2H); 7.20(2d, $J=8.84$ Hz, 4H); 7.31(b, 5H); 8.01(b, 2H).

$(\text{C}_{31}\text{H}_{32}\text{O}_9)_n$

calcd C 69.91 H 6.06

found C 69.59 H 6.01 N 0.07

1d



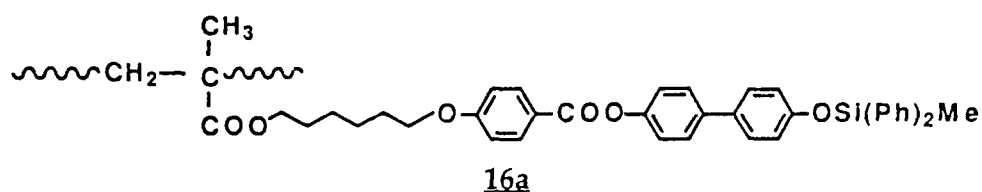
1d

yield: 74%

dp: ca 50

$^1\text{H-NMR}$ (300 MHz, $d_7\text{-DMF}$): δ 0.73(s, 1/2H); 0.96(b, 2H); 1.00(b, 2H); 1.45(b, 4H); 1.65(b, 2H); 1.76(b, 3H); 4.02(b, 2H); 6.89(b, $J=8.41$ Hz, 2H); 7.03(b, 2H); 7.44(b, 2H); 7.56(b, 2H); 8.06(b, 2H); 9.77(s, 1H).

Poly(hexyl-6-oxy-(4'-[4''-(4'''-diphenylmethylsiloxypheyl)phenyl]benzoyloxy)-methacrylate) (16a)



16a

FW: 670.84

dp: ca 100

yield: 80%

$^1\text{H-NMR}$ (300 MHz, CDCl_3): δ 0.73(s, 3H); 0.91(b, 2H); 1.04(b, 2H); 1.43(b, 4H); 1.55(b, 2H); 1.76(b, 3H); 3.94(d, 4H); 6.85(2d, $J=8.25$ Hz, 4H); 7.09(d, $J=8.41$ Hz, 2H); 7.36(m, 10H); 7.62(2d, $J=8.24$ Hz, 4H); 8.03(d, $J=8.88$ Hz, 2H).

$^{13}\text{C-NMR}$ (75 MHz, CDCl_3): δ -2.65(CH_3); 18.01(CH_3); 20.22(CH_3); 25.70(CH_2); 25.87(CH_2); 28.03(CH_2); 28.09(CH_2); 28.93(CH_2); 64.98(CH_2); 67.96(CH_2); 114.14(CH); 120.16(CH); 121.56(CH); 121.85(CH); 127.46(C); 127.54(CH); 127.83(C); 127.95(CH); 130.11(C); 132.19(CH); 133.58(C); 134.27(CH); 135.19(C); 138.24(C); 149.84(C); 154.58(C); 163.25(C); 164.73(C); 164.79(C).

$(\text{C}_{42}\text{H}_{42}\text{O}_6\text{Si})_n$

calcd C 75.19 H 6.31

found C 75.42 H 6.33 N < 0.06

$^1\text{H-NMR}$ (300 MHz, CDCl_3): δ 0.92(b, 2H); 1.06(b, 2H); 1.45(b, 4H); 1.60(b, 4H); 1.64(b, 4H); 1.77(b, 3H); 3.59(b, 1H); 3.94(b, 5H); 5.41(b, 1H); 6.88(d, $J=8.60$ Hz, 2H); 7.04(d, $J=8.80$ Hz, 2H); 7.13(d, $J=8.91$ Hz, 2H); 7.40(2d, $J=8.84$ Hz, 4H); 8.05(d, $J=8.89$ Hz, 2H).

$(\text{C}_{34}\text{H}_{38}\text{O}_7)_n$

calcd C 73.09 H 6.89

found C 73.58 H 6.93 N < 0.03

2.4.2.4: Deprotection of Polymers

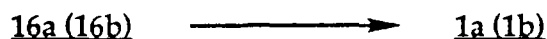


A single-necked 100 ml flask was charged with 0.800 g of 1d (1.460 mmoles) and THF (50 ml). To the clear solution that was obtained after stirring the contents for 20 min, acetic acid (15 ml) and water (6 ml) were added and stirring continued for 1h at room temperature. By the end of this time, the solution became slightly turbid and hence additional THF (10 ml) was added to get back a clear solution. After stirring the contents for 3h, the solution was poured into excess ether and the resulting suspension was refrigerated for 3h. The solid product was collected by suction filtration and dried in *vacuo* at 60°C for 20h. The solid product was characterized by $^1\text{H-NMR}$, IR and elemental analysis to be 1a.



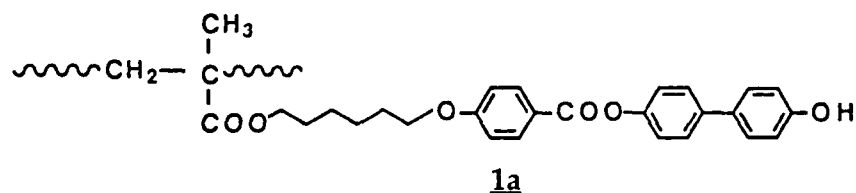
A single-necked 100 ml flask containing a stir bar was charged with 17 (0.250 g, 0.480 mmole of functional groups) and THF (25 ml). To the resultant clear solution, trifluoroacetic acid (3ml) and water (2 ml) were added and the contents stirred for additional 8h at room temperature. A homogeneous clear solution remained throughout the course of stirring. After 8h, the polymer was

precipitated into excess ether, filtered and dried in *vacuo* at 60°C for 20h. The polymer obtained by this deprotection was identified to be 1a.



A 100 ml single-necked flask containing a stir bar was charged with polymer 16a (0.575 g, 0.857 mmol of functional groups). THF (30 ml) was added *via* syringe and the contents were stirred at room temperature till a clear solution was obtained (ca 15 min). To the resultant homogeneous solution, added *via* syringe, trifluoroacetic acid (7.66 ml, 99.430 mmoles) followed by water (1.20 ml, 66.666 mmoles). The reaction flask was stoppered and contents were stirred at room temperature. Within 10 min, the solution became turbid and additional THF (10 ml) was added to keep the polymer from precipitating out of solution. The clear solution was stirred for additional 3h, concentrated and precipitated into excess ether. The resultant suspension was refrigerated for 2h following which, the polymer was collected by suction filtration and dried in *vacuo* at 60°C for 20h.

Poly(hexyl-6-oxy-[4'-[4''-(4'''-hydroxyphenyl)phenyl]benzoyloxy]methacrylate) (1a)



1a

FW: 474.53

dp: ca 100

yield: 90%

mp: 145-164°C

IR (KBr disc, ν_{\max} , cm^{-1}): 3410, 2942, 2850, 1734, 1705, 1604, 1582, 1511, 1500, 1468, 1442, 1420, 1401, 1263, 1216, 1164, 1079, 1002, 846, 820, 742.

^1H -NMR (300 MHz, d_7 -DMF): δ 0.96(b, 2H); 1.00(b, 2H); 1.45(b, 4H); 1.65(b, 2H); 1.76(b, 3H); 4.02(b, 4H); 6.89(d, $J=8.41$ Hz, 2H); 7.04(b, 2H); 7.23(b, 2H); 7.45(b, 2H); 7.56(b, 2H); 8.06(b, 2H); 9.78(s, 1H).

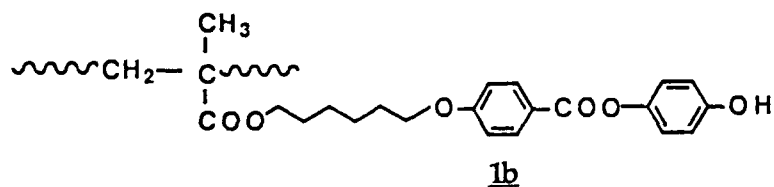
^{13}C -NMR (75 MHz, d_7 -DMF): δ 18.81(CH_3); 19.91(CH_3); 26.24(CH_2); 26.56(CH_2); 28.78(CH_2); 29.39(CH_2); 31.06(CH_2); 65.44(CH_2); 69.00(CH_2); 115.37(CH); 116.56(CH); 122.31(C); 122.83(CH); 127.67(CH); 128.52(CH); 131.49(C); 132.74(CH); 139.05(C); 150.69(C); 158.45(C); 162.88(C); 162.94(C); 164.30(C); 165.11(C)

($\text{C}_{29}\text{H}_{30}\text{O}_6$)_n calcd C 73.46 H 6.36

found C 73.38 H 6.34

Poly(hexyl-6-oxy-[4'-(4''-dimethylhexylsiloxylphenyl)benzoyloxy]methacrylate)

(**1b**)



1b

FW: 398.44

dp: ca 80

yield: 82%

IR (KBr disc, ν_{\max} , cm^{-1}): 3420, 2942, 2854, 1728, 1704, 1606, 1577, 1512, 1457, 1448, 1420, 1387, 1354, 1312, 1257, 1166, 1072, 1007, 873, 845, 822, 803, 762.

^1H -NMR (300 MHz, d_7 -DMF): δ 0.94(b, 2H); 1.08(b, 2H); 1.46(b, 4H); 1.65(b, 2H);

1.77(b, 3H); 4.05(b, 4H); 6.85(d, J=8.54 Hz, 2H); 7.04(2d, J=8.81 Hz, 4H); 8.04(d, J=8.80 Hz, 2H); 9.67(s, 1H).

$(C_{23}H_{26}O_6)_n$	calcd	C 69.33	H 6.58
	found	C 68.92	H 6.54

References

- (1) Blumstein, A., (ed) in *Mesomorphic Order in Polymers and Polymerization in Liquid Crystalline Media*, ACS Symp Ser., 1978, 74.
- (2) Shibaev, V. and Plate', N. A., *Polym. Sci. USSR.*, 1977, 19, 1065.
- (3) Blumstein, A. and Hsu, E.C., in *Liquid Crystalline Order in Polymers*, ed. Blumstein, A., (Academic Press, NY), 1978, 105.
- (4) Wendorff, J. H., in *Liquid Crystalline Order in Polymers*, *ibid.*, 1978, 1.
- (5) Finkleman, H. and Rehage, G., *Adv. Polym. Sci.*, 1984, 60/61, 99.
- (6) Finkleman, H., Ringsdorf, H. and Wendorf, J. H., *Makromol. Chem.*, 1978, 179, 273.
- (7) Finkleman, H., Happ, M., Portugall, M. and Ringsdorf, H., *Makromol. Chem.*, 1978, 179, 2541.
- (8) Blumstein, A., (ed) *Polymeric Liquid Crystals* (Plenum, NY), 1985.
- (9) Chapoy, L., (ed) *Recent Advances in Liquid Crystalline Polymers*, (Elsevier Applied Science, London), 1985.
- (10) Shibaev, V. P. and Plate', N. A., *Adv. Polym. Sci.*, 1984, 60/61, 173.
- (11) Cifferi, A., Krigbaum, W. and Meyer, R., (eds) *Polymer Liquid Crystals*, (Academic Press, NY), 1982.
- (12) Hinov, H., *Mol. Cryst. Liq Cryst.*, 1986, 136, 221.

- (13) Plate', N. A. and Shibaev, V. P., (eds) *Comb Shaped Polymers and Liquid Crystals*, (Plenum, NY), 1988.
- (14) Ringsdorf, H., Schlarb, B. and Venzmer, J., *Angew. Chem., Int. Ed. Engl.* 1988, 27, 113.
- (15) Griffin, A., Hall, C., Hoyle, C., Venkatram, K. and McArdle, C., *MaKromol. Chem. Rapid Commun.*, 1988, 9, 463.
- (16) Griffin, A., Bhatti, A. and Hung, R., *Proc. SPIE*, 1986, 682, 65.
- (17) Coles, H. and Simon, R., *Polymer*, 1985, 26, 1801.
- (18) Shibaev, V., Kostromin, S., Plate', N. A., Ivanov, S., Yu Vetrov, V. and Yakolev, I., *Polym. Commun.*, 1983, 24, 364.
- (19) Le Grange, J., Kuzyk, M. and Singer, K., *Mol. Cryst. Liq. Cryst.*, 1987, 150b, 567.
- (20) Meredith, G. R., Van Dusen, J. G. and Williams, D. J., *Macromol.*, 1982, 15, 1385.
- (21) Le Barny, P., *SPIE Conf. Proc.*, 1986, 682, 56.
- (22) Lux, M., Strohreigl, P. and Hocker, H., *Makromol. Chem.*, 1987, 188, 811.
- (23) Chapoy, L., Munck, D., Rasmussen, K., Diekman, E. and Sethi, R., in *Recent Advances in Liquid Crystalline Polymers*, ed: Chapoy, L. L., (Elsevier Applied Science, London), 1985.
- (24) Cabrera, I. and Krongauz, V. A., *Macromol.*, 1981, 20, 2713.
- (25) Krongauz, V. A., Goldburt, E. S., *Macromol.*, 1981, 114, 1382.
- (26) Goldburt, E. S., Shvartsman, F. and Krongauz, V. A., *Macromol.*, 1987, 17, 1876.
- (27) Sirlin, C., Bosio, L. and Simon, T. J., *J. Chem. Soc., Chem. Commun.*, 1987, 379.
- (28) Wenz, G., *Makromol. Chem. Rapid Commun.*, 1985, 6, 572.
- (29) Decobert, G., Soyer, F. and Dubois, J. C., *Polym. Bull.*, 1985, 14, 179.

- (30) Guglielminetti, J. M., Decobert, G. and Dubois, J. C., *Polym. Bull.*, 1986, 16, 411.
- (31) Shibaev, V. and Plate', N. A., *Pure and Appl. Chem.*, 1985, 57, 1589.
- (32) Shibaev, V., Kozlovsky, M., Bersenev, L., Blinov, L. and Plate', N. A., *Polym. Bull.*, 1984, 12, 299.
- (33) Janini, G. M., Laub, R. J. and Shaw, T. J., *Makromol. Chem. Rapid Commun.*, 1985, 6, 57.
- (34) Janini, G. M., Laub, R. J., Plyter, J. G. L. and Shaw, T. J., *Mol. Cryst. Liq. Cryst.*, 1987, 153, 479.
- (35) Loth, H. and Eushen, A., *Makromol. Chem. Rapid Commun.*, 1988, 9, 35.
- (36) Rodriguez-Parada, J. and Percec, V., *Polymer Preprints*, 1986, 27, 360.
- (37) Hall, P., Davies, G., Ward, I., McIntyre, J., Bannister, D. and LeBrocq, K., *Polym. Commun.*, 1986, 27, 98.
- (38) Hall, P., Davies, G., Ward, I. and McIntyre, J., *Polym. Commun.*, 1986, 27, 100.
- (39) Keller, H. and Hatz, R., *Handbook of Liquid Crystals*, (Verlag Chemie, Weinheim), 1980.
- (40) Gray, G. W., (ed) *Molecular Structure and the Properties of Liquid Crystals*, (Academic Press, London), 1962.
- (41) Gray, G. W., in *Polymer Liquid Crystals*, eds : Cifferi, A., Krigbaum, W. R. and Meyers, R. B., (Academic Press, London), 1982, 1.
- (42) Gray, G. W., *Phil. Trans. R. Soc. London*, 1983, A309, 77.
- (43) Gray, G. W., *Proc. R. Soc. London*, 1985, A462, 1.
- (44) Luckhurst, C. R. and Gray, G. W., in *Molecular Physics of Liquid Crystals*, eds: Luckhurst, G. R. and Gray, G. W., (Academic Press, London), 1979, 1.
- (45) Toyne, K. J., in *Thermotropic Liquid Crystals*, ed: Gray, G. W., (John Wiley, NY), 1987, 28.

- (46) Apfel, M. A., Finkelmann, H., Janini, G. M., Laub, R. J.,Luhman, B. H.,Price, A., Roberts, W. L., Shaw, T. J. and Smith, C. A., *Anal. Chem.*, **1985**, *57*, 651.
- (47) Bresci, V., Frosini, A., Lupinacci, D. and Magagnini, P. L., *Makromol. Chem. Rapid Commun.*, **1980**, *1*, 183.
- (48) Baccaredda, M., Magagnini, P. L., pizzarini, G. and Turchi, G., *J. Polym. Sci., Polym. Lett.*, **1971**, *9*, 303.
- (49) Magagnini, P.L., Marchetti, A., Matsa, F., Pizzirani, G. and Turchi, G., *Eur. Polym. J.*, **1974**, *10*, 585.
- (50) Lupinacci, P., Frosini, V. and Magagnini, P. L., *Makromol. Chem. Rapid Commun.*, **1980**, *1*, 671.
- (51) Alimoglu, A. K., Ledwith, A., Gemmel, P. A., Gray, W. and Lacey, D., *Polymer*, **1984**, *25*, 1342.
- (52) Duran, R.,Guillon, D., Gramain, A. and Skoulois, A., *Makromol. Chem. Rapid Commun.*, **1987**, *8*, 181.
- (53) Clough, S. B., Blumstein, A. and DeVries, A., *ACS Polymer Preprints*, **1977**, *18*, 1.
- (54) Finkleman,H., Ringsdorf, H., Siol, W. and Wendorff, J. H. in *Mesomorphic Order in Polymers and Polymerization in Liquid Crystalline Media*, ed: Blumstein, A., ACS Symp. Ser., **1978**, *7*, 22.
- (55) Geib, H., Hisgen, B., Pschorn, V., Ringsdorf, H. and Spiess, H. W., *J. Amer. Chem. Soc.*, **1982**, *104*, 917.
- (56) Wassmer, K. H., Ohmes, E., Portugall, M., Ringsdorf, H. and Kothe, G., *J. Amer. Chem. Soc.*, **1985**, *107*, 1511.
- (57) Spiess, H. W., *Pure Appl. Chem.*, **1985**, *57*, 1617.
- (58) Engel, M., Hisgen, B., Keller, R., Kreuder, W., Reck, B., Ringsdorf, H., Schmidt, H. W. and Tschirner, P., *Pure Appl. Chem.*, **1985**, *57*, 1009.

- (59) Cser, F. in *Liquid Crystals and Ordered Fluids*, eds: Griffin, A. C. and Johnson, J. F., (Plenum, NY), 1984, 4, 945.
- (60) Kriste, R. G. and Ohm, H. G., *Makromol. Chem. Rapid Commun.*, 1985, 6, 179.
- (61) Keller, P., Carvacho, J. P., Lambert, M., Moussa, F. and Pepy, G., *J. Phys. Lett.*, 1985, 46, 1065.
- (62) Elbert, R., Laschewsky, A. and Ringsdorf, H., *J. Amer. Chem. Soc.*, 1985, 107, 4134.
- (63) Kunitake, T., Nayai, H., Takarabe, K. and Nakashima, N., *J. Macromol. Soc. Chem.*, 1984, A 21, 1273.
- (64) Laschewsky, A., Ringsdorf, H., Schmidt, G. and Schneider, J., *J. Amer. Chem. Soc.*, 1985, 107, 4134.
- (65) Finkleman, H., *Angew. Chem., Int. Ed. Engl.*, 1987, 26, 816.
- (66) Hsu, C. S. and Percec, V., *Polym. Bull.*, 1987, 17, 49.
- (67) Engel, M., Hisgen, B., Keller, R., Kreuder, W., Reck, B., Ringsdorf, H., Schmidt, H. W. and Tschirner, P., *Pure Appl. Chem.*, 1985, 57, 1007.
- (68) Rodriguez-Parada, J. and Percec, V., *J. Polym. Sci., Polym. Chem. Ed.*, 1986, 24, 1363.
- (69) Percec, V., Rodriguez-Parada, J. and Ericson, C., *Polym. Bull.*, 1987, 17, 353.
- (70) Duran, R., Gramain, P., Guillon, D. and Skoulois, A., *Mol. Liq. Cryst. Lett.*, 1986, 3, 23.
- (71) Duran, R. and Gramain, P., *Makromol. Chem.*, 1987, 188, 2001.
- (72) Kostromin, S. G., Shibaev, V. P. and Plate', N. A., *Liquid Crystals*, 1987, 2, 195.
- (73) Kim, C. and Allcock, H. R., *Macromol.*, 1987, 20, 1726.

- (74) Shibaev, V. P., Kostromin, S. G. and Plate', N. A., *Eur. Polym. J.*, 1982, 18, 651.
- (75) Zentel, R. and Ringsdorf, H., *Makromol. Chem. Rapid Commun.*, 1984, 5, 393.
- (76) Percec, V., Rodriguez-Parada, J. M. and Ericson, C., *Polym. Bull.*, 1987, 17, 347.
- (77) Frosini, A., Levita, G., Lupinacci, D. and Magagnini, P. L., *Mol. Cryst. Liq. Cryst.*, 1981, 66, 21.
- (78) Han, B., Wendorff, J. H., Portugall, H. and Ringsdorf, H., *Coll. Polym. Sci.*, 1981, 259, 875.
- (79) Kreuder, W., Webster, O. W., and Ringsdorf, H., *Makromol. Chem. Rapid Commun.*, 1986, 7, 5.
- (80) Pugh, C. and Percec, V., *ACS Polymer Preprints*, 1986, 26, 303.
- (81) Rodriguez-Parada, J. and Percec, V., *J. Polym. Sci., Polym. Chem. Ed.*, 1986, 24, 1363.
- (82) Percec, V. and Tomazos, D., *Polym. Bull.*, 1987, 18, 239.
- (83) Rodriguez-Parada, J. and Percec, V., *J. Polym. Sci., Polym. Chem. Ed.*, 1987, 25, 2269.
- (84) Cser, F., Nyotrai, K., Horvath, J. and Hardy, G., *Eur. Polym. J.*, 1985, 21, 259.
- (85) Reck, B. and Ringsdorf, H., *Makromol. Chem. Rapid Commun.*, 1985, 6, 291.
- (86) Berg, S., Kronr, V. and Ringsdorf, H., *Makromol. Chem. Rapid Commun.*, 1986, 7, 381.
- (87) Engel, M., Hisge, B., Keller, R., Kreuder, W., Reck, B., Ringsdorf, H., Schmidt, H. W. and Tschirner, P., *Pure Appl. Chem.*, 1985, 57, 1009.
- (88) Zentel, R., Reckert, G. and Reck, B., *Liquid Crystals*, 1987, 2, 83.

- (89) Flory, P. J., *J. Amer. Chem. Soc.*, 1939, 61, 3334.
- (90) Morawetz, A. in *Chemical Reactions on Polymers*, eds: Benham, J.Z. and Kriste, J. K., ACS Symp. Ser., 1987, 364, 317.
- (91) Paleos, C. M., Fillippakis, S. E. and Leonidopoulou, G. M., *J. Polym. Sci., Polym. Chem. Ed.*, 1981, 19, 1427.
- (92) Paleos, C. M., Leonidopoulou, G. M., Fillippakis, S. E., Malliaris, A. and Dais, P., *J. Polym. Sci., Polym. Chem. Ed.*, 1982, 20, 2267.
- (93) Pugh, C. and Percec, V., *Polym. Bull.*, 1985, 16, 513.
- (94) Pugh, C. and Percec, V. in *Chemical Reactions on Polymers*, eds: Benham, J.Z. and Kriste, J. K., ACS Symp. Ser., 1987, 364, 97.
- (95) Singler, R. E., Willingham, R. A., Lenz, R. W., Furakawa, A. and Finkleman, H., *Macromol.*, 1987, 20, 1727.
- (96) Kim, C. and Allcock, H. R., *Macromol.*, 1987, 20, 1726.
- (97) Keller, P., *Macromol.*, 1985, 17, 2937.
- (98) Keller, P., *Mol. Cryst. Liq. Cryst. Lett.*, 1985, 2, 101.
- (99) Keller, P., *Macromol.*, 1985, 18, 2337.
- (100) Keller, P., *Makromol. Chem. Rapid Commun.*, 1985, 6, 707.
- (101) Keller, P., *Macromol.*, 1987, 20, 462.
- (102) Pugh, C. and Percec, V., *Polym. Bull.*, 1986, 16, 521.
- (103) Gray, G. W., Lacey, D., Nestor, G and White, M. S., *Makromol. Chem. Rapid Commun.*, 1986, 7, 71.
- (104) Nester, G., White, M. S., Gray, G. W., Lacey, D. and Toyne, K. J., *Makromol Chem.*, 1987, 188, 2759.
- (105) Auman, B. C., Percec, V., Schneider, H. A. and Cantow, H. J., *Polymer*, 1987, 28, 1407.
- (106) Auman, B. C., Percec, V., Schneider, H. A., Jishan, W. and Cantow, H. J., *Polymer*, 1987, 28, 119.

- (107) Finkleman, H., Kock, H. and Rehage, G., *Makromol. Chem. Rapid Commun.*, **1981**, 2, 317.
- (108) Zhou, Q. F. and Lenz, R. W., *J. Polym. Sci., Polym. Chem. Ed.*, **1983**, 21, 3313.
- (109) Blumstein, A. and Kitagawa, N., *Mol. Cryst. Liq. Cryst*, **1971**, 12, 215.
- (110) Tanaka, Y., Hitosuganagi, M., Shimura, V., Okada, A. Z. and Sukurada, T., *MaKromol. Chem.*, **1976**, 177, 3035.
- (111) Blumstein, A. and Hsu, E., in *Liquid Crystalline Order in Polymers.*, ed: Blumstein, A., **1978**, 110.
- (112) Shibaev, V. P., Kostromin, S. G. and Plate', N. A., *Eur. Polym. J.*, **1982**, 18, 651.
- (113) Gunter, P., (ed), *Electro-Optic and Photorefractive Materials*, (Springer-Verlag, NY), **1986**, 17.
- (114) Blinov, L. M., (ed), *Electro-Optical and Magneto-Optical Properties of Liquid Crystals*, (John Wiley, NY), **1983**, 36.
- (115) Carpenter, M. M., Prasad, P. N. and Griffin, A. C., *Thin Solid Films*, **1988**, 161, 315.
- (116) Vickers, A. J., Tredgold, R. G., Hodge, P., Khoshdel, E. and Girling, I., *Thin Solid Films*, **1985**, 134, 43.
- (117) Carr, N., Goodwin, M. J., McRoberts, A. M., Gray, G. W., Marsden, R. and Scrowston, R. M., *MaKromol. Chem. Rapid Commun.*, **1987**, 8, 487.
- (118) Bader, H., Dorn, K., Hupfer, B. and Ringsdorf, H., *Adv. Polym. Sci.*, **1985**, 64, 1.
- (119) Tredgold, R. H., Young, M. C. J., Hodge, P. and Khoshdel, E., *Thin Solid Films*, **1987**, 151, 441.
- (120) Ringsdorf, H., Schneider, J. and Schuster, A., *3rd Int. Conf. on Langmuir-Blodgett Films*, F. R. G., **1987**, July, 26-31.

- (121) Byson, D. J., Gray, G. W. and Worrall, B. N., *J. Chem. Soc.*, **1965**, 3706.
- (122) Otterholm, B., Alstermark, C., Flatischler, K., Dahlgren, A., Lagerwall, S. and Skark, K., *Mol. Cryst. Liq. Cryst.*, **1987**, 146, 189.
- (123) Plueddemann, E. P., *Compos. Mater.*, **1974**, 204.
- (124) Drzal, L. T., *Adhesion*, **1985**, 18, 49.
- (125) Piggott, M. R., Sanadi, A., Chua, P. S. and Andison, D., in *Composite Interfaces*, eds: Ishida, I. and Koenig, J. L., **1986**, 109.
- (126) Portugall, M., Ringsdorf, H. and Zentel, R., *Makromol. Chem.*, **1982**, 183, 2311.
- (127) Rehage, G. and Frenzel, J., *Br. Polym. J.*, **1982**, 14, 173.
- (128) Kelker, H. and Wirzing, U., *Mol. Cryst. Liq. Cryst.*, **1979**, 49, 175.
- (129) Beihofer, T. W. and Glass, J. E., *J. Polym. Sci., Part A., Polym. Chem. Ed.*, **1988**, 26, 343.
- ((130) Bailey, D., Tirrel, D. and Vogl, O., *J. Polym. Sci., Polym. Chem. Ed.*, **1976**, 14, 2725.
- (131) Georgieff, K., K., *J. Appl. Polym. Sci.*, **1965**, 19, 2009.
- (132) Kurland, J. J., *J. Polym. Sci., Polym. Chem. Ed.*, **1980**, 18, 1139.
- (133) Olcott, H. S., *J. Amer. Chem. Soc.*, **1937**, 59, 392.
- (134) Colvin, E., (ed) in *Silicon in Organic Synthesis*, (Butterworths, London), **1981**, 20.
- (135) Wetter, H., Oertle, K., *Tetrahedron Lett.*, **1985**, 26, 5515.
- (136) Chaudhary, S. K. and Hernandez, O., *Tetrahedron Lett.*, **1979**, 99.
- (137) Jackson, A. E. and Johnstone, R. A. W., *Synthesis*, **1977**, 685.
- (138) Anantharamiah, G. M. and Sivanandhiah, K. M., *J. Chem. Soc., Perkin Trans.*, **1977**, 1, 490.
- (139) Felix, A. M., Heimer, H. P., Lambros, T. J., Tzougraki, C. and Meienhofer, J., *J. Org. Chem.*, **1982**, 43, 4199.

- (140) Mikolajczyk, M. and Kielbasinski, P., *Tetrahedron*, 1981, 37, 233.
- (141) Neiser, B., Steglich, W., *Angew. Chem., Int. Ed. Engl.*, 1978, 17, 522.
- (142) Moore, J. S. and Stupp, S. I., *Macromol.*, 1990, 23, 65.
- (143) Odian, G., (ed) in *Principles of Polymerization*, (Wiley Interscience Publication, NY), 1981, 246.
- (144) Anwer, M. K. and Spatola, A. F., *Synthesis*, 1980, 929.
- (145) McOmie, J. F. W., (ed) in *Protective Groups in Organic Chemistry*, (Plenum Press, NY), 1973, 60.
- (146) Watanabe, Y., Maki, Y. and Kikuchi, K., *Chem. Ind., (London)*, 1984, 2, 272.
- (147) Otsuji, Y., Matsamura, N. and Imoto, E., *Bull. Chem. Soc. of Japan*, 1971, 44, 852.
- (148) Otsuji, Y., Matsamura, N. and Imoto, E., *Bull. Chem. Soc. of Japan*, 1968, 41, 1485.
- (150) Sommer, L. H., (ed), *Stereochemistry, Mechanism and Silicon*, (McGraw Hill, NY), 1965, 130.
- (150) Denmark, S. E., Hammer, R. P. Weber, E. J. and Habermas, K. L., *J. Org. Chem.*, 1987, 165.
- (151) Still, W. C., Kahn, M. and Mitra, A., *J. Org. Chem.*, 1978, 44, 2923.

CHAPTER 3

Properties of Hydroxy-Functionalized Monomers,

Polymers and Derivatives

3.1: Structure-Property Correlations in Liquid Crystalline Compounds

The relationship between mesomorphic behavior and chemical constitution has been studied extensively by many to address fundamental questions concerning mesomorphism and molecular structure in organic compounds. These studies can reveal structural requirements for mesomorphism and the manner in which the chemical constitution of a compound determines whether the mesophase exhibited is smectic, nematic or cholesteric. In addition, they can also assist in the molecular interpretation of changes in mesomorphic phase transition temperatures.

Attempts to obtain such correlations were initiated by Vorlander (1) and Lehmann (2) soon after the discovery of the first mesomorphic compound in 1888 (3). The fact that attempts continue in this direction today is an indication that the correlations are neither simple nor obvious. However, considerable progress has been made and the basic structural criteria for mesomorphism as well as the relationship between the mesophase exhibited and the chemical structure are now much more thoroughly understood. In fact, most present day studies center around the last point, and seek to relate quite small changes in smectic-nematic, smectic-isotropic or nematic-isotropic transition temperatures to controlled changes in molecular shape, polarity and polarizability.

3.1.1: Structural Criteria

Compounds which exhibit thermotropic mesomorphic properties vary

widely in chemical constitution, but all possess the common feature of molecular geometric anisotropy. This issue was briefly discussed in the preceding chapter and we return to this once again, with due emphasis on the influence of substituents on mesomorphism. In predicting whether or not a particular substituent will affect mesomorphism as a whole, its influence on intermolecular interactions must enter into consideration, together with purely geometric aspects of the molecule itself. These intermolecular attractions in turn may originate from dipole-dipole attractions, induced-dipole attractions or dispersion forces.

Considering the last type of interaction first, attractions as a result of dispersion forces as such depend on the polarizability of a molecule. Generally speaking, the polarizability of an atom increases with increasing atomic radius, and the polarizability of a bond between two atoms increases with increasing bond order. As a simple example, if we compare a *trans* *p*-*n* alkoxy cinnamic acid (4) with *p*-*n* alkoxy benzoic acid (5) of the same molecular length, cinnamic acid exhibits a more thermally stable smectic and nematic mesophase because of its higher polarizability. In addition, the position of the substituent itself on the benzene ring is an important factor in determining mesomorphism, as this can affect the linearity of a molecule. In most cases, *ortho*- or *meta*-disubstituted

compound	S \rightarrow N ($^{\circ}$ C)	N \rightarrow I ($^{\circ}$ C)
$\text{C}_8\text{H}_{17}\text{O}-\text{C}_6\text{H}_4-\text{COOH}$	108	147
$\text{C}_8\text{H}_{17}\text{O}-\text{C}_6\text{H}_4-\text{CH}=\text{CH}-\text{COOH}$	146	175

benzenes do not possess mesomorphism whilst para- isomers do. This is so because any substitution that broadens a rod-like molecule will hinder parallel orientation and therefore, molecules are forced apart. Consequently, the interaction energy which is inversely proportional to the power of r , the distance between the attracting centers, i. e.

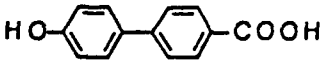
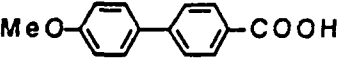
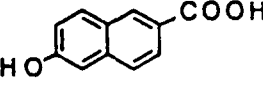
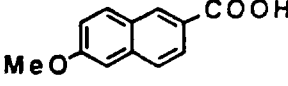
$$\text{Interaction energy} \propto \frac{1}{r^y} \quad (\text{where } y = 6 \text{ for the gas phase}) \quad \dots(3.1)$$

is affected adversely (6). For these reasons, most benzene derivatives which exhibit mesomorphism are para-substituted and on the same basis, 4,4'-disubstituted biphenyls and 4,4'-disubstituted p-terphenyls are frequently mesomorphic.

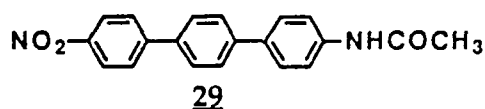
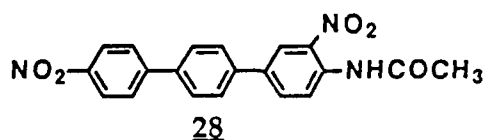
The introduction of dipolar groups into the parent molecule will undoubtedly increase the intermolecular interactions of the dipole-dipole and induced-dipole type, but again only if the separation of the molecular axes is not affected significantly. Commonly employed dipolar groups on the aromatic rings are -OR, -OCOR, -CO-, -COOH, NO₂ and -CN (7). Strong dipole-dipole interactions operate in most of these compounds in a favorable fashion. One particular type of intermolecular interaction that could assist mesomorphism in some cases and destroy this property in some others is the interaction *via* hydrogen bonding. For instance, association *via* hydrogen bonding has been claimed responsible for lack of mesomorphism associated with many phenolic and aromatic amino compounds (8-11). On the other hand, with carboxylic acids, this interaction has been shown to function in a reverse fashion (12, 13). Since phenolic compounds are the target systems for the present investigation, influence of intermolecular hydrogen bonding on mesomorphism in general merits some deeper attention.

3.1.1.1: Hydrogen Bonding and Mesomorphism

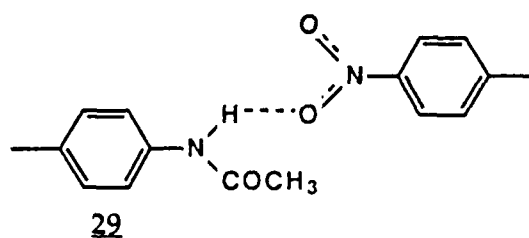
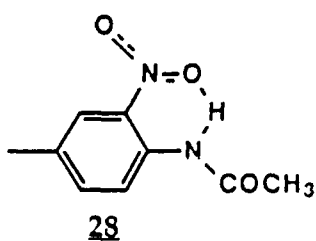
Hydrogen bonding in general, is of two types: intermolecular and intramolecular. When the association is of the former type, it increases the melting point of a compound significantly (5). This aspect in turn can have a profound influence on mesomorphism as a whole. The first examples of their influence on mesomorphism were provided by Gray and coworkers in the mid 1950's (8-10). Data from some of their investigations on phenolic compounds which emphasize the role of intermolecular association in these compounds is presented below. For instance, it was observed that phenolic compounds studied were non-mesomorphic, where as the corresponding alkoxy derivatives were indeed mesomorphic. This was attributed to the fact that in the former class of compounds, extensive intermolecular association is possible which raises the melting point of the compound significantly. Mesomorphism could be restored

Compound	Transition Temp. (°C)
	K 294 I (8, 9)
	K 258 N 300 I (8, 9)
	K 250 I (10)
	K 206 N 219 I (10)

by eliminating this association *via* hydrogen bonding by replacement of the phenolic hydrogen by an alkyl group. In a similar investigation with amino derivatives (11), they observed that two para-substituted terphenyl compounds, 28 and 29, had strikingly different properties. While 28 showed a nematic-isotropic transition around 230°C, 29 was found to be non-mesomorphic. This

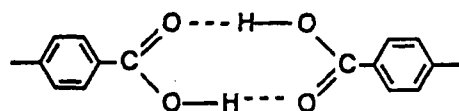


was in great contrast to the anticipated behavior based on their structural linearity. This anomalous behavior was explained on the basis that in the dinitro derivative, 28, only intramolecular hydrogen bonding is possible whilst in the mono derivative, intermolecular association occurs, as shown below. Based on these observations, Gray concludes: "*mesomorphic behavior is not to be expected in any system which will give rise to intermolecular hydrogen*

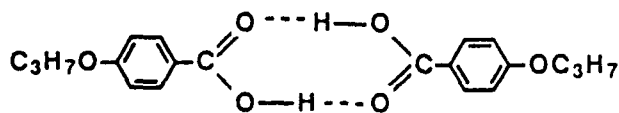
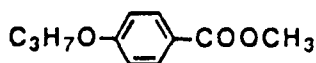


bonding effects as such an association not only increases the melting point markedly but also encourages the adoption of a non-linear arrangement of the molecules" (12).

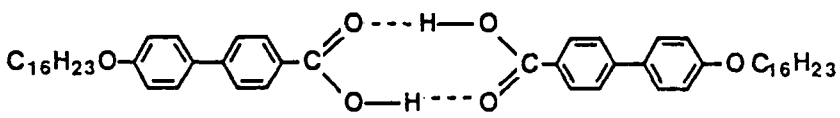
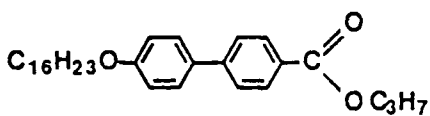
One particularly well recognized example of intermolecular hydrogen bonding has a reverse effect, increasing the tendency for mesophase formation by greatly lengthening the molecule. This refers to the dimerization of carboxylic acids by the intermolecular hydrogen bonding of the carboxyl groups as shown below:



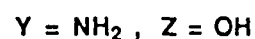
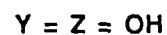
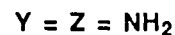
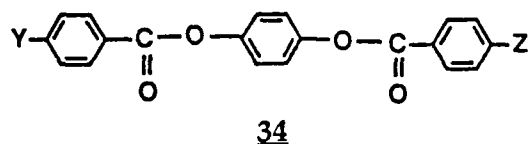
Such an association not only preserves the linearity of the molecule but also increases the molecular length, maintaining the intermolecular attractions at a suitably high level. The fact that this association is necessary in order that p-n alkoxy benzoic acids may exhibit mesophases is illustrated by the fact that these acids give non-mesomorphic alkyl esters. For instance, p-n-propyloxy benzoic acid (30) is mesomorphic where as the corresponding ester (31) is not (12). Only

3031

in the analogous biphenyl compounds are the lengths and polarizabilities of the monomeric esters great enough for mesomorphism to appear (13), although the thermal stabilities of their mesophases are much lower than those of the corresponding dimeric acids. Transition temperatures of compounds 32 and 33 shown below illustrate this point.

Compound	S \rightarrow I ($^{\circ}$ C)
 <p style="text-align: center;"><u>32</u></p>	241
 <p style="text-align: center;"><u>33</u></p>	91

Based on the guidelines discussed above, it is quite unsafe to make broad generalizations about the molecular characteristics which lead to mesomorphic behavior. To date, few exceptions to these generalizations on phenolic compounds are reported in the literature (14, 15). The fact that intermolecular hydrogen bonding is not a deterrent to mesomorphism in these compounds was first proven by Schroeder and Schroeder (14). They have reported mesomorphism in a series of aromatic diamines, phenols and amino phenols of the type shown as 34. Interestingly, in most of these compounds, smectic and nematic phases have been found to coexist in the liquid crystalline state.



Evidence in favor of this observation was derived from the fact that flashing nematic and focal-conic smectic textures coexist in these liquid crystalline melts. Their simultaneous occurrence has been ascribed to the end to end and sidewise hydrogen bonding possible in these compounds, such as that shown in figure 3.1. Vora and Gupta (15) have synthesized another extensive homologous series

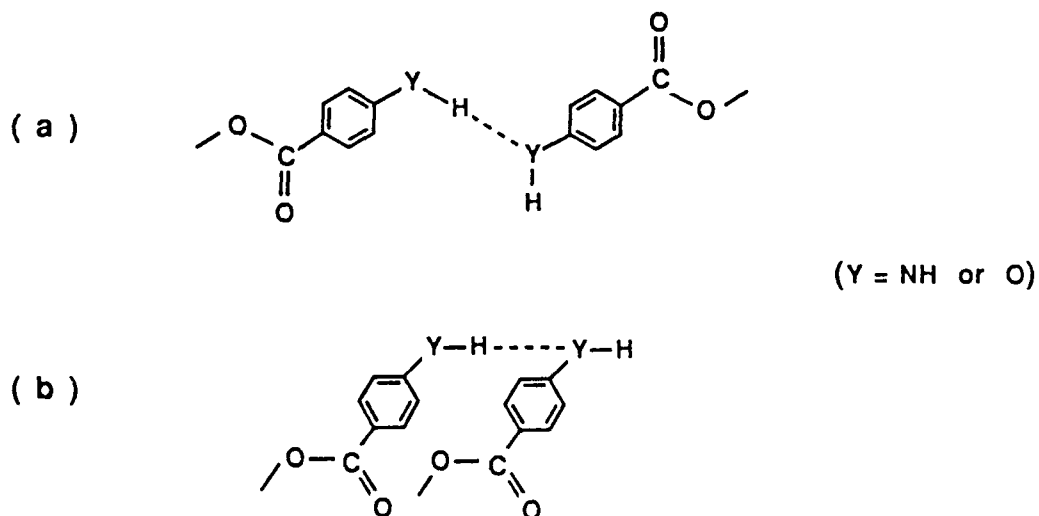
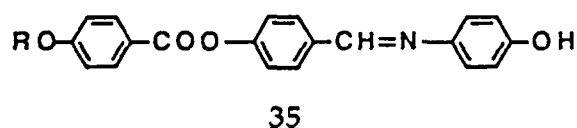


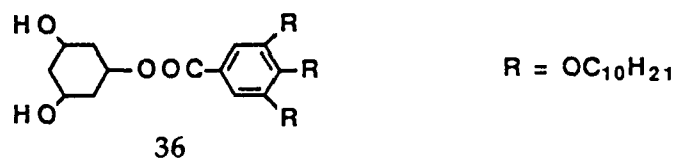
Figure 3. 1 : Schematic of (a) end to end and (b) sidewise hydrogen bonding that can lead to nematic and smectic ordering in phenolic compounds (14)

of phenolic derivatives of the type **35** that exhibit mesomorphic properties. Their finding is that nematic phases occur when R is small (C_1 - C_3), smectic and nematic phases occur with intermediate values of R (C_{10} - C_{14}) and only smectic phases result when R is long (C_{16} - C_{18}). These results are consistent with the

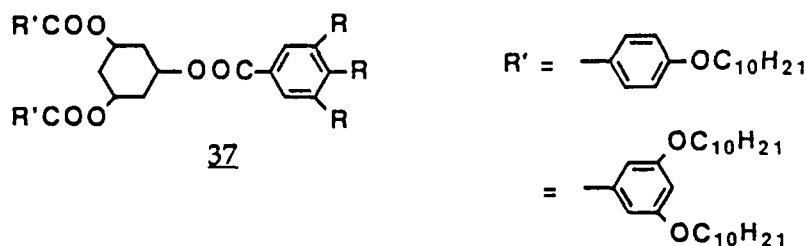
changes that occur when the length of the alkyl tail is altered (16). They propose end to end and sidewise hydrogen bonding mechanism of the type shown in figure 3.1 to explain the various mesophases formed in this series of compounds.



Very recently, the first examples of a new class of mesomorphic monomers containing hydroxyl groups of the type shown in 36 were reported by Lattermann and Stauffer (17). Somewhat contradictory to the earlier



generalizations, they report that the mesophase disappears following esterification of the two hydroxyl groups (as in 37) and conclude that association by hydrogen bonding is the main factor responsible for formation of liquid crystalline phases in these compounds.



3.1.2: Molecular Structure and Mesomorphism

In this section, very general structural requirements for compounds to exhibit smectic and nematic phases are presented. Considering the formation of a smectic mesophase first, the solid-smectic transition may be primarily viewed as weakening of the molecular attractions operating between the ends of molecules. Furthermore, since the smectic mesophase involves layers of parallel molecules that can move freely over one another, the cohesive forces between the sides of the molecules must be great enough to prevent molecules from moving out of the layers to form nematic or isotropic states. Thus, the obvious requirement for the formation of such a mesophase is that the lateral intermolecular attractions must be considerably greater than the terminal attractions. However, this is likely to be so in any system comprised of long narrow molecules, since the area of contact between the sides is so much greater than that between the ends of the molecules. Therefore, the probability that a smectic mesophase occurs in a compound must depend on the degree of difference between the terminal and lateral attractions, rather than the simple fact that a difference exists. Such a difference would be obviously enhanced by the presence of strong dipole moments operating across the major axes of the molecules, because with a suitable layer arrangement, dipole-dipole reinforcement would occur (figure 3.2). *Thus, a biphenylic core with strong dipolar substituents such as alkoxy, ester, nitrile or nitro groups usually encourage smectic mesophase formation(16).*

Nematic phases, on the other hand, may be derived either from a smectic phase or directly from a solid phase. The conditions necessary for the formation of this phase is that the terminal and lateral attractions must be roughly equal. *In general, if a molecule is long and narrow and possesses polarizable aromatic rings, but contains no strong dipole moments operating across the long axis, then*

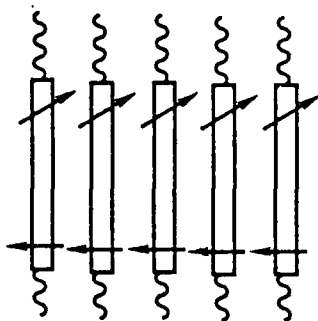


Figure 3.2 : The reinforcement of dipole moments which operate across the long axes of molecules arranged in a layer

the compound is most likely to exhibit nematic properties. That is, the absence of the structural characteristics most favorable for smectic mesophase formation is as useful a criterion as any that a structure is potentially nematogenic and the question of deciding between possible smectic or nematic tendencies is indeed a relative one. As far as identifying either of these mesophases is concerned, observing the texture under an optical microscope between cross polars is the most commonly employed technique (18, 19). However, a more conclusive tool for this purpose is x-ray diffraction technique (20-22). For a detailed analysis, the reader is referred to the numerous references available in the literature.

3.1.3: Influence of Substituents on Transition Temperatures

The influence of substituents on transition temperatures of various mesophases is a poorly understood subject at this stage. Research in this direction was initiated by Gray and coworkers (5) with a homologous series of alkoxy substituted mesomorphic compounds. They found no systematic correlations between the length of the alkyl tail and melting temperatures whereas correlations were possible with respect to clearing temperatures. Initial attempts to synthesize mesogenic compounds with various polar substituents to

study their influence on clearing temperatures were made by Vander Veen (23). In order to make quantitative predictions, he used the molecular statistical theory of Maier and Saupe (24) in which long range orientational order of the molecules was attributed to anisotropic dispersion forces alone, inferring that a linear relationship between T_{n-i} and the polarizability anisotropy of the $C_{Ar}-X$ bond must exist. In his paper, Vander Veen demonstrated this linear relationship for two series of compounds with five polar end groups ($-CH_3$, F, Cl, NO_2 and CN) and concluded that the polarizability anisotropy of the $C_{Ar}-X$ bond is a valuable parameter for predicting T_c . However, in similar studies by Griffin (25) with four new series of compounds and a new polar group (Br), this correlation was found to be inconsistent.

A more recent investigation by Barbera et al. (26) was aimed at predicting the clearing temperatures based on the empirical parameters of the substituents, such as molar refractivity to represent the anisotropy of the polarizability and the dipole moment. Based on the results obtained from their correlation studies, they conclude that these two empirical parameters can be used to predict the clearing temperatures quantitatively.

In addition to those described in the above three sections, closely dictated by the chemical constitution is yet another aspect of mesomorphic molecules - their alignment behavior on various substrates. Two substrates that are of relevance to this work are glass surfaces and carbon fibers. While studies with glass surfaces abound in the literature, little information is currently available on the influence of carbon substrates on the alignment of LCs. Furthermore, with glass surfaces as substrates, most investigations center around modifying the substrate surface, topologically or chemically, to induce a particular type of alignment of a given LC. On the contrary, the present investigation focuses on a given substrate and attempts to understand the alignment behavior of a series of

mesomorphic compounds as a function of chemical substituents.

3.1.4: Surface Phenomena

The various external fields that have an aligning influence on liquid crystals have already been mentioned in the first chapter. The surface of a solid substrate may be considered as a local external field and can be used to orient LC molecules. Because of its practical importance in display devices, the alignment of liquid crystals at a solid boundary has been extensively studied and an enormous amount of expertise on how to achieve a desired boundary alignment has been accumulated (27). A systematic survey of the different ways to align LCs is justified in order to predict the possible behavior of the newly synthesized mesomorphic compounds. Two terms that will recur in the discussion are homogeneous and homeotropic alignment, the former referring to the parallel uniaxial alignment of molecules on the substrate and the latter term referring to the perpendicular alignment as shown in figure 3.3.

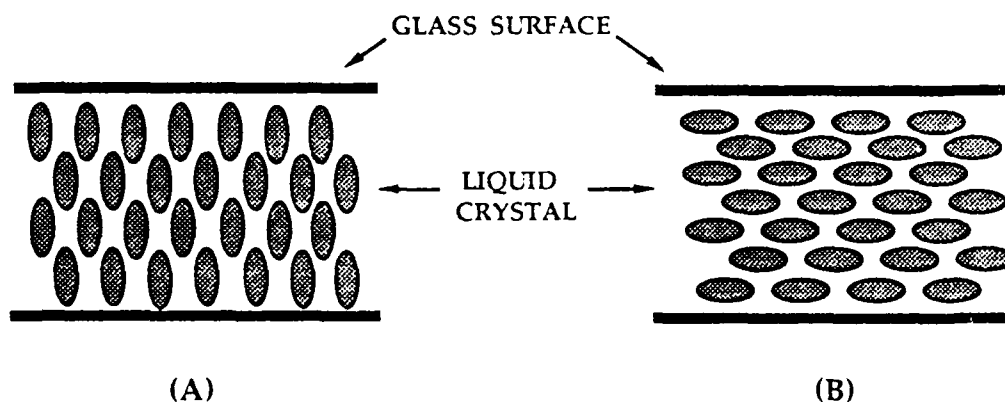


Figure 3.3 : Schematic showing (A) homeotropic and (B) homogeneous alignment of liquid crystals on glass surfaces

In general, the surfaces of glass, oxides and metals exhibit an aligning influence on liquid crystals. The cleaning procedures employed in the substrate preparation have also been shown to play a major role in the alignment behavior of LCs. For instance, some LCs of the Schiff base type align perpendicular to acid-treated surfaces (28, 29), but nonuniform alignment parallel to the substrate surface is obtained with fired (28) or detergent cleaned glasses (29, 30). Homeotropic alignment observed with several Schiff bases has been primarily ascribed to the presence of homeotropic aligning impurities (31) that these systems can easily be contaminated with.

Polymer coatings on glass substrates have also been successfully employed to align LCs, but film uniformity as well as the substrate used influence the observed results. Films of polyethylene, polybutadiene, poly(methyl methacrylate), poly(vinyl alcohol), poly(vinyl chloride), polyesters, polyamides and polyimides have been reported to induce parallel alignment on rubbed surfaces (27). Smooth films of these polymers also induce parallel but nonuniform alignments. Smooth and uniform coatings of teflon and silicones [poly(methyl siloxane), poly(methyl phenyl siloxane)] are the only polymers that have been reported to induce homeotropic alignment and have been extensively used in many commercial applications. However, no mechanistic details to explain the orienting behavior of these different films are currently available. Another common method to produce very uniform homeotropic alignment of LCs is by coating glass surfaces with polyfunctional compounds (32). Structures of some of these compounds that are of relevance to this investigation are presented in table 3.1.

In evaluation studies of alignment effects, classification of an LC alignment into parallel or perpendicular alignment is often an oversimplification. In fact, the nematic director of the LC molecules generally

makes an angle, θ , called the tilt angle which may be close to 0° or 90° or can have intermediate values. These intermediate θ values have been successfully achieved by oblique evaporation of SiO_x , MgF_2 and CaF_2 on glass substrates (33). Further modification of tilt angles have been made possible by coating obliquely evaporated surfaces with films that can induce homeotropic alignment (34).

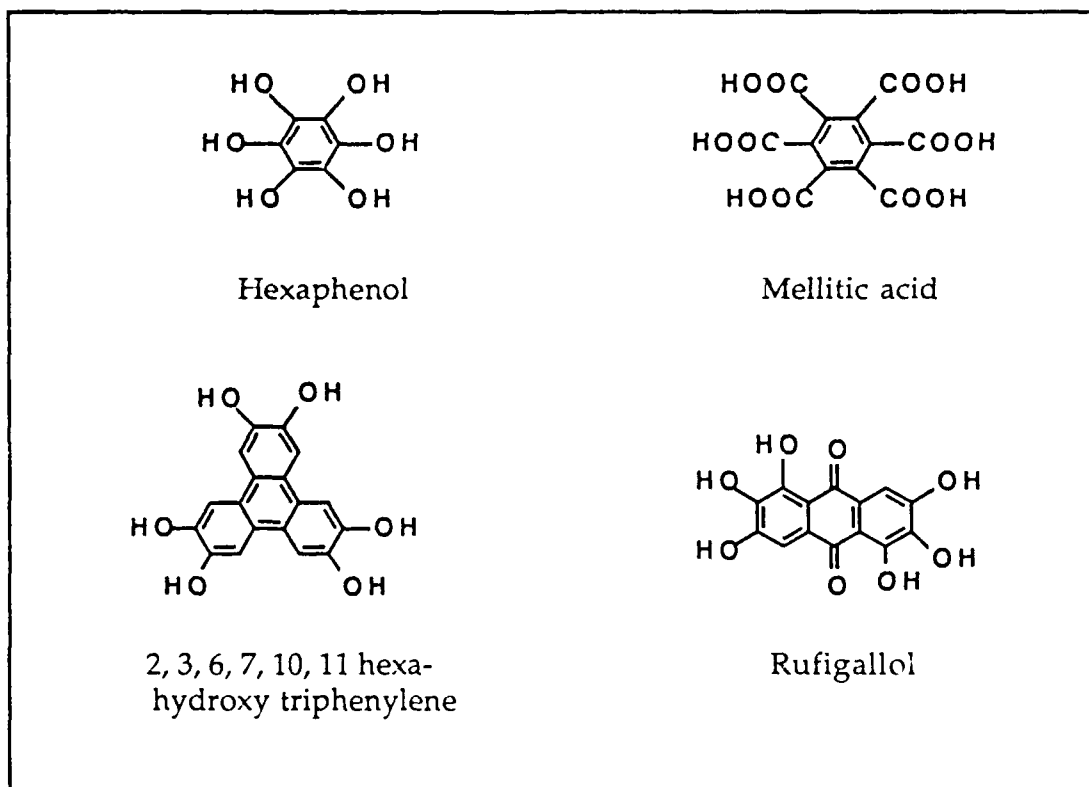


Table 3.1: Structures of some polyfunctional compounds commonly employed as coatings to induce homeotropic alignment on glass surfaces (32)

As far as the alignment behavior of LCPs is concerned, the known procedures for low molar mass liquid crystals described above have afforded only partial success in achieving the desired alignment. A few main chain polymers containing poly(alkylene oxide) spacers (35) and copolyesters based on

hydroquinone, pyrocatechol and terephthalic acid (36) show partial homeotropic alignment spontaneously upon heating on glass surfaces. However, no special structural modifications to specifically induce this kind of orientation either in low molar mass LCs or LCPs have been attempted to date. The present investigation may very well shed some light on the scope of such an approach.

Alignment Mechanisms

While the art of achieving the desired boundary alignment has been mastered, the basic understanding of the alignment mechanism is still lacking. The empirical rule that is widely supported by experimental data was postulated by Freidel, Creagh and Kmetz (FCK rule) (29). According to this rule, substrates with surface energy lower than the LC surface tension cause homeotropic alignment and conversely, those with higher surface tension will align molecules homogeneously. In other words,

$\gamma_c > \gamma_{LC}$Homeotropic alignment
$\gamma_c < \gamma_{LC}$Homogeneous alignment

where γ_c and γ_{LC} are the critical surface tension of the substrate and surface tension of the liquid crystal respectively. γ_{LC} may be viewed as the macroscopic description of the LC-LC interactions while the γ_c approximates the solid surface excess energy.

In order to have thermodynamic significance, the LC surface tension should be measured with an LC in equilibrium with its vapor. Most of the data available, however, are relevant to an air-LC interface, γ_{LA} . Moreover, considerable scatter is observed even with γ_{LA} values, due to the orientational dynamics of molecules at the LC-air interface. In general, the measured surface tensions of many commercially employed small molecule LCs are of the order of

25-40 ergs/cm² (37). Furthermore, since surface tension results from the excess surface energy of the molecules at the surface, it would be expected to vary according to whether the LC molecules are oriented parallel or perpendicular to the surface.

Precise measurements of these orientation dependent surface tension values have encountered considerable difficulty. Commonly employed techniques such as capillary, du Nuoy and Willhemy methods imply contact of LCs with solid surfaces. The orienting effect of solid surfaces on LCs have been found to influence the measured γ_{LA} values significantly. As LCs generally lie parallel to most solid surfaces, the above quoted methods should give a value close to that of characteristic $\gamma_{LA\parallel}$. Only in the hanging drop method, solid-LC interactions are minimized and the γ_{LA} values should be obtained fairly accurately. As LCs often orient perpendicular to free surfaces (38), γ_{LA} values obtained by this method are close to $\gamma_{LA\perp}$ (39).

While problems encountered in measuring the surface tension of LCs accurately are numerous, those associated with solid substrates are also ample. For instance, the measured surface tension values differ significantly from the theoretically predicted values, based on the excess surface energy resulting from the broken bonds (40). Atmospheric constituents that are strongly adsorbed on the surface are responsible for this discrepancy. Experimental procedures to measure the surface tension usually involves measuring contact angles with a homologous series of alkanes. From these measurements, the critical surface tension of a solid can be estimated and this is usually taken as a measure of the solid surface tension. However, the various approximations introduced in assessing the surface tensions of the two components make it difficult to reliably establish the validity of the FCK rule. In general, all of the above mentioned substrate modifications to induce parallel or perpendicular anchoring may be

viewed as methods to alter their surface tensions which in turn govern their orienting properties.

In the following section, properties of the target polymers, 1a and 1b, as well as those of their corresponding monomers are presented. In addition, properties of O-derivatized monomers and polymers are also presented. It is anticipated that such derivatives will elucidate the properties of the target polymers that are specifically conferred on these materials by the phenolic groups. Results of studies on the influence of fiber surface forces on the alignment of these various monomers and polymers are also included. These are of particular importance in the light of the fact that the target polymers have potential for use as coupling agents in carbon fiber-organic matrix composite materials. Finally, specific details regarding the preparation of some derivatives are offered in the experimental section. Experimental details concerning the characterization of the various monomers and polymers by calorimetric studies and optical observations are similar to those presented in chapter 1.

3.2: Results and Discussion

3.2.1: Properties of Hydroxy-Functionalized Monomers and Polymers

Target polymers 1a, 1b, and their corresponding monomers 8a and 8b (shown below) were successfully synthesized as described in the preceding chapter. Optical microscopy experiments were carried out using a thin layer of the sample placed between two very carefully cleaned glass discs. The layers had an average thickness of 1-5 μ , thinner at the centers and thicker at the peripheries. Monomer 8b revealed a crystalline texture at room temperature that melts directly into an isotropic phase around 96°C. On the other hand, as cast

films of the corresponding polymer 1b were clear and exhibited no optical anisotropy when viewed between cross polars in the microscope.

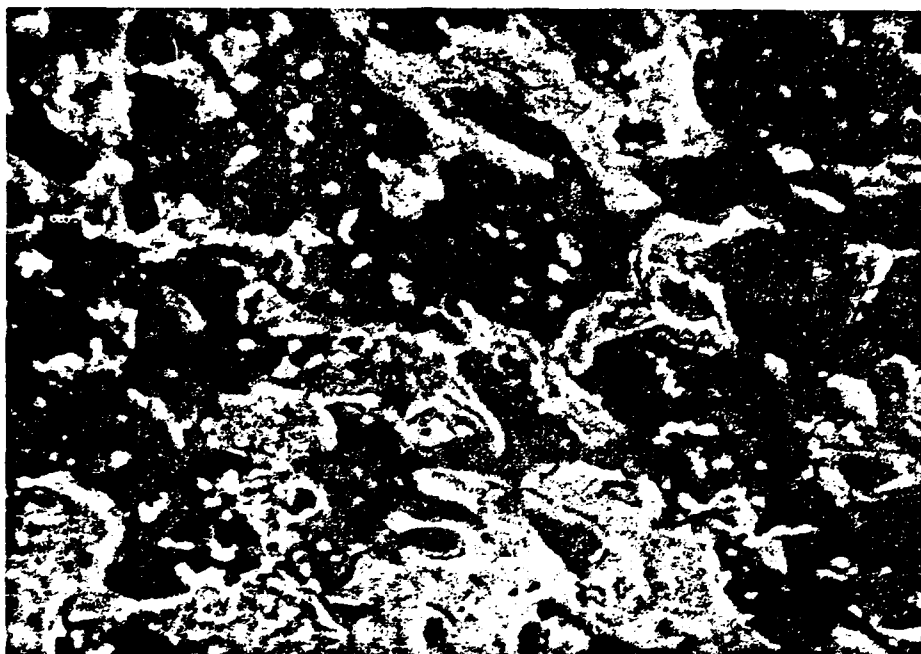
Sample no.	Structure
<u>8a</u>	$\text{CH}_2=\text{C} \begin{array}{l} \text{CH}_3 \\ \text{COO} \end{array} \text{CH}_2\text{CH}_2\text{CH}_2\text{CH}_2\text{CH}_2\text{CH}_2\text{CH}_2\text{O}-\text{C}_6\text{H}_4-\text{COO}-\text{C}_6\text{H}_4-\text{C}_6\text{H}_4-\text{OH}$
<u>8b</u>	$\text{CH}_2=\text{C} \begin{array}{l} \text{CH}_3 \\ \text{COO} \end{array} \text{CH}_2\text{CH}_2\text{CH}_2\text{CH}_2\text{CH}_2\text{CH}_2\text{CH}_2\text{O}-\text{C}_6\text{H}_4-\text{COO}-\text{C}_6\text{H}_4-\text{OH}$
<u>1a</u>	$\text{CH}_2-\text{C} \begin{array}{l} \text{CH}_3 \\ \text{COO} \end{array} \text{CH}_2\text{CH}_2\text{CH}_2\text{CH}_2\text{CH}_2\text{CH}_2\text{CH}_2\text{O}-\text{C}_6\text{H}_4-\text{COO}-\text{C}_6\text{H}_4-\text{C}_6\text{H}_4-\text{OH}$
<u>1b</u>	$\text{CH}_2-\text{C} \begin{array}{l} \text{CH}_3 \\ \text{COO} \end{array} \text{CH}_2\text{CH}_2\text{CH}_2\text{CH}_2\text{CH}_2\text{CH}_2\text{CH}_2\text{O}-\text{C}_6\text{H}_4-\text{COO}-\text{C}_6\text{H}_4-\text{OH}$

In great contrast to monomer 8b, the biphenylic monomer 8a revealed large spherulites at room temperature that melt into a birefringent fluid at 128°C. Upon continued heating, the field of view under cross polars begins to turn black in the vicinity of 135°C and by 147°C, most of the detectable birefringence disappears leaving more or less, a black field of view. An interference figure was obtained with the orthoscope set up as a conoscope to determine whether the black area was isotropic or contained a homeotropically aligned liquid crystal

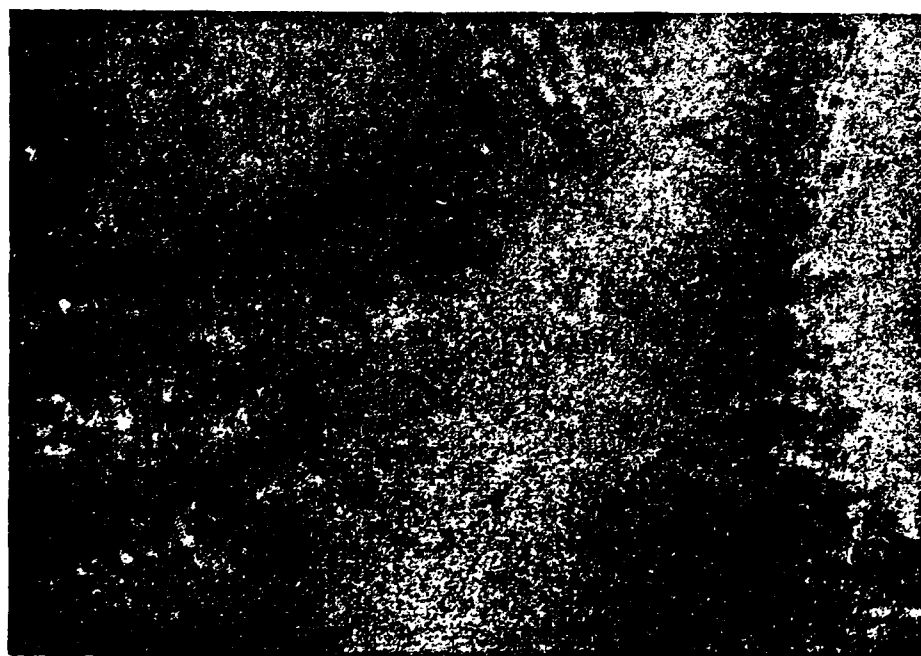
(molecules parallel to the optic axis). The resulting conoscopic image clearly revealed a cross pattern which corresponds to the uniaxial interference figure [as shown in figure 3.12(b)]. When the temperature is increased further to 156°C , the whole sample acquires a colorful *Schlieren* texture, as shown in figure 3.13(a). This texture exists over a narrow $3\text{--}4^{\circ}$ range. This transition was followed by tiny isotropic droplets developing in the medium which quickly grow, leaving a completely isotropic melt at approximately 176°C . Optical micrographs describing these various changes follow later in the discussion.

A similar experiment with the corresponding polymer **1a** revealed a frozen glassy texture at room temperature which changes texture around 158°C . Above this temperature, very faint flow was detected in the medium, but distinct changes in colors were noticed. Close to 218°C , the sample begins to appear black and by 233°C , large patches of black color were seen dispersed in a birefringent medium [as shown in figure 3.4(a)]. A clear conoscopic image could not be deciphered due to the presence of bright regions. However, the sample in these black regions when sheared, became fully birefringent [as shown in figure 3.4(b)] suggesting that the black regions were due to the homeotropically aligned molecules. The sample becomes fully birefringent once again around 238°C . The clearing point for this polymer was observed at 262°C , and this was preceded by a narrow $3\text{--}4^{\circ}\text{C}$ range where a finely dotted texture of bright and dark regions is observed.

Figures 3.5 and 3.6 show the DSC heating scans corresponding to the monomer **8a** and its polymer **1a** respectively. The scans presented are those of the first heating cycle for the monomer and the second heating cycle for the polymer. The DSC trace of the monomer reveals two endothermic transitions at 124°C and 171°C . That of the polymer also shows two endothermic peaks at 154°C and 256°C . Table 3.2 summarizes the optical and DSC temperature data of



(a)



(b)

Figure 3.4: Optical micrographs between cross polars of polymer 1a at 233°C showing (a) partial homeotropic alignment and (b) disappearance of this alignment when sheared (450x)

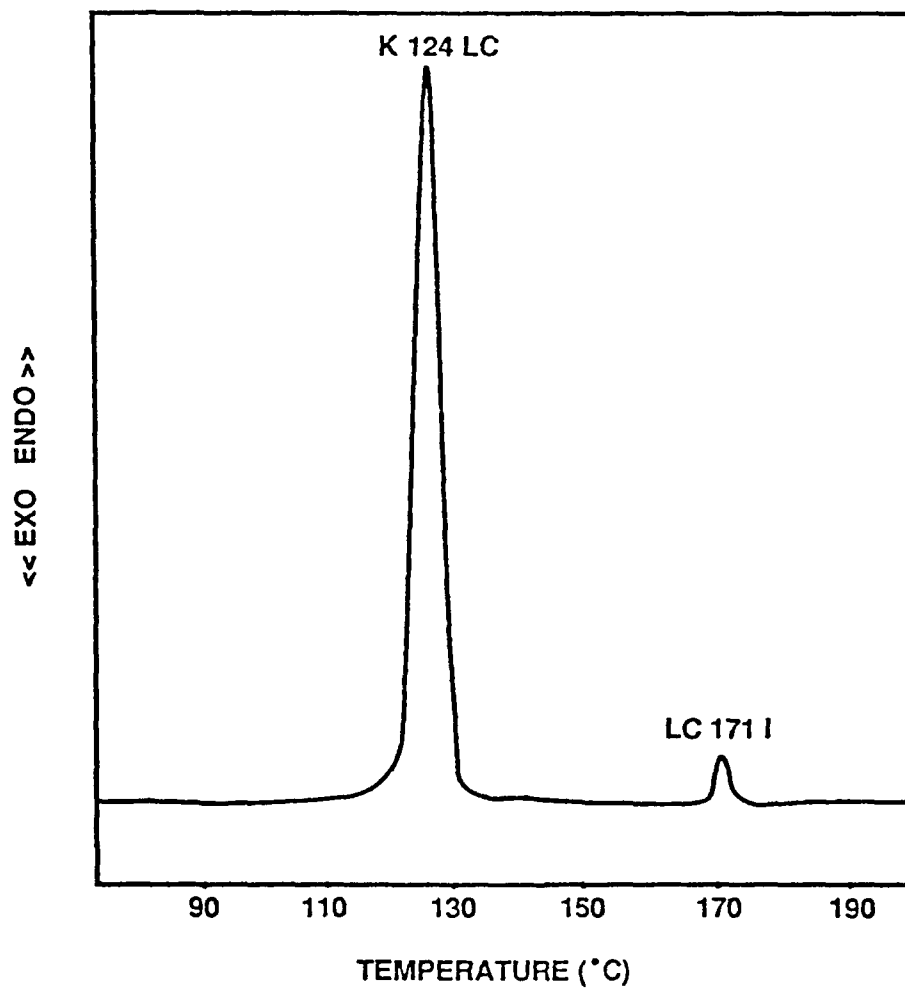


Figure 3.5: DSC scan of the phenolic monomer **8a** obtained at a heating rate of 10°C/min

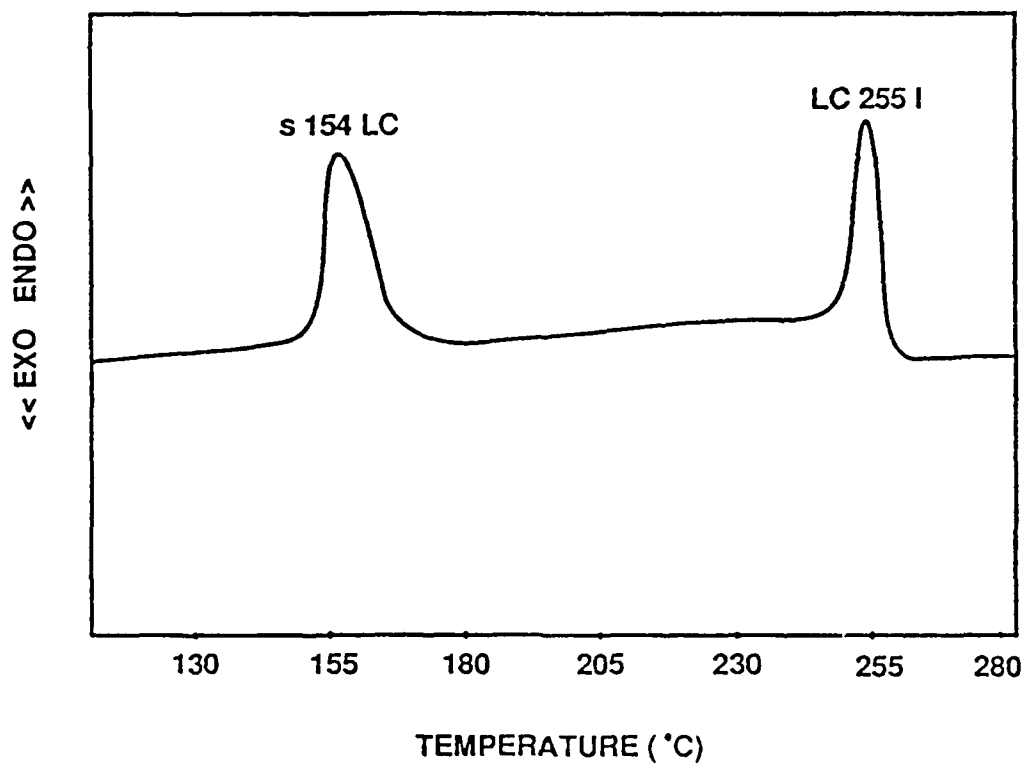


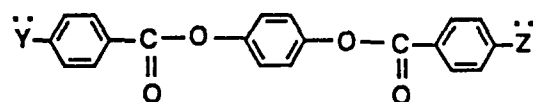
Figure 3.6 : DSC scan of the phenolic polymer 1a obtained at a heating rate of 10°C/min

the two hydroxylated monomers and polymers. Based on the optical observations, it is unclear if the solid state structure of the polymer corresponds to a glassy, semicrystalline or crystalline material. Therefore, 's' is in recognition of the undefined nature of the solid state texture.

Sample no.	Optical Transition Temp., °C	DSC Transition Temp., °C
<u>8a</u>	K 128 LC 176 I	K 124 LC 171 I
<u>1a</u>	s 158 LC 262 I	s 154 LC 256 I
<u>8b</u>	K 96 I	K 94 I
<u>1b</u>	Glass	Glass

Table 3.2: Transition temperatures of the hydroxylated monomers and polymers as obtained from DSC and optical microscopy studies

Optical observations with the phenolic monomer, 8a clearly reveal that this compound is mesomorphic in nature. The mesophase formation in this compound certainly disproves the common notion that phenolic compounds are not suitable for mesomorphism due to their strong tendency for intermolecular association *via* hydrogen bonding. This result is in accordance with few other exceptions that are cited in the literature (14, 15, 17). According to Schroeder and Schroeder (14), mesomorphism in the phenolic compounds that they have synthesized (of the type 34) is due to the highly dipolar structures



34

Y = Z = NH₂

Y = Z = OH

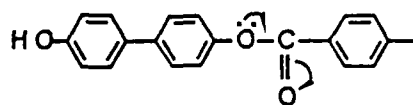
Y = NH₂ , Z = OH

that can result from these molecules. For instance, these investigators believe that electron donation by the terminal -OH to the ester carbonyl can produce high molecular polarity, as shown below. Powerful dipolar



intermolecular attractive forces that can result from such an electron delocalization have been claimed responsible for stable mesophases formed when these compounds melt.

Interestingly, in the present system, the mesogenic structure does not permit such a *resonance enhanced attraction* to come into play because the ester is linked to the electron rich aromatic ring via the -O- atom and not via a carbonyl group. Only a linear, highly polarizable mesogen can be the outcome of resonance in this case. Therefore, based on our observations, the validity of their

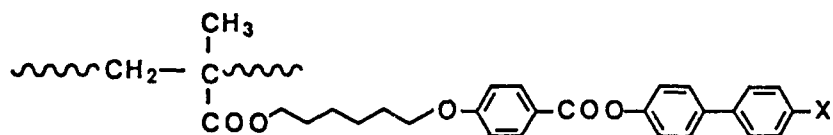


hypothesis that *special structural features that can involve strong dipolar interactions are necessary for phenolic compounds to exhibit mesomorphism* is questionable.

As far as evidence for the inter or intramolecular hydrogen bonding is concerned, this may be derived from the -OH stretching frequency range in the IR-spectrum of the molecule. Referring to this association as *intermesogenic hydrogen bonding* may be more appropriate in the present context. With the monomers, this would imply intermolecular association but in the case of polymers, this would include inter and intra molecular hydrogen bonding. The IR-spectra of all the phenolic monomers and polymers in the solid state show a broad peak in the range 3380-3440 cm^{-1} . This range is typical for phenolic compounds with extensive hydrogen bonding. Should there be no association of this kind, a free phenolic -OH stretching frequency would absorb in the range 3590-3650 cm^{-1} . The fact that no peak is observed in this range implies extensive intermesogenic hydrogen bonding in all of the phenolic compounds involved in this study. However, this information on solid state association may not be extrapolatable to the liquid crystalline phases.

An indirect evidence for the extent of hydrogen bonding may also be derived by comparing the transition temperatures of the phenolic polymer with those of the corresponding alkoxy derivatives. Reported in table 3.3 is the data from the literature (41) for one such alkoxy derivative of polymer **1a**. Association by hydrogen bonding, in general, is known to increase the melting point of organic compounds. In the present case, by comparing the melting temperatures of the two polymers, this increase may be approximated to 100°C. The fact that the clearing temperatures of the two polymers are comparable suggests that this parameter is more dependent on the interactions between the mesogenic cores (common for the two cases) rather than on the terminal interactions.

The strong intermesogenic bonding that is associated with these compounds may very well be the cause for lack of mesomorphism in polymer

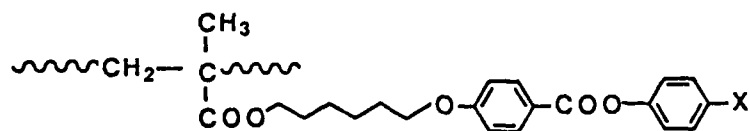


Sample no.	-X	Transition temp. (°C)
<u>1a</u>	-OH	s 158 LC 262 I
<u>38</u>	-OCH ₃	g 60 LC 258 I

Table 3.3: Transition temperatures of the phenolic polymer 1a and its corresponding methoxy analog (41)

1b. In this case, the mesogenic core comprised of two aromatic rings connected by an ester linkage, is as such only weakly prone to mesomorphism given the low aspect ratio. The corresponding methoxy derivative, 39, (21) and the methyl analog, 40, (42) do show mesomorphic behavior and the transition temperatures of these polymers are presented in table 3.4 for comparison. Consistent with their weak mesomorphic character, the mesophase stability in both these polymers spans only a narrow 15-20°C range. Therefore, lack of mesomorphism in 1b may be easily visualized as resulting from the melting point being raised to temperatures above the clearing temperature due to association *via* hydrogen bonding. But such an association yields a glassy instead of a crystalline material. The actual reason for vitrification rather than crystallization in polymer 1b is not clear at this point.

One peculiar feature of the phenolic monomer 8a, presumably facilitated by its tendency for extensive association, is its spontaneous organization perpendicular to glass surfaces upon heating. Such an organization extends over thousands of molecular layers that are confined between two glass surfaces.



Sample no.	-X	Transition temp. (°C)
<u>1b</u>	-OH	Glass
<u>39</u>	-OCH ₃	g 95 N 105 I
<u>40</u>	-CH ₃	g 70 N 84 I

Table 3.4: Transition temperatures of the mesomorphic derivatives of polymer 1b

Ascribing this feature mostly to the presence of the phenolic functionality on the monomer may not be incorrect, given the fact that glass surfaces coated with polyfunctional phenolic compounds (listed earlier in table 3.1) do promote homeotropic alignment of many commercial LCs. However, such an alignment behavior is not reported for other phenolic LCs cited in the literature. Therefore, the aligning tendencies of a few other phenolic LCs on glass surfaces need to be studied before any generalizations can be made about this class of functionalized compounds.

Mechanistically, interactions between the polar silanol bonds on the surface of glass and the phenolic groups on the monomer may be critical in aligning the first layer of molecules that are in contact with the surface. This layer in turn can dictate the alignment of subsequent layers, the driving force for which may be viewed as the cooperative behavior common among LC molecules in conjunction with their strong tendency for intermolecular attractions *via* hydrogen bonding. These monomeric molecules may be viewed

as amphiphilic molecules which have a polar and a nonpolar fragment at their ends, each having an affinity for a similar group. Thus, the alignment of these molecules between glass surfaces may be visualized as that shown in figure 3.7, where the left half shows a homeotropic smectic arrangement seen typically in smectic A and smectic C phases while the right half represents a nematic ordering. The smectic ordering shown in the left half actually corresponds to a bilayer structure of smectic A phase typically observed in melts derived from cyano substituted compounds (43, 44). The average lamellar spacing is about 1.4 times the molecular length in the case of 4-alkoxy-4'-cyano biphenyls, suggesting

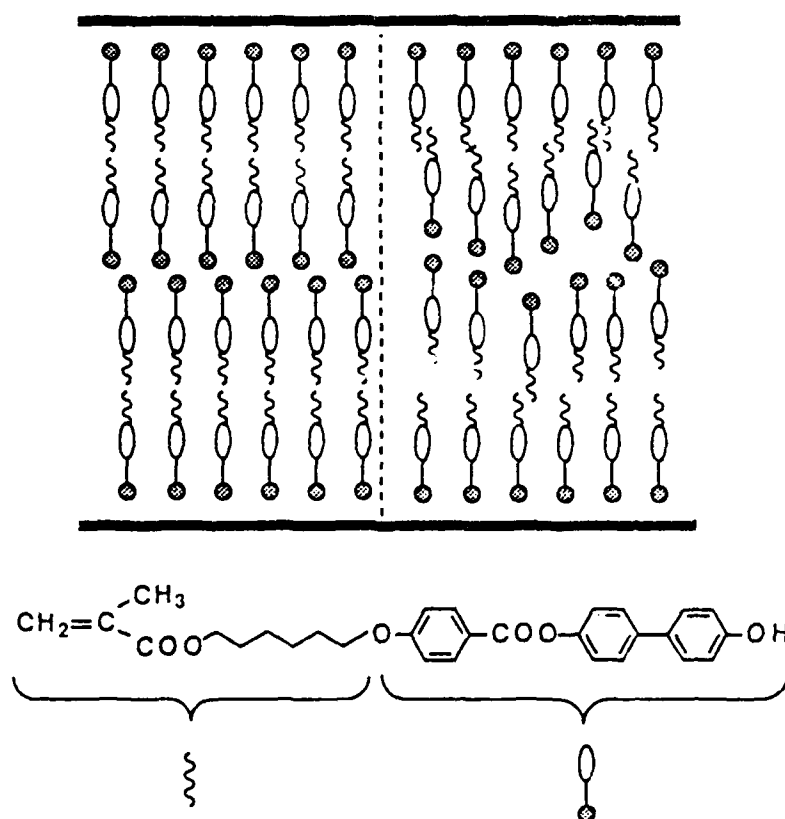


Figure 3.7 : Schematic showing bilayered smectic (left half) and nematic (right half) ordering in homeotropically aligned monomer on glass surface

that the layer structure in these compounds is of an interdigitated type (43).

As far as the exact nature of the mesophase in monomer 8a is concerned, a nematic phase is observed just before the sample clears into the isotropic state. This is based on the fact that a *Schlieren* texture, consisting of four and two brushes is seen before the clearing temperature is reached [as shown in figure 3.13(a)]. The DSC trace of this monomer reveals a melting endotherm around 124°C and another small endotherm at 171°C, corresponding to the nematic-isotropic transition.

In optical observations with polymer 1a, the observed texture of the birefringent melt does not easily relate to any of the classical textures of smectic or nematic phases. However, most polymers with similar mesogenic units and containing strong dipolar substituents have been reported to show smectic as well as nematic phases upon heating. But as such, the DSC trace (figure 3.6) shows only two peaks, one corresponding to the melting transition (at 154°C) and the other due to the mesophase-isotropic transition (at 256°C). In general, DSC analysis and optical observations of all these compounds need to be supplemented by electron diffraction studies to determine the nature of the mesophase unambiguously. Since the electron diffraction studies of these compounds are beyond the scope of this thesis, the various mesophases described thus far will simply be referred to as the LC state in the remainder of the chapter.

Lastly, in great contrast to the monomer 8a, polymer 1a does not show a very pronounced tendency for homeotropic alignment on glass surfaces. This tendency does exist to some extent, as is evident from the bright and dark regions in micrograph in figure 3.4. This observation was contrary to our expectation that the phenolic polymer should be more strongly prone to homeotropic alignment than the monomer. This was thought to be so because of the greater

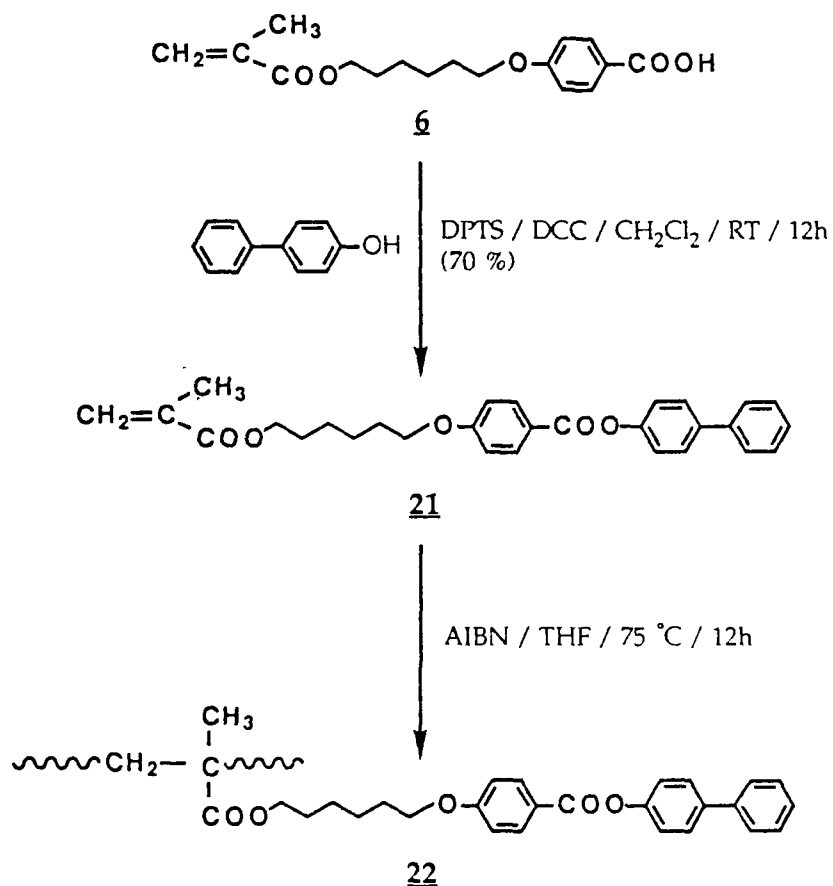
cooperative behavior of the mesogenic units enforced on them by a common linking backbone. The fact that it is not so may imply that mesogenic mobility is an important factor in this organizing process. Alternatively, the backbone entropy may be viewed as a limiting factor for polymeric chains to align homeotropically. Attempts to address this problem by aging the sample at 235°C were not fruitful as the sample begins to decompose even before any change in the extent of perpendicular alignment is noticed. Aging at temperatures below 235°C did not reveal any noticeable changes in behavior either.

3.2.2: Properties of O-Derivatized Monomers and Polymers

This section discusses the properties of monomers and polymers that were involved as intermediates in the synthesis of hydroxy-functionalized polymers. A few others that could be easily derived from the functionalized monomer are also included. It is anticipated that comparing the properties of these compounds would throw some light on the influence of terminal substituents on mesomorphic properties in general. In particular, the role of the phenolic groups in the spontaneous organization of molecules perpendicular to glass surfaces may be better understood from these studies.

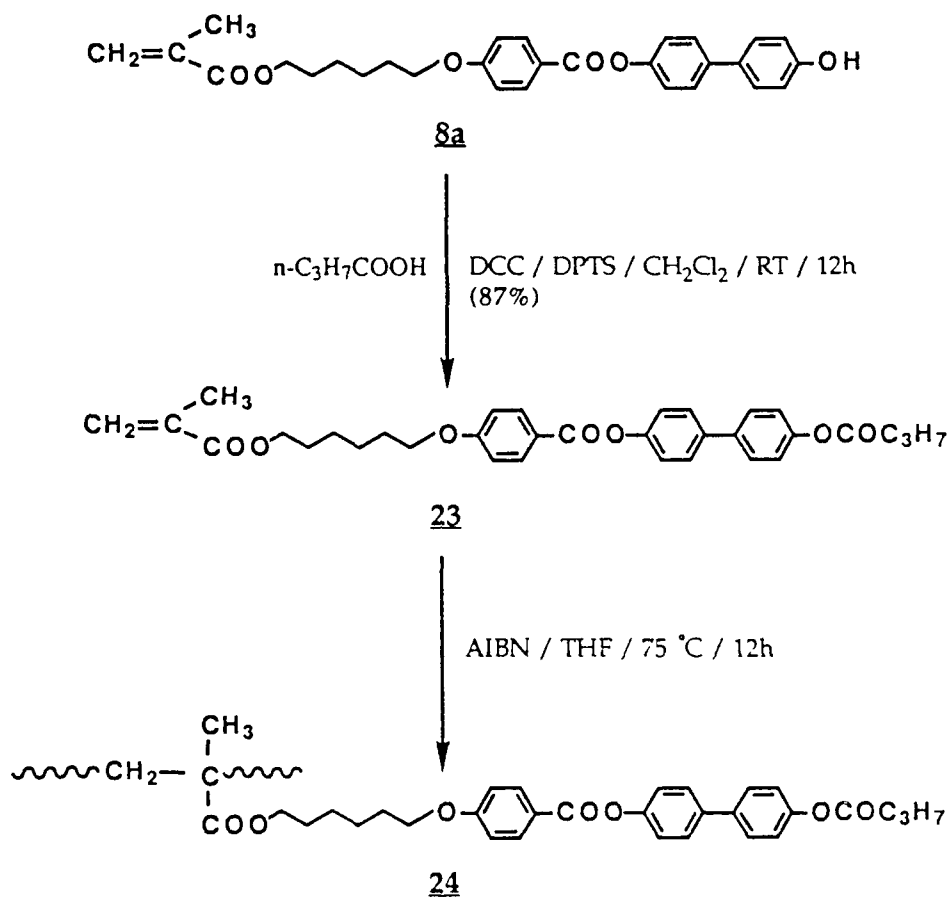
Synthesis of the monomer without any substituent in the para-position, 21, was easily accomplished by an esterification reaction of 6 with 4-hydroxybiphenyl (as shown in the scheme 3.1). The corresponding polymer 22 of dp ca 150 was prepared by standard polymerization procedure described in the preceding chapter.

SCHEME 3.1



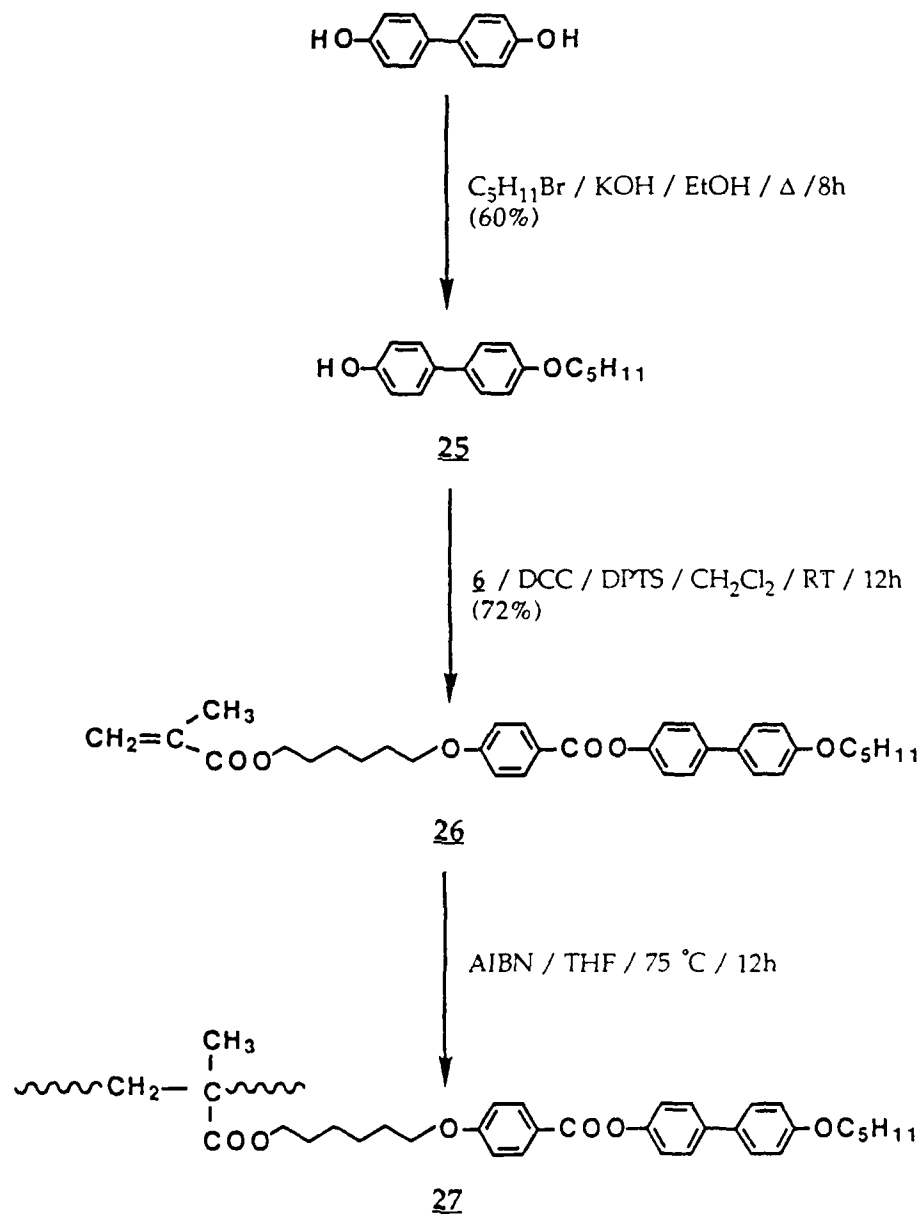
Polymer **24** with an ester substituent was synthesized by esterification of monomer **8a** with n-butyric acid, followed by polymerization, as shown in scheme 3.2. A polymer of dp ca 150 was isolated in 90 % yield.

SCHEME 3.2



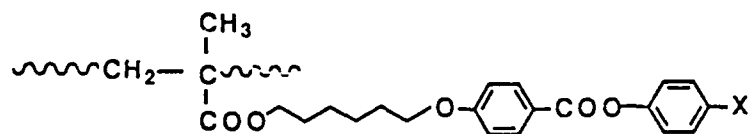
Synthesis of a polymer with pentyloxy substituent on the mesogen (27) first involved synthesis of the corresponding mesogenic fragment which could then be coupled with a polymerizable spacer (as shown in scheme 3.3). Thus, 4-(4'-pentyloxyphenyl)phenol, 25, was first synthesized by monoetherification of the dihydroxy compound as described by Marcos et al. (45) in 60 % yield. Esterification of 25 with 6 afforded monomer 26 in 72 % yield. Polymerization of this monomer yielded polymer 27 of dp ca 150 in 88 % yield.

SCHEME 3.3



The various monomers and polymers thus synthesized were studied by optical microscopy and DSC analysis. Data regarding their transition temperatures as obtained from optical observations are presented in tables 3.5 and 3.6. Table 3.5 covers data of the compounds which contain two phenyl rings

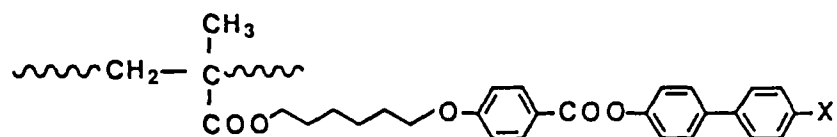
interconnected by an ester linkage (eg. **1b**). Table 3.6 includes data of the compounds which contain a biphenylic moiety linked to a benzoate group (eg. **1a**).



-X	Transition Temp.(°C) of	
	Monomer	Polymer
-OH	K 96 I	Glass
-OCOOBn	K 81 LC 86 I ^a	s 85 LC 100 I
-OΣ	liquid ^b	Glass
-ODPMS	liquid ^b	Glass

Table 3.5: Transition temperatures of O-derivatized monomers and polymers (^a monotropic, ^b isotropic liquid)

The mesomorphic properties of the compounds listed in table 3.6 are presented in a different manner to highlight their mesophase stabilities, in an increasing order of melting points in figure 3.8. The top graph in this figure represents the transition temperatures of the various monomers while the bottom one corresponds to those of the respective polymers. Shown in figure 3.9 are the clearing temperatures for the various biphenylic monomers and the corresponding polymers for comparison.



-X	Transition Temp.(°C) of	
	Monomer	Polymer
-OH	K 128 LC 176 I	s 158 LC 262 I
-H	K 64 LC 92 I	s 135 LC 163 I
-OCOC ₃ H ₇	K 74 LC 172 I	s 138 LC 270 I
-OC ₃ H ₁₁	K 105 LC 126 I	s 156 LC 249 I
-OCOObn	K 70 LC 105 I	s 138 LC 229 I
-OTHP	K 96 LC 150 I	s 138 LC 228 I
-OΣ	K 48 LC 62 I ^a	Glass
-ODPMS	K 57 I	Glass

Table 3.6: Transition temperatures of various monomer and polymer derivatives obtained from optical microscopy studies (^a refers to monotropic behavior)

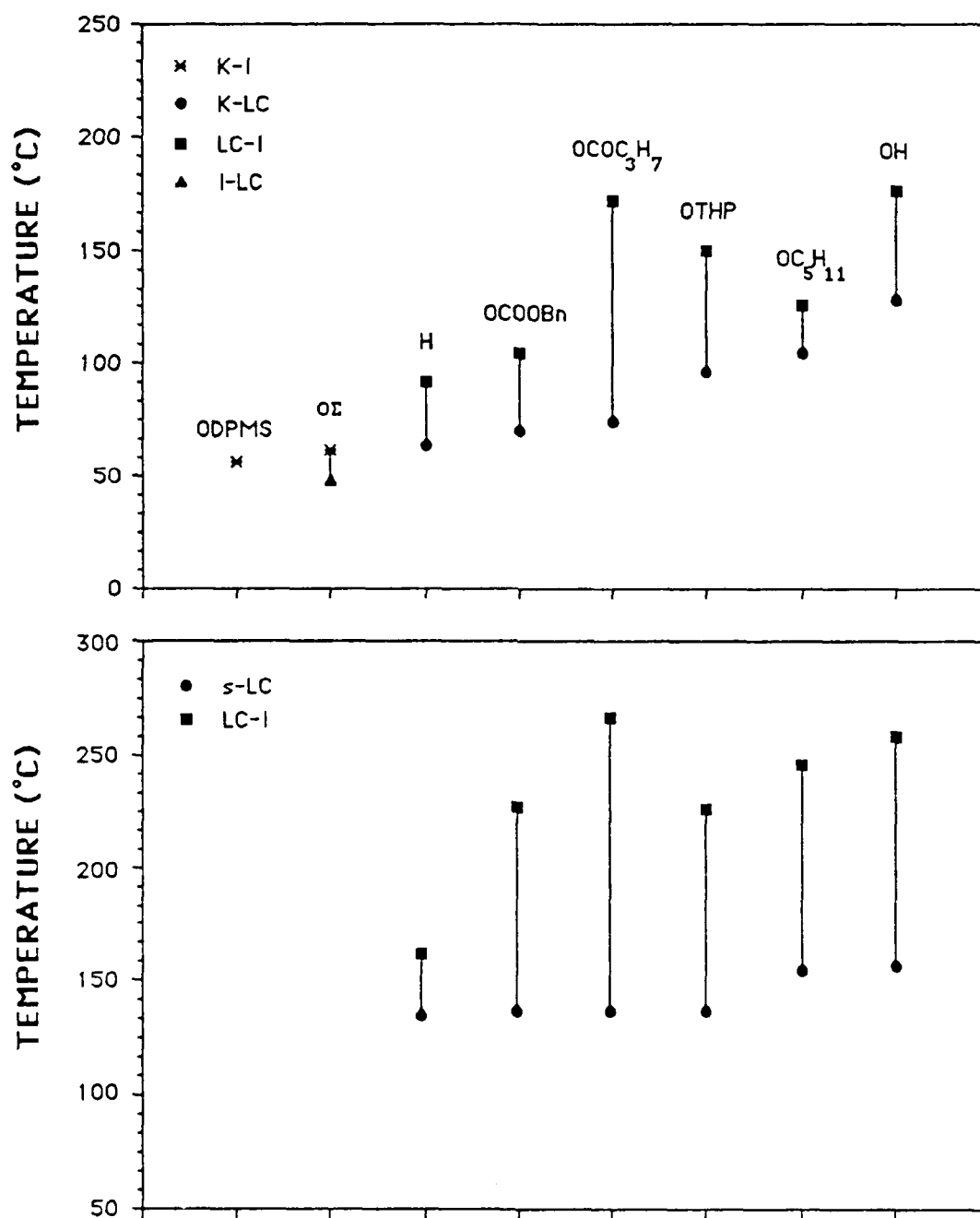


Figure 3.8: Comparison of the transition temperatures of various monomers (top) and corresponding polymers (bottom)

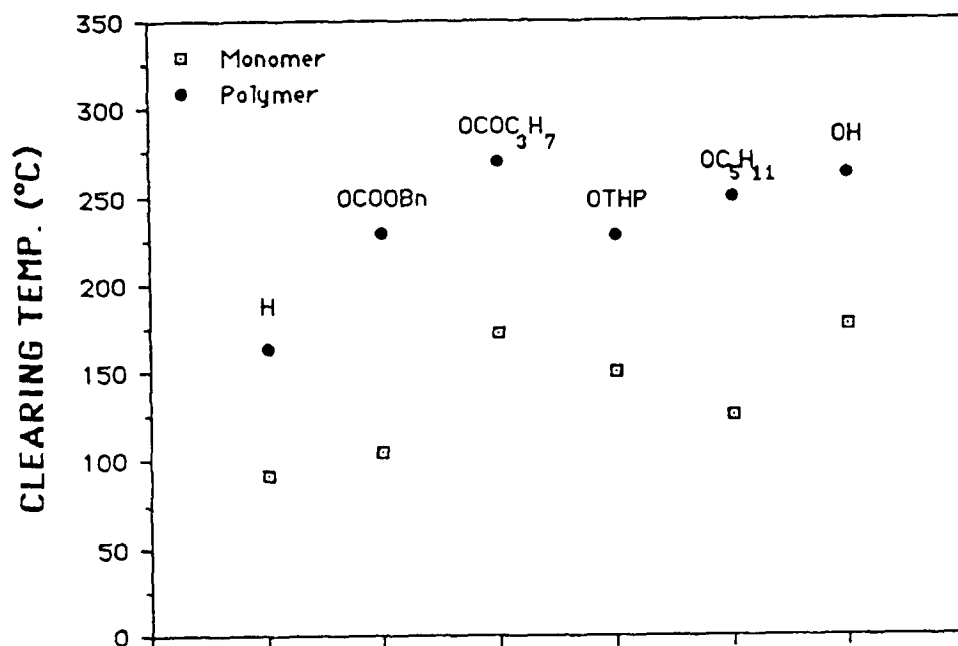


Figure 3.9: Comparison of the clearing temperatures of various biphenylic monomers and polymers

The most striking feature that surfaces by comparing the transition temperatures of monomers and polymers presented in figure 3.8 is regarding their mesophase stabilities. In most of the cases, a much higher mesophase stability is observed with the polymeric melts as opposed to the melts derived from the monomers. That is, stabilization of the mesophase is observed when the monomers are converted into polymers. In principle, this transformation conserves the chemical constitution of the mesogenic units and therefore the polarizability and anisotropy factors should remain constant. Therefore, the strong shift in phase behavior must be attributed to changes in density associated with polymerization reaction in general. A decrease in specific volume presumably turns on the attractive forces between the mesogenic units. If this is indeed so, a strong shift in phase behavior is to be expected in changing from monomer to the dimer, trimer etc. Eventually, this shift should vanish in the limiting case when an additional monomer does not alter the specific volume any further. Investigations in this regard by Finkleman do indicate that no shift in phase behavior is observed at high degrees of polymerization (46).

Comparing the behavior of the various monomers, the melting temperature of the phenolic monomer is higher than that of the others, consistent with the earlier discussion on hydrogen bonding. The mesophase stability of a terminal ester containing monomer is particularly high, presumably due to the strong ester bond dipoles. The observed mesophase stability of a terminal hydrogen substituted monomer 21 (as well as its polymer 22) is lower than most other cases. This has been ascribed to the lack of any dipole moment associated with this substituent (5). The presence of terminal silyl ether substituents on the mesogen seems to influence mesomorphism in these compounds as a whole. For instance, polymer 13 and 16a with terminal dimethylhexylsilyl ether (OS) and diphenylmethylsilyl ether (ODPMS) groups

respectively are totally amorphous in nature. Focussing specifically on the former type of substituent, it is observed that this monomeric compound (7a) is mesomorphic (monotropic) in nature where as the corresponding polymer (13) is amorphous. This particular case, in the light of the above discussion that stabilization of a mesophase occurs upon polymerization of monomers, is inconsistent with the expected behavior. Otherwise, the general lack of mesomorphism in these bulky silyl ether substituted polymers may very well be due to steric repulsions activated when polymerization occurs. These bulky terminal substituents may be viewed as units that weaken the intermolecular (intermesogenic) interactions. In general, if intermolecular forces are weak, only low melting solids result and cohesive forces between these may again be inadequate to maintain order in the fluid state. This does seem to be the case as both the silyl ether monomers, 7a and 11a are low melting compounds (62° and 57°C respectively). Shown in figures 3.10 and 3.11 are two different projections of the phenolic monomer 8a, O Σ protected monomer 7a, and ODPMS protected monomer 11a. From these graphical representations, it is evident that the bulky silyl ether substituents in effect broaden the mesogenic units. However, these are only qualitative projections that do not correspond to the minimum energy conformations. Studies regarding the minimum energy conformations will be addressed in the future.

The ordering behavior of the various biphenylic monomers and polymers synthesized are summarized in table 3.7. As far as the homeotropic aligning tendency is concerned, that of the phenolic monomer is by far unsurpassed. Most of its derivatives show only a faint tendency towards perpendicular alignment on glass surfaces. This behavior is somewhat more pronounced with the monomer and polymer containing terminal ester linkages (23 and 24 respectively). In these compounds, the terminal ester groups have orthogonal

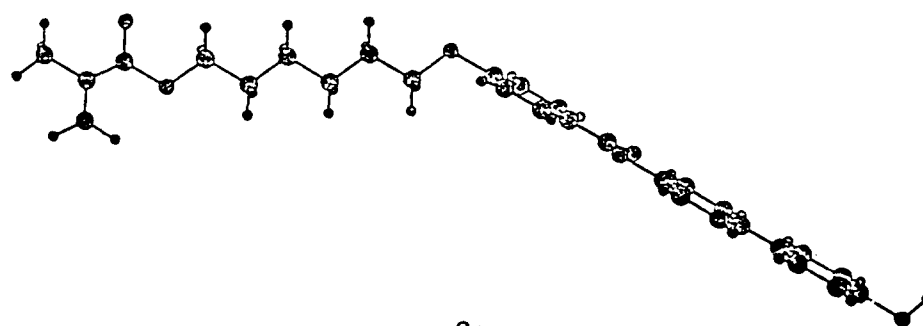
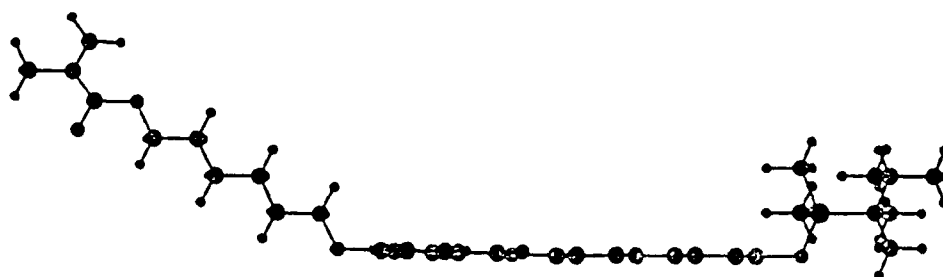
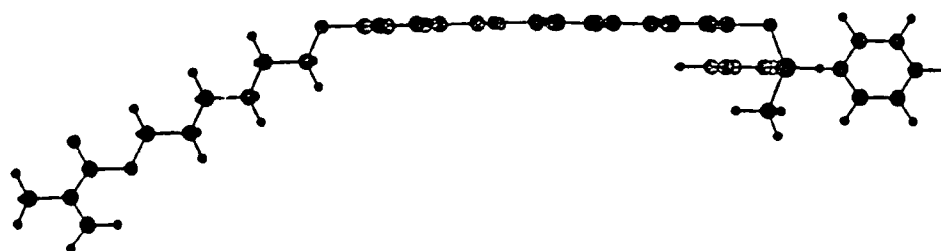
**8a****7a****11a**

Figure 3.10 : Ball and stick representation (Chem 3D) of the phenolic monomer, **8a**, O Σ protected monomer **7a**, and ODPMS protected monomer **11a**

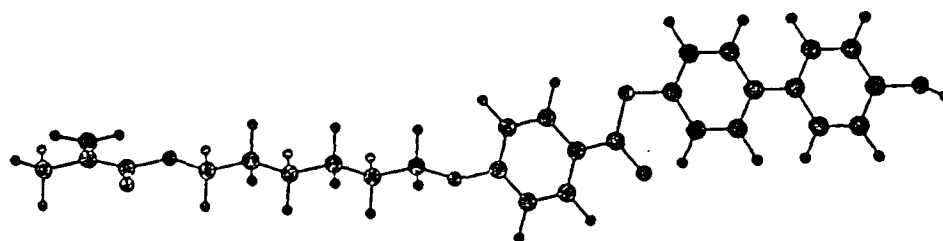
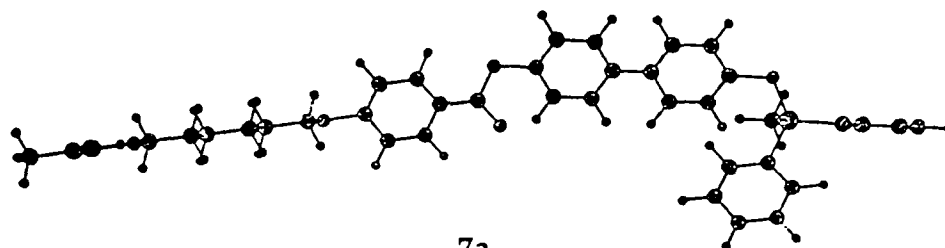
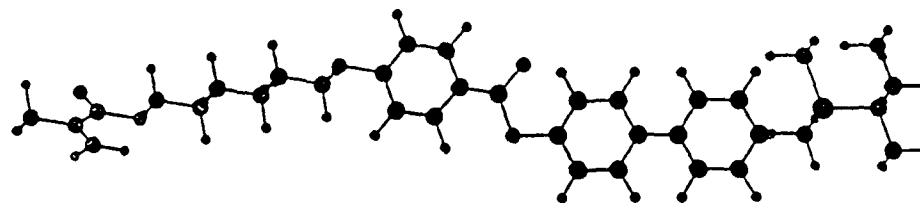
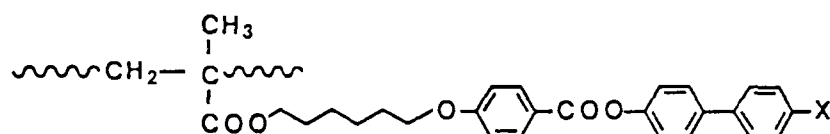
8a7a11a

Figure 3.11 : Aa alternative ball and stick representation of the phenolic monomer 8a, O Σ protected monomer 7a, and ODPMS protected monomer 11a showing the planar nature of the aromatic system

dipoles that could impede homeotropic alignment on glass surfaces. Even with nonpolar pentyloxy terminal groups such as in monomer **26** and its polymer **27**, the mesogenic units do show some inclination to align homeotropically. The micrograph in figure 3.12 shows this property of the polymer **27**. Even in these cases, the pentyloxy groups can deform to expose ether linkages to the



-X	Ordering Behavior of	
	Monomer	Polymer
-OH	v. strong	weak
-OCOC ₃ H ₇	medium	weak
-OC ₅ H ₁₁	weak	weak
-H	weak	weak
-OCOObn	weak	weak
-OTHP	weak	weak

Table 3.7: Summary of the ordering behavior of various liquid crystal monomers and polymers (strong, medium and weak refer to the tendency of molecules to align homeotropically on glass surfaces)

hydroxylated glass surfaces. Given the fact that the polar phenolic end groups have a strong influence in organizing the molecules uniformly on glass surfaces, the conclusion is that *specific chemical interactions such as hydrogen bonding*

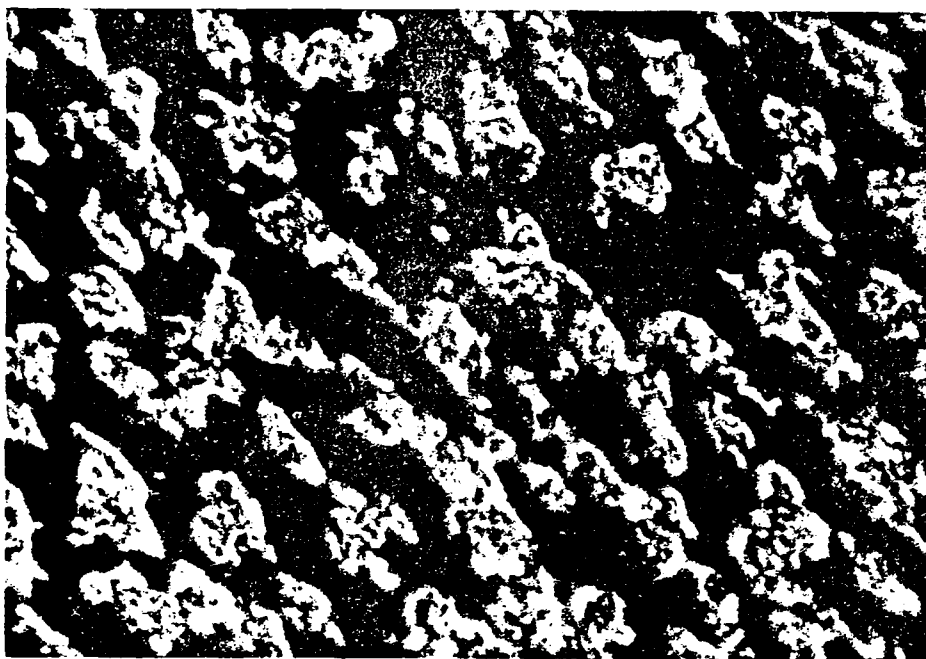


Figure 3.12 : Optical micrograph between cross polars revealing the partial homeotropic alignment of the polymer with pentyloxy substituents (27) (450x)

facilitate the orientational organization on glass surfaces. However, based on the orienting tendency of molecules with nonpolar pentyloxy groups (26, 27) and those without any terminal dipoles (21, 22), it may be inferred that the nature of substituents is not the only factor affecting the observed orientation of molecules on glass surfaces.

3.2.3: Influence of Fibers on Molecular Alignment

From the earlier studies on main chain LCPs (chapter 1), it is inferred that fiber surface forces exert an aligning influence on liquid crystal molecules. An ideally suited system at hand to study this guiding aspect of fibers is the phenolic monomer 8a, which undergoes spontaneous organization perpendicular to glass surfaces. In an optical microscopy experiment, any disturbing tendency by the fiber should be readily revealed through birefringence in the otherwise black field of view.

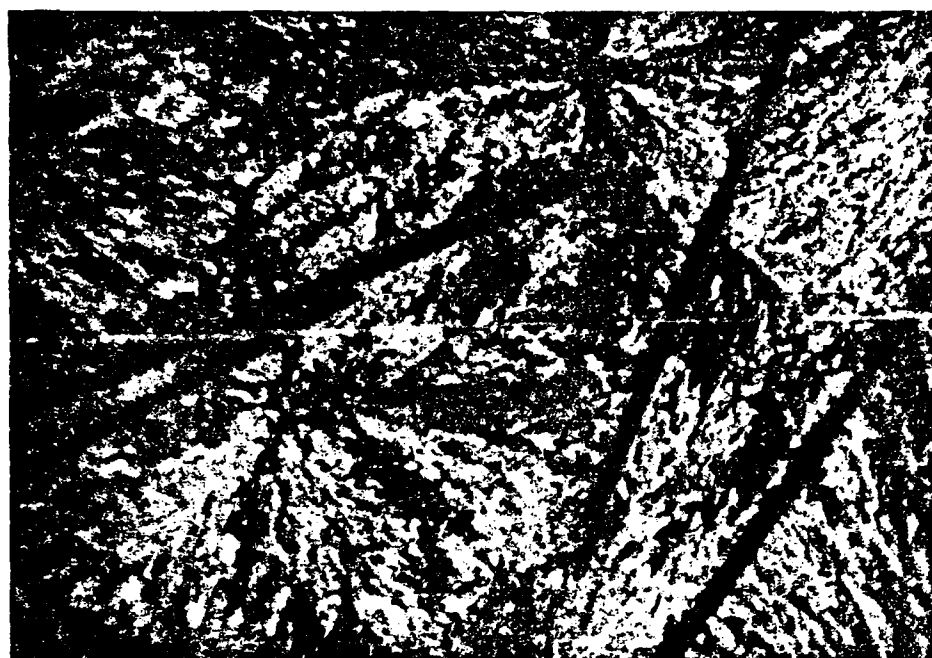
Samples for optical observations were prepared by the same procedure as before, except that 1-2 mm long fibers were dispersed in the medium. Since the sandwiched fibers are of an average diameter of 10 μ , the sample thickness should also be of the same order. Optical micrographs shown in figures 3.13-3.16 sequentially relate the changes that occur when the sample is heated.

Optical observations of the monomeric sample have already been described at length in the preceding section. Figure 3.13(a) shows the crystalline texture of the monomer with dispersed carbon fibers at room temperature. Figure 3.13(b) shows homeotropically aligned regions (in black color) that result upon heating the LC phase to 136°C. As heating continues, all of the sample becomes homeotropically aligned except in the vicinity of fibers at 150°C. This feature is clearly seen in figure 3.14(a) as a birefringent glow around the fibers. Figure 3.14(b) corresponds to the conoscopic image of the molecules aligned in

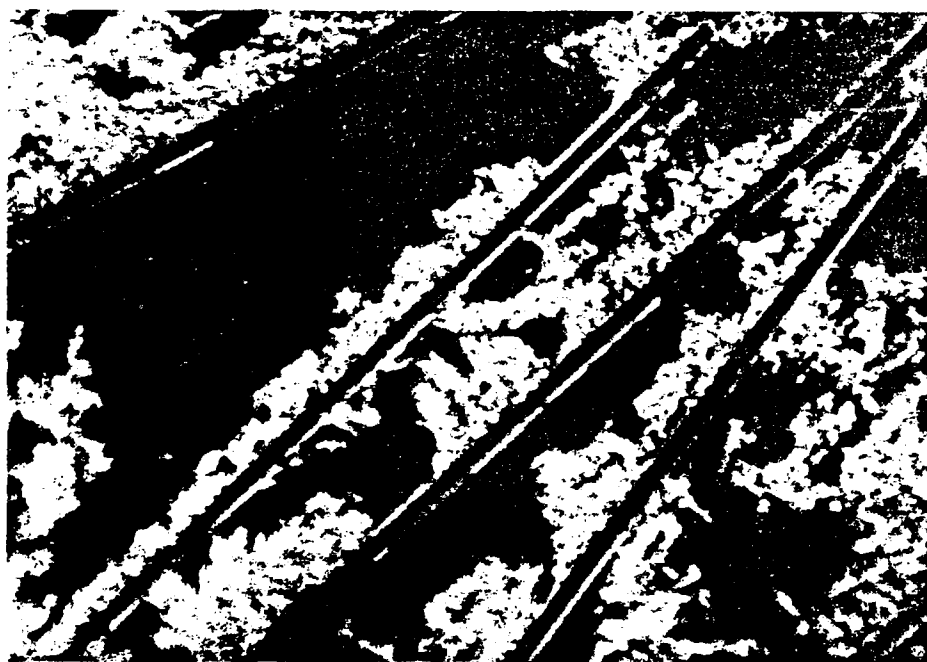
the bulk. Such an interference figure consisting of two black bars, or isogyres, that form a cross is typical for a uniaxially aligned sample. Figure 3.15(a) shows the colorful *Schlieren* texture that develops when the sample is heated to 157°C. The four and two brushes seen in this micrograph indicate nematic ordering of the molecules. The development of birefringence also provides an added confirmation to the fact that the black color in figure 3.14(a) is indeed due to the homeotropic (pseudoisotropic) orientation of molecules and not due to the presence of an isotropic fluid. Isotropic droplets develop around 172°C as shown in figure 3.15(b) and their isotropic nature was confirmed by shearing the sample and observing that the droplets do not disappear. All these transitions are reversed upon cooling the sample from its isotropic state. Shown in figure 3.16 is the crystallization of the sample at 114°C from its homeotropically aligned liquid crystalline melt.

Based on this experiment with fibers, it is very obvious that fiber surface forces influence the alignment of liquid crystalline molecules in their immediate neighborhood. Of the two competing forces (those of the glass surface and the fiber surface) acting on the molecules in the boundary zone, fiber surface forces seem to dominate in this region. Careful examination of the micrograph in figure 3.14(a) brings forth two important points concerning the boundary zone around the fibers. Firstly, this boundary zone is not seen as one continuous birefringent region but is divided into small compartments of irregular lengths. This feature of the boundary zone and its implication on the molecular alignment is discussed below.

Information regarding the second important point that is derived from micrograph in figure 3.14(a) concerns the dimensions of the boundary zone. It is observed that the thickness of this zone is of the same order as the fiber diameter. In other words, the influence exerted by the fiber surface spans approximately



(a)



(b)

Figure 3.13 : Optical micrographs between cross polars of the monomer 8a with dispersed carbon fibers showing the (a) crystalline texture of the sample at room temperature and (b) homeotropically aligned regions in the liquid crystalline phase (450x)

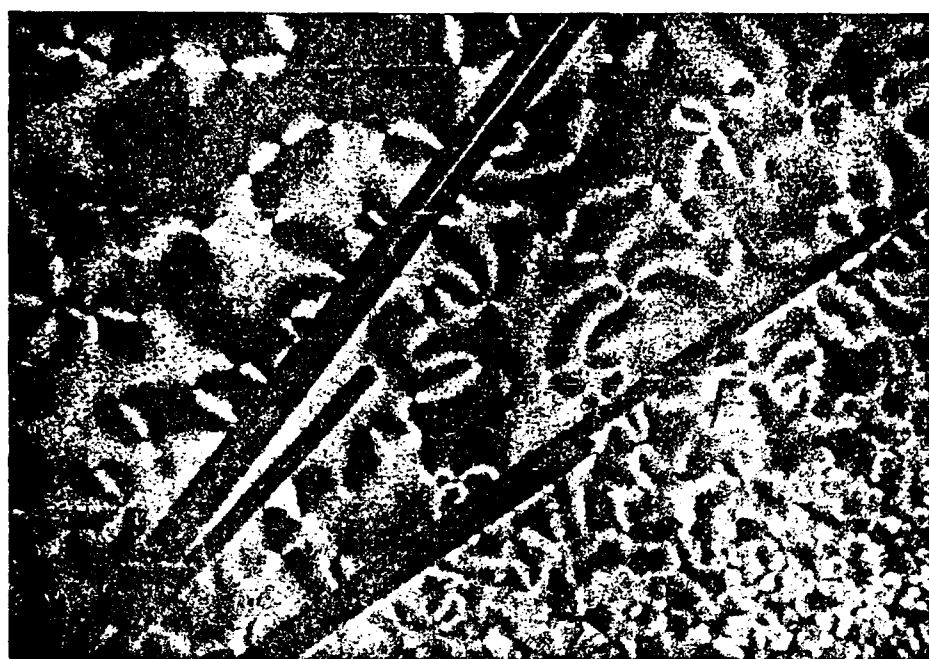


(a)

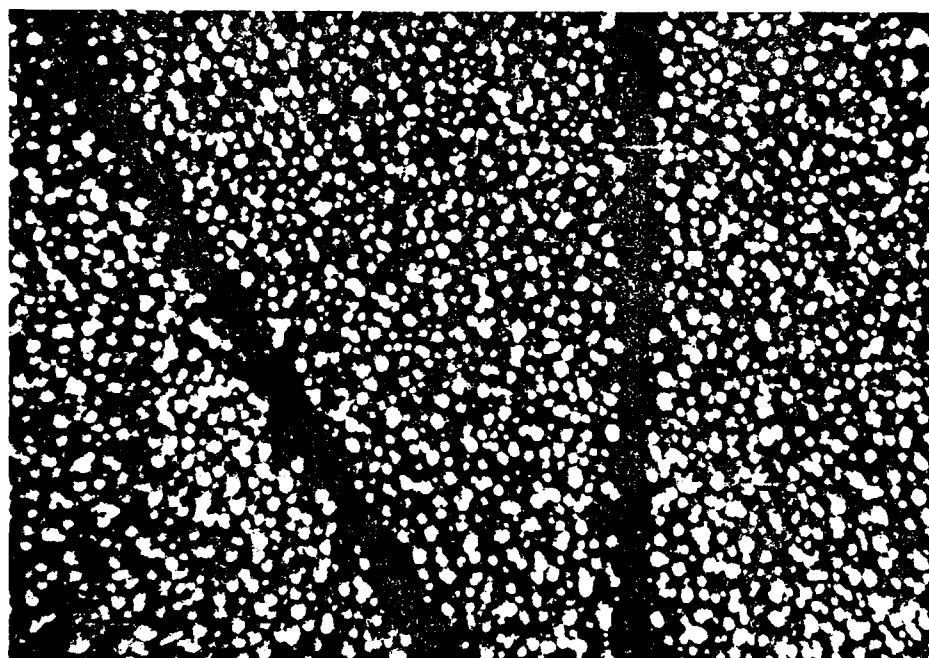


(b)

Figure 3.14: Optical micrographs revealing (a) the boundary zone around carbon fibers dispersed in a homeotropically aligned melt and (b) the conoscopic image confirming the uniaxial alignment of the molecules in the bulk (450x)



(a)



(b)

Figure 3.15 : Optical micrographs between cross polars revealing (a) nematic *Schlieren* texture of the monomeric melt at 157°C and (b) isotropic droplets at 172°C (450x)

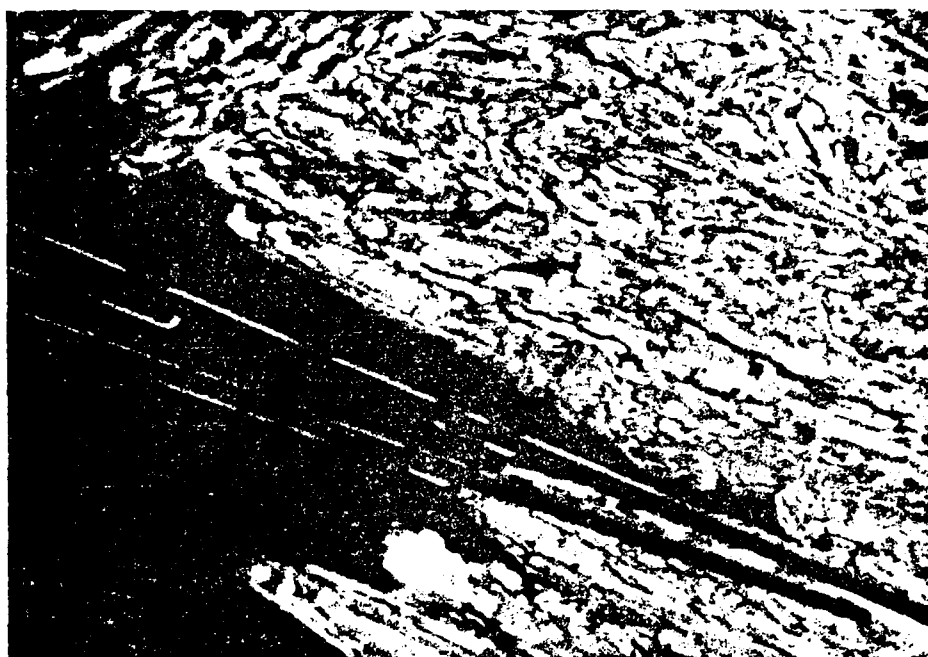


Figure 3.16 : Optical micrograph showing the crystallization of the monomer from the homeotropically aligned melt at 114°C (450x)

10 μ from its surface. An approximate calculation at the number of molecular layers stacked in the boundary zone affords a value close to 4000, assuming the mesogenic length to be about 25 \AA (47). That is, the alignment of thousands of molecular layers is dictated by the fiber surface. In principle, parallel, perpendicular or tilted alignment of molecules with respect to the fiber axis is possible. Upon rotating the sample stage, the birefringent zone around the fibers becomes bright and dim alternately, but never completely extinct. Should all the molecules be aligned parallel to the fiber axis, complete extinction should be observed. Since this is not observed, the possibility of parallel anchoring on the fiber surface is eliminated. This is further confirmed by studies with a compensator plate.

When a full wave compensator (gypsum) plate is introduced in the path of the transmitted light, the pseudoisotropic matrix appears pink in color whereas the boundary zone shows two distinct colors (*orange and blue*) as shown in figure 3.17(a). At this point, it is worth mentioning that a very clear boundary zone is not observed when carbon fibers are replaced by glass fibers. This aspect of the glass fiber surface is illustrated in figure 3.17(b). Furthermore, it is observed that the blue and orange sectors in figure 3.17(a) alternate, the switch in color occurring at the break points along the boundary zone. Upon rotating the stage, the boundary zone remains equally intense, but the color alternates between a single homogeneous color and two alternating colors. Implications of these observations become clearer once the role of a compensator is exemplified with a simple uniaxial crystal. But even before this is attempted, a brief review of the very origin of colors in anisotropic samples is useful.

When illuminated with white light, anisotropic samples viewed between crossed polars appear colored. These colors result from the unequal transmission by the analyzer of the component wavelengths of white light.



Figure 3.17: (a) Optical micrograph between cross polars, revealing the bicolored boundary zone that results when a full wave compensator plate is introduced in the path of transmitted light (450x)

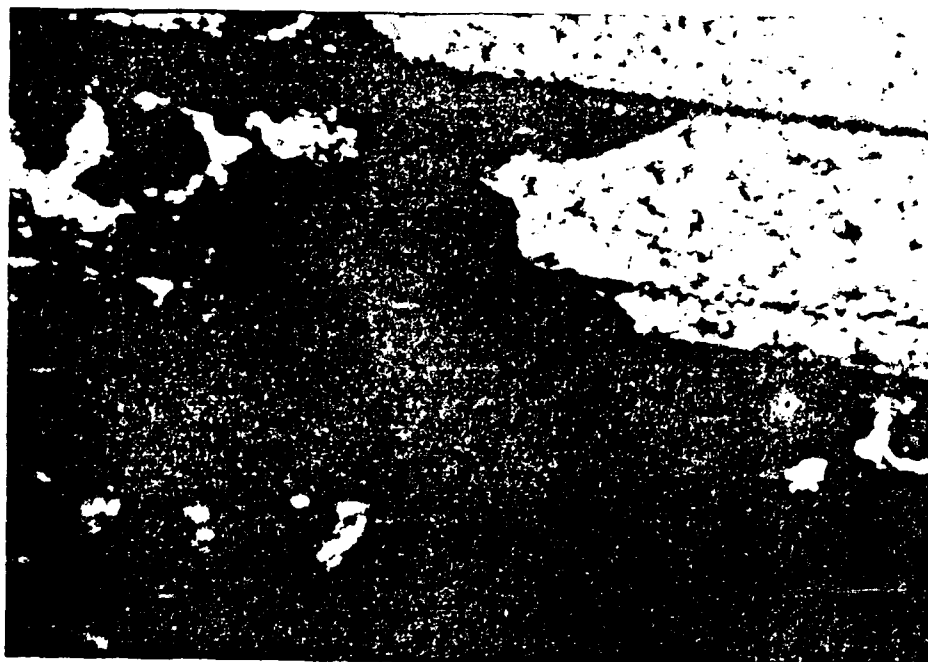


Figure 3.17: (b) Optical micrograph between cross polars, of the functionalized monomer 8a in contact with glass fibers revealing the absence of a distinct boundary zone around fibers (450x)

The particular wavelength that the analyzer transmits depends upon the amount of *retardation* (Δ) produced in the light by its prior passage through the sample. Retardation, in turn, is the path difference between two perpendicularly polarized wave trains and is related to the difference in refractive indices between these two wave trains by,

$$\Delta = t (N_c - n_c) \quad \text{.....(3. 2)}$$

where t is the thickness of the anisotropic sample (crystal), n_c and N_c are the refractive indices along the the crystal's fast and slow directions respectively. Thus, particular values of retardation produce specific interference colors. The relationship between the retardation values and the interference colors characteristic of them are available in the literature (48).

Compensators are accessories particularly useful in studying uniaxial crystals. In general, they are of three different types : a simple quartz wedge, a first order red (gypsum) plate and a quarter-wave plate. Each of these possess two mutually perpendicular principal directions, one called the slow direction (marked as \vec{N}) and the other called the fast direction, \vec{n} . Light waves that vibrate parallel to the 'N' direction while passing through the accessory plate will travel more slowly than do those that vibrate parallel to the 'n' direction during their transmission. Consequently, after emergence from the accessory plate, the slow wave is retarded with respect to the fast wave.

The three different compensators mentioned above possess slightly different retarding characteristics. Thus, the quartz wedge when inserted with its thin end first, produces increasingly higher retardations as its thicker portions successively move into the light path. The first order red or gypsum plate, on the other hand, is of a constant thickness throughout. Its birefringence and

thickness are such that it produces a Δ of 575 m μ . Similarly, a quarter-wave mica plate is generally a thin plate of mica that produces a retardation of 150 m μ . With this background, a simple calculation with a uniaxial crystal is attempted in order to predict the color that this crystal would have with a compensator. Restricting ourselves to a full wave gypsum plate which was employed in all the optical experiments, this would produce a retardation of 575 m μ . Also, the birefringent zone around the fiber is first order yellow in color and the retardation value corresponding to this color as obtained from the literature is 150 m μ (48).

Consider a uniaxial sample of $\Delta=150$ m μ , to be aligned 45° off extinction between cross polars. Insertion of a gypsum plate so that its N direction (slow direction) is parallel to that of the crystal should change the observed retardation color to *second order blue* ($\Delta=725$ m μ). After emergence from the crystal, the wave that vibrated parallel to N_c in the crystal is 150 m μ behind that which had vibrated parallel to n_c . Upon entering the gypsum plate, this already retarded wave, since it vibrates parallel to N while within the gypsum plate, is retarded an additional 575 m μ , finally lagging 725 m μ behind the first ray [figure 3.18(A)]. If viewed between crossed polars, an interference color corresponding to 725 m μ (that is *second order blue*) should be observed. Assume the crystal to have been rotated 90° so that its n and N principal directions have exchanged positions [figure 3.18(B)]. The retarded wave that vibrated within the crystal parallel to N_c , the crystal's slow direction, would be as before 150 m μ behind the fast wave upon emergence from the crystal. However, when it enters the gypsum plate, the formerly slow wave vibrates parallel to the fast direction whereas the formerly fast wave vibrates parallel to the slow direction of the gypsum plate. Thus, the original faster wave is retarded by 425 m μ (575 m μ -150 m μ). The retardation color corresponding to 425 m μ is *second order orange*.

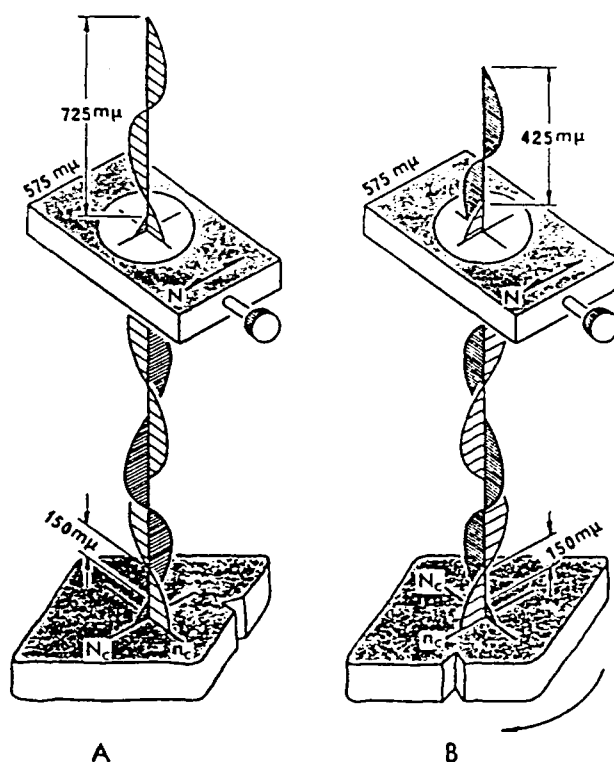


Figure 3.18 : Crystal of retardation 150 mμ at 45° off extinction in (A) additive position and (B) subtractive position with respect to the first order gypsum (575 mμ) plate (48)

Upon extending this knowledge to the bicolored boundary zone observed around the fibers (as in figure 3.17), the following important result emerges. *In the boundary zone two different orientations of molecules exist at an angle to each other close to 90°.* A schematic of such a boundary zone with two molecular orientations is shown in figure 3.19. The detailed molecular architecture within a segment in the boundary region is shown in figure 3.20.

A schematic such as that shown in figure 3.19 raises two very fundamental questions. The first of these concerns the tendency of the molecules to acquire tilted orientations on the fiber surface. The origin of tilted alignment may be

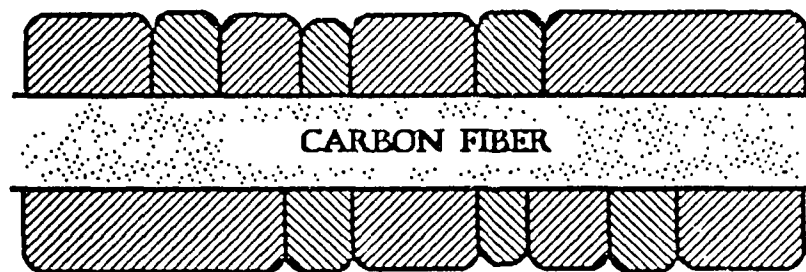


Figure 3.19 : Schematic showing the two different alignments of monomer molecules on the fiber surface

related to the fact that the molecules are in contact with a surface which has a very specific symmetry. Alternatively, this may also be a direct consequence of two competing forces acting on the molecules in this region. While the aligning tendency of the glass surface is clearly established by microscopy studies, it is unknown if the preferred orientation by the fiber alone is parallel or perpendicular to its axis. Therefore, in order to resolve this problem unambiguously, the guiding influence by fiber surface needs to be established.

Recently STM studies have been successfully employed by Smith et al. to determine the orientation of LCs on graphite substrates (49). Their experimental samples were monolayers of nitrile substituted biphenylic compounds of the type shown below (42), deposited on graphite substrates. Two of their important



conclusions based on these studies are of particular relevance in the present context. Firstly, *the structure of the adsorbed molecules in contact with these surfaces is different from those in the bulk. More importantly, the phenyl groups do not lie flat on the graphite surface, but instead, stand on their sides so*

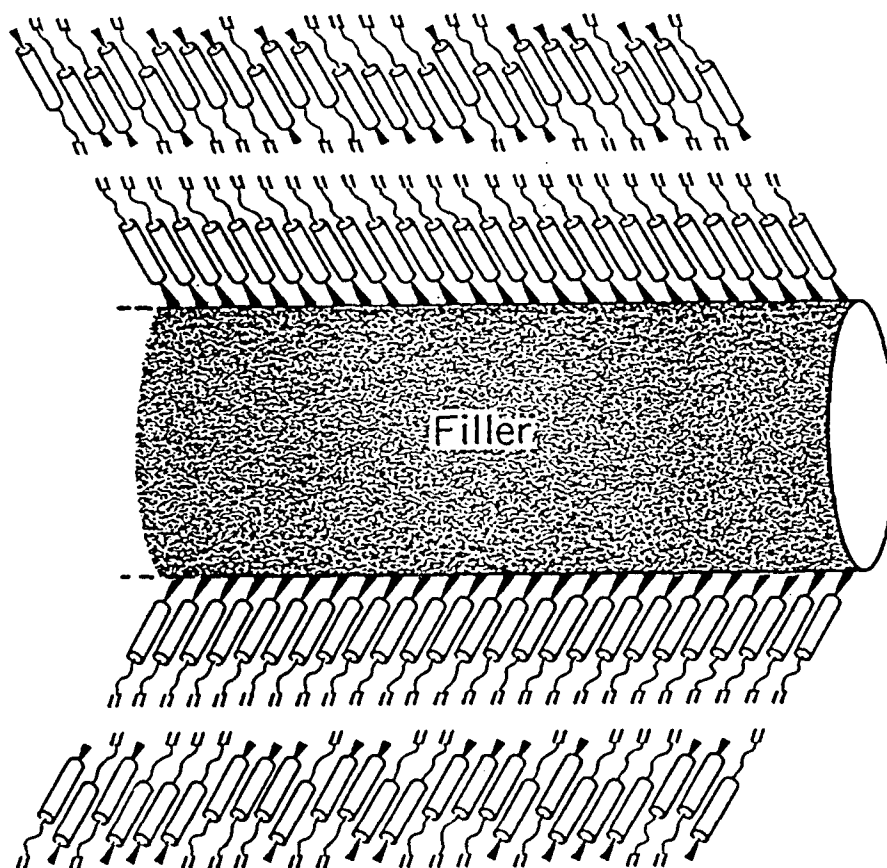


Figure 3.20 : Detailed molecular architecture within a segment in the boundary zone seen around fibers

that the hydrogens of the phenyl rings on one side bond to the graphite and those on the other point normal to the surface. In other words, this result suggests that the molecules prefer to orient in such a way that their long axis is parallel to the graphite plane. However, the nature of the terminal substituents in these molecules, which might play a significant role in this orienting process, is quite different from those in monomer 8a. STM experiments with monomer 8a on graphite substrates that are currently underway in our laboratory are anticipated to give valuable information that might be extended to understand the guiding influence of carbon fiber surfaces better.

The second question that stems from this study is regarding the very origin of breakpoints in the boundary zone around the fiber. Since this experiment involved carboxy-functionalized fibers, it was originally suspected that the carboxyl functionalities were responsible for this feature. But masking these groups by an esterification reaction does not alter this situation either. This aspect of the boundary zone was also observed with fibers coated with a sizing agent as well as with untreated fibers. Scanning electron microscopy studies with these carbon fibers did not reveal any topological features that could be related to the observed phenomenon. Surface defects in the basal planes, inherent in all these fibers may be the cause of this effect. Alternatively, these surface defects may themselves be chemical functions which are present in all fibers at populations above some critical size which is unknown at this point. On the whole, the peculiarities of molecular organization within interphase regions are very interesting as well as scientifically challenging and need to be addressed in the future. Briefly described below are results of additional experiments that were performed to understand these surface phenomena better.

Optical microscopy experiments were conducted with monomer 8a in contact with glass fibers. These fibers revealed nonuniform boundary zones

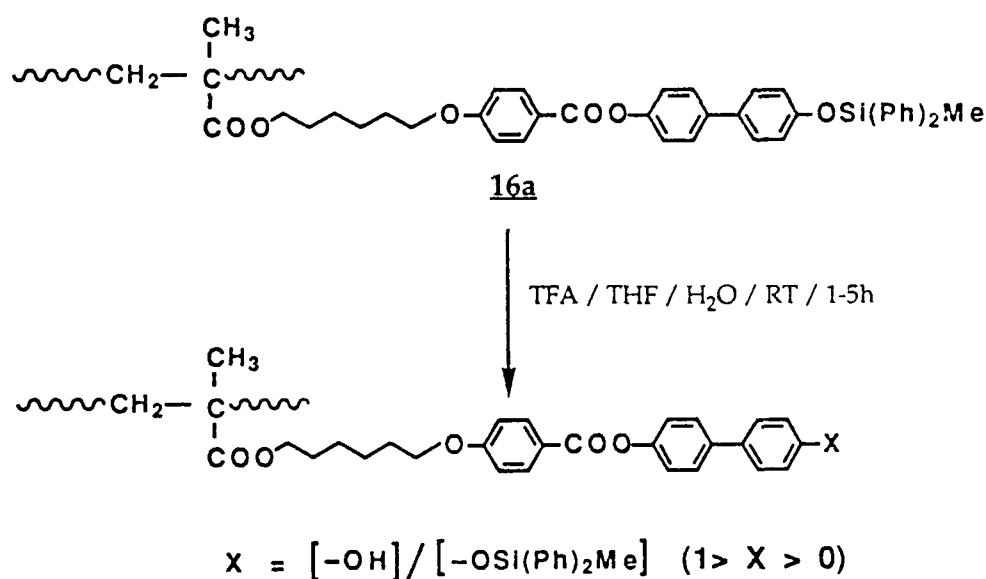
around them. While some portions of the fiber did not reveal any birefringence around them, some others had a faint boundary zone. This probably is the case due to the perpendicular anchoring of molecules on the glass disc as well as on the glass fibers. In another experiment, glass surfaces coated with In_2O_3 layer were used to study their influence on the aligning behavior of molecules. No visible changes were observed in the microscopic studies. In fact, In_2O_3 films have been used to induce perpendicular alignment of liquid crystals (50). So, in this case, the oxide coating may only have a slight stabilizing influence on the already observed homeotropic alignment. Lastly, this tendency of the monomer molecules towards homeotropic alignment was tested on grooved surfaces. In general, such featured surfaces induce parallel alignment of LCs (51, 52). Results from our experiment with monomer **8a** on grooved glass surfaces revealed the same pronounced tendency of the monomer to align perpendicularly. This finding is in accordance with an observation by Guyon et al. (53). They report that silanes and silicones deposited on grooved surfaces are capable of inducing homeotropic alignment of several LCs, just as they do on smooth surfaces. This result may imply that the major orienting factor with these compounds is the chemical interactions at the surface, with topological effects taking precedence only when chemical anchoring is weak.

3.2.4: Partially Protected Hydroxy-Functionalized Polymers

Our strategy to synthesize hydroxylated polymers involved deprotection of silyl ether protected polymers. Partially deprotected polymers were isolated on several occasions while optimizing these deprotection reaction conditions. Optical observations of polymers that were incompletely deprotected revealed an interesting feature of these materials. It was observed that upon heating, a liquid crystalline phase resulted, that soon adopted a biphasic texture over a finite

temperature range before complete isotropization was observed. However, the liquid crystalline melts derived from the the fully deprotected polymers did not show such a biphasic behavior. This observation motivated us to systematically obtain a series of polymers (as shown in scheme 3.4) with increasing extent of deprotection to study their optical behavior.

SCHEME 3.4



Three different approaches were initiated towards the synthesis of this target polymer series. The first of these involved conducting several deprotection reactions with polymer **16a** simultaneously (TFA/THF/H₂O), but varying the time of each deprotection reaction. Therefore, the reaction mixtures were quenched after 1, 2, 3, 4 and 5h successively by precipitation with ether and the products were dried in *vacuo* at 60°C for 24h. Unfortunately, this approach afforded only 25% and 30% deprotected polymers with 1 and 2h of reaction times respectively and 100% deprotection with longer reaction times. Intermediate

compositions could not be isolated even when the reaction intervals were reduced.

The second approach of carefully controlling the reaction temperatures was not successful either and yielded products of extreme compositions only. The third approach was based on controlling the pH of the reaction medium by altering the concentration of water in the reaction mixture. Increasing the amount of water progressively decreased the pH and therefore, increased the extent of deprotection progressively by small amounts. By this method, polymers over a wide range of composition were isolated. The ^1H -NMR spectra of these polymers is shown in figure 3.21. The extent of deprotection in these polymers could be easily inferred from the disappearance of the silyl methyl protons around δ 0.73 as well as disappearance of the silyl phenyl peak around δ 7.36. The integral height of the phenolic peak around δ 9.80 was used to estimate the -OH content in the polymer. On this basis, the -OH content was estimated to be 37, 61, 75, 89 and 100%.

Optical microscopy experiments revealed that the polymer with 37% -OH content exhibited no optical anisotropy at room temperatures or upon heating. On the other hand, all the polymers with a higher -OH content do show liquid crystalline phases upon melting. When the -OH content is 61%, the polymer melts into an LC phase at 130°C and clears at 154°C . With subsequent increase in -OH content, to 75 and 89%, the polymers melt at 146° and 153°C respectively. In addition, these melts show a biphasic region spanning over 38°C in the former case and about 16°C in the latter sample. In these regions, the birefringent and the isotropic fluid coexist, as shown in figure 3.22. With further increase in -OH content to 100%, as described earlier, the polymer melts at 158°C and clears over a narrow $3\text{-}4^\circ\text{C}$ range without showing any conspicuous biphasic behavior.

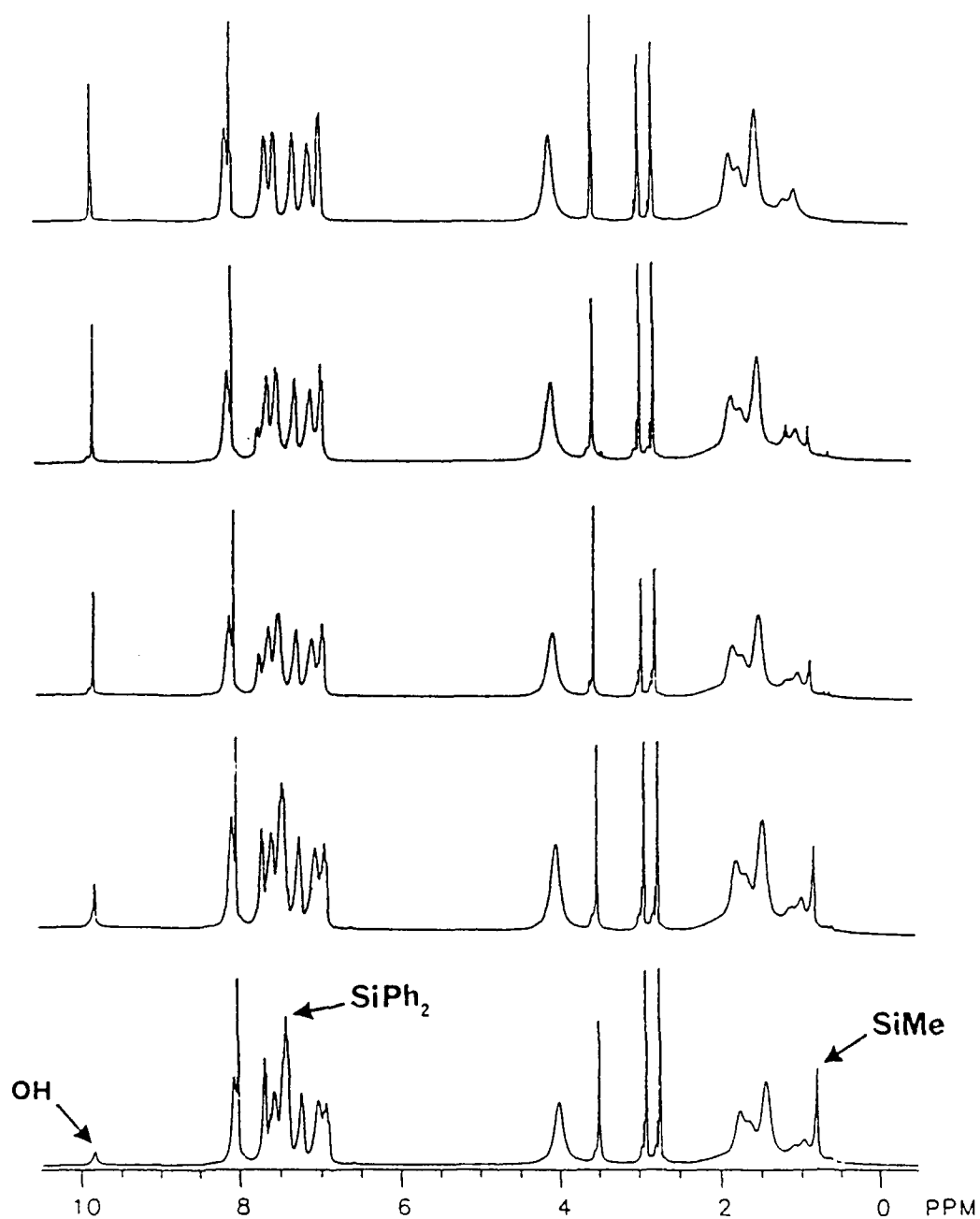


Figure 3.21 : ^1H -NMR spectra of the diphenylmethoxypoly(methylsiloxane) (ODPMS) protected polymers as a function of increasing extent of deprotection

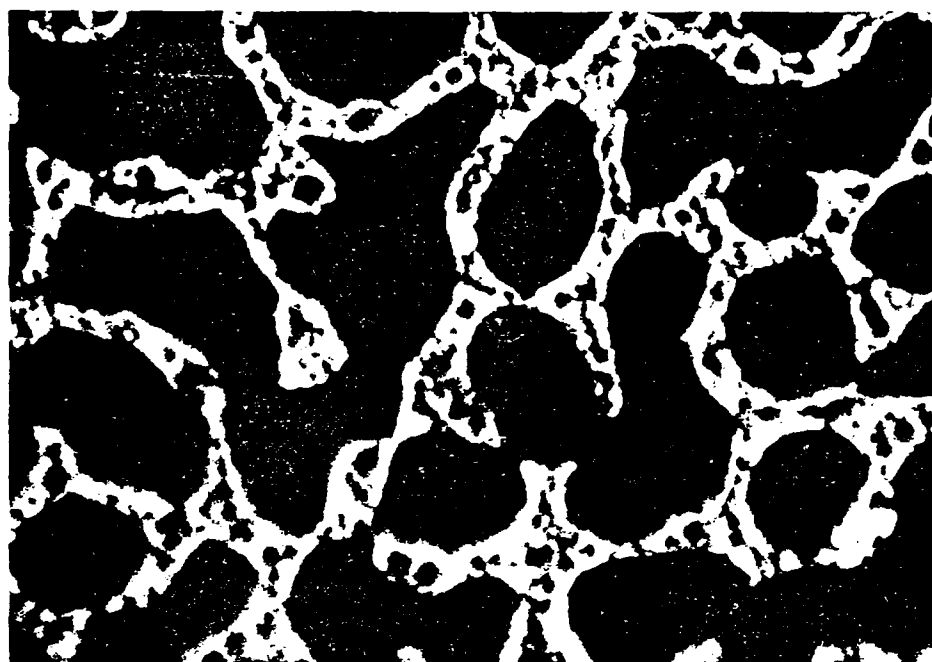


Figure 3.22 : Optical micrograph showing the biphasic nature of the melt derived from polymer with 75%-OH groups at 201°C (450x)

Results of the microscopy studies with this series of polymers are summarized in table 3.8.

Extent of Deprotection (%)	Transition Temperatures (°C)	Biphasic Range (°C)
0	Glass	—
37	Glass	—
61	s 130 LC 154 I	—
75	s 146 LC 227 I	38
89	s 152 LC 249 I	16
100	s 158 LC 262 I	—

Table 3.8: Transition temperatures of the partially protected polymers as obtained from optical microscopy experiments

DSC experiments were conducted with these polymers at a heating rate of 10°C/min. DSC traces of the polymers with 37, 61 and 75% -OH content did not reveal any peak corresponding to the melting or clearing transitions. Polymer with 89% -OH groups showed two broad endotherms around 144°C and 239°C corresponding to the s-LC and LC-isotropic transitions. As shown in figure 3.6, the polymer with 100% -OH content reveals two peaks at 154°C and 256°C corresponding to the melting and clearing transitions respectively.

From the data presented in table 3.8, it is evident that the polymers exhibit

liquid crystalline behavior only above a threshold level of -OH content, which in this case, ranges between 37-61%. The fact that the polymer with 37% -OH groups is amorphous in nature may be explained in terms of its structural composition. Based on its structure, this polymer may also be classified as a copolymer containing mesogenic (functionalized) monomer and nonmesogenic (silyl ether protected) monomer. The presence of a nonmesogenic comonomer dilutes the concentration of the mesogenic units. Consequently, the copolymer loses its mesomorphic behavior below a minimum mesogenic concentration. This is similar to several other side chain copolymeric systems reported in the literature (54-57) which reveal that a minimum amount of mesogenic monomer is required to preserve liquid crystalline phases in these compounds. This situation is frequently encountered when nonmesogenic dyes are copolymerized with mesogenic monomers for nonlinear optical properties (58, 59).

Melts derived from polymers with 75 and 89% -OH content show a clear biphasic behavior before complete isotropization is observed. In general, biphasic behavior observed in polymeric materials has been attributed to the inhomogeneity among the chains that comprise the sample. The first source of inhomogeneity that could occur in most polymeric systems is molecular weight. However, this problem is eliminated right away in the present case because all the partially deprotected polymers are derived from the same protected polymer, of which only some show this biphasic behavior. The next possibility to consider would be chemical inhomogeneity that could exist amongst the various chains. Considering the polymer with 75% -OH content, the 25% protecting groups may be randomly distributed in the sample. If this is the case, some chains may contain more of these protecting groups and these would go into the isotropic state at temperatures lower than those that have a higher -OH content. This would be so because the clearing temperatures of the samples (given in table 3.8)

increase with increasing -OH content. Therefore, segregation of chains on the basis of protecting group distribution may be the cause for the observed phase separation at high temperatures.

In order to address this issue regarding the origin of phase separation in polymers, Stupp et al. (60) have studied two main chain polymers of which one was an ordered and the other a disordered polyester of oxybenzoate, pimelate and dioxyphenyl structural units. Using computer simulation, they have shown that in the disordered polymer, a wide variation in oxybenzoate composition about a global composition of 0.33 exists which translates into a wide variation in persistence length values. Based on the observation that the disordered polymer shows a broad biphasic behavior while the ordered polymer does not, they conclude that *polyflexibility leads to the observed gradual phase separation*.

Results of their computer simulation of disordered chains are presented in figure 3.23 which shows the biphasic width of the system as affected by the distribution in the molar fraction of oxybenzoate structural units. In the copolymeric system which comprises of 75% -OH groups and 25% silyl ether groups, a similar distribution in chain composition may exist which can account for the observed biphasic behavior. The fact that this phase separation does not occur in the polymer with 61% -OH content may be attributed to the low clearing temperature of this sample (154°C). Also, the narrower biphasic range in the polymer with 89% -OH content (16°C) may be related to the narrower distribution in chemical inhomogeneity that this system can have as opposed to the earlier case with 25% protecting groups.

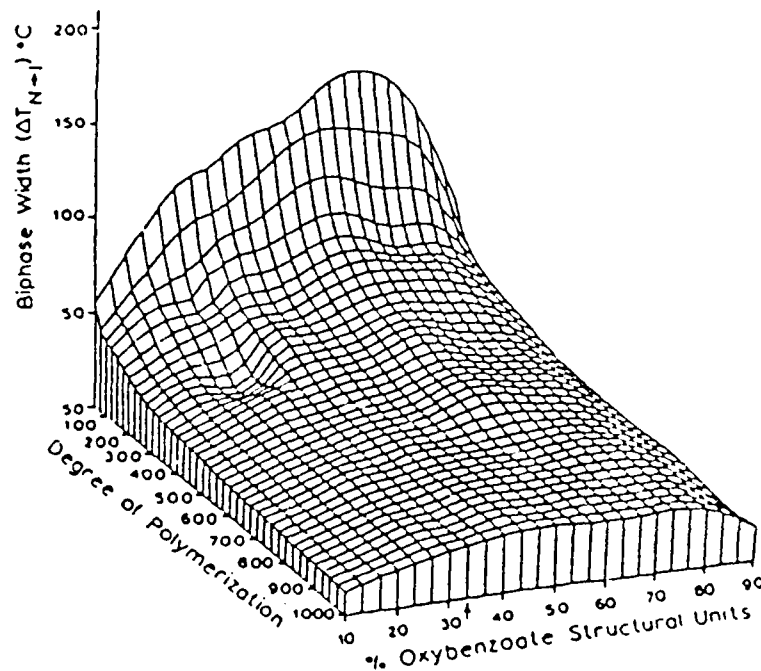
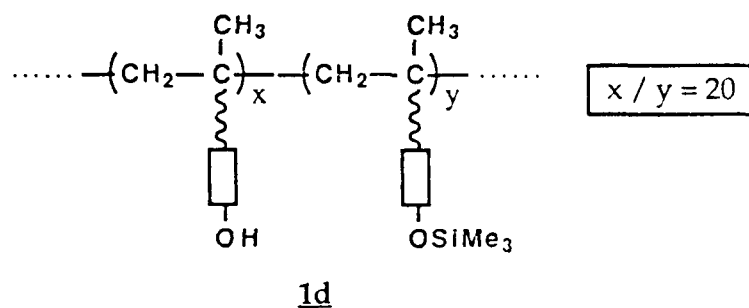


Figure 3.23 : Results of computer simulation showing the biphase width of a polymeric system as affected by the degree of polymerization and composition distribution of oxybenzoate structural units (61)

Another member of the family of partially deprotected polymers that was alluded to in the earlier chapter is **1d**. The structure of this polymer based on its ^1H -NMR is shown below:



In an optical microscopy experiment, this sample melts around 135°C into a birefringent fluid. At temperatures between 151°C and 173°C , this melt shows obvious flow and has a typical *Schlieren* texture corresponding to nematic ordering of the constituent mesogens. More interestingly, the polymeric chains align very uniformly, perpendicular to glass surfaces when heated to about 204°C . A clear conoscopic image was seen, confirming the perpendicular alignment of the mesogenic units. Upon heating to temperatures close to 218°C , isotropic droplets develop which coalesce over a 10° range to yield a fully isotropic fluid. As a result of its high propensity to align homeotropically, distinct boundary zones could be clearly observed when this sample is heated or cooled in the presence of carbon fibers. Micrograph in figure 3.24 clearly shows the homeotropically aligned sample in the bulk as well as the boundary zone around fibers when cooled from its isotropic state to 198°C . Neither of these features were clearly seen with the fully deprotected polymer **1a**. Micrograph (a) shown in figure 3.25 reveals a distinct boundary zone frozen around the fiber when the sample is cooled to room temperature. The fact that such an interphase is a highly ordered one is revealed by the uniform color of the

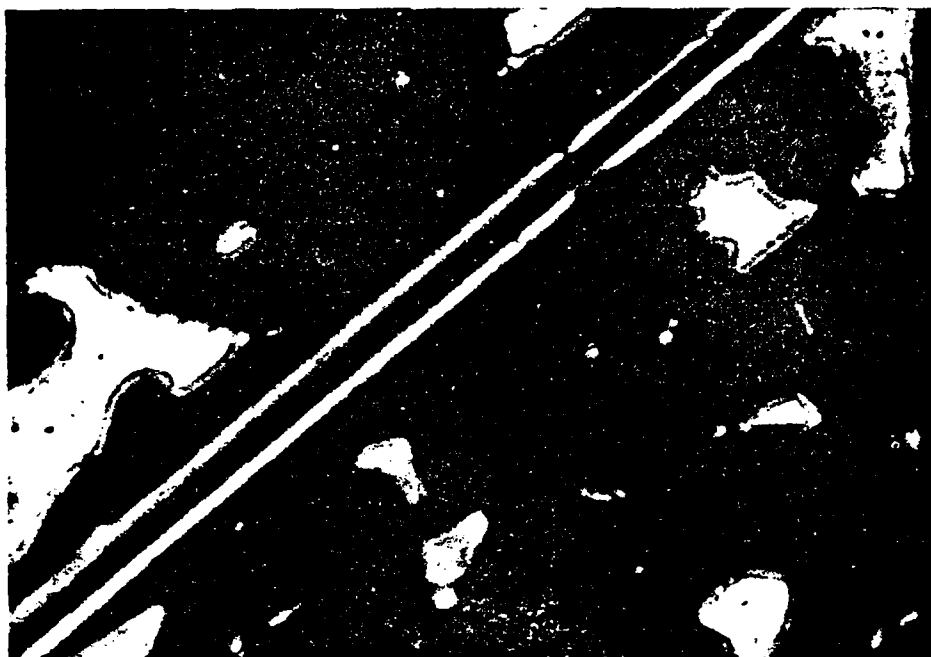
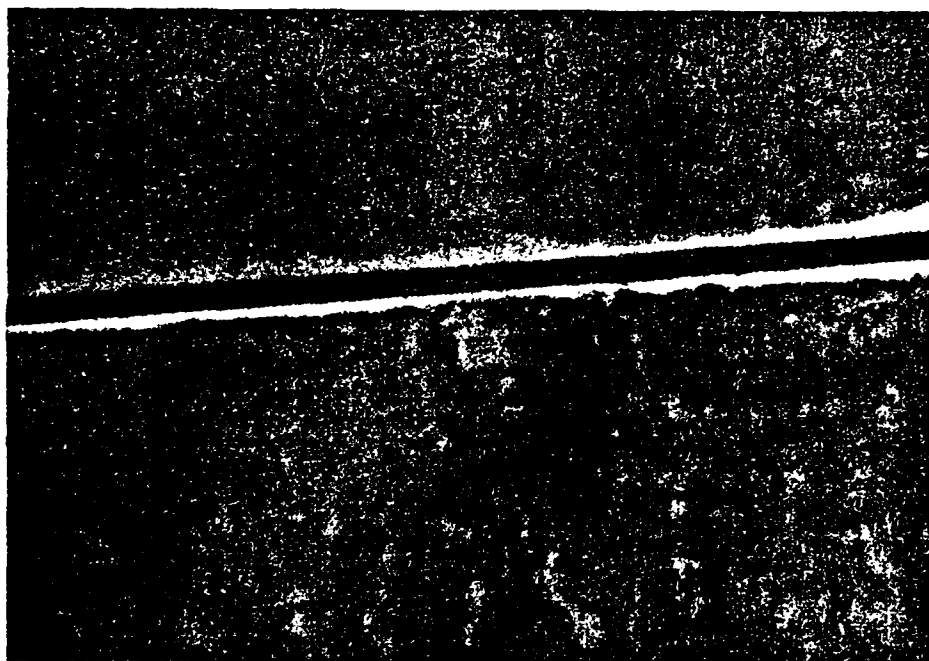


Figure 3.24 : Optical micrograph showing the homeotropic alignment of mesogens comprising 1d at 198°C (450x)



(a)



(b)

Figure 3.25 : Optical micrographs showing the vitrified boundary zone around fiber at ambient temperature without a compensator (a) and with a compensator (b) (450x)

boundary zone when viewed through a compensator [micrograph (b) in fig. 3.25].

The properties of this sample, i. e. its obvious flow characteristics, its nematic texture and its strong tendency for homeotropic alignment are in great contrast to those of the fully deprotected polymer (1a) derived from this intermediate. These properties imply the greater mobility of the mesogenic units due to the incorporation of bulky terminal trimethylsilyl ether substituents. These terminal groups may be viewed as units that disrupt the high ordering of the phenolic mesogens. The improved tendency of the copolymer chains to align on carbon and glass surfaces suggests that the mobility of mesogenic units is an important factor for the molecular organization of polymeric chains on surfaces.

3.3: Summary

Phenolic monomer 8a and its corresponding polymer 1a, both show liquid crystalline phases upon heating. This is in contrast to the expected behavior of phenolic compounds that are extensively associated *via* hydrogen bonding. Molecules in the liquid crystalline phase derived from monomer 8a have a very high tendency to align perpendicular to glass surfaces upon heating. The corresponding polymer, however, does not reveal this feature to such a pronounced extent. This property of the monomer molecules seems to be dictated quite strongly by the phenolic functionality. This inference is drawn from some comparative studies with monomers and polymers that have various other chemical substituents on the mesogen.

Carbon fiber surfaces also have a dramatic influence on the alignment of these molecules. This influence spans over a few thousand molecular layers from the fiber surface, revealed as a distinct boundary zone around the fibers in

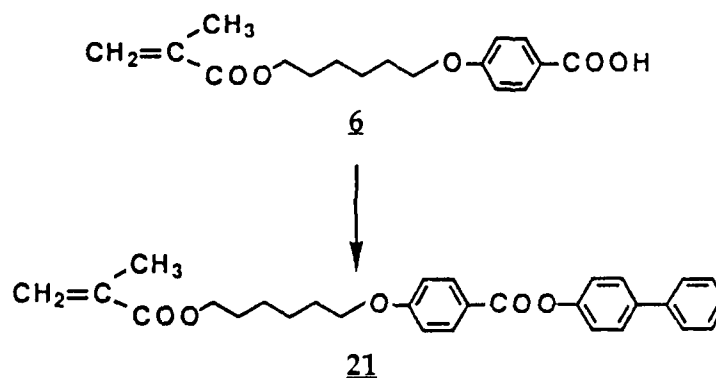
optical microscopy experiments. The alignment of the molecules under the influence of both carbon and glass surface guiding forces is tilted in two different directions with respect to the fiber axis.

A new series of copolymers containing varying fractions of a nonmesogenic monomer (DPMS ether protected form of 8a) and a mesogenic monomer (phenolic monomer, 8a) has been successfully synthesized. Optical microscopy studies with polymers containing 75% and 89% hydroxyl groups reveal that their melts are associated with a biphasic behavior over a finite temperature range before complete isotropization is observed. This is presumably due to the segregation of chains on the basis of functional group distribution. In contrast to that of the fully hydroxylated system, orientation of copolymer chains containing 95%-OH and 5% trimethylsilyl ether groups is strongly influenced by glass and carbon surfaces.

3.4: Experimental

3.4.1: Synthesis of O-Derivatized Monomers and Polymers

Hexyl-6-oxy-[4'-(4''-(4'''-phenyl)phenyl)benzoyloxy]methacrylate (21)



A 50 ml single-necked flask equipped with a Claisen adapter connected to nitrogen inlet and a septum was charged with **6** (0.800 g, 2.162 mmole), 4-hydroxybiphenyl (0.489 g, 2.871 mmole), DPTS (0.153 g, 0.521 mmole) and 1,3-dicyclohexylcarbodiimide (0.808 g, 3.914 mmole). The reaction flask was flushed thoroughly with nitrogen and then dry dichloromethane (20 ml) was added *via* syringe. The solution remained slightly turbid for 10 min after which it became momentarily clear and this was immediately followed by precipitation of urea. After stirring the contents at room temperature for 12h under nitrogen atmosphere, the solid was filtered off and the solution concentrated. Purification was achieved by flash chromatography (silica, 20% acetone in petroleum ether) and recrystallization from heptane.

21

MW: 458.53

yield. 70% after recrystallization

mp: 63-64°C

MS (70 eV): 458(23, M⁺), 291(55), 290(100), 219(22), 203(61).

¹H-NMR (300 MHz, CDCl₃): δ 1.44(m, 4H); 1.63(m, J=6.72 Hz, 2H); 1.75(m, J=6.57 Hz, 2H); 1.87(s, 3H); 4.03(t, J=6.41 Hz, 2H); 4.10(t, J=6.59 Hz, 2H); 5.51(s, 1H); 6.21(s, 1H); 6.98(d, J=8.98 Hz, 2H); 7.26(d, J=8.68 Hz, 2H); 7.48(m, 3H); 7.61(2d, J=8.72 Hz, 4H); 8.21(d, J=8.78 Hz, 2H).

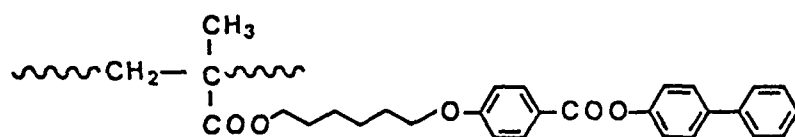
¹³C-NMR (75 MHz, CDCl₃): δ 17.93(CH₃); 25.24(CH₂); 25.35(CH₂); 28.90(CH₂); 28.55(CH₂); 64.11(CH₂); 67.57(CH₂); 113.84(CH); 121.05(CH₂); 121.72(CH); 124.83(C); 126.54(CH); 126.88(CH); 127.53(CH); 128.38(CH); 131.83(CH); 135.99(C); 137.74(C); 139.01(C); 150.12(C); 163.01(C); 164.02(C); 166.35(C).

C₂₉H₃₀O₅

calcd C 75.96 H 6.59

found C 75.78 H 6.57

Poly(hexyl-6-oxy-[4'-(4''-(4'''-phenyl)phenyl]benzoyloxy)methacrylate) (22)



22

22

FW: 458.53

dp: ca 150

yield: 90%

mp: 135-144°C

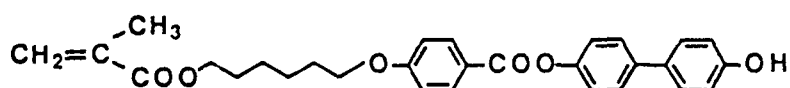
¹H-NMR (300 MHz, CDCl₃): δ 0.91(b, 2H); 1.07(b, 2H); 1.45(b, 4H); 1.64(b, 2H); 1.78(b, 3H); 3.94(b, 4H); 6.86(b, 2H); 7.50(b, 5H); 8.08(b, 2H).

(C₂₉H₃₀O₅)_n

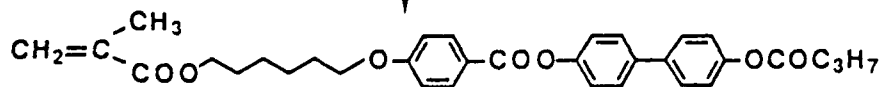
calcd C 75.96 H 6.59

found C 75.78 H 6.57 N 0.06

Hexyl-6-oxy-[4'-(4''-(4'''-propyloxycarbonylphenyl)phenyl]benzoyloxy]-methacrylate (23)



8a



23

A single-necked flask fitted with a Claisen adapter connected to a nitrogen inlet and a septum was charged with **8a** (0.200 g, 0.420 mmole), DPTS (0.026 g, 0.087 mmole) and 1,3-dicyclohexylcarbodiimide (0.130 g, 0.630 mmole) and flushed thoroughly with nitrogen. Dry dichloromethane (15 ml) was added *via* syringe and after stirring the contents for 5 min, n-butyric acid (0.040 g, 0.382 mmole) was added to the reaction mixture. Stirring continued at room temperature overnight under inert atmosphere. The next morning, urea was filtered off and the solution concentrated. Analytical grade monomer was obtained by flash chromatography (silica, 12% acetone in petroleum ether).

23

MW: 544.62

yield: 87% after purification

mp: 72-74°C

MS (70 eV): 544(15, M⁺), 290(100), 203(23), 186(25), 185(33).

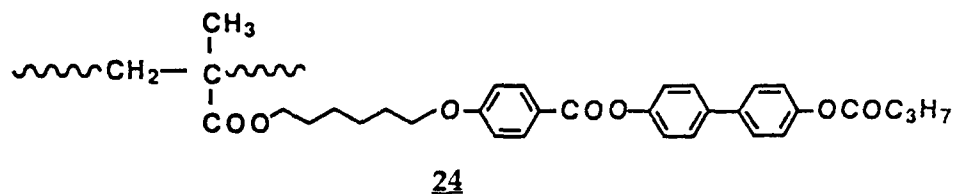
¹H-NMR (300 MHz, CDCl₃): δ 0.87(t, J=7.07 Hz, 3H); 1.3(m, J=7.05 Hz, 2H); 1.43(m, 4H); 1.62(m, J=6.72 Hz, 2H); 1.75(m, J=6.57 Hz, 2H); 1.87(s, 3H); 2.54(t, J=7.01 Hz, 2H); 4.02(t, J=6.5 Hz, 2H); 4.19(t, J=6.5 Hz, 2H); 5.68(s, 1H); 6.14(s, 1H); 6.99(d, J=8.89 Hz, 2H); 7.21(d, J=8.67 Hz, 2H); 7.34(d, J=8.89 Hz, 2H); 7.68(2d, J=8.99 Hz, 4H); 8.24(d, J=9.00 Hz, 2H).

C₃₃H₃₆O₇

calcd C 72.77 H 6.66

found C 72.75 H 6.66

Poly(hexyl-6-oxy-[4'-[4''(4'''-propyloxycarbonylphenyl)phenyl]benzoyloxy]-methacrylate) (24)



24

FW: 544.62

dp: ca 150

yield: 90%

mp: 138-149°C

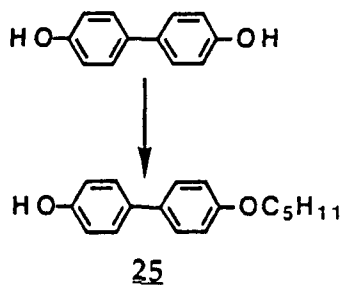
¹H-NMR (300 MHz, CDCl₃): δ 0.96(b, 2H); 0.99(m, J=6.81 Hz, 4H); 1.31(b, 5H); 1.60(b, 2H); 1.74(b, 5H); 2.96(t, J=6.99 Hz, 2H), 3.90(b, 4H); 6.76(b, 2H); 7.03(d, J=8.78 Hz, 2H); 7.34(2d, J=8.80 Hz, 4H); 8.04(d, J=8.90 Hz, 2H).

(C₃₃H₃₆O₇)_n

calcd C 72.77 H 6.66

found C 72.58 H 6.59 N<0.06

4-(4'-Pentyloxyphenyl)phenol (25)



A 100 ml three-necked flask equipped with a stir bar, connected to a reflux condenser and an addition funnel was charged with 4,4'-dihydroxybiphenyl (5.590 g, 0.030 mole), n-pentyl bromide (4.530 g, 0.030 mole) and absolute ethanol (25 ml). With constant stirring, the mixture was slowly heated to its reflux temperature in an oil bath maintained at 110°C. A solution of KOH (1.800 g, 0.030 mole in 4 ml water) was added dropwise over a period of 30 min. The pH of the reaction mixture at the end of this addition was 8.0. Reflux temperature was maintained for an additional 8h following which the contents were cooled and transferred to a separatory funnel containing 50 ml ether. The organic layer was washed with KOH solution (3x25) and the combined aqueous layers were acidified with 10% HCl upon which a white solid precipitated out. The solid was collected by suction filtration and purified by recrystallization from a mixture of hexane and ethanol.

25

MW: 256.34

yield: 60% after recrystallization

mp: 92-93°C

MS (70 eV): 256(38, M⁺), 187(14), 186(100), 158(10), 43(11).

¹H-NMR (300 MHz, CDCl₃): δ 0.86(t, J=7.07 Hz, 3H); 1.30(m, J=7.06 Hz, 2H); 1.68(m, J=7.06 Hz, 2H); 3.93(t, J=6.52 Hz, 2H); 6.78(d, J=8.56, 2H); 6.92(d, J=8.73 Hz, 2H); 7.38(d, J=8.59 Hz, 2H); 7.43(d, J=8.69 Hz, 2H); 9.44(s, 1H).

¹³C-NMR (75 MHz, d₆-DMSO): δ 13.98(CH₃); 22.15(CH₂); 27.19(CH₂); 28.68(CH₂); 67.48(CH₂); 114.69(CH); 115.79(CH); 126.98(CH); 127.22(CH); 130.89(C); 132.69(C); 156.74(C); 157.67(C).

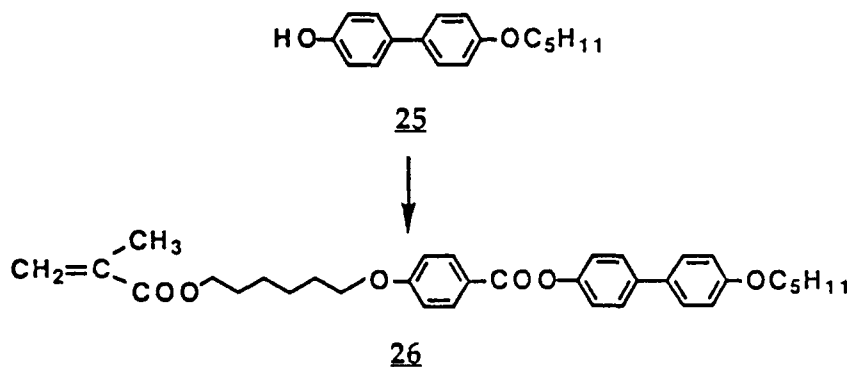
C₁₇H₂₀O₂

calcd C 79.65 H 7.86

found C 79.44 H 7.88

Hexyl-6-oxy-[4'-[4''(4'''-pentyloxyphenyl)phenyl]benzoyloxy]methacrylate

(26)



A 50 ml single-necked flask round-bottomed flask equipped with a Claisen adapter connected to a nitrogen inlet and a septum was charged with 6 (0.869 g, 2.837 mmole), 25 (0.800 g, 3.121 mmole), DPTS (0.167 g, 0.567 mmole) and 1,3-dicyclohexylcarbodiimide (0.878 g, 4.255 mmole). The reaction flask was thoroughly flushed with nitrogen followed by addition of dry dichloromethane (25 ml). The contents were stirred at room temperature under nitrogen atmosphere overnight. The next morning, urea from the reaction mixture was filtered off and the solution concentrated. The residue was first purified by flash chromatography (silica, 10% ethyl acetate in dichloromethane) and subsequently by recrystallization from a mixture of heptane and isopropanol.

26

MW: 544.6

yield: 72% after recrystallization

mp: 104-106°C

MS (70 eV): 544(13, M⁺), 290(19), 289(100), 122(50), 69(11).

¹H-NMR (300 MHz, CDCl₃): δ 0.87(t, J=7.07 Hz, 3H); 1.30(m, J=7.05 Hz, 4H); 1.43(m, 4H); 1.62(m, J=6.72 Hz, 2H); 1.68(m, J=6.60 Hz, 2H); 1.87(s, 3H); 3.93(t, J=6.6 Hz, 2H);

4.04(t, J=6.5 Hz, 2H); 4.18(t, J=6.5 Hz, 2H); 5.65(s, 1H); 6.01(s, 1H); 6.90(2d, J=8.70 Hz, 4H); 7.26(d, J=8.68 Hz, 2H); 7.48(d, J=8.67 Hz, 2H); 7.61(d, J=8.73 Hz, 2H); 8.21(d, J=8.84 Hz, 2H).

^{13}C -NMR (75 MHz, CDCl_3): δ 13.88(CH_3); 18.51(CH_3); 22.31(CH_2); 25.48(CH_2); 25.58(CH_2); 28.02(CH_2); 28.32(CH_2); 28.79(CH_2); 28.81(CH_2); 64.36(CH_2); 67.76(CH_2); 67.82(CH_2); 114.03(CH); 114.54(CH); 121.35(CH_2); 121.76(CH); 125.07(CH); 127.33(CH); 127.80(CH); 132.05(CH); 132.39(C); 136.23(C); 138.18(C); 149.75(C); 158.51(C); 163.20(C); 164.69(C); 167.18(C).

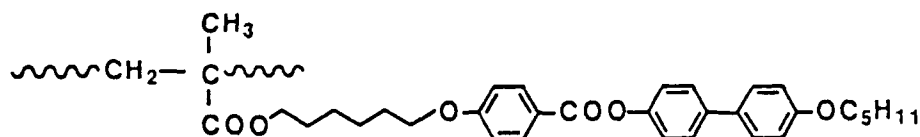
$\text{C}_{34}\text{H}_{40}\text{O}_6$

calcd C 74.97 H 7.40

found C 75.07 H 7.46

Poly(hexyl-6-oxy-[4'-[4''(4'''-pentyloxyphenyl)phenyl]benzoyloxy]methacrylate)

(27)



27

27

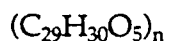
FW: 544.62

dp: ca 150

yield: 88%

mp: 156-164 $^{\circ}\text{C}$

^1H -NMR (300 MHz, CDCl_3): δ 0.87(m, 5H); 0.95(b, 2H); 1.39(b, 8H); 1.64(b, 2H); 1.77(b, 5H); 3.90(b, 6H); 6.85(2d, J=8.56 Hz, 4H); 7.10(d, J=8.16 Hz, 2H); 7.37(2d, J=8.38 Hz, 4H); 8.06(d, J=8.48 Hz, 2H).



calcd C 74.97 H 7.40

found C 74.48 H 7.46 N<0.06

References

- (1) Vorlander, D., *Kristallinish-flussige Substanzen*, 1908, 53.
- (2) Lehmann, O., *Z. Phys. Chem. (Leipzig)*, 1906, 56, 750.
- (3) Reinitzer, F., *Monatsch*, 1888, 9, 421.
- (4) Gray, G. W. and Jones, B., *J. Chem. Soc.*, 1954, 1467.
- (5) Gray, G. W. and Jones, B., *J. Chem. Soc.*, 1953, 4179.
- (6) Gray, G. W. (ed) in *Molecular Structure and the Properties of Liquid Crystals*, (Academic Press, NY), 1962, 151.
- (7) Gray, G. in *Liquid Crystals and Plastic Crystals*, eds: Gray, G. W. and Winsor, P. A. (Halstead Press, NY), 1974, 103.
- (8) Gray, G. W., Hartley, J. B. and Jones, B., *J. Chem. Soc.*, 1955, 1462.
- (9) Gray, G. W., Jones, B. and Marson, F., *J. Chem. Soc.*, 1957, 393.
- (10) Gray, G. W. and Jones, B., *J. Chem. Soc.*, 1954, 2556.
- (11) Culling, P., Gray, G. W. and Lewis, D., *J. Chem. Soc.*, 1960, 2699.
- (12) Gray, G. W. (ed) in *Molecular Structure and the Properties of Liquid Crystals*, (Academic Press, NY), 1962, 152.
- (13) *ibid*, 154.
- (14) Schroeder, D. C. and Schroeder, J. P., *J. Org. Chem.*, 1976, 41, 2566.
- (15) Vora, R. A. and Gupta, R. S., *Mol. Cryst. Liq. Cryst.*, 1979, 56, 31.
- (16) Gray, G. W. (ed) in *Molecular Structure and the Properties of Liquid Crystals*, (Academic Press, NY), 1962, 166.
- (17) Lattermann, G. and Stauffer, G., *Liquid Crystals*, 1989, 4, 347.

- (18) Hartshorne, N. H. (ed) in *The Microscopy of Liquid Crystals*, (Microscopy Publications Ltd., London), 1974, 1.
- (19) Demus, D. and Richter, L., (eds) in *Textures of Liquid Crystals*, (Verlag Chemie, Weinheim), 1978, 14.
- (20) De Vries, A., *Mol. Cryst. Liq. Cryst.*, 1970, 10, 31.
- (21) Wendorff, J. H., Finkleman, H. and Ringsdorf, H. in *Mesomorphic Order in Polymers and Polymerization in Liquid Crystalline Media*, ACS Symp. Ser., 1978, 74, 12.
- (22) Wendorff, J. H. in *Liquid Crystalline Order in Polymers*, ed: Blumstein, A. (Academic Press, NY), 1978, 7.
- (23) Vanderveen, J., *J. Phys. (Paris)*, 1975, 36, 375.
- (24) Maier, W. and Saupe, Z. *Naturforsch*, 1958, 13A, 564; 1959, 14A, 882; 1960, 15A, 287.
- (25) Griffin, A. C., *Mol. Cryst. Liq. Cryst., Lett.*, 1976, 34, 111.
- (26) Barbera, J., Marcos, M., Ros, M. B. and Serrano, J. L., *Mol. Cryst. Liq. Cryst.*, 1988, 163, 139.
- (27) Cognard, J., *Mol. Cryst. Liq. Cryst., Suppl. Ser.*, 1, 1982.
- (28) Porte, G., *J. Phys. (Paris)*, 1976, 37, 1245.
- (29) Creagh, L. T. and Kmetz, A. R., *Mol. Cryst. Liq. Cryst.*, 1973, 24, 59.
- (30) Proust, J. E., Ter-Minassian-Saraga, L. and Guyon, E., *Solid State Commun.*, 1972, 11, 1227.
- (31) Uchida, T., Watanabe, H. and Wada, M., *Jap. Appl. Phys.*, 1972, 11, 1559.
- (32) Vaucher, C., Zann, A., Le Barny, P., Dubois, J. C. and Billard, J., *Mol. Cryst. Liq. Cryst.*, 1981, 66, 103.
- (33) Cognard, J., *Mol. Cryst. Liq. Cryst., Suppl. Ser.*, 1982, 32.
- (34) Urbach, W., Boix, M. and Guyon, E., *Appl. Phys. Lett.*, 1974, 479, 25.

- (35) Gallie, G., Chienellini, E., Ober, C. K., and Lenz, R. W., *Makromol. Chem.*, **1982**, 183, 2693.
- (36) Sek, D., *Polym. J.*, **1985**, 17, 427.
- (37) Gannon, M. J. and Faber, T. E., *Phil. Mag.*, **1978**, 37, 117.
- (38) Parson, J. D., *Mol. Cryst. Liq. Cryst.*, **1975**, 31, 79.
- (39) Krishnaswamy, S. and Shashidhar, R., *Mol. Cryst. Liq. Cryst.*, **1976**, 35, 253.
- (40) Adamson, A. W. in *Physical Chemistry of Surfaces*, 2 ed. (Inter Science Publishers, NY), **1960**, 272.
- (41) Finkleman, H. in *Polymer Liquid Crystals*, eds: Ciferri, A., Krigbaum, W. R. and Meyer, R. B. (Academic Press, NY), **1982**, 45.
- (42) Kelker, H. and Wirzing, U., *Mol. Cryst. Liq. Cryst.*, **1979**, 49, 175.
- (43) Leadbetter, A. J., Durrant, J. L. A. and Rugman, M., *Mol. Cryst. Liq. Cryst.*, **1977**, 34, 231.
- (44) Leadbetter, A. J., Frost, J. C., Gaugha, J. P., Gray, G. W. and Mosley, A., *J. Phys. (Paris)*, **1979a**, 40, 375.
- (45) Marcos, M., Melendez, E. and Serrano, J. L., *Mol. Cryst. Liq. Cryst.*, **1983**, 91, 157.
- (46) Finkleman, H. in *Polymer Liquid Crystals*, eds: Ciferri, A., Krigbaum, W.R. and Meyer, R. B. (Academic Press, NY), **1982**, 53.
- (47) Ober, C. K., Jin, J. and Lenz, R. W., *Advances in Polymer Sci.*, **1984**, 59, 114.
- (48) Bloss, F. D. in *An Introduction to the Methods of Optical Crystallography*, (Holt, Rhinehart and Winston Inc.), **1961**, 144.
- (49) Smith, D. P. E., Horber, H. and Gerber, C. H. and Binnig, G., *Science*, **1989**, 245, 43.

- (50) Uchida, T., Oghawara, M. and Shibata, Y., *Mol. Cryst. Liq. Cryst.*, 1983, 98, 149.
- (51) Berreman, D. W., *Mol. Cryst. Liq. Cryst.*, 1973, 23, 215.
- (52) Wolff, V., Greubel, W. and Kruger, H., *Mol. Cryst. Liq. Cryst.*, 1973, 23, 187.
- (53) Guyon, F. and Urbach, W. in *Non Emissive Electrooptic Displays*, eds: Kmetz, A. R. and Wonwillison, P. (Plenum Press, NY), 1976.
- (54) Plate', N. A., Talroze, R. V. and Shibaev, V. P., *Makromol. Chem., Suppl. Ser.*, 1984, 8, 47.
- (55) Engel, M., Hisgen, B., Keller, R., Kreuder, W., Reck, B., Ringsdorf, H., Schmidt, H. W. and Tschirner, P., *Pure Appl. Chem.*, 1985, 57, 1009.
- (56) Shibaev, V. P. and Plate', N. A., *Adv. Polym. Sci.*, 1984, 60/61, 173.
- (57) Ringsdorf, H. and Schmidt, H. W., *Makromol. Chem.*, 1984, 185, 1327.
- (58) Ringsdorf, H., Schmidt, H. W., Baur, G., Kiefer, K. and Windsscheid, F., *Liq. Cryst.*, 1986, 1, 319.
- (59) Ringsdorf, H., Schmidt, H. W., Ellingsfeld, H. and Etzback, K. H., *Makromol. Chem.*, 1987, 188, 1355.
- (60) Stupp, S. I., Moore, J. S. and Martin, P. G., *Macromol.*, 1988, 21, 1228.
- (61) Martin, P. G., Ph. D. Thesis, University of Illinois at Urbana-Champaign, 1988.

FINAL CONCLUSIONS

This investigation focussed on a new generation of composite materials containing thermotropic liquid crystalline polymers. Two different types of polymers were synthesized for this study: main chain and side chain liquid crystal polymers. The main chain polymer was prepared by melt phase transesterification of p-acetoxybenzoic acid, diacetoxyhydroquinone and pimelic acid for studies on magnetic field orientation of an LCP matrix in the presence of carbon fibers. Characterization by high resolution ^{13}C NMR led to the conclusion that the polymer is best described as a random terpolymer of the three structural units. Optical microscopy studies revealed that this polymer exhibits a nematic phase at temperatures above 135°C and a broad biphasic texture between 220° and 320°C . Magnetic orientation rate of this polymeric melt was enhanced significantly in the presence of carbon fibers, suggesting that the external magnetic field and guiding surface forces act synergistically in orienting polymer chains. Polarized optical microscopy was used to analyze interfacial zones in the composite samples. Large orientational domains were observed when carbon fibers were dispersed in the LCP fluid. Fiber surfaces were also found to stabilize nematic ordering of the polymer as the melt was heated towards complete isotropization or cooled from its isotropic state. SEM analysis of these composite specimens revealed a poor interfacial adhesion and also a poor wetting of fibers by the matrix polymer. On the other hand, grafting of nematogenic chains by in-situ polymerization was found to induce excellent wetting of these surfaces by the matrix polymer. Evidence for grafted polymeric chains on fiber surfaces was derived from XPS and SEM analyses.

New hydroxy-functionalized side chain liquid crystal polymers have been synthesized. This synthesis involved identifying a suitable protection-

polymerization-deprotection route for preparation of phenolic polymers by addition polymerization mechanism. Trimethylsilyl, diphenylmethylsilyl and tetrahydropyranyl ether groups were found to be satisfactory protecting groups for this purpose. Contrary to earlier generalizations that phenolic compounds are non-mesomorphic, the phenolic monomer **8a** and its corresponding polymer **1a**, both show liquid crystalline phases upon heating. Furthermore, monomeric molecules in this phase spontaneously organize perpendicular to glass surfaces. However, fibers that are dispersed in this melt perturb such an organization of molecules in their immediate surroundings. As a consequence, when viewed under an optical microscope between cross polars, distinct "boundary zones" are observed around the fibers, the molecular orientations within which are tilted in two different directions with respect to the fiber axis. In an effort to elucidate the role of phenolic groups in orienting behavior of these molecules, a number of other similar compounds with different terminal substituents were synthesized. Optical microscopy reveals that the polar phenolic groups on mesogenic units are mainly responsible for the perpendicular alignment of mesogens on glass surfaces. However, the slight tendency of molecules with non-polar tails for similar anchoring suggests that this property is not merely a function of the terminal substituent alone. In great contrast to the monomer, the orienting tendency of phenolic polymer side chains on surfaces (glass or carbon) is not very obvious. This is presumably related to lack of sufficient mobility in these polymeric chains. In order to address this aspect of the polymer, bulky non-polar silyl ether substituents were introduced in varying fractions so as to disrupt the high ordering between the phenolic mesogens. Interesting findings with copolymers containing diphenylmethylsilyl ether and phenolic groups are: low -OH contents (0-37%) yield amorphous materials while polymers with -OH content in the range 75-89% show LC phases with biphasic behavior. Finally, the

ordering tendency of copolymer chains that contain a small fraction of trimethylsilyl ether groups was improved significantly, presumably through the plasticizing effect that these substituents can have on the polymer chains.

VITA

Satya Bhama Sastri was born in India on December 24, 1960. After graduating from Stanley Girls' High School in Hyderabad, in June of 1976, she received a Bachelor of Science degree in Chemistry from University of Delhi in May of 1980. During her two year Master's program in Indian Institute of Technology (1980-1982), she was fascinated by the field of polymer science and decided to go for an M. Tech. program in Polymer Science and Technology in June of 1982. Her goal soon drifted towards a doctoral degree in Polymer Science which brought her to the Department of Materials Science and Engineering, University of Illinois at Urbana-Champaign in August of 1986. Research was initiated upon a new generation of composite materials containing liquid crystal polymers under the direction of Professor Samuel Stupp. While in graduate school, she was the recipient of the Whirlpool Fellowship in 1988 and 1989 in recognition of her research work. Her work has been presented at the Materials Research Society Meeting (1988) and the American Physical Society Meetings (1988 and 1989). She is the co-author of three publications based on her M. Tech. and Ph. D research work.